Development of biomimetic 3D platforms for the culture and redifferentiation of pancreatic beta cells

Caterina Aloy Reverté

DOCTORAL THESIS

Title	Development of biomimetic 3D platforms for the culture and redifferentiation of pancreatic beta cells
Presented by	Caterina Aloy Reverté
Centre	IQS School of Engineering
Department	Bioengineering
Directed by	Carlos E. Semino Eduard Montanya

A la meva família

i a l'Aleix

ACKNOWLEDGMENTS

En primer lloc m'agradaria donar les gràcies al Dr. Carlos Semino. *Carlos, muchas gracias por haberme dado la oportunidad de hacer la tesis en tu laboratorio y poder trabajar en un proyecto tan interesante. Me has transmitido la pasión por el mundo de la medicina regenerativa y enseñado a llevar un proyecto de investigación. Durante estos cuatro años he crecido profesionalmente y personalmente. Has confiado en mí y me has dado libertad en todo momento, incluso durante esas etapas en las que parecía que no salía nada. Gracias a ello he aprendido a no darme por vencida y a ser una persona más optimista y perseverante. ¡Gracias por todo!*

També m'agradaria fer especial menció a tots els integrants del grup de recerca en diabetis, nutrició i malalties endocrines (IDIBELL), dirigit pel Dr. Eduard Montanya, amb qui hem tingut la sort de portar a terme el projecte de la Marató. Amb tots vosaltres m'he pogut submergir en el món de la diabetis, el qual m'ha fascinat. Ha estat una experiència molt enriquidora, de la qual n'he gaudit molt. He après molt de la vostra forma de treballar i també he pogut compartir moments personals dels quals m'emporto un molt bon record. Eduard, moltes gràcies per haver estat el co-director de la tesi i haver-te implicat tant en aquesta última fase. Durant aquests anys he après molt amb la teva visió de la ciència i també amb els teus consells. Montse, gràcies per tot el que m'has ensenyat al llarg d'aquests anys, per la teva paciència i per fer-ho tot tan fàcil. I la persona amb qui més he pogut compartir, el Pepelu. *He sido muy afortunada de tenerte como compañero, hemos recorrido este camino juntos y la verdad es que no podría pensar en otra persona mejor. Trabajar contigo ha sido todo un placer, siempre con esa alegría y salero que te caracteriza. Mil gracias!* També voldria donar les gràcies a la resta del grup: Cris, Noèlia, Eli i Sandra.

Per altra banda agrair a totes aquelles persones que han contribuït al desenvolupament d'alguna de les parts de la tesi. Agrair a la Dra. Sara Cervantes del IDIBAPS per facilitar-nos la línia cel·lular INS-1E, amb la qual hem pogut portar a terme experiments molt importants per la tesi. Moltes gràcies al Dr. Salvador Borrós, del grup de Materials de l'IQS, per les facilitats donades a l'hora de fer servir els seus equips. En especial, voldria donar moltes gràcies a l'Anna Mas per la seva implicació en la modificació de les membranes i a la Marina, pel temps que ens va dedicar amb el microscopi de força atòmica (AFM). També agrair al Dr. Jordi Abellà del laboratori de Mètodes Electromètrics del IQS per l'ajuda aportada amb l'obtenció de les imatges de microscòpia electrònica (SEM). També als Centres Científics i Tecnològics de la UB, pels serveis de microscòpia electrònica (SEM). Finalment, donar les gràcies a la Dra. Mª Pilar Armengol, responsable del servei de genòmica de l'IGTP de l'Hospital Germans Tries i Pujol de Badalona. Gràcies per les facilitats que ens has donat a l'hora de venir a fer servir els teus aparells i sobretot per l'ajuda proporcionada, i també al Dr. Marco Antonio Fernández, responsable del servei de citometria de flux.

Durant tots aquests anys al laboratori he tingut la sort de conèixer a moltes persones, i de viure moltes experiències. Ha estat una mica com una muntanya russa, moments de molta

feina i estressants, moments de diversió, decepcions, alegries....tots ells els trobaré a faltar. Vull donar les gràcies a totes les persones que han format part del laboratori de Teixits. Recordo amb molta alegria el grup que érem quan vaig començar, Mire, Patri, Cris, Tere, Lou i Vero, ara totes unes doctores que fan enveja! Mire amb tu vaig tenir una connexió especial des del primer dia. Quants moments hem viscut juntes, quan els recordo se'm dibuixa un somriure gairebé sense adonar-me'n. Segur que em quedo curta al descriure com d'important ets per mi. Ara estàs molt lluny, però seguim compartint les nostres converses infinites amb dubtes existencials inclosos i sobretot moltes risses. Gràcies per ser com ets i per compartir-ho amb mi! Patri, un altre regal que m'ha donat la tesi. Amb tu vaig compartir una part llarga del doctorat i he tingut la sort de tornar a coincidir i de seguir gaudint dia a dia de la nostra amistat. Em meravella lo forta i positiva que ets, i m'encanta la teva part més esbojarrada. Has estat molt present durant tota l'etapa de redacció, amb converses i àudios infinits, menys mal que tu tens tarifa plana! Mil gràcies pel teu suport i els teus consells! Cris, durant l'últim any de doctorat vam agafar més relació i vam fer el nostre petit grup, juntament amb la Vere i la Júlia (i el Verenito). Tot i que ens costa horrors trobar un dia que ens vagi bé a totes per quedar, quan ho fem val molt la pena! Gràcies també pels ànims que m'heu donat totes tres, sou genials! També vull agrair a totes les persones que han anat passant per Teixits: Anna, Astrid, Júlia, Vere, Juli, Oscar, Gerard, Sílvia, Ana, Alex... Amb alguns de vosaltres he pogut treballar conjuntament i ha estat un plaer. *Astrid, I got to share great moments with you, not only at work but also outside. Very good memories from our evenings with Cris and Miquel... beer and plenty of chocolate! Ben & Jerry's will always remind me of you!* Anna, vaig gaudir molt del temps que vam compartir juntes al laboratori, sobretot perquè vam poder compartir moltes aficions, música, comilones, cine... Vere i Júlia, els dos *torbellinos*! Teniu una alegria i vitalitat que es contagia, encantada de tenir-vos a la meva vida. Tot i que no formen part de Teixits, vull agrair especialment al Miquel, Pol i Míguel tots els moments que hem passat junts, us vaig conèixer a la uni gràcies a la Patri i juntament amb ella i la Mire, he gaudit dels moments més esbojarrats del doctorat, amb tardes i nits de birres, sortides i risses impossibles d'oblidar!

També vull agrair als companys del grup de Biomaterials, amb qui hem compartit espai de treball: Pam, Pere, Leti, Sejin, Joan, Robert, Anna, Pol, German, Nathaly... i la resta, que sou molts! Ha estat una experiència molt grata. Merci a tots! *Pam, aunque ahora estás muy lejos y nos veamos muy poquito, siempre te tengo presente. Geniales momentos los que hemos pasado juntas y el más especial el de tu boda…que bien nos lo pasamos con Mire y Albita! Gracias!* Agrair també al Pere, Anna, Joan i Robert per aquestes últimes setmanes, que al tornar a IQS m'han fet sentir com si no hagués marxat. També agrair a la gent de Bioquímica: Victoria, Estela, Cris, Hugo, Ellen, Albita...Sempre tan amables i disposats a ajudar. *Ellen y Albita me llevo muy buenos recuerdos de vosotras, sois un cielo!*

Agrair també als nous companys del BST els ànims que m'heu donat durant aquesta última etapa: Nausica, Eva M, Tatiana, Núria, Marisa, Eva V, Ana B, Sergi, Jesús, Patricia... i la resta, que també sou molts! *Ricardo, muchas gracias por tus sabios consejos y por confiar en mí.*

Durant aquesta etapa de la meva vida també he estat acompanyada per persones de fora del laboratori, especialment de les meves amigues de tota la vida, les *Modernillas y* especialment les *anguiletes*. No se que faria sense *vatros*, estic orgullosa de poder dir que tinc unes amigues

que són un tresor i així m'ho heu demostrat, donant-me els ànims necessaris per donar la última empenta. Mil gràcies truxetes! També vull donar les gràcies a la meva loqueta (Xus) i a l'Andrea. Meri faltes tu! Gràcies per acompanyar-me durant aquesta etapa, aviat podrem reprendre les nostres sortides pels *mercadillos* i les comilones.

Finalment, els agraïments a la meva família. No tinc paraules per expressar l'agraïda que estic als meus pares i germana. Durant tota la tesi, però sobretot aquests últims mesos m'heu donat un suport incondicional i tot i que ens hem pogut veure molt poc, us he sentit més prop que mai. Aquesta tesi ha estat possible gràcies a *vatros*, a la vostra comprensió i estima (candeles incloses). Em fa molta gràcia recordar la frase que sempre em dieu: vinga filla meua, ànims que ja acabes! Ara ja es veritat! I Chloe, que he de dir de la nova incorporació a la família? La meva filloleta, quina cosa més ben feta Maria i David! Una de les seves rialles et dona forces per fer això i molt més! I com no, agrair als meus xiquets, Carlitos i Elisabeth, un dels motors de la meva vida. Una estoneta amb vosaltres i carrego les piles a l'instant. També vull donar les gràcies als meus tiets, cosines i pares de l'Aleix, pel seu continu interès. I ara ja si, només quedes tu, Aleix. El meu company i millor amic. No acabaria mai de donar-te les gràcies, per *aguantar-me* durant tot el procés, i fer-ho de la manera que ho has fet, amb paciència, relativitzant els problemes i amb humor, millor impossible vaja. És l'agraïment que més em costa de fer perquè sento que es queda petit. Gràcies infinites per estar al meu costat i per fer-me confiar en mi mateixa en tot moment!

Caterina, 4 de juliol de 2017

Aquesta tesi ha estat possible gràcies al finançament de la Fundació La Marató de TV3 (subprojecte 121131) i al pressupost de l'IQS per al laboratori d'Enginyeria de Teixits.

SUMMARY

Diabetes is a disease that has reached epidemic proportions. This metabolic disorder is characterized by chronic hyperglycemia and it is associated with a high cardiovascular mortality and a reduced life expectancy. Type 1 diabetes mellitus (T1DM) is caused by the autoimmune destruction of the insulin producing beta cells in the pancreatic islets of Langerhans. Replacement of the lost beta cell mass is a promising treatment for T1DM patients that aims to restore normoglycemia. Pancreatic islet transplantation (IT) has proved its potential as a cell replacement therapy, but faces several obstacles that severely limit its clinical application. The main hurdle is related to the scarcity of pancreatic islets available for transplantation due to the shortage of organ donors. Thus, new strategies aimed to generate an abundant source of insulin-producing cells are needed. A promising approach is the expansion of human adult beta cells. However, the *in vitro* expansion of adult beta cells implies the loss of the beta cell phenotype. This is probably a consequence of the isolation and subsequent dissociation of pancreatic islets into single cells, which completely alters cell-cell and cell-matrix contacts due to the destruction of the islet microenvironment. Tissue engineering (TE) can help to overcome these issues by creating functional 3D tissues, using cells combined with biomaterials that mimic the native extracellular matrix (ECM).

We hypothesize that the functionalization of nanofibrous 3D matrices with ECM-derived signaling motifs could reconstitute the islet microenvironment and induce the redifferentiation of the expanded human islet cells. The rat beta cell surrogate INS-1E was used as a proof of concept for the functionalized 3D model. The non-instructive self-assembling peptide (SAP) RAD16-I was functionalized with the integrin-binding motifs RGD, YIG, IKVAV, GEF and TWY. Characterization of the functionalized matrices showed that RAD16-I maintained its characteristic β-sheet structure when the bioactive motifs RGD, YIG, and IKVAV were added. Therefore, INS-1E cells were encapsulated with the biomimetic RAD16-I scaffolds, which supported cell survival and promoted the formation of cell clusters, resembling the *in vivo* conformation of pancreatic islets. Furthermore, an enhanced insulin secretion was observed in YIG and IKVAV-functionalized matrices.

Based on these results, we aimed to adapt the developed 3D model to promote the redifferentiation of expanded human islet-derived cells. The encapsulation of dedifferentiated expanded cells in RAD16-I scaffold was not an adequate system, but the embedding of cells in a sandwich configuration proved to be a suitable culture model. Expanded cells were induced to reaggregate forming islet-like cell clusters (ICCs) in order to promote cell-cell contacts. ICCs conformation was maintained and evolved in RAD16-I sandwich cultures with excellent viability values. Furthermore, RGD and IKVAV adhesion motifs promoted the re-expression of the crucial beta cell markers Ins, Pdx1, Nkx6.1 and MafA. These results indicate that RGD and IKVAV-functionalized RAD16-I sandwiches are a promising 3D platform to induce the redifferentiation towards a beta cell phenotype, and to generate insulin-expressing cells that could be used in diabetes cell therapy.

RESUMEN

La diabetes es una enfermedad que ha alcanzado proporciones epidémicas. Este trastorno metabólico se caracteriza por la hiperglucemia crónica y está asociado con una elevada mortalidad cardiovascular y la reducción de la esperanza de vida. La diabetes mellitus tipo 1 (T1DM) está causada por la destrucción autoinmune de las células beta pancreáticas productoras de insulina. El reemplazo de la masa de células beta es un tratamiento prometedor para los pacientes de T1DM, que tiene como objetivo restaurar la normoglucemia. El trasplante de islotes pancreáticos ha demostrado su potencial como terapia de reemplazo celular, aunque su aplicación se encuentra limitada por diversos obstáculos como la escasez de islotes pancreáticos. Por lo tanto, se necesitan nuevas estrategias dirigidas a generar una fuente abundante de células productoras de insulina. Un enfoque prometedor es la expansión de las células beta adultas. Sin embargo, la expansión *in vitro* de las células beta implica la pérdida de su fenotipo, probablemente como consecuencia del aislamiento y la posterior disociación de los islotes en células individuales. Dichos procesos destruyen el microambiente celular, alterando los contactos célula-célula y célula-matriz. La ingeniería de tejidos (TE) puede ayudar a superar estos problemas creando tejidos tridimensionales (3D), mediante el uso combinado de células y biomateriales que imitan la matriz extracelular (ECM) nativa.

La hipótesis de trabajo se basó en que la funcionalización de las matrices 3D con motivos de señalización derivados de la ECM podría reconstituir el microambiente de los islotes, induciendo la rediferenciación de las células expandidas. La línea de células beta de rata INS-1E, se utilizó como prueba de concepto para el modelo 3D funcionalizado. El péptido autoensamblable RAD16-I se funcionalizó con los motivos de unión a integrina RGD, YIG, IKVAV, GEF y TWY. La caracterización de las matrices funcionalizadas evidenció que el péptido RAD16-I mantenía su estructura característica de hoja beta al añadir los motivos bioactivos RGD, YIG e IKVAV. Por lo tanto, las células INS-1E se encapsularon con los *scaffolds* biomiméticos, los cuales promovieron la supervivencia celular y la formación de agregados celulares, mimetizando la conformación in vivo de los islotes pancreáticos. Además, se observó una mayor secreción de insulina en las matrices funcionalizadas con los péptidos YIG e IKVAV.

Basándonos en estos resultados, se intentó adaptar el modelo 3D para promover la rediferenciación de las células expandidas de los islotes humanos. La encapsulación de las células desdiferenciadas en la matriz de RAD16-I no resultó ser un sistema adecuado, por ese motivo se establecieron cultivos en configuración sándwich. Previamente, se indujo la formación de agregados celulares (ICCs), propiciando así los contactos célula-célula. La conformación de los ICCs se mantuvo y evolucionó en los cultivos en sándwich con excelentes valores de viabilidad. Además, los motivos de adhesión RGD e IKVAV promovieron la reexpresión de los marcadores de célula beta Ins, Pdx1, Nkx6.1 y MafA. Estos resultados indican que los cultivos en configuración sándwich funcionalizados con RGD e IKVAV, son una plataforma 3D prometedora para inducir la rediferenciación hacia un fenotipo de célula beta, generando así células que puedan ser utilizadas en la terapia celular de la diabetes.

RESUM

La diabetis és una malaltia que ha assolit proporcions epidèmiques. Aquest trastorn metabòlic es caracteritza per la hiperglucèmia crònica i està associat amb una elevada mortalitat cardiovascular i la reducció de l'esperança de vida. La diabetis mellitus tipus 1 (T1DM) està causada per la destrucció autoimmune de les cèl·lules beta pancreàtiques productores d'insulina. El reemplaçament de la massa de cèl·lules beta és un tractament prometedor per als pacients de T1DM, que té com a objectiu restaurar la normoglucèmia. El trasplantament d'illots pancreàtics ha demostrat el seu potencial com a teràpia de reemplaçament cel·lular, encara que la seva aplicació es troba limitada per diversos obstacles com l'escassetat d'illots pancreàtics. Per tant, es necessiten noves estratègies dirigides a generar una font abundant de cèl·lules productores d'insulina. Un enfocament prometedor és l'expansió de les cèl·lules beta adultes. No obstant, l'expansió *in vitro* de les cèl·lules beta implica la pèrdua del seu fenotip, probablement com a conseqüència de l'aïllament i la posterior dissociació dels illots en cèl·lules individuals. Aquests processos destrueixen el microambient cel·lular, alterant els contactes cèl·lula-cèl·lula i cèl·lula-matriu. L'enginyeria de teixits (ET) pot ajudar a superar aquests problemes creant teixits tridimensionals (3D), mitjançant l'ús combinat de cèl·lules i biomaterials que imitin la matriu extracel·lular (ECM) nativa.

La hipòtesi de treball es va basar en el fet que la funcionalització de les matrius 3D amb motius de senyalització derivats de la ECM podria reconstituir el microambient dels illots, induint la rediferenciació de les cèl·lules expandides. La línia de cèl·lules beta de rata INS-1E, es va utilitzar com a prova de concepte per al model 3D funcionalitzat. El pèptid autoensamblable RAD16-I es va funcionalitzar amb els motius d'unió a integrina RGD, YIG, IKVAV, GEF i TWY. La caracterització de les matrius funcionalitzades va evidenciar que el pèptid RAD16-I mantenia la seva estructura característica de fulla beta en afegir els motius bioactius RGD, YIG i IKVAV. Per tant, les cèl·lules INS-1E es van encapsular amb els *scaffolds* biomimètics, els quals van promoure la supervivència cel·lular i la formació d'agregats cel·lulars, mimetitzant la conformació *in vivo* dels illots pancreàtics. A més, es va observar una major secreció d'insulina en les matrius funcionalitzades amb els pèptids YIG i IKVAV.

Basant-nos en aquests resultats, es va intentar adaptar el model 3D per promoure la rediferenciació de les cèl·lules expandides dels illots humans. L'encapsulació de les cèl·lules desdiferenciades en la matriu de RAD16-I no va resultar ser un sistema adequat, per aquest motiu es van establir cultius en configuració sandvitx. Prèviament, es va induir la formació d'agregats cel·lulars (ICCs), propiciant així els contactes cèl·lula-cèl·lula. La conformació dels ICCs es va mantenir i va evolucionar en els cultius en sandvitx amb excel·lents valors de viabilitat. A més, els motius d'adhesió RGD i IKVAV van promoure la reexpressió dels marcadors de cèl·lula beta Ins, Pdx1, Nkx6.1 i MAFA. Aquests resultats indiquen que els cultius en configuració sandvitx, funcionalitzats amb RGD i IKVAV, són una plataforma 3D prometedora per induir la rediferenciació cap a un fenotip de cèl·lula beta, generant així cèl·lules que puguin ser utilitzades en la teràpia cel·lular de la diabetis.

LIST OF CONTENTS

LIST OF FIGURES

LIST OF TABLES

LIST OF ABBREVIATIONS

2D:	two-dimensional
3D:	three-dimensional
ADA:	american diabetes association
AFM:	atomic force microscopy
AM:	acetomethyl ester
ATP:	adenosine triphosphate
BM:	basement membrane
CD:	circular dichroism
Coll:	collagen
CVD:	cardiovascular disease
DAPI:	4'6-diamidino-2-phenylindole dihydrochloride
DM:	diabetes mellitus
DMSO:	dimethyl sulfoxide
E-Cad:	E-cadherin
ECM:	extracellular matrix
EMT:	epithelial to mesenchymal transition
EV:	enteroviruses
FAs:	focal adhesions
FBS:	fetal bovine serum
FN:	fibronectin
GAGs:	glycosaminoglycans
GDM:	gestational diabetes mellitus
GSIS:	glucose-stimulated insulin secretion
HEMA-MMA:	hydroxyethyl methacrylate-methyl methacrylate
hPSCs:	human pluripotent stem cells
HSPG:	heparan sulfate proteoglycans
ICCs:	islet-like cell clusters
IEQ:	islets equivalents
Ins:	insulin
IT:	islet transplantation
KRBH:	krebs-ringer bicarbonate hepes
LM:	laminin
MACS:	magnetic activated cell sorting
MafA:	V-maf musculoaponeurotic fibrosarcoma oncogene homolog A
MafB:	V-maf musculoaponeurotic fibrosarcoma oncogene homolog B
MDI:	multiple daily injections
MET:	mesenchymal epithelial transition
MSC:	mesenchymal stem cell
MTT:	3-(4,5-dimethylthiazolyl-2)-2,5-diphenyltetrazolium bromide
N-Cad:	N-cadherin
NCAM:	neural cell adhesion molecule
NeuroD1:	neurogenic Differentiation Factor 1

Ngn3:	neurogenin 3
NID:	nidogen
Nkx6.1:	NK6 homeobox
PDCs:	pancreatic ductal cells
Pdx1:	pancreatic and duodenal homeobox 1
PEG:	Poly (ethylene glycol)
PFA:	paraformaldehyde
PFM:	pentafluorophenyl methacrylate
PGA:	poly (glycolic acid)
PgPFM:	plasma grafting of pentafluorophenyl methacrylate
PLA:	poly (lactic acid)
PLGA:	poly [(lactic acid)-co-(glycolic acid)]
PP:	polypeptide-secreting
PSA:	polysialic acid
PTE:	pancreatic tissue engineering
PTFE:	polytetrafluoroethylene
QCM-D:	quartz crystal microbalance with dissipation monitoring
RER:	rough endoplasmic reticulum
RIN:	RNA integrity
RPLP0:	human large ribosomal protein
RPMI:	Roswell park memorial institute's medium
RQ:	relative quantification
SAP:	self-assembling peptide
SEM:	scanning electron microscopy
SMA:	smooth-muscle actin
T1DM:	type 1 diabetes mellitus
T2DM:	type 2 diabetes mellitus
TBP:	TATA-box binding protein
TE:	tissue engineering
TGN:	trans-Golgi Network
TRITC:	tetramethylrhodamine B isothiocyanate
UKPDS:	UK Prospective Diabetes Study
VDCC:	voltage-dependent Ca^{2+} channels
VEGF-A:	vascular endothelial growth factor-A
Vim:	vimentin
VN:	vitronectin
WHO:	world health organization

CHAPTER 1

INTRODUCTION

1.1 BACKGROUND

1.1.1 OVERVIEW

The term Diabetes mellitus (DM) refers to a metabolic disorder characterized by chronic hyperglycemia (high blood glucose)[1]. Diabetes prevalence is dramatically increasing and has reached epidemic proportions during the last century[2]. Currently, an estimated 415 million adults are afflicted with diabetes worldwide (one in eleven adults), being one of the most common chronic diseases in almost every country[2,3] (Figure 1.1). Specifically, in Europe 8% of the population suffers from diabetes[4]. According to the World Health Organization (WHO), high blood glucose is the third higher risk factor for premature mortality after high blood pressure and tobacco use[5].

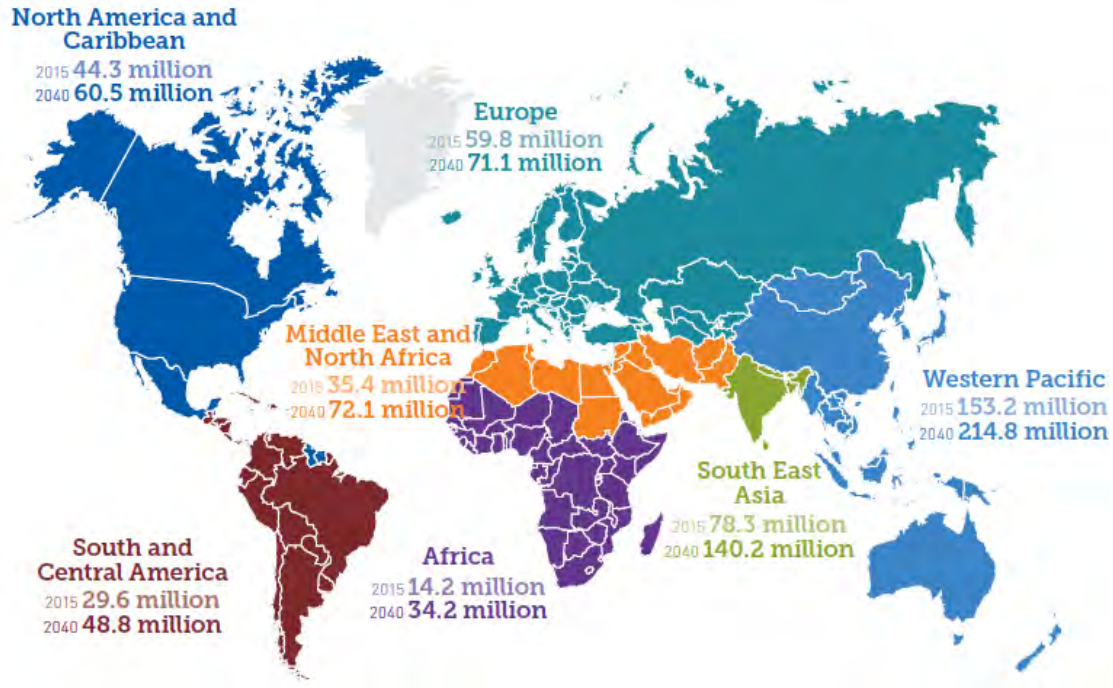

Figure 1.1. Estimated number of people, aged 20-79, with diabetes in 2015 and 2040 in 220 countries. The prevalence of diabetes continues to increase around the glove. One of the major concerns is that much of this increase will take place in developing countries. From the International Diabetes Federation Atlas[2].

Diabetic patients suffer from long-term complications such as macrovascular and microvascular diseases. Macrovascular complications include coronary heart disease, peripheral vascular disease and cerebrovascular disease[6]. On the other hand, diabetes is also associated with the progressive development of severe microvascular complications, such as retinopathy with potential blindness, nephropathy that could lead to renal failure and neuropathy with risk of foot ulcers and amputation among others[1]. These devastating complications are associated with a reduced life expectancy, being cardiovascular disease

(CVD) one of the leading causes of premature death[2,7,8]. This macrovascular complication accounts for approximately 50% of early deaths among people with diabetes[2]. Specifically, in 2015 around 5.0 million people under the age of 60 died from diabetes, which is equivalent to 14.5% of all-cause mortality[2].

Moreover, diabetes entails a large economic burden for patients and health care systems[2,9,10]. People who suffer from diabetes consume two to three times more resources than non-diabetic people[11]. According to the International Diabetes Federation, in 2015 the 12% of the global health care expenditure was attributable to diabetes[2,11,12]. These costs were estimated to range from USD 673 billion to USD 1.197 billion[2].

1.1.2 BASICS OF PANCREATIC PHYSIOLOGY AND FUNCTION

1.1.2.1 Pancreas physiology

The pancreas is an organ comprised of separated functional units, the exocrine and the endocrine parts, which regulate two major physiological processes, protein and carbohydrate digestion and blood glucose homeostasis, respectively (Figure 1.2). The exocrine pancreas conforms the 80% of the organ tissue mass and is composed of a branched network of acinar and duct cells that produce and deliver enzymes important to digestion. The exocrine tissue surrounds the endocrine regions that are spheroidal clusters of cells scattered throughout the pancreas (islets of Langerhans).

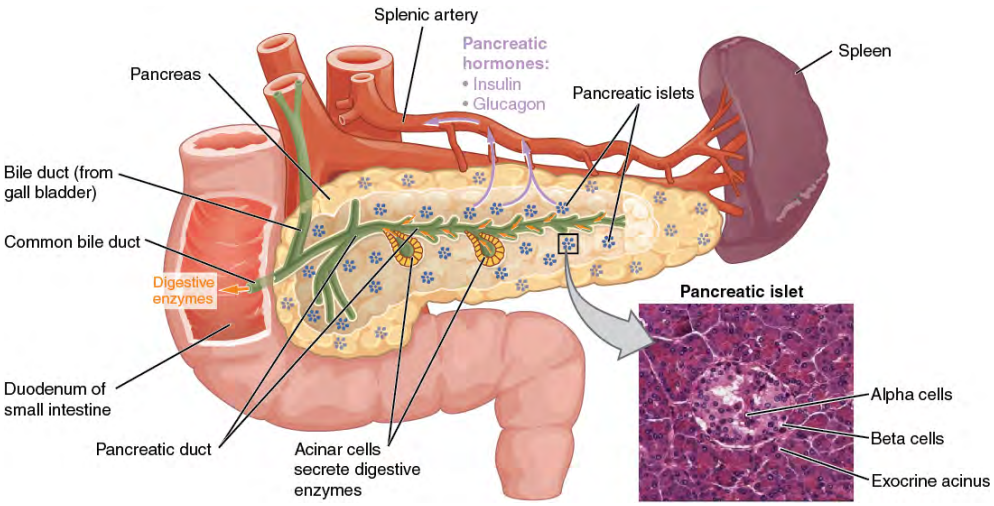

Figure 1.2. Anatomy of the pancreas, the exocrine and the endocrine compartments. The pancreas is formed by the exocrine and the endocrine glands. The exocrine tissue composes the bulk of the pancreatic mass, producing and secreting digestive enzymes that are transported by the pancreatic duct into the duodenum, the first part of the small intestine. The endocrine pancreas, formed by the Islets of Langerhans, secretes hormones as insulin and glucagon into the blood stream. Micrograph image shows an islet of Langerhan surrounded by the exocrine acini. From OpenStax under the license of Creative Commons, Attribution 4.0 International (CC by 4.0)[13].

Discovered in the 1869 by the German pathological anatomist Paul Langerhans (1847-1888), the islets of Langerhans are responsible for the production and secretion of hormones and are highly vascularized structures, which allows the access of hormones to the blood system. In particular, each islet is largely vascularized by direct arteriole blood flow, being the islet capillary network density five times higher than the present on the exocrine compartment [14,15]. A healthy human adult pancreas contains over 1 million islets[16], most of them measuring 50-200 µm in diameter[14], although they represent only 1 to 2 % of the entire organ.

The islets of Langerhans are composed of different cell types that function together to maintain normoglycemia (normal blood glucose levels)[17,18]. Within each islet there are five types of cells, the insulin-secreting beta cells (β), glucagon-secreting alpha cells (α), pancreatic polypeptide-secreting PP cells, somatostatin-secreting delta cells (δ) and ghrelin-secreting epsilon cells (ε)[19] (Figure 1.3). Glycemic control depends mainly on the secretion of insulin and glucagon hormones. Both hormones respond oppositely to changes in blood glucose concentrations. Insulin is secreted in response to rising levels of blood glucose, meanwhile glucagon secretion is stimulated when blood glucose levels are low (hypoglycemic conditions). On the other hand, somatostatin inhibits the secretion of both hormones[20].

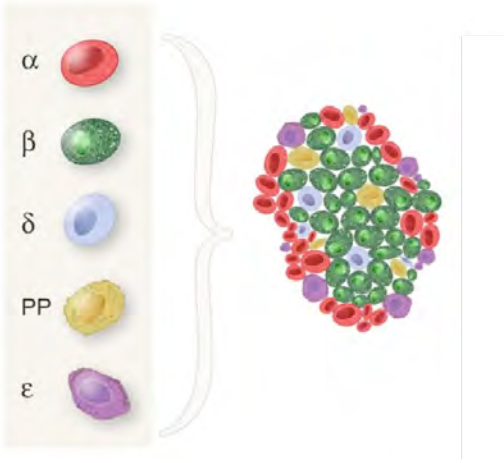

Figure 1.3. Schematic representation of the islets of Langerhans. The different cell types that conform the islets of Langerhans synthesize and secrete hormones responsible for the maintenance of normal blood glucose levels. Within each islet there are five types of cells, the insulin-secreting beta cells (β), glucagon-secreting alpha cells (α), pancreatic polypeptide-secreting PP cells, somatostatin-secreting delta cells (δ) and ghrelin-secreting epsilon cells (ε). The most abundant are the beta cells, followed by the α cells. Adapted from www.symmation.com.

Cell islet composition and architecture varies between species and within species, yet, in rodent and human species, beta cells are the most abundant cell type[18]. Pancreatic islets in rodent species are characterized by a central core of beta cells that represents 60-80% of the islet cells, and a mantle of alpha (15-20%), delta (<10%), and PP cells (<1%) cells segregated to the periphery[21]. In contrast, human islets have a lower proportion of insulin-containing cells

and a larger proportion of alpha cells than rodent islets; approximately 50-70 % of the islet cells are beta cells, 30-40% alpha cells, 10% delta cells and few PP cells[18,21–23]. Concerning the cell organization within human islets, some reports stated that endocrine cells were randomly distributed thorough the islets[22,24]. Nevertheless, more recently, various authors have proved that small islets (40-60 µm in diameter) maintain the segregated cell type distribution (mantle-core arrangement) present in rodent islets[23,25–27]. They have also seen that larger islets consist of fusion of cell aggregates subunits, in which each subunit preserves the mantle-core arrangement. Alpha and beta cells present in these subunits are closely associated with the islet microvasculature[23,25,26].

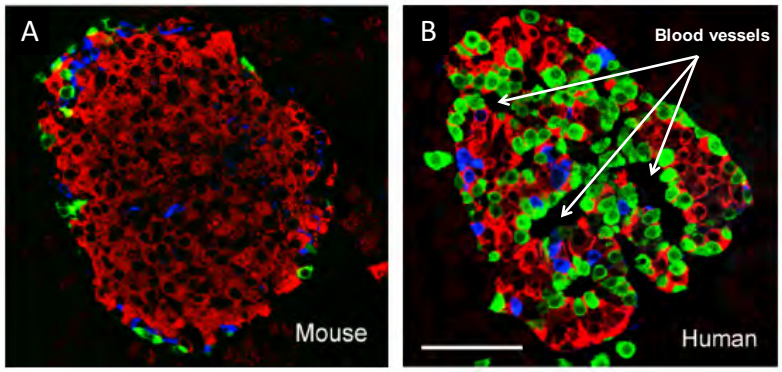

Figure 1.4. Cellular organization of rodent and human pancreatic islets. (A) Rodent pancreatic endocrine cells display a mantle-core arrangement, with beta cells located in the core of the islets and alpha, delta, PP and epsilon cells at the periphery. (B) Human islets structure seems to be similar to that of rodent islets, with various mantle-core subunits and a strong association among beta and alpha cells with the islet microvasculature. Insulin red, glucagon green and somatostatin blue. Scale bar of 50 µm. Adapted from Caicedo[21].

1.1.2.2 Glucose homeostasis in the healthy pancreas

The endocrine pancreas, through the action of its various hormones, especially insulin and glucagon, is responsible for the maintenance of normal blood glucose levels. Glucose is the main human's body source of energy and the sole source of energy for the brain or red blood cells.

After a meal, insulin is secreted proportionally to the increment in blood glucose levels caused by glucose entrance into the circulation due to food absorption and digestion. Insulin secretion reduces liver glucose production and promotes liver glucose uptake, which is stored as glycogen (glycogenesis). It also stimulates glucose utilization by the insulin-dependent tissues (skeletal muscle and adipocytes). The excess of glucose is stored as glycogen in the skeletal muscle or as lipids in adipose cells for long-term energy use. Thus, insulin lowers blood glucose levels, reestablishing glucose homeostasis. Conversely, between meals or at night, when blood

glucose levels tend to decrease, glucagon is released stimulating the breakdown of stored glycogen to glucose (glycogenolysis) in liver and skeletal muscle. Thus, glucose is then ready to be used as energy in muscle cells and released into the bloodstream by liver cells. Moreover, glucagon also promotes the conversion of aminoacids and lipids into glucose (gluconeogenesis) during prolonged periods of low blood glucose levels. These actions prevent the occurrence of hypoglycemia (low blood glucose) (Figure 1.5) [4,28,29].

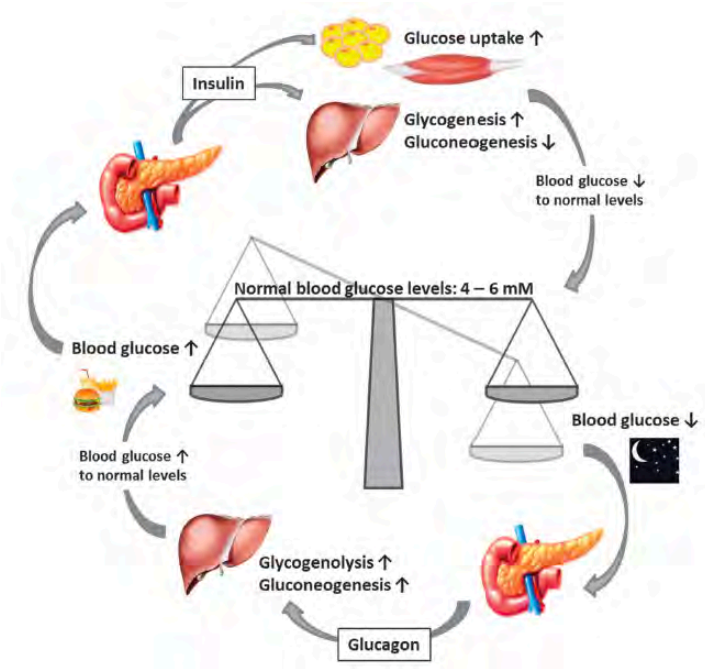

Figure 1.5. Maintenance of glucose homeostasis by insulin and glucagon action. When blood glucose levels are high, insulin is secreted by the beta cells of the pancreas to stimulate glucose uptake by the liver and the insulin-dependent tissues (skeletal muscle and adipocytes), and the storage as glycogen in the liver and muscles. Insulin also triggers the conversion of excess of glucose into fat. When blood glucose levels are low, the alpha cells of the pancreas release glucagon, which promotes liver cells to break down glycogen and release glucose into the bloodstream. From Röder *et al* [30].

Thus, thanks to the hormonal control, glucose levels are maintained within a narrow range in the human body. The disturbance of the glucose homeostasis can lead to metabolic disorders.

1.1.2.3 Insulin structure, biosynthesis and secretion

The insulin secreted by the beta cells is a polypeptide of 51 aminoacids (5.8 KDa), although the insulin gene encodes a 110-aminoacid precursor named preproinsulin[31]. In humans, preproinsulin is encoded by a single gene, whereas in rats and mice two non-allelic insulin genes are present[32]. Among other factors, the synthesis of insulin (Figure 1.6) is regulated by blood glucose levels at the transcriptional and post-transcriptional levels. This is mostly

controlled by the promoter region of the insulin gene, that presents several binding sites for islet-enriched transcriptional factors, such as Pdx1, NeuroD1 and MafA[33,34].

Preproinsulin is composed of A-, B- and C-chains and is synthesized in the cytoplasm along with a signal peptide, a molecule commonly found on secreted proteins (Figure 1.6). The signal peptide is rich in hydrophobic residues that facilitate the penetration into the rough endoplasmic reticulum (RER). Hence, the nascent preproinsulin is translocated into the lumen of the RER, and is converted to proinsulin by removal of the signal peptide[35–37]. Proinsulin consists of the A- and B-chains of insulin in a continuous single chain linked through a region called C-peptide (connective peptide)[38]. In the lumen of the RER proinsulin undergoes accurate folding in which two disulfide bonds between A- and B-chains are formed[37,39]. Then, proinsulin is delivered to the Trans-Golgi Network (TGN) where it is packed into immature secretory granules. The maturation of the granule involves the cleavage of proinsulin to yield insulin and C-peptide, which are secreted together in nearly equimolar amounts[35,40]. Acidification of the milieu is necessary to facilitate the conversion from proinsulin to insulin by prohormone convertases PC1/3 and PC2[35,41]. Under such conditions insulin crystallization within the mature granule takes place. Insulin monomers tend to form dimers and in the presence of Zn^{+2}, dimers associate to form insoluble hexameric units coordinated by two zinc ions[37,42], leading to the formation of the dense-core granules (Figure 1.7)[31,37,43]. C-peptide is more soluble and does not crystalize with insulin, so it is found surrounding the dense-core granules[37].

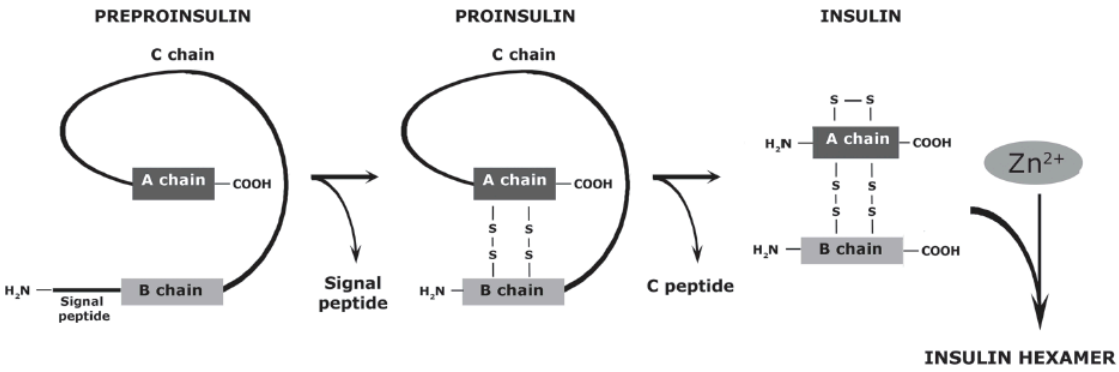

Figure 1.6. Schematic view of insulin biosynthesis. The processing of insulin entails the cleavage of the preproinsulin signal peptide, which gives rise to proinsulin precursor. Afterwards, the C-peptide is removed to yield mature insulin (A and B chains bond by two disulfide bridges). Zinc-stabilized hexamers are then formed and stored in secretory granules. From Skelin *et al*[44].

As previously mentioned, upon glucose stimulation beta cells secrete insulin. The glucose-stimulated insulin secretion (GSIS) is a multistep process involving the transport and oxidation of glucose, electrophysiological changes and fusion of the insulin granules with the beta cell plasma membrane. Firstly, glucose enters the cell by the action of glucose transporters (GLUT2 in rodents, GLUT1 in humans). Then, glucose is metabolized to generate adenosine triphosphate (ATP). Increased cytosolic ATP causes closure of ATP sensitive K^+ channel (K_{ATP}), depolarizing the plasma membrane and leading to the opening of voltage-dependent Ca^{2+}

channels (VDCC), which allows Ca^{2+} influx[4,35]. The resultant increase in intracellular Ca^{2+} concentration induces the release of insulin stored in the densely clustered granules, which occurs via exocytosis[45,46] (Figure 1.8).

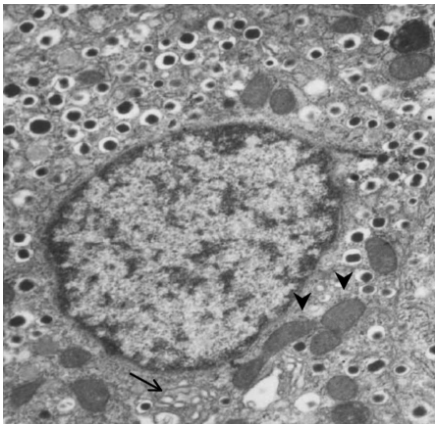

Figure 1.7. Electron microscope picture showing insulin granules. Dense-core insulin granules at the cytoplasm of a beta cell. Golgi apparatus (arrow) and mitochondria (arrowheads). From Kulkarni[47].

In order to be secreted, insulin secretory granules must be transported to the beta cell plasma membrane along the microtubules of the cytoskeleton. After fusion of the insulin granules with the plasma membrane, insulin is released[37].

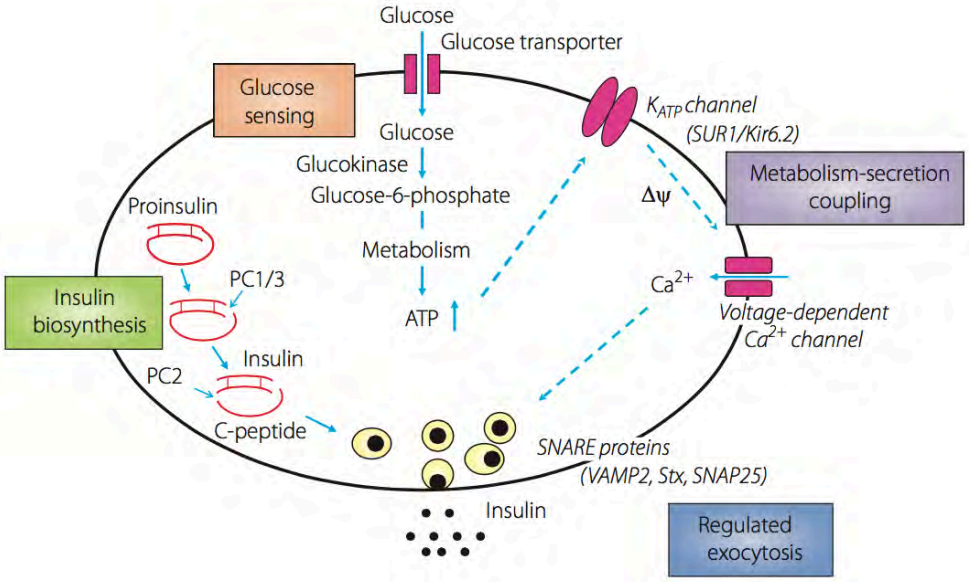

Figure 1.8. Generalized mechanism of glucose-stimulated insulin secretion in pancreatic beta cells. Glucose entering beta cells through glucose transporters is metabolized, leading to an increase in the ATP concentration, closure of the K_{ATP}, depolarization of the beta cell membrane and opening of the voltage-dependent Ca^{2+} channels. The resultant rise in intracellular Ca^{2+} triggers soluble N-ethylmaleimide-sensitive factor attachment protein receptor (SNARE)-dependent exocytosis of insulin granules. From Minami and Seino[48].

1.1.2.4 Regulation of the pancreatic beta cell mass

The pancreatic beta cell mass is dynamic and increases and decreases to maintain the glycemic levels within the physiological range. In conditions where pancreatic islets must meet an increased metabolic demand, such as obesity, pregnancy, partial pancreatectomy, glucose infusion or islet transplantation, the beta cell mass has been shown to increase[49]. Specifically, the beta cell mass is determined by the number and size of beta cells. The mechanisms that dictate beta cell mass variations at cellular and molecular level in humans are not completely known, but it is accepted that the beta cell number is determined by the balance between replication from preexisting beta cells, neogenesis (formation of new islets through the differentiation from progenitor or stem cells), and cell death. On the other hand, beta cell size relies on processes such as hypertrophy and atrophy[49–51]. Transdifferentiation and dedifferentiation processes also play a role in the regulation of the beta cell mass.

The embryonic development

The exocrine and the endocrine pancreas have a common cell origin, the endoderm[47]. During the embryonic development, the endoderm gives rise to the primitive gut that will form the digestive system[52]. From the gut, the epithelium buds ventrally and dorsally giving place to a single organ, the pancreas[52,53]. Differentiation from progenitor cells to beta cells occurs mostly during this period and several transcription factors are involved[47]. With genetic lineage-tracing studies, the key transcription factors that participate in this process have been elucidated. Figure 1.9 shows that all the different mature pancreatic cell types have their origin in progenitors cells expressing Pdx1 and or Ptf1a transcriptions factors[54–56]. Specifically, the islet cell types emerge from a subset of these progenitors that express the transcription factor neurogenin 3 (Ngn3). Going on with the differentiation process, beta cells eventually express high levels of Pdx-1, Nkx6.1, Nkx2.2 and Pax6 transcription factors[52,54]. The fate of the endocrine progenitors cells is also driven by other factors such as nutrients, hormones and growth factors[47]. Therefore, neogenesis is the predominant form of beta cell formation through the embryonic development.

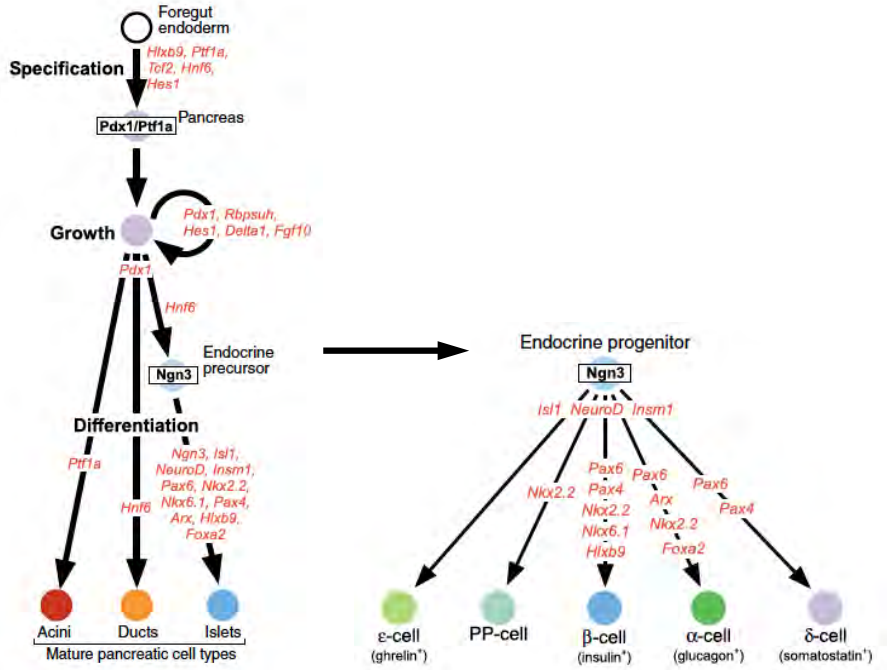

Figure 1.9. Schematic view of pancreatic progenitors' differentiation toward different lineages. The different pancreatic phenotypes originate from endoderm progenitors, which give rise to acini, ductal and endocrine progenitors. These endocrine progenitors then differentiate into the four endocrine islet cells (α-, β-, δ-, PP- and ε- cells). Adapted from Murtaugh[54].

Neonatal growth

During late gestation and neonatal development, there is a massive increase in beta cell mass, being replication the dominant pathway[57–60]. This replication rate is considerably higher during this period than after weaning[59]. Specifically, the perinatal period is when this replication rate is higher and declines steadily over the first month of life in rodents[58]. In parallel to the enhanced replication rate, apoptosis, which is the programmed cell death indispensable for the normal cell turnover, experiences an increase rate during this period[58,60,61]. Other studies provide evidence that over the first month, neogenesis is also present in order to compensate for this lost beta cell mass[58,62–64]. Neogenesis during this stage would account for the 30% of the newly formed beta cell mass and proliferation for the 70% in rats according to Bonner-Weir group[65]. The most accepted model for neogenesis after birth is that in the epithelial ductal tissue exists a population of stem cells capable of giving rise to insulin-producing beta cells, since islet cells appear to be budding from the ducts[66]. However, several studies have questioned the formation of new beta cells from progenitor cells in the postnatal stage[55,67,68].

From childhood to adulthood

Even though after weaning beta cells replicative rate experiences a considerable decrease, it has been proved that beta cells maintain the proliferative capacity throughout life[49,52,69]. In rats, during the initial months of life, beta cell mass increases proportionally to body weight and besides from cell number, cell size also increase. Therefore, within the first months of life,

hyperplasia and hypertrophy contribute to the increment of the beta cell mass[49,66]. The replicative rate stabilizes after these months in adult rats and although being low, is able to maintain the beta cell mass[49,70]. In old rats, however, only cell size increases[49,66,69]. Conversely, beta cell apoptosis is low and stable from month 1 to 20 (old rats)[49]. Since in the postnatal stage the growth rate ranges from 2 to 3% per day and the apoptotic rate is approximately 0.5%, the lifespan of a rat beta cell has been estimated as approximately 58 days[49,52,69,71]. Thus, although adult beta cells divide very slowly, they maintain the proliferative capacity.

Dor *et al* showed by genetic linage tracing studies in mice, that progenitor cell differentiation drives beta cell growth mass in utero, while postnatal expansion takes place mainly through replication from pre-existing beta cells[72]. Authors labelled mouse adult beta cells and observed that 12 months after the pulse, no dilution of the labelled population took place despite the number of beta cells increased by 6.5-fold. Therefore, this result suggests that differentiated beta cells retain a proliferative capacity during adulthood, able to sustain the turnover and maintenance of beta cell homeostasis[72]. Nevertheless, this study does not exclude the presence of stem or progenitor cells that could play a role in the normal beta cell growth. In addition to the hypothesis of beta cell differentiation from stem/progenitor cells located in epithelial ducts, there are several works proposing other sources of new beta cells, such as the transdifferentiation of adult acinar cells to beta cells[73,74] or bone marrow cells[75]. As for the transdifferentiation from acinar to beta cells Solar *et al* reported with lineage tracing assays that ductal cells give rise to only ductal and not beta cells[67].

Most of the previous studies have been performed in rodents. In humans, on the other hand, the main drawback when investigating the contribution of existing beta cells or stem cells to the beta cell growth mass is the impossibility of performing lineage cell tracing experiments. Thus, this is carried out through immunohistochemistry and morphometric analysis. Nevertheless, it seems clear that rodents present a higher capacity for beta cell replication than humans[70]. Meier *et al* conducted these analyses in human pancreases from subjects of 2 weeks to 21 years old and the conclusions were the following:

- Beta cell mass expands by several folds from childhood to adulthood, being the highest increment in infancy (before 2 years old).
- The greatest growth in beta cell mass is characterized by increased numbers of beta cells per islets, instead of increased number of islets.
- Frequency of beta cell replication is parallel to the rate of increase in beta cell mass.
- The two previous statements support the evidence that replication from differentiated beta cells is the predominant mechanism for postnatal beta cell growth[76].

Regeneration of beta cells after injury

Regeneration of pancreatic tissue has been studied using two different models, partial pancreatectomy[77] and duct ligation[78], although there is some controversy around the duct ligation model. As expected, replication from pre-existing beta cells takes place after injury, however, there is strong evidence that neogenesis also occur. Yet, as in the case of normal

growth of the beta cell mass after birth, there is some controversy about the existence of this pathway upon tissue damage due to the lack of specifics markers of pancreatic progenitors and the contradictory results obtained in lineage-tracing experiments.

After partial pancreatectomy, regeneration is not as robust as in the case of the liver and there is not a complete recovery of the original pancreatic volume[52]. Nonetheless in both types of injury an important regeneration with new lobes containing islets has been obtained and besides replication from differentiated cells, part of it has been attributed to neogenesis from ductal epithelium tissue[77–82]. In more detail, Inada *et al* carried out lineage tracing studies in mice and proposed that adult ductal cells partially dedifferentiate after replication in order to generate new islet cells[82]. This hypothesis is based on the presence of several ductal genes in the newly formed beta cells after injury[78,83]. On the other hand, other studies using lineage cell tracing show that replication is the only mechanism by which regeneration is carried out[68,72,84].

A recent study, though, provided evidences for the existence of beta cells progenitors in the adult pancreas[85]. Xu *et al* proved that after partial duct ligation rapid proliferation occurs relying on the recruitment of islet progenitor cells[85]. This islet cell precursors would be a population of cells located in the epithelial ducts that express Ngn3, which is known to be a very specific marker for endocrine progenitors during embryogenesis[55]. However, the methodologies used to quantify the beta cell mass after duct ligation have been questioned. More recent studies using more innovative techniques have shown no detectable contribution to beta cells mass by neogenesis from duct-derived cells after duct ligation[86,87].

1.1.3 DIABETES MELLITUS: PATHOGENESIS AND CLASSIFICATION

1.1.3.1 Diabetes pathogenesis

According to the American Diabetes Association (ADA) and the World Health Organization (WHO), Diabetes Mellitus (DM) is a heterogeneous group of metabolic disorders characterized by chronic hyperglycemia with abnormalities of carbohydrate, fat and protein metabolism. The hyperglycemia is due to the development of several pathogenic processes, resulting from defects in insulin secretion and/or insulin action. Characteristic symptoms of marked hyperglycemia are polydipsia (excessive thirst), polyuria (excessive urination volume), and weight loss. In the most serious forms of uncontrolled diabetes, other life-threatening conditions can occur, as for instance ketoacidosis or the nonketotic hyperosmolar syndrome[1,88]. Ketoacidosis takes place when the body produces ketones using fat as an energy source, since there is no glucose available. Ketones make the blood's pH more acidic, which could lead to a diabetic coma or even death. Nonketotic hyperosmolar syndrome occurs when the body tries to get rid of the excess of blood sugar by passing it into the urine. Eventually, this could lead to severe dehydration being a cause of death. Nevertheless, in some other cases, diabetes presents no symptoms, with persistent hyperglycemia until diagnosis is made.

As mentioned previously, diabetic patients are more likely to suffer from long-term health problems than non-diabetic subjects. Specifically, chronic hyperglycemia can lead to the damage, dysfunction, and failure of different organs such as heart, blood vessels, eyes, kidneys and nervous system. Nonetheless, these complications can be prevented, or at least delayed, by maintaining blood glucose levels as normal as possible [1,2].

1.1.3.2 Classification of Diabetes Mellitus

Currently, the classification of diabetes entails different degrees of hyperglycemia depending on the disease process. Basically, there are three main types of diabetes: type 1 diabetes, type 2 diabetes and gestational diabetes. Figure 1.10 shows the different disorders of glycemia and the different stages of each type.

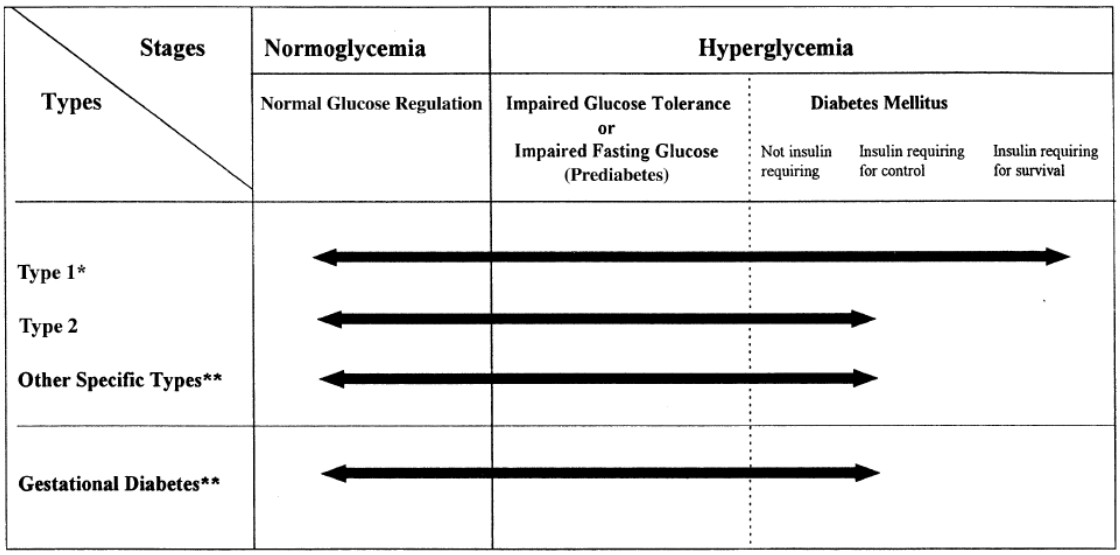

Figure 1.10. The different disorders of glycemia, stages and types. The current classification considers multiple degrees of hyperglycemia regardless of the disease process. Some diabetic patients can achieve a proper glycemic control with weight reduction, exercise and/or oral glucose-lowering drugs, avoiding the need for exogenous insulin. In contrast, when there is extensive beta cell damage and therefore no insulin secretion, exogenous insulin is required for survival. From ADA[88].

Type 1 diabetes

Although type 1 diabetes mellitus (T1DM) accounts only for the 5-10% of all DM cases[88], is one of the most common prevalent chronic disorders among children and adolescents, with a peak incidence in children aged 5-7 and/or 10-14 years[89]. About 50-60% of people with T1DM develop the disease before 16-18 years of age[88,90,91]. Nevertheless, the disease can appear at any age[92]. Nowadays, the incidence of this type of diabetes is increasing at a 2-5% annual rate worldwide[91].

T1DM is due to the autoimmune destruction of the pancreatic beta cells, resulting in an absolute deficiency of insulin[88,90,93]. In this type of diabetes daily exogenous insulin is required for survival in order to prevent ketoacidosis, which could lead to coma and eventually dead[1]. Therefore, T1DM patients are insulin dependent. Islets inflammation (insulitis) is one of the hallmarks of T1DM and is characterized by an infiltration limited to the pancreatic islets, consisting predominantly of T-cells ($CD8^+$ and $CD4^+$ cells), which deliver proinflammatory cytokines causing beta cell death[91,94]. Moreover, a B-cell response with production of different autoantibodies against beta cell antigens has also been found. However, the precipitating antigen causing the inflammatory response remains unknown[91,95,96].

T1DM is triggered by environmental factors in genetically predisposed individuals[97]. Genes located at the HLA-DQ locus on chromosome 6 account for 45% of the genetic susceptibility and the rest is due to non-HLA genetic polymorphisms[98,99]. Yet, only a small population with the mentioned genetic alterations develops eventually the disease[100]. Hence, other factors must trigger the disease on the genetically predisposed individuals. Some relevant variations affecting the onset of T1DM have been observed:

- Seasonal variations on the diagnosis of T1DM, such as a higher onset of the disease during the winter months, have been observed[101].
- Birth month has also shown to influence the likelihood of developing T1DM, with people being born in the spring having higher probabilities of suffering the disease[102].
- On the other side, there are also geographical variations affecting the incidence of T1DM, even within Caucasians, being Finland the country with a highest annual rate (54/100,000 children) whereas Macedonia has the lowest rate (3.2/100,000 children)[90,97,103].

Therefore, there are multiple evidences that environmental factors have a critical role on the development of T1DM[100,104]. Even though the environmental triggers have not been completely uncovered, a variety of them are under study:

- **Viruses:** so far, viruses are one of the major candidates as environmental risk factors. In particular, enteroviruses (EV) are the ones causing more human diseases. Several studies have shown a temporal relationship among the appearance of the first T1DM associated autoantibodies and EV infections, which could imply that EV infections constitute a risk factor for the development of beta cell autoimmunity[105,106]. Other types of viruses linked to T1DM are rotavirus, cytomegalovirus, rubella, retroviruses, etc. Moreover, it has been observed that viral structures and beta cell antigens present structural homology[100].
- **Dietary factors:** children and young adults diet factors seem to influence the onset and progression of T1DM. Some studies report that short breastfeeding may influence the appearance of beta cell autoimmunity[107,108]. It has already been proven that breastfeeding protects against EV infections, therefore it seems plausible that breastfeeding lowers the possibility of an enterovirus-mediated beta cell autoimmunity[109,110]. Other studies have shown an association between the early

introduction of cow milk proteins in the diet and a higher risk of beta cell autoimmunity[107,108,111,112]. In fact, several authors have found increased concentrations of antibodies against cow milk proteins in children that have been recently diagnosed with T1DM[113–115]. In the same way, other studies have proven that the early introduction of cereals is related to the autoimmunity present in T1DM[116,117]. Finally, the lack of vitamin D is also thought to contribute to beta cell autoimmunity. The EURODIAB study of 1999 pointed out that vitamin D supplementation decreased the risk of having T1DM[118]. Nonetheless, further research in this field is needed since many of the studies remain controversial.

- **Gut microbiota:** this area of research has gained importance during the last years since there seems to be a strong interplay between T1DM and a variety of aberrant intestinal microbiota, alterations of the intestinal permeability and altered mucosal immunity[119]. A recent study has shown that gut microbiota in children with T1DM differ significantly from that of healthy children[120]. Moreover, different genera of bacteria were present in lower amounts in T1DM children compare to the healthy children. The authors claim that these differences could be responsible for the increased gut permeability found in T1DM patients, which facilitates the absorption of antigens that could damage beta cell[121–123].

The degree of long-term glycemic control in T1DM patients is closely related to the onset or progression of microvascular (retinopathy, nephropathy and neuropathy) and macrovascular (cardiovascular, cerebrovascular and peripheral vascular disease) complications. Besides these long-term complications, another complication related to limitations of the disease treatment are hypoglycemic (low blood sugar) episodes, which are a considerable obstacle to the achievement of glycemic control with the present treatment approaches[91]. Currently, most T1DM patients are treated with multiple daily injections (MDI) of insulin combined with a tailored diet. Novel insulin formulations, subcutaneous insulin pumps and continuous glucose monitoring systems have improved glycemic control giving as a result a lower rate of diabetes associated complications[91,124].

Type 2 diabetes

Type 2 diabetes (T2DM) is the predominant form of diabetes, comprising approximately 90% of DM cases[1]. Nowadays, this form of diabetes is having a major raise in developing countries, mainly China and India, rather than in developed countries, since in the latter the prevalence is already high[125]. This increase is closely related to changes in lifestyle in developing countries, such as the introduction of high-energy diets and decreased physical activity[126]. In developed countries the majority of people having T2DM are older than 60 years, meanwhile in developing countries 40-60 years[3,127]. Another major concern is the increasing incidence of T2DM in children, teenagers and adolescents[93].

T2DM is a heterogeneous metabolic disorder developed when the inadequate beta cell

function and low beta cell mass cannot fulfil the increased insulin demands caused by the insulin resistance[128]. The epidemic of T2DM results basically from the epidemic of obesity and physical inactivity[4]. Insulin resistance state is defined as a decreased response of the peripheral tissues to insulin action[129]. In obese people, several factors contribute to the development of insulin resistance, such as the release of increased amounts of non-esterified fatty acids, glycerol, hormones and proinflammatory cytokines by the adipose tissue[130]. Specifically, in muscle, insulin resistance causes reduced glucose uptake and storage as glycogen in the liver, an increased hepatic glucose production, and finally in adipose tissue, an increased free fatty acid mobilization[131,132]. It has been seen that more than 60-90% of T2DM patients are obese[133], which could imply that obesity is the main cause of insulin resistance in T2DM patients. Thus, obesity is a major risk factor for developing the disease.

Nevertheless, most obese insulin-resistant people do not develop the disease[134]. In non-diabetic obese individuals, pancreatic islet beta cells try to overcome the impaired insulin action by increasing the beta cell mass and thereby increasing their insulin secretion and maintaining glucose tolerance within normal levels[130,135]. But in some cases, when beta cells are put under a major stress in order to compensate for the increased insulin demand, this beta cell adaptation fails. As a consequence, plasma glucose levels increase giving place to the onset of T2DM[136]. Therefore, even though insulin resistant individuals are predisposed to progress to T2DM, a beta cell dysfunction must exist in order to develop the disease.

Pancreatic beta cell dysfunction in T2DM patients can be caused by a deficit in beta cells, an increased beta cell apoptosis along with a diminished regeneration, beta cell exhaustion due to the long-term insulin resistance, lipid toxicity and amyloid deposition in pancreatic islets among others[137]. Nowadays, it seems clear that some kind of defect in beta cell function exist in all T2DM patients, even before the disease is diagnosed[138]. According to the UK Prospective Diabetes Study (UKPDS) study, in T2DM patients, beta cell function was decreased about 50% at the time of diagnosis[139].

As for the beta cell mass, it has been reported to be reduced in T2DM individuals[4]. A recent study performed with European subjects, has shown a 35% reduction on average in beta cell mass[140]. The loss of beta cell mass has been attributed mainly to a higher beta cell death because of apoptosis[128,141]. Nonetheless, due to the highly heterogeneity of the disease and the difficulty of measuring the amount of beta cells *in vivo*, it is not completely clear whether the reduction in beta cell mass in T2DM individuals is due to a deficiency of beta cells early in life, a failure when increasing the beta cell mass in response to a reduced insulin sensitivity or because of a progressive loss of beta cells due mainly to apoptosis[142].

T2DM has a strong genetic component, with an estimated heritability higher than 50%[127]. Despite the highly heritability component of the insulin resistance condition[143], and the fact that the vast majority of T2DM patients present some degree of insulin resistance[132], there is no genetic evidence that the disease is caused exclusively by this condition[144]. Interestingly, the genome-wide association studies showed that the majority of the genetic loci associated to T2DM play a key role in beta cell function rather than insulin resistance or obesity[145]. Some

of these genes regulate cell cycle, which implies that the burst in beta cell replication that takes place during the postnatal period could be affected[137].

As in the case of T1DM, T2DM disorder is also influenced by environmental factors. Firstly, high-fat and high-energy diets, and a sedentary lifestyle are closely related to insulin resistance[146]. In particular, weight loss in obese T2DM patients has normalized insulin sensitivity[147]. Another environmental factor that is thought to play a role takes place in the utero when poor nutrition change the metabolism, favoring the storage of nutrients[148]. On the other hand, gut microbiota is considered a new environmental factor that regulates fat storage[149], and it has been found to be different in T2DM subjects[150].

Most T2DM patients do not require insulin treatment to survive. The current treatments are based on drugs known as insulin sensitizers, which treat the insulin resistance problems. Yet, there is a need to develop treatments focused on the preservation of beta cell function, since it is the main pathogenic abnormality in T2DM[151].

Gestational diabetes

Gestational diabetes mellitus (GDM) is defined as glucose intolerance with onset or first recognition during pregnancy [88].

During the latter half of pregnancy, the levels of insulin resistance experience a progressive increment, reaching levels similar to those of T2DM[152,153]. The insulin resistance condition in pregnant women could result from a combination of increased maternal adiposity and the insulin-desensitizing effect of hormones coming from the placenta[152]. Thereby, to maintain glucose homeostasis during pregnancy, the beta cells of the mother increase their insulin secretion, in order to compensate for the insulin resistance and meet the body's requirements[154,155]. Pregnant women with GDM are unable to increase insulin production to match the increased insulin needs occurring in late pregnancy[152,154], which is thought to occur due to a chronic beta cell dysfunction[156].

1.1.4 T1DM CELL REPLACEMENT THERAPY

As mentioned previously, T1DM treatment consists of daily insulin injections. Nevertheless, administration of exogenous insulin fails to mimic the physiological activity of the islet, which results in chronic hyperglycemia and the development of long-term complications. Moreover, a side effect of the intensive insulin therapy are the hypoglycemic events, which can lead to confusion, loss of consciousness, seizures and even death[157]. Nowadays, hypoglycemia is still a limiting factor in the glycemic management for T1DM patients. Recurrent hypoglycemic episodes impair the counter-regulatory responses and hypoglycemia awareness. In particular, 30-40% of T1DM patients suffer from impaired hypoglycemic awareness, which confers a 3 to 6-fold increased risk of severe hypoglycemic episodes[158].

Replacement of the lost beta cell mass is a promising option for T1DM patients that aims to achieve strictly normal glucose levels. This replacement can be achieved by whole pancreas transplantation or by pancreatic islet transplantation from cadaveric organ donors.

1.1.4.1 Pancreatic islet transplantation

Whole pancreas transplantation was first performed in 1966 and nowadays it is accepted as an alternative therapy for diabetic patients, usually in the context of simultaneous kidney transplant performed because of end stage chronic kidney disease in diabetic nephropathy [159]. Nevertheless, whole organ transplantation is a major surgical procedure, which implies significant risks[160]. Conversely, compared to whole organ, islet transplantation (IT) is a simpler procedure with minimal invasion and low morbidity, and also less costly[159]. In 1972, Ballinger and Lacy were able to reverse chemical-induced diabetes in rats with IT[161], and by the 1980s the first successful islet autograft was reported in humans.

Currently, IT is a procedure reserved for T1DM patients with repeated episodes of severe hypoglycemia or severe metabolic instability [162]. As mentioned previously, the achievement of an acceptable glycemic control is crucial in order to prevent or delay long-term complications associated to diabetes.

After pancreas procurement from a cadaveric organ donor and prior to transplantation, islets must be isolated. To that purpose, exocrine tissue of the pancreas is digested with collagenase via ductal perfusion. Afterwards, the pancreas is placed on a digestion chamber and islets are separated from the exocrine tissue by enzymatic and mechanic digestion. Finally, islets are purified using density gradient centrifugation[163] and cultured for 2 days in order to allow cell recovery from the isolation process[164] (Figure 1.11). Although it depends on the transplantation center expertise and the number of islets in the donor, in the best-case scenario, an estimated 300,000 – 600,000 islets equivalents (IEQ) are obtained from one single pancreas (one IEQ is considered to be equivalent to an islet with a diameter of 150 μm)[165]. Considering that a minimum of 10,000 IEQs/Kg are needed to achieve insulin independence[166], usually more than one donor is required to obtain the needed number of islets to treat a single patient. This is due to the loss of more than 50% of the islet mass during the isolation process[167].

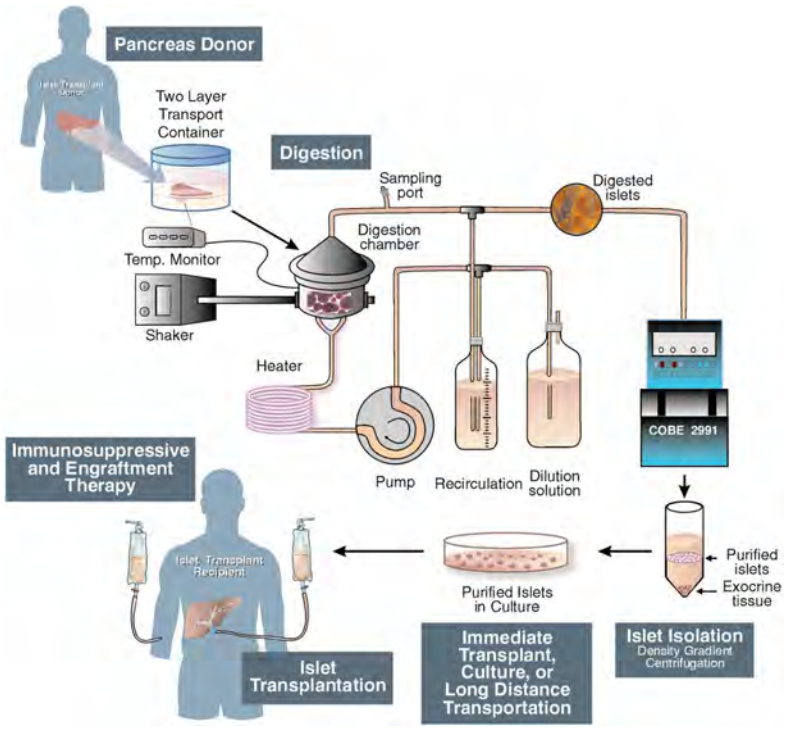

Figure 1.11. Pancreatic islets isolation process. After pancreas procurement from cadaveric organ donors, the exocrine tissue is digested with collagenase enzyme. Subsequently, density gradient centrifugation is carried out in order to isolate pancreatic islets. Finally, islets are cultured for two days before transplantation to the recipient. From Merani and Shapiro[166].

After isolation, islets are ready to be transplanted. To that end, islets are infused via a catheter into the portal vein of the liver with ultrasound guidance. Once infused, the islets are transported by the bloodstream into the peripheral branches of the portal vein, where they lodge and start releasing insulin[162,168]. This minimally invasive procedure is performed under local anesthesia and sedation and lasts approximately 1 hour[167]. Figure 1.12 illustrates the IT process.

In the past century, the success of IT was rather limited. Specifically, only a 10% of transplanted patients showed insulin independence after 1 year[169]. Multifactorial mechanisms such as immune reaction, cell stress and the limited ability of the islet cells to respond to the generated stress were the main hurdles of IT. Immunosuppressive agents induce insulin resistance and cause beta cell dysfunction and probably apoptosis[170]. In 2000, Shapiro and colleagues obtained remarkable results in seven T1DM patients using a steroid-free protocol and islets from more than 1 donor with an approximate number of approximately 850,000 IEQ (Edmonton protocol)[170]. This protocol introduced other improvements such as the limitation of prolonged cold ischemia, avoidance of culture and the elimination of exposure to xenoproteins. One year after transplantation, all transplanted patients were insulin independent and no severe hypoglycemic episodes were observed[170]. Nevertheless, long-term follow-up from Shapiro and other groups who also used the Edmonton protocol showed that the insulin independence rate was declining over time, being approximately 70% after 1 year

post-transplant, 50% at two years, 30% at 3 years and 10% at 5 years[4,171–175]. Yet, these patients experienced 50-60% reduction in insulin requirement. A more encouraging clinical trial showed that after 3 years post-transplant, 8 out of 14 transplanted patients (57%) still remained insulin independent[176]. More recently, Bellin *et al* reported even better results with rates of insulin independence of 74% one year after transplantation, 50% at 3 years and 50% at 5 years. Moreover, severe hypoglycemic episodes were absent in 80% of the transplanted patients at 1-3 years after transplantation[177]. As for the long-term diabetic complications, results are favorable, with a reduced progression or stabilization of retinopathy, improvement of neuropathy, reduced nerve dysfunction and improved cardiovascular function[167].

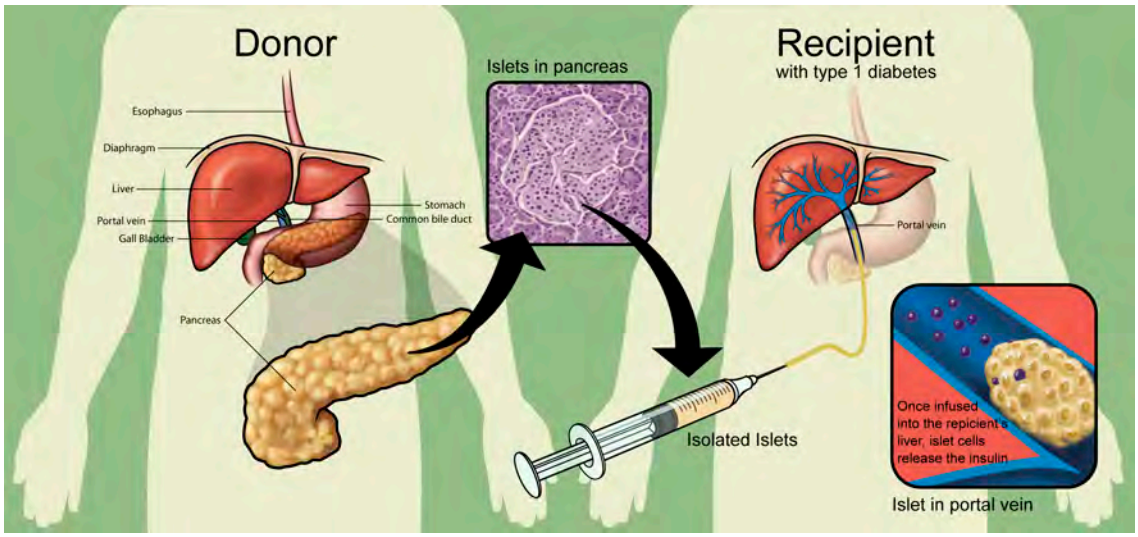

Figure 1.12. Pancreatic islets transplantation procedure. Upon islets isolation, transplantation is performed via infusion to the portal vein of the liver. Once infused, the islets are transported by the blood flow into the liver where they embolize in the smaller branches of the portal vein and start releasing the amount of insulin needed to maintain blood glucose homeostasis. Adapted from Naftanel and Harlan[168].

Despite the continuous improvements, IT is still an experimental procedure that needs to overcome many obstacles. The main hurdle is the limited supply of islets available for transplantation, basically due to the shortage of organs donors. Several factors contribute to the outcome of IT, for instance the long-term requirement of immunosuppressive agents, complications related to the transplant process, the recurrence of auto-immunity, etc. Many of the immunosuppressive agents used to avoid rejection present antiproliferative and antiangiogenic effects, that could decreased beta cell viability, regeneration, engraftment and vascularization[167]. On the other hand, pancreatic islets are extremely vulnerable during the first days after transplantation[178]. Approximately, 50-70% of the islets are destroyed due to an inflammatory reaction developed during islet infusion or to stress-induced apoptosis[166,179,180]. Another impediment that needs to be overcome is the poor oxygen concentration found in the peripheral portal veins, which induces chronic hypoxia and premature apoptosis[166]. Thus, alternative implantation sites for IT are being explored[181].

In conclusion, IT is a promising cell therapy that can reduce glycemic variability, eliminate severe hypoglycemia, reestablish hypoglycemia awareness and allow insulin independence by restoring endogenous insulin secretion in T1DM patients[177]. Moreover, compared to whole organ transplantation, IT is less costly and presents less clinical complications. Yet, some important limitations need to be addressed, in particular the shortage of organ donors.

1.1.5 TISSUE ENGINEERING

As in the case of T1DM, a large number of diseases result in the loss or failure of an organ or tissue. Although transplantation is very successful, the demand for organ donors and tissues drastically exceeds the supply. Hence, it is necessary to develop new strategies in order to provide the needed tissue. From this need emerged the field of tissue engineering (TE)[182]. Defined two decades ago by Langer and Vacanti as an interdisciplinary field that applies the principles of engineering and the life sciences, toward the development of biological substitutes that restore, maintain or improve the function of human damaged tissue[183]. Since then, TE field has evolved in a very rapid manner, with the discovery of new sources of cells, materials and technologies.

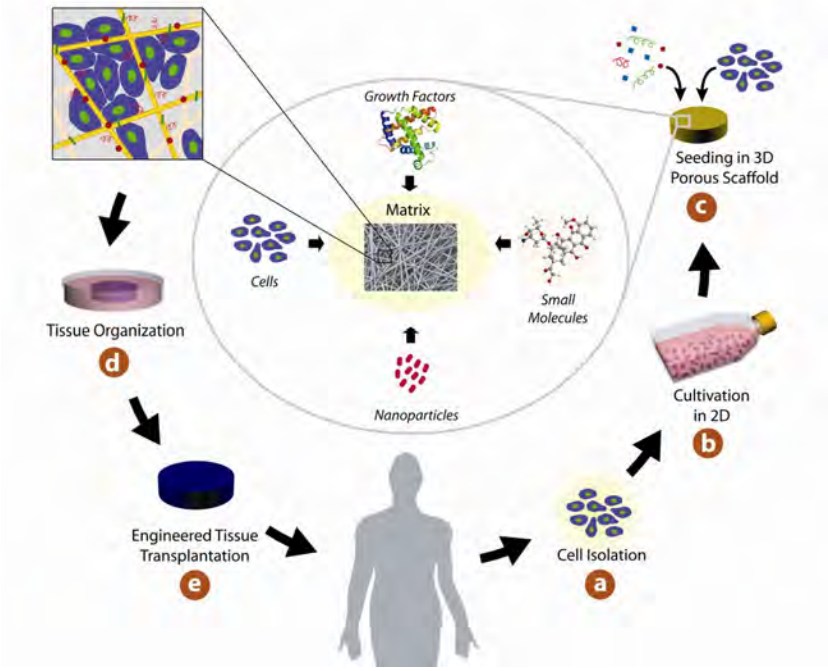

Figure 1.13. Example of a tissue engineering concept. (A) Cells are isolated from the patient and (B) are cultivated *in* vitro in two-dimensional surfaces for efficient expansion. (C) Next, cells are seeded in scaffolds, which serve as mechanical support, (D) and provide a 3D microenvironment to facilitate cellular organization into a functioning tissue, a tissue-like construct. (E) Once a functioning tissue has been successfully engineered, the construct is transplanted on the defect to restore function. From Dvir *et al*[185].

The concept of TE is based on the creation of functional 3D substitutes using cells combined with scaffolds or devices that facilitate cell growth, organization and differentiation[184]. A second application of tissue engineering is the development of *in vitro* 3D models based on human cells[184], in order to test new clinical therapies and drugs or to study human physiology.

1.1.5.1 The extracellular matrix milieu

The basic premise of TE is to combine the appropriate cells with a material under conditions that lead to tissue formation[186]. To that purpose, scaffolds engineered with ECM-like biomaterials are used to mimic the 3D architecture and functions of the *in vivo* tissues[187].

There are two main types of macromolecules conforming the ECM, fibrous proteins and proteoglycans. Fibrous proteins include collagen, elastin, fibronectin and laminin. Collagen is the major component of the ECM and is responsible for providing strength to the matrix, and elastin gives elasticity to the matrix. Fibronectin and laminin contribute to organize the matrix and mediate the cellular attachment to it. These proteins present specific binding sites for other matrix macromolecules, such as proteoglycans and collagen fibers, and for adhesion receptors on the cell surface, which are mainly integrins.

The second class of ECM macromolecules, proteoglycans, consists of a protein backbone with covalently attached highly anionic glycosaminoglycans (GAGs). These molecules are the polysaccharide components of the ECM and, in fact, all of them except for hyaluronic acid, are linked to a protein making-up the proteoglycans. The functions of these macromolecules derive from the physicochemical characteristics of their strongly hydrophilic glycosaminoglycan components with the capacity of developing hydrated gels. These structures provide hydration and swelling pressure to the tissue, enabling it to withstand compressional forces, therefore providing mechanical support to the tissue. Moreover, these gel-like structures present variable pore size and charge density, which regulate the traffic of soluble biomolecules according to their size, charge or both of them, modulating their signaling activity. These soluble biomolecules, which include growth factors, cytokines and enzymes are also a component of the ECM[188].

The organization and distribution of the ECM molecules confers a unique and specialized architecture and function to every specific tissue. For instance, mesenchymal cells are surrounded by an interstitial matrix that provides specific biomechanical properties to the connective tissue[189]. On the other hand, the basal surface of epithelial and endothelial cells is in contact with an specialized type of ECM, the basement membrane (BM), which confers specific mechanical strength and physiology to the epithelia (Figure 1.14)[190].

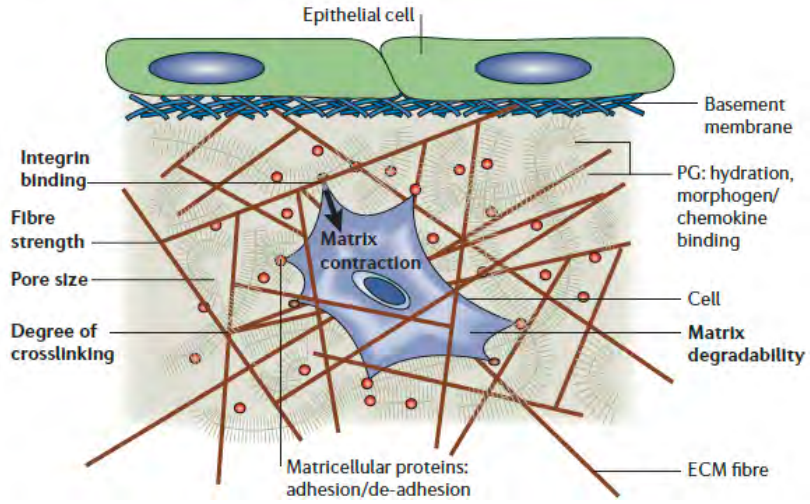

Figure 1.14. Schematic representation of the extracellular matrix. Mesenchymal cells are surrounded by ECM proteins whereas epithelial cells are in contact with a thin layer of extracellular matrix, the basement membrane.

Besides the fundamental scaffolding functions that the ECM provides to the cells, serving as a substrate for cell anchorage, the ECM is also responsible for transmitting environmental signals to the cells. Therefore the cellular crosstalk with the surrounding ECM modulates crucial aspects of cell life, such as cell adhesion, migration, proliferation, differentiation and apoptosis[191]. ECM molecules interact with receptors on the cell surface, which are responsible for the transmission of signals across the cell membrane to the cytoplasm. Integrins are the most important group of cell surface receptors that mediate cell adhesion to the ECM proteins[192]. Thanks to the cell-matrix adhesion, cells are able to respond to the mechanical and biochemical changes of the ECM through the crosstalk between integrins and the actin cytoskeleton[193] (Figure 1.15). Integrin receptors are glycoproteins composed of α and β transmembrane heterodimers, 18 α subunits and 8 β subunits, that associate non-covalently into 24 α/β distinct combinations[193,194]. Precisely, this α/β combination is what dictates specificity for ligands. For instance, α2β1 binds to selected collagen family members, α5β1 binds to fibronectin, and αvβ3 binds to a number of ligands including fibronectin, vitronectin and fibrinogen[195].

Each heterodimer is composed of a large extracellular domain, a transmembrane domain and a generally short intracellular cytoplasmic tail domain[192]. Therefore, one side of the integrin faces the extracellular space interacting with specific ligands present on the ECM molecules (also known as cues), as for instance the RGD signaling motif, whereas the other side faces the interior of the cell[194]. The cytoplasmic domain connects with the tensile members of the cytoskeleton (actin filaments) through adaptor proteins, such as talin, vinculin, paxillin or α-actinin for instance, forming adhesion complexes known as focal adhesions (FAs)[192]. Ligand binding to integrins cause integrin clustering which transmit adhesive and traction forces that activate a cascade of intracellular signaling pathways (outside-in signaling), leading to changes

in gene expression and affecting most aspects of cell behavior. On the other hand, intracellular signals induce changes in integrin conformation and activation altering their ligand-binding activity, which is known as inside-out signaling. Through these interactions, integrin receptors provide a bi-directional signaling across the cell membrane connecting the intracellular and the extracellular compartments[196].

The composition, architecture and the degree of crosslinking of the ECM dictate its mechanical properties and control how mechanical forces are transmitted to cells[184]. On the other hand, the dynamic assembly and disassembly of adhesion structures applies different levels of force to the matrix that, in turn, regulates and varies matrix rigidity and composition[196]. Cells respond through changes in the distribution of cell surface integrin receptors and cytoskeleton organization, regardless of whether the resistance derives from normal tissue matrix, synthetic substrate or even an adjacent cell[197]. Therefore, ECM stiffness can regulate integrin adhesion and, as a consequence, tissue phenotype, playing a key role in multiple cellular functions such as differentiation, organization, morphology, migration and cell survival[198].

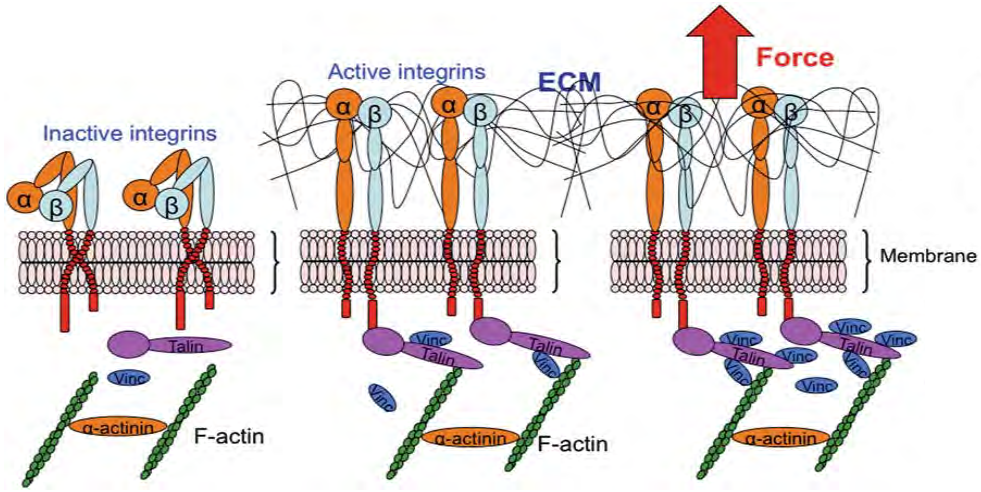

Figure 1.15. Example of cell-matrix adhesion mediated through integrin receptors. The extracellular domain of integrins binds to the ECM, whereas the intracellular domain binds to different cytoplasmic proteins in order to control adhesion-dependent processes. Therefore, integrins provide a bi-directional communication between the extracellular and the intracellular compartments. Adapted from Khalili *et al*[199].

1.1.5.2 Pancreatic tissue engineering

Beta cell replacement therapies have been proposed as a curative treatment for diabetes and IT has provided proof of concept that cell therapy may achieve insulin-independence and restore normoglycemia in T1DM patients[200]. The improvements and subsequent success of the Edmonton protocol for pancreatic IT were based on two main modifications, the increase in the number of transplanted islets and the use of more benign steroid-free

immunosuppressants. However, the widespread application of IT is hampered by the severely shortfall of available human islets and the need for long-life immunosuppression, that entails serious side effects for the patients and the transplanted islets. Hence, pancreatic endocrine tissue engineering (PTE) aims to overcome these limitations using alternative cell sources, and reducing or even eliminating the need for the immunosuppressive regimen needed for the survival of the graft[201].

Moreover, there is another hurdle associated with islet isolation that influences islets engraftment. During pancreatic islet isolation, islet cells are exposed to a variety of cellular stresses. Among them, the disruption of cell-ECM relationships, internal vascularization and innervation[202]. As a result, there is an islet cell death over time[203–205]. Several works have demonstrated that re-establishment of cell-ECM relationships is crucial to maintain beta cell function and survival over time, which may increase the long-term success of islet transplantation[204,206–212]. Therefore, TE strategies aim to restore the islet microenvironment, enhancing the efficacy of cell-based therapies for T1DM[213]. The optimal 3D scaffold for supporting islet function should be designed to improve islet survival, glucose responsiveness and maintenance of differentiation[214].

Thus, an initial approach of PTE is the combination of islet cells or another type of cells with the most appropriate biomaterial to either maintain their function after transplantation in the case of islet cells, or induce the differentiation towards an insulin-producing phenotype when other sources of cells are used with transplantation purposes. The most common practice in PTE is the generation of encapsulation systems to transplant the insulin-producing cells within a semipermeable barrier to address the problem of the immune response. According to their origin, cells can be allo- or xenogeneic (porcine islets for instance), or autologous cells. A second approach is based on the development of pancreatic *in vitro* 3D models to closely mimic the *in vivo* microenvironment. These models provide a valuable tool to better understand the behavior of islets or beta cell surrogates, as compared to traditional monolayer cultures.

1.1.5.3 Alternatives sources of insulin-producing cells

As mentioned previously, the scarcity of pancreatic islets from cadaveric organ donors is one of the major limitations to the widespread practice of IT. The limited availability of donor islet tissue could be overcome by the development of new strategies to generate an abundant source of insulin-producing cells. Several alternative forms to generate insulin-producing cells are being explored and are discussed below[48,215,216].

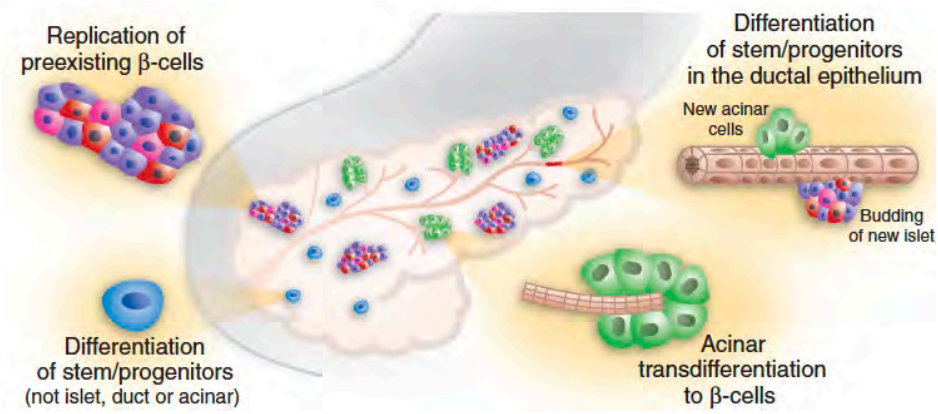

Figure 1.16. Representation of distinct methodological approaches to generate new beta cells for diabetes therapy. The pancreas is one of the main sources of new insulin-producing cells. The different processes have been proposed including the replication of pre-existing beta cells, differentiation of progenitors within the ductal epithelium, transdifferentiation of acinar cells and differentiation of pancreatic stem/progenitor cells that are not of beta, ductal or acinar origin. Non-pancreatic sources include liver cells and pluripotent stem cells (not shown in the figure). From Bonner-Weir and Weir[215].

Generation of beta cell lines

Given the explained difficulties of pancreatic isolation and expansion, different researchers have developed continuous beta cell lines, which has implied a significant progress in understanding beta cell biology[200]. These cells are either tumoral cells or cells that have been immortalized by genetic manipulation. Many rodent tumor cell lines have been established from primary cultures of insulinomas developed in transgenic rodent models and showing glucose-responsive secretion of endogenous insulin. On the other hand, human beta cell lines are way more difficult to establish due to the dedifferentiation process when expanded. Nevertheless, in 2005 a human beta cell line that appears to be equivalent in function to primary beta cells was established[217]. However, most of the human beta cell lines present an unstable phenotype. Some of the most commonly used rodent beta cell lines are MIN-6 (mice), INS-1 and INS-1E (rat), RINm5F (rat), etc.

In vitro expansion of existing beta cells

Beta cell expansion seems the most rational approach for obtaining abundant insulin-producing beta cells to be used in transplantation[218,219]. *In vivo,* human beta cells present replicative capacity, although at a very low rate. *In vitro* conditions, in particular suspension cultures, allow the preservation of insulin expression and glucose responsiveness in human islets. Nevertheless, islet cells do not replicate under these conditions[147]. On the other hand, when islet cells are allowed to attach to the Petri dish surface, although a massive proliferation is achieved, beta cells dedifferentiate losing the phenotype and therefore insulin expression[219–221]. Lineage tracing studies demonstrated that human beta cells cultured *in vitro* undergo an

epithelial to mesenchymal transition (EMT), which implies the loss of the beta cell phenotype[222]. The aim of this approach is to culture and expand intact islets or isolated beta cells to obtain a large amount of islet-derived cells and achieve the subsequent redifferentiation towards a beta cell phenotype[218].

Further analysis of this approach will be carried out in Chapter 4 as the main motivation of the present thesis. Results obtained using this strategy will be also presented.

Transdifferentiation from adult somatic cells (acinar and liver cells)

Acinar cells are a byproduct obtained in the isolation of pancreatic islets. Thus, it makes sense to use these cells as a possible source of beta cell surrogates. Acinar cells are the most abundant cell type in the adult pancreas and from the point of view of the embryonic development these cells are closely related to the endocrine cells[55]. Bowens *et al* proposed in 1998 this approach based on previous studies that confirmed the presence of intermediate forms of acinar and islet cells[223]. The isolation of acinar cells from the adult pancreas induces a dedifferentiation into progenitor-like cells[224]. In this particular moment, these cells can be treated with specific agents in order to induce the transdifferentiation to beta-like cells. Different groups have succeeded applying this approach in murine models using growth factors and small molecules. Baeyens *et a*l achieved diabetes reversal in 64% of the treated mice using growth factors[225]. Other authors have also obtained encouraging results by means of genetic manipulation. In 2008, Zhou *et al* carried out an *in* vivo study in mice reprogramming acinar cells into beta cell surrogates, using three pancreatic transcription factors (Ngn3, Pdx1, MafA)[226].

The pancreas and the liver have a common origin, the endoderm. Therefore, transdifferentiation from liver cells seems to be a logical strategy. Moreover, this would allow the use of liver cells from the same patient. Usually, the transdifferentiation is achieved by the introduction of key transcription factors in liver cells. For instance, the expression of the transcription factor Pdx-1 in adult human liver cells induced the transdifferentiation into insulin-producing cells[227].

Generation of beta cells from adult/stem ductal cells

Although the contribution of neogenesis to the regeneration of the beta cell mass still remains controversial, convincing data suggest the existence of stem or progenitor cells budding from the pancreatic ducts giving rise to new beta cells[59]. Many efforts have been dedicated to identify stem or progenitor cells in the adult pancreas. Suzuki *et al* managed to isolate pancreatic progenitor cells with flow cytometry from the adult mouse pancreas using cell surface markers[228]. These cells formed colonies *in vitro* and expressed acinar, ductal and islet, as well as neural markers. In another work, Peck *et al* obtained *in vitro*-grown islets from cultures of pancreatic stem cells from the adult mouse pancreas[229]. Recently, El-Gohary *et al* found pancreatic ductal structures residing within young mice and human islets. Further

lineage tracing experiments confirmed that pancreatic ductal cells can convert into new beta cells [230].

Other works have studied the potential of adult pancreatic ductal cells (PDCs) to convert into beta-like cells. For instance, Lee *et al* were able to isolate PDCs expressing solely ductal markers and through genetic conversion using the transcription factors Pdx1, MafA, Ngn3, and Pax6, obtained beta cell differentiation[231].

Generation of beta cells from pluripotent stem cells

Human pluripotent stem cells (hPSCs) have been the most widely investigated cells during the last decade as a source of insulin-producing cells. Undoubtedly, their unlimited proliferation and the high differentiation potential make them a very attractive option for beta cell replacement strategies[232]. Notwithstanding the promising potential of these cells, most of the beta cell surrogates generated from hPSCs lack many functional characteristics of mature beta cells[216]. Thanks to the previous studies on pancreatic development, several research teams have differentiated *in vitro* hPSCs into pancreatic endocrine precursor cells and pancreatic progenitor cells[233–235]. Despite producing insulin, these cells were not able to respond to glucose stimulation, requiring further *in vivo* maturation in rodents (3-4 months). However, this long *in vivo* maturation process is not well understood and uncertain to occur in humans. Recently, three groups have reported hopeful results with the *in vitro* differentiation of hPSCs into functional human beta cells without any genetic modification[236–238]. The main concern about these cells is their potential for teratoma formation once implanted into the recipient.

1.1.5.4 Pancreatic islet microenvironment

The islet microenvironment consists of a network of ECM, mesenchymal cells, nerves and blood vessels[239]. The islet composition, cell-cell contacts and contacts with the surrounding tissues and environmental cues determine glucose responsiveness and insulin secretion. As in many other tissues, ECM is one of the main components of the islet microenvironment, and as shown in many works plays a key role in islet survival [204,209,210,240–242], proliferation[240,243,244] and insulin secretion[204,207,210,211,240,242,245–248]. A deep knowledge of islets ECM composition and architecture is needed in order to design the most suitable 3D scaffolds with ECM-like biomaterials. It must be taken into account that islets ECM composition experiments a continuous remodeling from embryonic development until the adult stage.

The ECM of adult human pancreatic islets is formed by a continuous peri-islet BM that surrounds the entire islet and co-invaginates into the islet tissue together with blood vessels[249]. Moreover, islets blood vessels form their own BM, where endothelial cells attach and migrate[250,251]. This form of BM is known as the vascular BM, which is believed to be in close contact with nearly each beta cell. The intraislet endothelial cells and their BM are crucial for islet revascularization, survival and function after transplantation[24,252]. Furthermore, the

vascular BM binds and releases growth factors required for revascularization and maintenance of the islet phenotype, such as the vascular endothelial growth factor-A (VEGF-A)[253]. Hence, in contrast to rodents, blood vessels in human islets are surrounded by a unique double BM, one probably derived from the endothelial cells and the other coming from the epithelial islets cells (Figure 1.17).

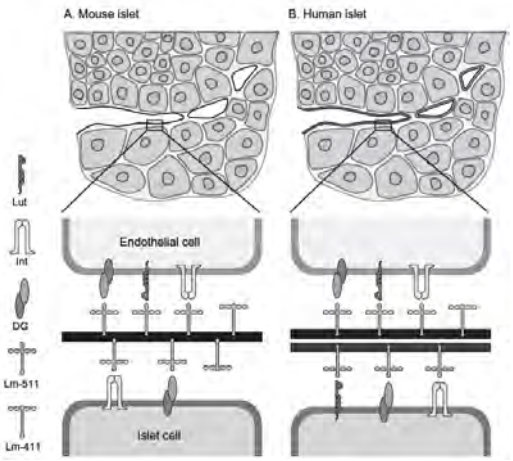

Figure 1.17. Schematic representation of the main differences between mouse and human islets basements membranes (BM). The main difference is the presence of a double BM surrounding the blood vessels on human islets, whereas mouse islets present only one endothelial BM. From Otonkoski[249].

The main structural components of the peri-islet and the vascular BM are laminin (LM)[252], and collagen IV[245,252]. Nonetheless, other ECM proteins such as fibronectin (FN), nidogen (NID), vitronectin (VN) and other types of collagens are also present[14], in addition to heparan sulfate proteoglycans (HSPG), such as perlecan and syndecan[214] (Figure 1.18). A more detailed description of the most abundant islet-ECM components and its interactions with integrin cell receptors is detailed below.

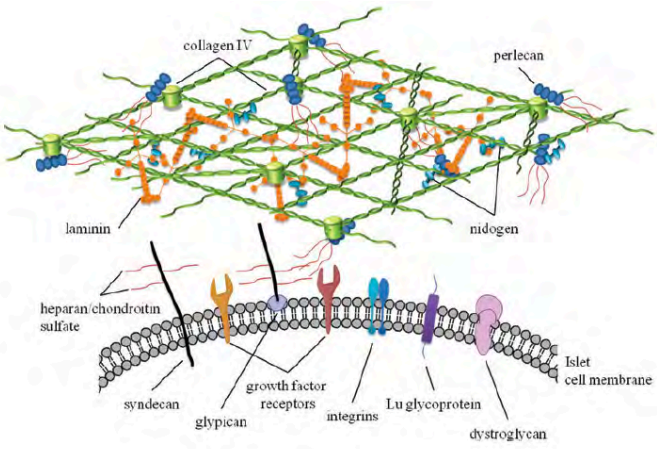

Figure 1.18. Schematic representation of islet matrix components. The pancreatic ECM consists of laminin, collagen IV, fibronectin, perlecan and other components[214].

Collagen: The great tensile strength of collagen fibers provides structural support to the cells. Different types of collagen have been found in the islet ECM, Coll-I, II, III, IV and VI, being Coll-IV the most abundant type[204,254]. Despite being the collagen form most frequently found in islets ECM, its role remains unclear. While Coll-IV proved to be more efficient than Coll I promoting the survival of intact islets[255], another work showed that Coll-IV decreased insulin production and secretion in purified beta cells[211]. The main integrin binding Coll-IV is α1β1[14]. Although the β1 integrin chain has been found to be expressed by islet cells, the presence of α1 chain remains controversial[204,245]. Kaido *et al* showed that integrin α1β1 allowed human fetal beta cells to attach, migrate and secrete insulin when adhered to Coll-IV (Kaido 2004), meanwhile Wang *et al* were not able to find α1 integrin in hamster, canine, porcine and human pancreas[256]. Therefore, the lack of clear Coll-IV binding integrin pathways suggests that islet cells have a low level of interaction with Col-IV despite the abundance of this protein and their close proximity[14]. Probably, non-integrin receptors of Coll-IV play a more important role in islets physiology[214].

Laminin: Together with Coll-IV, laminins are the most abundant structural proteins of the islet ECM. Coll-IV and laminins form polymer networks bound together by nidogen and perlecan[214]. 12 isoforms of laminin have been identified so far. Among other, LM-411 and 511, are present at the double BM of human islets and are thought to play an important role in beta cell proliferation and insulin transcription[251,252]. Laminin interaction with cells is given by integrin and non-integrin receptors. We will focus on integrin receptors, which are the following, β1 subfamily (α1β1, α2β1, α3β1, α6β1, α7β1, and α9β1), αv subfamily (αvβ3, αvβ5, and αvβ8), and the α6β4 integrin. To date, α3, β1 and α6 integrins have been shown to be expressed in islet BM[251,257]. Furthermore, many laminin isoforms contain the RGD sequence (Arg-Gly-Asp), although their activity it is under debate[14].

Fibronectin: Fibronectins are high molecular weight glycoproteins commonly present in the ECM of many cell types. The interactions between fibronectin and integrin cell receptors are one of the most well-characterized cell-matrix interactions[14]. Cells adhere to fibronectin through the recognition of the RGD motif. This signaling domain is recognized by a variety of integrins, including α3β1, α4β1, α5β1, α4β7, α8β1, αvβ1, αvβ3, αvβ5, αvβ6, and αIIbβ3[258]. Fibronectin has been localized in the adult islet periphery, islet ductal pole and perivascular areas, being often associated with collagens and laminin[214]. The majority of integrins expressed in adult human islets recognize the RGD motif. Specifically, integrin subunits α3 and α5 have been co-localized with fibronectin in the developing pancreatic tissue[204,259]. Moreover, RGD-dependent adhesions have been shown to inhibit apoptosis in mature human islets[255].

In short, the integrin receptor composition of human islets is complex and still remains controversial. Nevertheless, up to date there are several studies reporting the presence of α3, α5, αv, β1, β3 and β5 integrins in adult human islets[14]. Interestingly, despite the abundance of Collagen IV in both forms of islets BM, receptor compositions of beta cells suggest that the vast majority of their binding interactions are with Laminin rather than Collagen IV.

1.1.5.5 Biomaterials and methodologies in PTE

The main challenge in TE is to design scaffolds capable of closely mimic the most important features of the ECM. Thus, the ideal biomaterial should be able to resemble the dynamic biochemical, structural, and mechanical properties of the natural ECM. Therefore, it should present water retention capacity, porosity to allow cell growth, stimulate cell-substrate interactions and an easy and scalable production. Some other properties that should possess are biocompatibility and biodegradability[187,260,261].

A wide variety of biomaterials have been used so far in PTE. The first classification to establish is by its nature, like natural or synthetic biomaterials. Natural ECM-derived biomaterials like collagen, laminin, alginates or chitosan have been used in PTE. These materials have been most widely used due to their easy accessibility and the fact that they provide the spectrum of chemical and physical cues necessary to induce morphogenesis and function from many cells. However, they present some important limitations regarding their use in TE. Cells cultured in matrices of natural origin are exposed to the influence of a large variety of unknown biochemical signals that makes it difficult to attribute outcomes to specific matrix components. Moreover, the scaffold properties such as mechanics, nanostructure and degradation rate cannot be modified. Furthermore, since they are usually isolated from animal tissue, they suffer from batch to batch variations and when implanted into the human body an immunogenic reaction may develop. For all these reasons, the use of natural occurring biomaterials makes it difficult to exert a precise control over the extracellular microenvironment[194,260,262]. Conversely, synthetic biomaterials can be tailored to mimic ECM properties, such as the mechanical properties or the degradation time, providing well-controlled and reproducible cellular environments[184]. The lack of cell-recognition signals allows for the functionalization with specific cell-binding motifs in order to recreate the most appropriate ECM[262,263].

Several methods have been applied to obtain proper three-dimensional environments for the culture or transplantation of insulin-producing cells. The nature of the biomaterial varies depending on the selected methodology. As mentioned previously, the most common approach is the encapsulation of islets or other insulin-secreting cells. This methodology aims to immunoprotect the transplanted cells, usually from an allogeneic source, coating them with a semipermeable membrane, which allows the passage of low molecular weight nutrients and metabolites, such as insulin, but excludes larger antibodies and cytotoxic cells from the host[201,264]. Thus, the need for immunosuppressants could be avoided.

There are several methods of cell encapsulation, but the most commonly used is the microencapsulation, which consists on the encapsulation of a single islet or a small number of islets within a thin layer of polymer gel[202]. Nowadays alginates are the most widely employed polymers used for generation of microcapsules[265,266]. Alginate is a natural biomaterial, a polysaccharide obtained from brown seaweeds that creates three-dimensional structures when reacting with multivalent ions[267]. Microcapsules are transplanted in the peritoneal cavity or the kidney capsule.

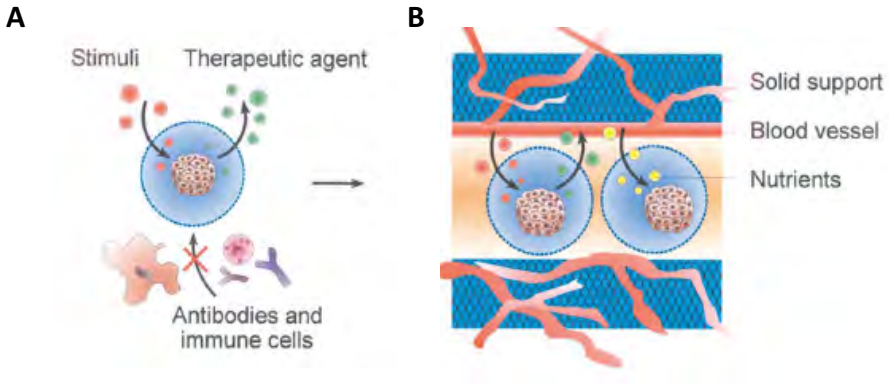

Figure 1.19. Pancreatic islet microencapsulation technique. (A) The membrane allows the diffusion of nutrients, oxygen and stimuli, whereas antibodies and immune cells are excluded. (B) A more sophisticated prevascularized system to provide an adequate nutrition to the encapsulated cells. Adapted from Orive[264].

Other three-dimensional scaffolds have been used in order to improve cell viability and function when transplanting pancreatic islets, or to induce the differentiation towards a beta cell phenotype when using other cell sources. Moreover, these materials can act as carriers for cell transplantation. Some examples of natural biomaterials are collagen[205,268], fibrin gel[269] and chitosan[270] among others. On the other hand synthetic biomaterials include poly(glycolic acid) (PGA)[271], poly(ethylene glycol) (PEG) diacrylate[272], hydroxyethyl methacrylate-methyl methacrylate (HEMA-MMA)[273], PEG hydrogels[274,275] and self-assembling peptides (SAP) nanofibers[206,276–280].

The present thesis is based on the combination of a rat beta cell line or expanded human islets cells with a self-assembling peptide (SAP) nanofiber gel. Results are presented in Chapter 3 (rat beta cell line) and 4 (expanded human islets cells).

1.2 HYPOTHESIS AND GENERAL AIMS

Beta cell replacement has been proposed as a treatment for diabetes. The *in vitro* expansion of beta cells obtained from human cadaveric organ donors is a potential approach to generate an abundant source of insulin-producing cells. Nevertheless, the growth of islets cells in monolayer cultures implies the loss of the beta cell phenotype. This dedifferentiation could be a consequence of pancreatic islet isolation and dispersion into single cells, which causes the disruption of the islet microenvironment.

Thus, this thesis is based on the development of a three-dimensional (3D) biomimetic culture platform for pancreatic tissue engineering (PTE). Our working hypothesis is that the functionalization of nanofibrous 3D matrices with ECM-derived signaling motifs could reconstitute the islet microenvironment and induce the redifferentiation of the expanded cells. With this aim, the non-instructive self-assembling peptide RAD16-I was functionalized with bioactive motifs, to promote the redifferentiation of expanded human islet-derived cells towards a beta cell like phenotype. Prior to the establishment of the RAD16-I culture platforms based on the expanded human islet cells, a rat beta cell surrogate was used as a proof of concept for the functionalized 3D model. Therefore, the general aims of the present thesis are the following:

1) To develop a biomimetic 3D culture model based on the insulin-producing cell line INS-1E, and to evaluate its potential to maintain or improve beta cell viability and function (Chapter 3).

2) To develop and study the potential of different functionalized 3D culture platforms to induce the redifferentiation of expanded human beta cells, that could eventually be used in diabetes therapy (Chapter 4).

1.3 REFERENCES

1. Alberti, K. G. & Zimmet, P. Z. Definition, diagnosis and classification of diabetes mellitus and its complications. Part 1: diagnosis and classification of diabetes mellitus provisional report of a WHO consultation. *Diabet. Med.* **15,** 539–553 (1998).

2. IDF. *International Diabetes Federation. IDF Diabetes Atlas 7th ed. Brussels, Belgium* (2015). Available at: http://www.diabetesatlas.org/.

3. Shaw, J. E., Sicree, R. A. & Zimmet, P. Z. Global estimates of the prevalence of diabetes for 2010 and 2030. *Diabetes Res. Clin. Pract.* **87,** 4–14 (2016).

4. DeFronzo R. A., Ferrannini E., Zimmet P., G. A. *International Textbook of Diabetes Mellitus*. (John Wiley & Sons, 2015).

5. WHO. Global Health Risks: Mortality and burden of disease attributable to selected major risks. *Bull. World Health Organ.* **87,** 646–646 (2009).

6. Cade, W. T. Diabetes-Related Microvascular and Macrovascular Diseases in the Physical Therapy Setting. *Phys. Ther.* **88,** 1322 LP-1335 (2008).

7. Gregg, E. W. *et al.* Changes in Diabetes-Related Complications in the United States, 1990–2010. *N. Engl. J. Med.* **370,** 1514–1523 (2014).

8. Angelantonio, D., Kaptoge, Wormser, Gao, Wood, Nietert, K., Wallace, Trevisan, Cooper, Howard, S., Casiglia, Jukema, Woodward, Brunner, S. & Danesh. Association of cardiometabolic multimorbidity with mortality. *JAMA* **314,** 52–60 (2015).

9. Hex, N., Bartlett, C., Wright, D., Taylor, M. & Varley, D. Estimating the current and future costs of Type 1 and Type 2 diabetes in the UK, including direct health costs and indirect societal and productivity costs. *Diabet. Med.* **29,** 855–862 (2012).

10. Hodgson, T. A. & Cohen, A. J. Medical Care Expenditures for Diabetes, Its Chronic Complications, and Its Comorbidities. *Prev. Med. (Baltim).* **29,** 173–186 (1999).

11. Zhang, P. *et al.* Global healthcare expenditure on diabetes for 2010 and 2030. *Diabetes Res. Clin. Pract.* **87,** 293–301 (2010).

12. Alwan, A. *Global status report on noncommunicable diseases 2010.* (World Health Organization, 2011).

13. OpenStax. *Anatomy & Physiology*. (OpenStax CNX).

14. Stendahl, J. C., Kaufman, D. B. & Stupp, S. I. Extracellular matrix in pancreatic islets: Relevance to scaffold design and transplantation. *Cell Transplant.* **18,** 1–12 (2009).

15. Camussi, G., Zanone, M. M. & Favaro, E. From endothelial to β cells: insights into pancreatic islet microendothelium. *Curr. Diabetes Rev.* **4,** 1–9 (2008).

16. Weir, G. C. & Bonner-Weir, S. Islets of Langerhans: the puzzle of intraislet interactions and their relevance to diabetes. *J. Clin. Invest.* **85,** 983 (1990).

17. Ishihara, H., Maechler, P., Gjinovci, A., Herrera, P.-L. & Wollheim, C. B. Islet β-cell secretion determines glucagon release from neighbouring α-cells. *Nat. Cell Biol.* **5,** 330–335 (2003).

18. Steiner, D. J., Kim, A., Miller, K. & Hara, M. Pancreatic islet plasticity: interspecies comparison of islet architecture and composition. *Islets* **2,** 135–145 (2010).

19. Wierup, N., Svensson, H., Mulder, H. & Sundler, F. The ghrelin cell: a novel developmentally regulated islet cell in the human pancreas. *Regul. Pept.* **107,** 63–69 (2002).

20. Strowski, M. Z., Parmar, R. M., Blake, A. D. & Schaeffer, J. M. Somatostatin Inhibits Insulin and Glucagon Secretion via Two Receptor Subtypes: An in Vitro Study of Pancreatic Islets from Somatostatin Receptor 2 Knockout Mice. *Endocrinology* **141,** 111–117 (2000).

21. Caicedo, A. Paracrine and autocrine interactions in the human islet: more than meets the eye. in *Seminars in cell & developmental biology* **24,** 11–21 (Elsevier, 2013).

22. Cabrera, O. *et al.* The unique cytoarchitecture of human pancreatic islets has implications for islet cell function. *Proc. Natl. Acad. Sci. U. S. A.* **103,** 2334–2339 (2006).

23. Bonner-Weir, S., Sullivan, B. A. & Weir, G. C. Human Islet Morphology Revisited Human and Rodent Islets Are Not So Different After All. *J. Histochem. Cytochem.* **63,** 604–612 (2015).

24. Brissova, M. *et al.* Assessment of human pancreatic islet architecture and composition by laser scanning confocal microscopy. *J. Histochem. Cytochem.* **53,** 1087–1097 (2005).

25. Bosco, D. *et al.* Unique arrangement of α-and β-cells in human islets of Langerhans. *Diabetes* **59,** 1202–1210 (2010).

26. Bonner-Weir, S. & O'Brien, T. D. Islets in type 2 diabetes: in honor of Dr. Robert C. Turner. *Diabetes* **57,** 2899–2904 (2008).

27. Wang, X. *et al.* Regional differences in islet distribution in the human pancreas-preferential beta-cell loss in the head region in patients with type 2 diabetes. *PLoS One* **8,** e67454 (2013).

28. Copstead-Kirkhorn, L.-E. C. & Banasik, J. L. *Pathophysiology*. (Elsevier/Saunders, 2014).

29. Berg, J. M., Tymoczko, J. L. & Stryer, L. *Biochemistry*. (W. H. Freeman, 2002).

30. Röder, P. V, Wu, B., Liu, Y. & Han, W. Pancreatic regulation of glucose homeostasis. *Exp. Mol. Med.* **48,** e219 (2016).

31. Fu, Z., R Gilbert, E. & Liu, D. Regulation of insulin synthesis and secretion and pancreatic Beta-cell dysfunction in diabetes. *Curr. Diabetes Rev.* **9,** 25–53 (2013).

32. Melloul, D., Marshak, S. & Cerasi, E. Regulation of insulin gene transcription. *Diabetologia* **45,** 309–326 (2002).

33. Andrali, S. S., Sampley, M. L., Vanderford, N. L. & Özcan, S. Glucose regulation of insulin gene expression in pancreatic β-cells. *Biochem. J.* **415,** 1–10 (2008).

34. Melloul, D. Transcription Factors in Islet Development and Physiology: Role of PDX-1 in Beta-Cell Function. *Ann. N. Y. Acad. Sci.* **1014,** 28–37 (2004).

35. Hou, J. C., Min, L. & Pessin, J. E. Insulin granule biogenesis, trafficking and exocytosis. *Vitam. Horm.* **80,** 473–506 (2009).

36. Dodson, G. & Steiner, D. The role of assembly in insulin's biosynthesis. *Curr. Opin. Struct. Biol.* **8,** 189–194 (1998).

37. Rhodes, C. J., Shoelson, S., Halban, P. A., Joslin, E. P. & Kahn, C. R. *Insulin biosynthesis, processing, and chemistry*. *Joslin's diabetes mellitus* (Lippincott Williams & Wilkins, 2005).

38. Espinal, J. *Understanding Insulin Action: Principles and Molecular Mechanisms*. (Springer Science & Business Media, 2013).

39. Lipson, K. L. *et al.* Regulation of insulin biosynthesis in pancreatic beta cells by an endoplasmic reticulum-resident protein kinase IRE1. *Cell Metab.* **4,** 245–254 (2006).

40. Steiner, D. F. The proinsulin C-peptide—a multirole model. *Exp. Diabetes Res.* **5,** 7–14 (2004).

41. Zhu, X. *et al.* Severe block in processing of proinsulin to insulin accompanied by elevation of des-64, 65 proinsulin intermediates in islets of mice lacking prohormone convertase 1/3. *Proc. Natl. Acad. Sci.* **99,** 10299–10304 (2002).

42. Dunn, M. F. Zinc–ligand interactions modulate assembly and stability of the insulin hexamer–a review. *Biometals* **18,** 295–303 (2005).

43. Wang, Z. & Thurmond, D. C. Mechanisms of biphasic insulin-granule exocytosis–roles of the cytoskeleton, small GTPases and SNARE proteins. *J. Cell Sci.* **122,** 893–903 (2009).

44. Skelin, M., Rupnik, M. & Cencic, A. Pancreatic beta cell lines and their applications in diabetes mellitus research. *ALTEX* **27,** 105–113 (2010).

45. Ma, L. *et al.* Direct imaging shows that insulin granule exocytosis occurs by complete vesicle fusion. *Proc. Natl. Acad. Sci. U. S. A.* **101,** 9266–9271 (2004).

46. Lang, J. Molecular mechanisms and regulation of insulin exocytosis as a paradigm of endocrine secretion. *Eur. J. Biochem.* **259,** 3–17 (1999).

47. Kulkarni, R. N. The islet β-cell. *Int. J. Biochem. Cell Biol.* **36,** 365–371 (2004).

48. Minami, K. & Seino, S. Current status of regeneration of pancreatic β-cells. *J. Diabetes Investig.* **4,** 131–141 (2013).

49. Montanya, E., Nacher, V., Biarnés, M. & Soler, J. Linear correlation between ß-cell mass and body weight throughout the lifespan in Lewis rats. *Diabetes* **49,** 1341–1346 (2000).

50. Karaca, M., Magnan, C. & Kargar, C. Functional pancreatic beta-cell mass: involvement in type 2 diabetes and therapeutic intervention. *Diabetes Metab.* **35,** 77–84 (2009).

51. Montanya, E. & Téllez, N. Pancreatic remodeling: beta-cell apoptosis, proliferation and neogenesis, and the measurement of beta-cell mass and of individual beta-cell size. *Type 2 Diabetes Methods Protoc.* 137–158 (2009).

52. Bouwens, L. & Rooman, I. Regulation of pancreatic beta-cell mass. *Physiol. Rev.* **85,** 1255–1270 (2005).

53. Slack, J. M. Developmental biology of the pancreas. *Development* **121,** 1569–1580 (1995).

54. Murtaugh, L. C. Pancreas and beta-cell development: from the actual to the possible. *Development* **134,** 427–438 (2007).

55. Gu, G., Dubauskaite, J. & Melton, D. A. Direct evidence for the pancreatic lineage: NGN3+ cells are islet progenitors and are distinct from duct progenitors. *Development* **129,** 2447–2457 (2002).

56. Murtaugh, L. C. & Melton, D. A. Genes, signals, and lineages in pancreas development. *Annu. Rev. Cell Dev. Biol.* **19,** 71–89 (2003).

57. Georgia, S. & Bhushan, A. β cell replication is the primary mechanism for maintaining postnatal β cell mass. *J. Clin. Invest.* **114,** 963–968 (2004).

58. Bonner-Weir, S., Aguayo-Mazzucato, C. & Weir, G. C. Dynamic development of the pancreas from birth to adulthood. *Ups. J. Med. Sci.* 1–4 (2016).

59. Bonner-Weir, S. Life and death of the pancreatic β cells. *Trends Endocrinol. Metab.* **11,** 375–378 (2000).

60. Kassem, S. A., Ariel, I., Thornton, P. S., Scheimberg, I. & Glaser, B. Beta-cell proliferation and apoptosis in the developing normal human pancreas and in hyperinsulinism of infancy. *Diabetes* **49,** 1325–1333 (2000).

61. Scaglia, L., Cahill, C. J., Finegood, D. T. & Bonner-Weir, S. Apoptosis Participates in the Remodeling of the Endocrine Pancreas in the Neonatal Rat 1. *Endocrinology* **138,** 1736–1741 (1997).

62. Hellerström, C. & Swenne, I. Functional maturation and proliferation of fetal pancreatic β-cells. *Diabetes* **40,** 89–93 (1991).

63. Chintinne, M. *et al.* Contribution of postnatally formed small beta cell aggregates to functional beta cell mass in adult rat pancreas. *Diabetologia* **53,** 2380–2388 (2010).

64. Peng, S. *et al.* Heterogeneity in mitotic activity and telomere length implies an important role of young islets in the maintenance of islet mass in the adult pancreas. *Endocrinology* **150,** 3058–3066 (2009).

65. Bonner-Weir, S. *et al.* Islet neogenesis: a possible pathway for beta-cell replenishment. *Rev Diabet Stud* **9,** 407–416 (2012).

66. Bonner-Weir, S. *et al.* β-cell growth and regeneration: replication is only part of the story. *Diabetes* **59,** 2340–2348 (2010).

67. Solar, M. *et al.* Pancreatic exocrine duct cells give rise to insulin-producing β cells during embryogenesis but not after birth. *Dev. Cell* **17,** 849–860 (2009).

68. Teta, M., Rankin, M. M., Long, S. Y., Stein, G. M. & Kushner, J. A. Growth and regeneration of adult β cells does not involve specialized progenitors. *Dev. Cell* **12,** 817–826 (2007).

69. Wang, R. N., Bouwens, L. & Klöppel, G. Beta-cell growth in adolescent and adult rats treated with streptozotocin during the neonatal period. *Diabetologia* **39,** 548–557 (1996).

70. Butler, P. C., Meier, J. J., Butler, A. E. & Bhushan, A. The replication of β cells in normal physiology, in disease and for therapy. *Nat. Clin. Pract. Endocrinol. Metab.* **3,** 758–768 (2007).

71. Finegood, D. T., Scaglia, L. & Bonner-Weir, S. Dynamics of β-cell mass in the growing rat pancreas: estimation with a simple mathematical model. *Diabetes* **44,** 249–256 (1995).

72. Dor, Y., Brown, J., Martinez, O. I. & Melton, D. A. Adult pancreatic β-cells are formed by self-duplication rather than stem-cell differentiation. *Nature* **429,** 41–46 (2004).

73. Minami, K. *et al.* Lineage tracing and characterization of insulin-secreting cells generated from adult pancreatic acinar cells. *Proc. Natl. Acad. Sci. U. S. A.* **102,** 15116–15121 (2005).

74. Song, K.-H. *et al.* In vitro transdifferentiation of adult pancreatic acinar cells into insulin-expressing cells. *Biochem. Biophys. Res. Commun.* **316,** 1094–1100 (2004).

75. Ianus, A., Holz, G. G., Theise, N. D. & Hussain, M. A. In vivo derivation of glucose-competent pancreatic endocrine cells from bone marrow without evidence of cell fusion. *J. Clin. Invest.* **111,** 843–850 (2003).

76. Meier, J. J. *et al.* β-cell replication is the primary mechanism subserving the postnatal expansion of β-cell mass in humans. *Diabetes* **57,** 1584–1594 (2008).

77. Bonner-Weir, S., Baxter, L. A., Schuppin, G. T. & Smith, F. E. A second pathway for regeneration of adult exocrine and endocrine pancreas: a possible recapitulation of embryonic development. *Diabetes* **42,** 1715–1720 (1993).

78. Wang, R. N., Klöppel, G. & Bouwens, L. Duct-to islet-cell differentiation and islet growth in the pancreas of duct-ligated adult rats. *Diabetologia* **38,** 1405–1411 (1995).

79. Peshavaria, M. *et al.* Regulation of pancreatic β-cell regeneration in the normoglycemic 60% partial-pancreatectomy mouse. *Diabetes* **55,** 3289–3298 (2006).

80. Misfeldt, A. A., Costa, R. H. & Gannon, M. β-Cell proliferation, but not neogenesis, following 60% partial pancreatectomy is impaired in the absence of FoxM1. *Diabetes* **57,** 3069–3077 (2008).

81. Bonner-Weir, S., Trent, D. F. & Weir, G. C. Partial pancreatectomy in the rat and subsequent defect in glucose-induced insulin release. *J. Clin. Invest.* **71,** 1544 (1983).

82. Inada, A. *et al.* Carbonic anhydrase II-positive pancreatic cells are progenitors for both endocrine and exocrine pancreas after birth. *Proc. Natl. Acad. Sci. U. S. A.* **105,** 19915–19919 (2008).

83. Sharma, A. *et al.* The homeodomain protein IDX-1 increases after an early burst of proliferation during pancreatic regeneration. *Diabetes* **48,** 507 LP-513 (1999).

84. Lee, R. H. *et al.* Multipotent stromal cells from human marrow home to and promote repair of pancreatic islets and renal glomeruli in diabetic NOD/scid mice. *Proc. Natl. Acad. Sci.* **103,** 17438–17443 (2006).

85. Xu, X. *et al.* β cells can be generated from endogenous progenitors in injured adult mouse pancreas. *Cell* **132,** 197–207 (2008).

86. Yu, K., Fischbach, S. & Xiao, X. Beta Cell Regeneration in Adult Mice: Controversy Over the Involvement of Stem Cells. *Curr. Stem Cell Res. Ther.* **11,** 542–546 (2016).

87. Kopp, J. L. *et al.* Sox9+ ductal cells are multipotent progenitors throughout development but do not produce new endocrine cells in the normal or injured adult pancreas. *Development* **138,** 653–665 (2011).

88. American Diabetes Association. Diagnosis and classification of diabetes mellitus. *Diabetes Care* **37,** S81 (2014).

89. Harjutsalo, V., Sjöberg, L. & Tuomilehto, J. Time trends in the incidence of type 1 diabetes in Finnish children: a cohort study. *Lancet* **371,** 1777–1782 (2008).

90. Atkinson, M. A., Eisenbarth, G. S. & Michels, A. W. Type 1 diabetes. *Lancet* **383,** 69–82 (2014).

91. Daneman, D. Type 1 diabetes. *Lancet* **367,** 847–858 (2006).

92. Atkinson, M. A. & Eisenbarth, G. S. Type 1 diabetes: new perspectives on disease pathogenesis and treatment. *Lancet* **358,** 221–229 (2001).

93. Zimmet, P., Alberti, K. & Shaw, J. Global and societal implications of the diabetes epidemic. *Nature* **414,** 782–787 (2001).

94. Willcox, A., Richardson, S. J., Bone, A. J., Foulis, A. K. & Morgan, N. G. Analysis of islet inflammation in human type 1 diabetes. *Clin. Exp. Immunol.* **155,** 173–181 (2009).

95. In't Veld, P. Insulitis in human type 1 diabetes: the quest for an elusive lesion. *Islets* **3,** 131–138 (2011).

96. Eizirik, D. L., Colli, M. L. & Ortis, F. The role of inflammation in insulitis and β-cell loss in type 1 diabetes. *Nat. Rev. Endocrinol.* **5,** 219–226 (2009).

97. Knip, M. *et al.* Environmental triggers and determinants of type 1 diabetes. *Diabetes* **54,** S125–S136 (2005).

98. Pociot, F. & McDermott, M. F. Genetics of type 1 diabetes mellitus. *Genes Immun.* **3,** 235–249 (2002).

99. Pociot, F. *et al.* Genetics of type 1 diabetes: what's next? *Diabetes* **59,** 1561–1571 (2010).

100. Knip, M. & Simell, O. Environmental triggers of type 1 diabetes. *Cold Spring Harb. Perspect. Med.* **2,** a007690 (2012).

101. Moltchanova, E. V, Schreier, N., Lammi, N. & Karvonen, M. Seasonal variation of diagnosis of Type 1 diabetes mellitus in children worldwide. *Diabet. Med.* **26,** 673–678 (2009).

102. Kahn, H. S. *et al.* Association of type 1 diabetes with month of birth among US youth the SEARCH for Diabetes in Youth Study. *Diabetes Care* **32,** 2010–2015 (2009).

103. Group, E. A. S. Variation and trends in incidence of childhood diabetes in Europe. *Lancet* **355,** 873–876 (2000).

104. Åkerblom, H. K., Vaarala, O., Hyöty, H., Ilonen, J. & Knip, M. Environmental factors in the etiology of type 1 diabetes. *Am. J. Med. Genet.* **115,** 18–29 (2002).

105. Lönnrot, M. *et al.* Enterovirus infection as a risk factor for beta-cell autoimmunity in a prospectively observed birth cohort: the Finnish Diabetes Prediction and Prevention Study. *Diabetes* **49,** 1314–1318 (2000).

106. Oikarinen, S. *et al.* Enterovirus RNA in blood is linked to the development of type 1 diabetes. *Diabetes* **60,** 276–279 (2011).

107. Kimpimaki, T. *et al.* The first signs of β-cell autoimmunity appear in infancy in genetically susceptible children from the general population: the Finnish Type 1 Diabetes Prediction and Prevention Study. *J. Clin. Endocrinol. Metab.* **86,** 4782–4788 (2001).

108. Holmberg, H., Wahlberg, J., Vaarala, O. & Ludvigsson, J. Short duration of breast-feeding as a risk-factor for β-cell autoantibodies in 5-year-old children from the general population. *Br. J. Nutr.* **97,** 111–116 (2007).

109. Knip, M. *et al.* Dietary intervention in infancy and later signs of beta-cell autoimmunity. *N. Engl. J. Med.* **363,** 1900–1908 (2010).

110. Knip, M., Virtanen, S. M. & Åkerblom, H. K. Infant feeding and the risk of type 1 diabetes. *Am. J. Clin. Nutr.* **91,** 1506S–1513S (2010).

111. Virtanen, S. M. *et al.* Infant feeding in Finnish children< 7 yr of age with newly diagnosed IDDM. *Diabetes Care* **14,** 415–417 (1991).

112. Virtanen, S. M. *et al.* Early introduction of dairy products associated with increased risk of IDDM in Finnish children. *Diabetes* **42,** 1786–1790 (1993).

113. Savilahti, E., Akerblom, H. K., Tainio, V. M. & Koskimies, S. Children with newly diagnosed insulin dependent diabetes mellitus have increased levels of cow's milk antibodies. *Diabetes Res.* **7,** 137–140 (1988).

114. Dahlquist, G., Savilahti, E. & Landin-Olsson, M. An increased level of antibodies to β-ltoglobulin is a risk determinant for early-onset Type 1 (insulin-dependent) diabetes mellitus independent of islet cell antibodies and early introduction of cow's milk. *Diabetologia* **35,** 980–984 (1992).

115. Virtanen, S. M. *et al.* Diet, cow's milk protein antibodies and the risk of IDDM in Finnish children. *Diabetologia* **37,** 381–387 (1994).

116. Norris, J. M. *et al.* Timing of initial cereal exposure in infancy and risk of islet autoimmunity. *Jama* **290,** 1713–1720 (2003).

117. Ziegler, A.-G., Schmid, S., Huber, D., Hummel, M. & Bonifacio, E. Early infant feeding and risk of developing type 1 diabetes–associated autoantibodies. *Jama* **290,** 1721–1728 (2003).

118. Group, E. S. 2 S. Vitamin D supplement in early childhood and risk for Type I (insulin-dependent) diabetes mellitus. *Diabetologia* **42,** 51–54 (1999).

119. Vaarala, O., Atkinson, M. A. & Neu, J. The 'perfect storm' for type 1 diabetes the complex interplay between intestinal microbiota, gut permeability, and mucosal immunity. *Diabetes* **57,** 2555–2562 (2008).

120. Murri, M. *et al.* Gut microbiota in children with type 1 diabetes differs from that in healthy children: a case-control study. *BMC Med.* **11,** 1 (2013).

121. Bosi, E. *et al.* Increased intestinal permeability precedes clinical onset of type 1 diabetes. *Diabetologia* **49,** 2824–2827 (2006).

122. Lee, A. S. *et al.* Gut barrier disruption by an enteric bacterial pathogen accelerates insulitis in NOD mice. *Diabetologia* **53,** 741–748 (2010).

123. Vehik, K. & Dabelea, D. The changing epidemiology of type 1 diabetes: why is it going through the roof? *Diabetes. Metab. Res. Rev.* **27,** 3–13 (2011).

124. Group, D. C. and C. T. R. The effect of intensive treatment of diabetes on the development and progression of long-term complications in insulin-dependent diabetes mellitus. *N Engl j Med* **1993,** 977–986 (1993).

125. Chen, L., Magliano, D. J. & Zimmet, P. Z. The worldwide epidemiology of type 2 diabetes mellitus—present and future perspectives. *Nat. Rev. Endocrinol.* **8,** 228–236 (2012).

126. Chan, J. C. N. *et al.* Diabetes in Asia: epidemiology, risk factors, and pathophysiology. *Jama* **301,** 2129–2140 (2009).

127. Nolan, C. J., Damm, P. & Prentki, M. Type 2 diabetes across generations: from pathophysiology to prevention and management. *Lancet* **378,** 169–181 (2011).

128. Butler, A. E. *et al.* β-cell deficit and increased β-cell apoptosis in humans with type 2 diabetes. *Diabetes* **52,** 102–110 (2003).

129. Xu, H. *et al.* Chronic inflammation in fat plays a crucial role in the development of obesity-related insulin resistance. *J. Clin. Invest.* **112,** 1821–1830 (2003).

130. Kahn, S. E., Hull, R. L. & Utzschneider, K. M. Mechanisms linking obesity to insulin resistance and type 2 diabetes. *Nature* **444,** 840–846 (2006).

131. Lebovitz, H. E. Type 2 diabetes: an overview. *Clin. Chem.* **45,** 1339–1345 (1999).

132. Gerich, J. E. Contributions of insulin-resistance and insulin-secretory defects to the pathogenesis of type 2 diabetes mellitus. in *Mayo Clinic Proceedings* **78,** 447–456 (Elsevier, 2003).

133. Felber, J. P. & Golay, A. Pathways from obesity to diabetes. *Int. J. Obes. Relat. Metab. Disord.* **26,** (2002).

134. Polonsky, K. S. Dynamics of insulin secretion in obesity and diabetes. *Int. J. Obes.* **24,** S29–S31 (2000).

135. Rhodes, C. J. Type 2 Diabetes-a Matter of ß-Cell Life and Death? *Science (80-.).* **307,** 380–384 (2005).

136. Donath, M. Y. & Halban, P. A. Decreased beta-cell mass in diabetes: significance, mechanisms and therapeutic implications. *Diabetologia* **47,** 581–589 (2004).

137. Costes, S., Langen, R., Gurlo, T., Matveyenko, A. V & Butler, P. C. β-Cell failure in type 2 diabetes: a case of asking too much of too few? *Diabetes* **62,** 327–335 (2013).

138. Kahn, S. E. The importance of β-cell failure in the development and progression of type 2 diabetes. *J. Clin. Endocrinol. Metab.* **86,** 4047–4058 (2001).

139. Matthews, D. R., Cull, C. A., Stratton, I. M., Holman, R. R. & Turner, R. C. UKPDS 26: sulphonylurea failure in non-insulin-dependent diabetic patients over six years. *Diabet. Med.* **15,** 297–303 (1998).

140. Rahier, J., Guiot, Y., Goebbels, R. M., Sempoux, C. & Henquin, J.-C. Pancreatic β-cell mass in European subjects with type 2 diabetes. *Diabetes, Obes. Metab.* **10,** 32–42 (2008).

141. Lingohr, M. K., Buettner, R. & Rhodes, C. J. Pancreatic β-cell growth and survival–a role in obesity-linked type 2 diabetes? *Trends Mol. Med.* **8,** 375–384 (2002).

142. Cnop, M. *et al.* Mechanisms of pancreatic β-cell death in Type 1 and Type 2 diabetes many differences, few similarities. *Diabetes* **54,** S97–S107 (2005).

143. Stern, M. P. Strategies and prospects for finding insulin resistance genes. *J. Clin. Invest.* **106,** 323–327 (2000).

144. McIntyre, E. A. & Walker, M. Genetics of type 2 diabetes and insulin resistance: knowledge from human studies. *Clin. Endocrinol. (Oxf).* **57,** 303–311 (2002).

145. Prokopenko, I., McCarthy, M. I. & Lindgren, C. M. Type 2 diabetes: new genes, new understanding. *Trends Genet.* **24,** 613–621 (2008).

146. Kahn, B. B. & Flier, J. S. Obesity and insulin resistance. *J. Clin. Invest.* **106,** 473–481 (2000).

147. Beck-Nielsen, H., Pedersen, O. & Lindskov, H. O. Normalization of the insulin sensitivity and the cellular insulin binding during treatment of obese diabetics for one year. *Acta Endocrinol. (Copenh).* **90,** 103–112 (1979).

148. Hales, C. N. & Barker, D. J. P. Type 2 (non-insulin-dependent) diabetes mellitus: the thrifty phenotype hypothesis. *Diabetologia* **35,** 595–601 (1992).

149. Bäckhed, F. *et al.* The gut microbiota as an environmental factor that regulates fat storage. *Proc. Natl. Acad. Sci. U. S. A.* **101,** 15718–15723 (2004).

150. Qin, J. *et al.* A metagenome-wide association study of gut microbiota in type 2 diabetes. *Nature* **490,** 55–60 (2012).

151. DeFronzo, R. A. From the triumvirate to the ominous octet: a new paradigm for the treatment of type 2 diabetes mellitus. *Diabetes* **58,** 773–795 (2009).

152. Buchanan, T. A., Xiang, A., Kjos, S. L. & Watanabe, R. What is gestational diabetes? *Diabetes Care* **30,** S105–S111 (2007).

153. Barbour, L. A. *et al.* Cellular mechanisms for insulin resistance in normal pregnancy and gestational diabetes. *Diabetes Care* **30,** S112–S119 (2007).

154. Reece, E. A., Leguizamón, G. & Wiznitzer, A. Gestational diabetes: the need for a common ground. *Lancet* **373,** 1789–1797 (2009).

155. Catalano, P. M., Huston, L., Amini, S. B. & Kalhan, S. C. Longitudinal changes in glucose metabolism during pregnancy in obese women with normal glucose tolerance and gestational diabetes mellitus. *Am. J. Obstet. Gynecol.* **180,** 903–916 (1999).

156. Buchanan, T. A. Pancreatic B-cell defects in gestational diabetes: implications for the pathogenesis and prevention of type 2 diabetes. *J. Clin. Endocrinol. Metab.* **86,** 989–993 (2001).

157. Seaquist, E. R. *et al.* Hypoglycemia and diabetes: A report of a workgroup of the american diabetes association and the endocrine society. *J. Clin. Endocrinol. Metab.* **98,** 1845–1859 (2013).

158. Geddes, J., Schopman, J. E., Zammitt, N. N. & Frier, B. M. Prevalence of impaired awareness of hypoglycaemia in adults with type 1 diabetes. *Diabet. Med.* **25,** 501–504 (2008).

159. Ryan, E. A. *et al.* Clinical outcomes and insulin secretion after islet transplantation with the Edmonton protocol. *Diabetes* **50,** 710–719 (2001).

160. Farney, A. C. *et al.* Simultaneous cadaver pancreas living-donor kidney transplantation: a new approach for the type 1 diabetic uremic patient. *Ann. Surg.* **232,** 696–703 (2000).

161. Ballinger, W. F. & Lacy, P. E. Transplantation of intact pancreatic islets in rats. *Surgery* **72,** 175–186 (1972).

162. de Kort, H., de Koning, E. J., Rabelink, T. J., Bruijn, J. A. & Bajema, I. M. Islet transplantation in type 1 diabetes. *Bmj* **342,** d217 (2011).

163. Ricordi, C., Lacy, P. E. & Scharp, D. W. Automated islet isolation from human pancreas. *Diabetes* **38,** 140–142 (1989).

164. Ichii, H. *et al.* Improved human islet isolation using nicotinamide. *Am. J. Transplant.* **6,** 2060–2068 (2006).

165. Korsgren, O. *et al.* Current status of clinical islet transplantation. *Transplantation* **79,** 1289–1293 (2005).

166. Merani, S. & Shapiro, A. M. J. Current status of pancreatic islet transplantation. *Clin. Sci.* **110,** 611–625 (2006).

167. Efrat, S. *Stem Cell Therapy for Diabetes*. (Springer Science & Business Media, 2010).

168. Naftanel, M. A. & Harlan, D. M. Pancreatic islet transplantation. *PLoS Med* **1,** e58 (2004).

169. Bretzel, R. G. *et al.* Improved survival of intraportal pancreatic islet cell allografts in patients with type-1 diabetes mellitus by refined peritransplant management. *J. Mol. Med.* **77,** 140–143 (1999).

170. Shapiro, A. M. J. *et al.* Islet transplantation in seven patients with type 1 diabetes mellitus using a glucocorticoid-free immunosuppressive regimen. *N. Engl. J. Med.* **343,** 230–238 (2000).

171. Ryan, E. A. *et al.* Five-year follow-up after clinical islet transplantation. *Diabetes* **54,** 2060–2069 (2005).

172. Ryan, E. A., Bigam, D. & Shapiro, A. M. Current indications for pancreas or islet transplant. *Diabetes, Obes. Metab.* **8,** 1–7 (2006).

173. Shapiro, A. M. J. *et al.* International trial of the Edmonton protocol for islet transplantation. *N. Engl. J. Med.* **355,** 1318–1330 (2006).

174. Wade, R. J. & Burdick, J. A. Engineering ECM signals into biomaterials. *Mater. Today* **15,** 454–459 (2012).

175. Ryan, E. A. *et al.* Successful islet transplantation continued insulin reserve provides long-term glycemic control. *Diabetes* **51,** 2148–2157 (2002).

176. Vantyghem, M.-C. *et al.* Primary graft function, metabolic control, and graft survival after islet transplantation. *Diabetes Care* **32,** 1473–1478 (2009).

177. Bellin, M. D. *et al.* Potent induction immunotherapy promotes long-term insulin independence after islet transplantation in type 1 diabetes. *Am. J. Transplant.* **12,** 1576–1583 (2012).

178. Davalli, A. M. *et al.* Vulnerability of islets in the immediate posttransplantation period: dynamic changes in structure and function. *Diabetes* **45,** 1161–1167 (1996).

179. Moberg, L. *et al.* Production of tissue factor by pancreatic islet cells as a trigger of detrimental thrombotic reactions in clinical islet transplantation. *Lancet* **360,** 2039–2045 (2002).

180. Biarnés, M. *et al.* β-cell death and mass in syngeneically transplanted islets exposed to short-and long-term hyperglycemia. *Diabetes* **51,** 66–72 (2002).

181. Merani, S., Toso, C., Emamaullee, J. & Shapiro, A. M. J. Optimal implantation site for pancreatic islet transplantation. *Br. J. Surg.* **95,** 1449–1461 (2008).

182. Vacanti, J. & Vacanti, C. A. Chapter One - The History and Scope of Tissue Engineering BT - Principles of Tissue Engineering (Third Edition). *Hist. Scope Tissue Eng.* 3–6 (2007). doi:http://dx.doi.org/10.1016/B978-012370615-7/50005-6

183. Langer, R. & Vacanti, J. P. Tissue Engineering. *Science (80-.).* **260,** 920–926 (1993).

184. Griffith, L. G. & Swartz, M. A. Capturing complex 3D tissue physiology in vitro. *Nat. Rev. Mol. Cell Biol.* **7,** 211–24 (2006).

185. Dvir, T., Timko, B. P., Kohane, D. S. & Langer, R. Nanotechnological strategies for engineering complex tissues. *Nat. Nanotechnol.* **6,** 13–22 (2011).

186. Lavik, E. & Langer, R. Tissue engineering: current state and perspectives. *Appl. Microbiol. Biotechnol.* **65,** 1–8 (2004).

187. Dutta, R. C. & Dutta, A. K. Cell-interactive 3D-scaffold; advances and applications. *Biotechnol. Adv.* **27,** 334–339 (2009).

188. Petreaca, M. & Martins-Green, M. in *Principles of Tissue Engineering* 161–187 (Elsevier Inc., 2013).

189. Suki, B., Ito, S., Stamenović, D., Lutchen, K. R. & Ingenito, E. P. Biomechanics of the lung parenchyma: critical roles of collagen and mechanical forces. *J. Appl. Physiol.* **98,** 1892–1899 (2005).

190. Breitkreutz, D., Mirancea, N. & Nischt, R. Basement membranes in skin: Unique matrix structures with diverse functions? *Histochem. Cell Biol.* **132,** 1–10 (2009).

191. Geiger, B., Bershadsky, A., Pankov, R. & Yamada, K. M. Transmembrane crosstalk between the extracellular matrix--cytoskeleton crosstalk. *Nat. Rev. Mol. Cell Biol.* **2,** 793–805 (2001).

192. Hynes, R. O. Integrins: Bidirectional, allosteric signaling machines. *Cell* **110,** 673–687 (2002).

193. Kim, S. H., Turnbull, J. & Guimond, S. Extracellular matrix and cell signalling: The dynamic cooperation of integrin, proteoglycan and growth factor receptor. *J. Endocrinol.* **209,** 139–151 (2011).

194. Rahmany, M. B. & Van Dyke, M. Biomimetic approaches to modulate cellular adhesion in biomaterials: A review. *Acta Biomater.* **9,** 5431–5437 (2013).

195. Bellis, S. L. Advantages of RGD peptides for directing cell association with biomaterials. *Biomaterials* **32,** 4205–4210 (2011).

196. Berrier, A. L. & Yamada, K. M. Cell–matrix adhesion. *J. Cell. Physiol.* **213,** 565–573 (2007).

197. Engler, A. J., Sen, S., Sweeney, H. L. & Discher, D. E. Matrix Elasticity Directs Stem Cell Lineage Specification. *Cell* **126,** 677–689 (2006).

198. Dado, D. & Levenberg, S. Cell-scaffold mechanical interplay within engineered tissue. *Semin. Cell Dev. Biol.* **20,** 656–64 (2009).

199. Khalili, A. A. & Ahmad, M. R. A Review of cell adhesion studies for biomedical and biological applications. *Int. J. Mol. Sci.* **16,** 18149–18184 (2015).

200. Limbert, C., Päth, G., Jakob, F. & Seufert, J. Beta-cell replacement and regeneration: Strategies of cell-based therapy for type 1 diabetes mellitus. *Diabetes Res. Clin. Pract.* **79,** 389–399 (2008).

201. Sambanis, A. in *Principles of Tissue Engineering* 849–868 (Academic Press, 2014).

202. Kaviani, M. & Azarpira, N. Insight into microenvironment remodeling in pancreatic endocrine tissue engineering: Biological and biomaterial approaches. *Tissue Eng. Regen. Med.* **13,** 475–484 (2016).

203. Ilieva, A. *et al.* Pancreatic islet cell survival following islet isolation: the role of cellular interactions in the pancreas. *J. Endocrinol.* **161,** 357–364 (1999).

204. Wang, R. N. & Rosenberg, L. Maintenance of beta-cell function and survival following islet isolation requires re-establishment of the islet-matrix relationship. *J. Endocrinol.* **163,** 181–190 (1999).

205. Daoud, J., Petropavlovskaia, M., Rosenberg, L. & Tabrizian, M. The effect of extracellular matrix components on the preservation of human islet function in vitro. *Biomaterials* **31,** 1676–1682 (2010).

206. Navarro-Alvarez, N. *et al.* Reestablishment of microenvironment is necessary to maintain in vitro and in vivo human islet function. *Cell Transplant.* **17,** 111–9 (2008).

207. Nagata, N. *et al.* Evaluation of insulin secretion of isolated rat islets cultured in extracellular matrix. *Cell Transpl.* **10,** 447–451 (2001).

208. Salvay, D. M. *et al.* Extracellular matrix protein-coated scaffolds promote the reversal of diabetes after extrahepatic islet transplantation. *Transplantation* **85,** 1456 (2008).

209. Hammar, E. *et al.* Extracellular Matrix Protects Pancreatic β-Cells Against Apoptosis. *Diabetes* **53,** 2034–2041 (2004).

210. Weber, L. M., Hayda, K. N. & Anseth, K. S. Cell-matrix interactions improve beta-cell survival and insulin secretion in three-dimensional culture. *Tissue Eng. Part A* **14,** 1959–68 (2008).

211. Kaido, T. *et al.* Impact of defined matrix interactions on insulin production by cultured human beta-cells: effect on insulin content, secretion, and gene transcription. *Diabetes* **55,** 2723–9 (2006).

212. Lim, D.-J. *et al.* Enhanced Rat Islet Function and Survival *In Vitro* Using a Biomimetic Self-Assembled Nanomatrix Gel. *Tissue Eng. Part A* **17,** 399–406 (2011).

213. Amer, L. D., Mahoney, M. J. & Bryant, S. J. Tissue engineering approaches to cell-based type 1 diabetes therapy. *Tissue Eng. Part B. Rev.* **20,** 455–67 (2014).

214. Cheng, J. Y. C. C., Raghunath, M., Whitelock, J. & Poole-Warren, L. Matrix components and scaffolds for sustained islet function. *Tissue Eng. Part B. Rev.* **17,** 235–47 (2011).

215. Bonner-Weir, S. & Weir, G. C. New sources of pancreatic beta-cells. *Nat. Biotechnol.* **23,** 857–61 (2005).

216. Domínguez-Bendala, J., Lanzoni, G., Klein, D., Álvarez-Cubela, S. & Pastori, R. L. The Human Endocrine Pancreas: New Insights on Replacement and Regeneration. *Trends Endocrinol. Metab.* **27,** 153–162 (2016).

217. Narushima, M. *et al.* A human β-cell line for transplantation therapy to control type 1 diabetes. *Nat. Biotechnol.* **23,** 1274–1282 (2005).

218. Russ, H. A. *et al.* Insulin-producing cells generated from dedifferentiated human pancreatic beta cells expanded in vitro. *PLoS One* **6,** e25566 (2011).

219. Ouziel-Yahalom, L. *et al.* Expansion and redifferentiation of adult human pancreatic islet cells. *Biochem. Biophys. Res. Commun.* **341,** 291–298 (2006).

220. Beattie, G. M. *et al.* Sustained proliferation of PDX-1+ cells derived from human islets. *Diabetes* **48,** 1013–9 (1999).

221. Russ, H. A., Bar, Y., Ravassard, P. & Efrat, S. In vitro proliferation of cells derived from adult human β-cells revealed by cell-lineage tracing. *Diabetes* **57,** 1575–1583 (2008).

222. Russ, H. A., Ravassard, P., Kerr-Conte, J., Pattou, F. & Efrat, S. Epithelial-mesenchymal transition in cells expanded in vitro from lineage-traced adult human pancreatic beta cells. *PLoS One* **4,** e6417 (2009).

223. Bouwens, L. Transdifferentiation versus stem cell hypothesis for the regeneration of islet beta-cells in the pancreas. *Microsc. Res. Tech.* **43,** 332–336 (1998).

224. Rooman, I., Heremans, Y., Heimberg, H. & Bouwens, L. Modulation of rat pancreatic acinoductal transdifferentiation and expression of PDX-1 in vitro. *Diabetologia* **43,** 907–914 (2000).

225. Baeyens, L. *et al.* Transient cytokine treatment induces acinar cell reprogramming and regenerates functional beta cell mass in diabetic mice. *Nat. Biotechnol.* **32,** 76–83 (2014).

226. Zhou, Q., Brown, J., Kanarek, A., Rajagopal, J. & Melton, D. A. In vivo reprogramming of adult pancreatic exocrine cells to beta cells. *Nature* **455,** 627–632 (2008).

227. Sapir, T. *et al.* Cell-replacement therapy for diabetes: Generating functional insulin-producing tissue from adult human liver cells. *Proc. Natl. Acad. Sci.* **102,** 7964–7969 (2005).

228. Suzuki, A., Nakauchi, H. & Taniguchi, H. Prospective isolation of multipotent pancreatic progenitors using flow-cytometric cell sorting. *Diabetes* **53,** 2143–2152 (2004).

229. Ramiya, V. K. *et al.* Reversal of insulin-dependent diabetes using islets generated in vitro from pancreatic stem cells. *Nat. Med.* **6,** 278–282 (2000).

230. El-Gohary, Y. *et al.* Intraislet pancreatic ducts can give rise to insulin-positive cells. *Endocrinology* **157,** 166–175 (2015).

231. Lee, J. *et al.* Expansion and conversion of human pancreatic ductal cells into insulin-secreting endocrine cells. *Elife* **2,** e00940 (2013).

232. Corritore, E., Lee, Y.-S., Sokal, E. M. & Lysy, P. A. β-cell replacement sources for type 1 diabetes: a focus on pancreatic ductal cells. *Ther. Adv. Endocrinol. Metab.* 2042018816652059 (2016).

233. D'Amour, K. A. *et al.* Production of pancreatic hormone–expressing endocrine cells from human embryonic stem cells. *Nat. Biotechnol.* **24,** 1392–1401 (2006).

234. Kroon, E. *et al.* Pancreatic endoderm derived from human embryonic stem cells generates glucose-responsive insulin-secreting cells in vivo. *Nat. Biotechnol.* **26,** 443–452 (2008).

235. Rezania, A. *et al.* Maturation of human embryonic stem cell–derived pancreatic progenitors into functional islets capable of treating pre-existing diabetes in mice. *Diabetes* **61,** 2016–2029 (2012).

236. Pagliuca, F. W. *et al.* Generation of functional human pancreatic β cells in vitro. *Cell* **159,** 428–439 (2014).

237. Rezania, A. *et al.* Reversal of diabetes with insulin-producing cells derived in vitro from human pluripotent stem cells. *Nat. Biotechnol.* **32,** 1121–1133 (2014).

238. Russ, H. A. *et al.* Controlled induction of human pancreatic progenitors produces functional beta-like cells in vitro. *EMBO J.* **34,** 1759–1772 (2015).

239. Roscioni, S. S., Migliorini, A., Gegg, M. & Lickert, H. Impact of islet architecture on [beta]-cell heterogeneity, plasticity and function. *Nat. Rev. Endocrinol.* (2016).

240. Beattie, G. M. *et al.* A novel approach to increase human islet cell mass while preserving beta-cell function. *Diabetes* **51,** 3435–9 (2002).

241. Ris, F. *et al.* Impact of integrin-matrix matching and inhibition of apoptosis on the survival of purified human beta-cells in vitro. *Diabetologia* **45,** 841–50 (2002).

242. Weber, L. M. & Anseth, K. S. Hydrogel encapsulation environments functionalized with extracellular matrix interactions increase islet insulin secretion. *Matrix Biol.* **27,** 667–73 (2008).

243. Parnaud, G. *et al.* Proliferation of sorted human and rat beta cells. *Diabetologia* **51,** 91–100 (2008).

244. Hayek, A. *et al.* Growth Factor/Matrix-Induced Proliferation of Human Adult β-Cells. *Diabetes* **44,** 1458–1460 (1995).

245. Kaido, T., Yebra, M., Cirulli, V. & Montgomery, A. M. Regulation of human beta-cell adhesion, motility, and insulin secretion by collagen IV and its receptor alpha1beta1. *J. Biol. Chem.* **279,** 53762–9 (2004).

246. Parnaud, G. *et al.* Blockade of β1 Integrin–Laminin-5 Interaction Affects Spreading and Insulin Secretion of Rat β-Cells Attached on Extracellular Matrix. *Diabetes* **55,** 1413–1420 (2006).

247. Hammar, E. B. *et al.* Activation of NF-kappaB by extracellular matrix is involved in spreading and glucose-stimulated insulin secretion of pancreatic beta cells. *J. Biol. Chem.* **280,** 30630–7 (2005).

248. Bosco, D., Meda, P., Halban, P. A. & Rouiller, D. G. Importance of cell-matrix interactions in rat islet beta-cell secretion in vitro: role of alpha6beta1 integrin. *Diabetes* **49,** 233–243 (2000).

249. Otonkoski, T., Banerjee, M., Korsgren, O., Thornell, L. & Virtanen, I. Unique basement membrane structure of human pancreatic islets: implications for β-cell growth and differentiation. *Diabetes, Obes. Metab.* **10,** 119–127 (2008).

250. Kragl, M. & Lammert, E. in *The Islets of Langerhans* 217–234 (Springer, 2010).

251. Virtanen, I. *et al.* Blood vessels of human islets of Langerhans are surrounded by a double basement membrane. *Diabetologia* **51,** 1181–91 (2008).

252. Nikolova, G. *et al.* The vascular basement membrane: a niche for insulin gene expression and Beta cell proliferation. *Dev. Cell* **10,** 397–405 (2006).

253. Brissova, M. *et al.* Pancreatic islet production of vascular endothelial growth factor-a is essential for islet vascularization, revascularization, and function. *Diabetes* **55,** 2974–2985 (2006).

254. Van Deijnen, J. H. M., Van Suylichem, P. T. R., Wolters, G. H. J. & Van Schilfgaarde, R. Distribution of collagens type I, type III and type V in the pancreas of rat, dog, pig and man. *Cell Tissue Res.* **277,** 115–121 (1994).

255. Pinkse, G. G. M. *et al.* Integrin Signaling via RGD Peptides and Anti beta 1 Antibodies Confers Resistance to Apoptosis in Islets of Langerhans. *Diabetes* **55,** 312–317 (2006).

256. Wang, R. N., Paraskevas, S. & Rosenberg, L. Characterization of Integrin Expression in Islets Isolated from Hamster , Canine , Porcine , and Human Pancreas. **47,** 499–506 (1999).

257. Kantengwa, S. *et al.* Identification and characterization of alpha 3 beta 1 integrin on primary and transformed rat islet cells. *Exp. Cell Res.* **237,** 394–402 (1997).

258. Johansson, S., Svineng, G., Wennerberg, K., Armulik, A. & Lohikangas, L. Fibronectin-integrin interactions. *Front Biosci* **2,** d126–d146 (1997).

259. Wang, R. *et al.* Role for β1 integrin and its associated α3, α5, and α6 subunits in development of the human fetal pancreas. *Diabetes* **54,** 2080–2089 (2005).

260. Sengupta, D. & Heilshorn, S. C. Protein-engineered biomaterials: highly tunable tissue engineering scaffolds. *Tissue Eng. Part B Rev.* **16,** 285–293 (2010).

261. Holmes, T. *et al.* Extensive neurite outgrowth and active synapse formation on self-assembling peptide scaffolds. *PNAS* **97,** 6728–6733 (2000).

262. Kim, B.-S. & Mooney, D. J. Development of biocompatible synthetic extracellular matrices for tissue engineering. *Trends Biotechnol.* **16,** 224–230 (1998).

263. Lutolf, M. P. & Hubbell, J. A. Synthetic biomaterials as instructive extracellular microenvironments for morphogenesis in tissue engineering. *Nat. Biotechnol.* **23,** 47–55 (2005).

264. Orive, G. *et al.* Cell encapsulation: promise and progress. *Nat. Med.* **9,** 104–107 (2003).

265. Lim, F. & Sun, A. M. Microencapsulated islets as bioartificial endocrine pancreas. *Science (80-.).* **210,** 908–910 (1980).

266. Basta, G. *et al.* Long-Term Metabolic and Immunological Follow-Up of Nonimmunosuppressed Patients With Type 1 Diabetes Treated With Microencapsulated Islet Allografts Four cases. *Diabetes Care* **34,** 2406–2409 (2011).

267. Murua, A. *et al.* Cell microencapsulation technology: Towards clinical application. *J. Control. Release* **132,** 76–83 (2008).

268. Zhang, Y. *et al.* Three-dimensional scaffolds reduce islet amyloid formation and enhance survival and function of cultured human islets. *Am. J. Pathol.* **181,** 1296–1305 (2012).

269. Bhang, S. H. *et al.* Mutual effect of subcutaneously transplanted human adipose-derived stem cells and pancreatic islets within fibrin gel. *Biomaterials* **34,** 7247–7256 (2013).

270. Roshanbinfar, K. & Salahshour Kordestani, S. Encapsulating beta islet cells in alginate, alginate-chitosan and alginate-chitosan-PEG microcapsules and investigation of insulin secretion. *J. Biomater. Tissue Eng.* **3,** 185–189 (2013).

271. Chun, S. *et al.* Adhesive growth of pancreatic islet cells on a polyglycolic acid fibrous scaffold. in *Transplantation proceedings* **40,** 1658–1663 (Elsevier, 2008).

272. Cruise, G. M. *et al.* In vitro and in vivo performance of porcine islets encapsulated in interfacially photopolymerized poly (ethylene glycol) diacrylate membranes. *Cell Transplant.* **8,** 293–306 (1998).

273. Sefton, M. V, May, M. H., Lahooti, S. & Babensee, J. E. Making microencapsulation work: conformal coating, immobilization gels and in vivo performance. *J. Control. Release* **65,** 173–186 (2000).

274. Weber, L. M., He, J., Bradley, B., Haskins, K. & Anseth, K. S. PEG-based hydrogels as an in vitro encapsulation platform for testing controlled beta-cell microenvironments. *Acta Biomater.* **2,** 1–8 (2006).

275. Weber, L. M., Hayda, K. N., Haskins, K. & Anseth, K. S. The effects of cell-matrix interactions on encapsulated beta-cell function within hydrogels functionalized with matrix-derived adhesive peptides. *Biomaterials* **28,** 3004–11 (2007).

276. Khan, S., Sur, S., Newcomb, C. J., Appelt, E. A. & Stupp, S. I. Self-assembling glucagon-like peptide 1-mimetic peptide amphiphiles for enhanced activity and proliferation of insulin-secreting cells. *Acta Biomater.* **8,** 1685–1692 (2012).

277. Stendahl, J. C., Wang, L.-J., Chow, L. W., Kaufman, D. B. & Stupp, S. I. Growth factor delivery from self-assembling nanofibers to facilitate islet transplantation. *Transplantation* **86,** 478 (2008).

278. Chow, L. W., Wang, L., Kaufman, D. B. & Stupp, S. I. Self-assembling nanostructures to deliver angiogenic factors to pancreatic islets. *Biomaterials* **31,** 6154–6161 (2010).

279. Zhao, M. *et al.* The three-dimensional nanofiber scaffold culture condition improves viability and function of islets. *J. Biomed. Mater. Res. Part A* **94,** 667–672 (2010).

280. Uzunalli, G. *et al.* Improving pancreatic islet in vitro functionality and transplantation efficiency by using heparin mimetic peptide nanofiber gels. *Acta Biomater.* **22,** 8–18 (2015).

CHAPTER 2

MATERIALS AND METHODS

2.1 MATERIAL CHARACTERIZATION

2.1.1 FUNCTIONALIZED SELF-ASSEMBLING PEPTIDES PREPARATION

Self-assembling peptide (SAPs) scaffolds were made by diluting 1% (w/v in water) prototypic RAD16-I peptide (PuraMatrix^{TM}, 354250, Corning) in 14% sucrose to achieve a final concentration of 0.3%. The different tailor-made peptide sequences were commercially synthesized by Peptide 2.0 Inc. (Chantilly, VA, USA) with purity above 95%. The lyophilized peptides were dissolved in deionized water at 10 mg/mL (stock solution) and sonicated for 30 min. Then, peptides were further diluted with 14% sucrose to a final concentration of 0.3%. At this point, prototypic RAD16-I peptide was combined with the each one of the tailor-made peptides in a 95:5 blending.

2.1.2 FUNCTIONALIZED SELF-ASSEMBLING PEPTIDES CHARACTERIZATION

2.1.2.1 Congo red staining

Congo red dye binds to β-sheet structures present in RAD16-I nanofibers[1]. Therefore, when RAD16-I is tailored with peptide signaling motifs, it allows the study of these secondary structures by visual examination. RAD16-I and tailor-made peptides sequences were diluted at a final concentration of 0.3% (w/v) and samples were prepared. To that end, 40 µL of each one of the peptides was loaded in a cell culture insert (PICM01250, Merck Millipore) placed in a 24 well culture plate. Then, 100 µL of phosphate buffered saline (PBS) (L0615, Biowest) were added underneath the insert membrane in order to induce the self-assembling process. Samples were incubated during 30 min to allow the gelation process of the constructs. Then, samples were washed with PBS and incubated with 100 µL of 0.1% (w/v) Congo Red (75758, Sigma-Aldrich) for 10 min. After that time, extensive washing with PBS was carried out to remove the excess of Congo red solution. Finally, samples were analyzed in a stereoscopic microscope (Nikon SMZ660).

2.1.2.2 Circular dichroism spectroscopy

Circular dichroism (CD) spectra were acquired on a JASCO-715 spectropolarimeter (Jasco Corp.) equipped with a Peltier system. Each peptide was dissolved at 1% (w/v) (stock solution) in deionized water and sonicated for 30 min. Stock solution was then diluted to a working concentration varying from 6 to 50 µM, and samples were analyzed in a quartz cuvette with a path length of 1 cm. Spectra were obtained in a range of 195-250 nm and scan speed of 20 nm/min.

2.1.2.3 Atomic force microscopy (AFM)

Peptide stock solutions (1%, 10 mg/mL) were sonicated for 30 min. Afterwards, samples were diluted to a concentration of 0.005% (conventional RAD16-I and pure TWY), and 0.01% (pure RGD and RAD16-I/RGD) with deionized water. Then, 10 µL of each peptide were loaded onto a freshly cleaved mica surface of 9.9 mm diameter and air-dried. Images were obtained at a resolution of 256 x 256 pixels, using a XE-100 Atomic force microscope (AFM) (Park Systems), operating in non-contact mode. A silicon cantilever (ACTA 10M, Park Systems), resonance frequency of 300 KHz, force constant 40N/m, tip curvature radius < 10nm, and 125 µm was used to perform the analysis.

2.1.3 RAD16-I COATED PTFE MEMBRANES

2.1.3.1 Membrane modification by plasma grafting of PFM

Hydrophilic PTFE (polytetrafluoroethylene) membranes (JHWP02500, Merck Millipore) were cut obtaining a diameter of 20 mm. Afterwards, membranes were modified by graft polymerization of PFM (pentafluorophenyl methacrylate) (Apollo Scientific Ltd.), in order to obtain a thin coating of RAD16-I peptide, as described in Wu *et al* work[2]. The PFM modification was performed in a stainless steel vertical plasma reactor[3]. The polymerization was carried out by a 2 step process[2]. First, PTFE membranes were activated by argon plasma, which was introduced into the reactor chamber at a pressure around 1,2·10-1 mbar, and plasma was generated at 25W during 15 min. Next, argon inflow was closed and PFM vapor was introduced at 75ºC and allowed to polymerize during 25 minutes. Membranes modification by plasma grafting was performed by Anna Mas from the Materials Engineering group of IQS-School of Engineering.

2.1.3.2 Quartz crystal microbalance with dissipation monitoring (QCM-D)

The adsorption of NH_2-RAD16-I solution onto PFM-modified PTFE membranes was studied using a quartz crystal microbalance with dissipation monitoring (QCM-D, Q-Sense E1, BiolinScientific AB, Frölunda, Sweden). To that end, PTFE QCM-D sensors (QSX331, BiolinScientific AB) were coated with PFM by plasma grafting following the same procedure than in PTFE membranes. PFM offer highly reactive ester groups with affinity towards amines[4]. Thus, NH_2- GG-RAD16-I can be immobilized onto PFM-coated substrates through its terminal amino group. To assess the interaction of NH_2-GG-RAD16-I with the PFM-coated sensor the following procedure was carried out. Firstly, a baseline was acquired by flowing a PBS solution through the QCM-D chamber. Next, 0.2 % (w/v) NH_2-RAD16-I solution was flown through the chamber, causing the adsorption of the peptide molecules onto the sensor's

surface. A PBS wash was then performed in order to eliminate the excess of NH_2-RAD16-I molecules that did not reacted with the PFM coating. Finally, a MilliQ water wash was performed to demonstrate that NH_2-GG-RAD16-I molecules were covalently bound to the PFM coating. By flowing MilliQ water after the PBS wash we are changing the ionic strength of the environment. The interactions that are purely electrostatic are disrupted with a change of ionic strength, whereas covalent bonds are not broken. The experiment was performed at 25ºC. QCM-D monitoring was performed in collaboration with the Materials Engineering group of IQS-School of Engineering.

2.1.3.3 PTFE membrane coating with RAD16-I peptide layer

Once PTFE membranes were modified by plasma grafting of PFM (PTFE/PgPFM), they were soaked overnight in an aqueous solution of NH_2-GG-RAD16-I (5 mg/mL) at room temperature and soft shaking, so that RAD16-I molecules became immobilized onto PTFE membranes surface (PTFE/PgPFM/RAD16-I). The following day, PTFE/PgPFM/RAD16-I membranes were rinsed with 70% ethanol and autoclaved at 120ºC during 20 min. Then, PTFE/PgPFM/RAD16-I membranes were covered with 100 µL of RAD16-I peptide (PuraMatrix, 354250, Corning), and incubated for 1 h without the addition of culture medium, leading to a thin coating of modified membranes. Thus, gelation occurred in a more controlled and slower way through the contact with the immobilized RAD16-I strands, as compared to the usual self-assembling process initiated by the increased ionic strength due to the addition of culture medium (Figure 2.1). Finally, the coated membranes were dipped 10 times in deionized water in order to remove the non-assembled peptide and left in PBS or culture medium until needed. We followed the procedure described in Wu *et al*[2], although with some modifications.

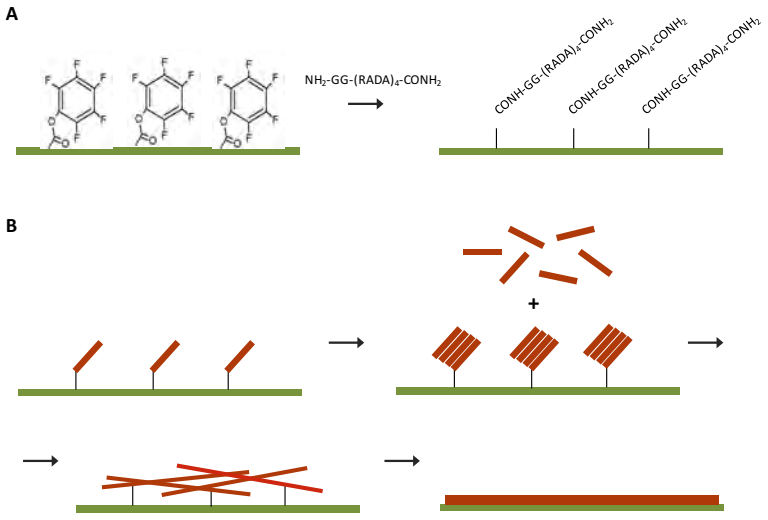

Figure 2.1. Coating of PFM-modified PTFE membranes with nanometric RAD16-I peptide layers. (A) After plasma deposition of pentafluorophenyl methacrylate (PFM) on porous membranes surfaces, modified membranes were incubated with an aqueous solution of NH_2-RAD16-I allowing the immobilization of RAD16-I molecules to the deposited PFM. (B) After immobilization of RAD16-I molecules onto membranes surface, they were covered with commercial RAD16-I peptide, and using RAD16-I strands as attachment points, a thin layer of peptide was assembled. Adapted from Wu *et al*[2].

2.1.3.4 Scanning electron microscopy (SEM)

Modified PTFE membranes were examined under a scanning electron microscope (SEM) in order to study the presence of RAD16-I nanofibers after treatment. First, modified membranes were washed with PBS and fixed with 2% (w/v) paraformaldehyde (PFA) for 40 min. Afterwards, four washing steps with PBS were performed (2 min each). Then, samples were dehydrated in a multi-step process consisting of several immersions in increasing concentrations of ethanol solutions of 10 min each: once in 50% (v/v) ethanol, twice in 60% (v/v) ethanol, twice in 70% (v/v) ethanol, twice in 80% (v/v) ethanol, three times in 90% (v/v) ethanol, three times in 96% (v/v) ethanol and three times in 100% (v/v) ethanol. Once dehydrated, samples were dried using a CO_2 critical point dryer (Emitech K850). Bare PTFE membranes and membranes thinly coated with RAD16-I peptide were gold-coated using a Polaron SC7620 Sputter Coater and examined with a field emission SEM (JOEL JSM-5310) at an accelerating voltage of 15 kV. On the other hand, PTFE membranes incubated with the aqueous solution of NH_2-GG-RAD16-I (PTFE/PgPFM/RAD16-I) were coated with a thin layer of graphite (Emitech K950X) and examined under a JEDL J-7100 field emission SEM (Cathodeluminiscence spectrometer GATAN MONO-CL4, EDS detector, retroscattered electron detector) at an accelerating voltage of 15 kV. A control condition of a membrane without PFM modification, but covered with RAD16-I peptide, was included.

2.2 2D CELL CULTURE

2.2.1 HUMAN PANCREATIC ISLET CELL ISOLATION FROM ORGAN DONORS

Pancreatic islets were isolated from adult cadaveric organ donors by collagenase digestion (Collagenase NB1 Premium Grade with Neutral Protease NB, Serva Electrophoresis GmbH) using the Ricordi method[5] with some modifications[6]. The islets were purified on a refrigerated COBE 2991 cell processor (COBE BCT, Lakewood, CO, USA) with a continuous density gradient. Islet purity was determined by staining with dithizone (D5130, Sigma-Aldrich). Isolated islets were cultured in CMRL 1066 medium (15-110-CV, Mediatech Inc., Corning Cellgro) containing 5.6 mM glucose and supplemented with 10% ABO-compatible human serum (Blood and Tissue Bank, BST, Barcelona), 2 mM L-glutamine (25030-024, Gibco), 10 mM HEPES (SH30237.01, GE Healthcare), 40 µg/mL gentamycin (636183, Braun), 0.25 µg/mL fungizone (A294250 Sigma-Aldrich), 20 µg/mL ciprofloxacin (619064, Fresenius-Kabi), 10 mM nicotinamide (N5535, Sigma-Aldrich) and 5 mM sodium pyruvate (P3662, Sigma-Aldrich)[7]. Cells were culture for 24-48h until dissociated into single cells with 0.16 mg/ml trypsin (T4799, Sigma-Aldrich) and 0.1 mM EDTA (ED2SS, Sigma-Aldrich) and sorted. Single endocrine cells were purified by magnetic activated cell sorting (MACS)[8], using a MiniMACS magnetic cell separation system according to the manufacturer instructions (Miltenyi Biotech). PSA-NCAM antibody (130-092-966, Miltenyi Biotech) was used as a positive selection marker of endocrine cells. As a result of the purification an enriched-endocrine fraction was obtained. Islet isolation and purification was

performed by the research group on Diabetes, Nutrition and Endocrine diseases, at the Institute of Biomedical Research of Bellvitge (IDIBELL). The experiments were approved by the Ethics Committee of the Hospital Universitari de Bellvitge. Written informed consent was obtained from the relatives of organ donors.

2.2.2 2D CULTURE OF HUMAN PANCREATIC SORTED CELLS

The enriched-endocrine fractions resulting from the isolation and purification of human pancreatic islets were seeded in monolayer and cultured with CMRL 1066 5.6 mM glucose, supplemented with 10% fetal bovine serum (FBS) (10270-106, Gibco), 2 mM L-glutamine (25030-024, Gibco), 10 mM HEPES (SH30237.01, GE Healthcare), 40 µg/mL gentamycin (636183, Braun), 0.25 µg/mL fungizone (A294250 Sigma-Aldrich), 20 µg/mL ciprofloxacin (619064, Fresenius-Kabi), 10 mM nicotinamide (N5535, Sigma-Aldrich) and 5 mM sodium pyruvate (P3662, Sigma-Aldrich) (expansion media). The medium was changed twice a week, and the islet cell population was split 1:2 once a week using 0.25% trypsin-EDTA (T4049, Sigma-Aldrich) and expanded in culture up to 12 passages. Cells were maintained at 37ºC in a humidified incubator with 5% CO_2. Expansion of sorted cells was performed by the research group on Diabetes, Nutrition and Endocrine diseases, at the Institute of Biomedical Research of Bellvitge (IDIBELL).

2.2.3 INDUCTION OF ISLET-LIKE CELL CLUSTERS (ICCs) FORMATION

At passage 7-8, expanded cells were trypsinized and seeded on non-adherent bacteriological Petri dishes (90 x 14 mm, 200209, Deltalab) at a cell density of 100,000 cells/mL, and cultured in expansion media. After 48 h the cells clustered and formed independent cell colonies (islet-like cell clusters, ICCs) that were seeded into the cell culture inserts (see 3D cell culture section).

2.2.4 2D CULTURE OF INS-1E CELL LINE

INS-1E rat insulinoma cell line was kindly provided by Dr. Sara Cervantes from the Diabetes and Obesity research laboratory, at August Pi i Sunyer Biomedical Research Institute (IDIBAPS). INS-1E cells were cultured on 25 and 75 cm^2 traditional plastic flasks with Roswell Park Memorial Institute's medium (RPMI) 1640 (31870-025, Gibco), containing 11.2 mmol/L glucose and supplemented with 10% (v/v) Fetal Bovine Serum (FBS, DE14-801F, Lonza), 100 U/ml penicillin and 100 µg/ml streptomycin (L0022, Biowest), 10 mmol/L HEPES (L0180, Biowest), 2 mmol/L L-glutamine (X0550, Biowest), 1 mmol/L sodium pyruvate (S8636, Sigma-Aldrich) and 50 µM β-

mercaptoethanol (M7522, Sigma-Aldrich). All experiments were performed at 70-80% confluence and cells were used between passages 43 and 49. Cells were maintained at 37ºC in a humidified incubator with 5% CO_2.

2.3 2D CELL CULTURE CHARACTERIZATION

2.3.1 IMMUNOSTAINING OF HUMAN PANCREATIC ISLET-DERIVED CELLS

Immunostaining was performed to characterize the cell population in MACS-purified dispersed human islet cells and after expansion in monolayer cultures. Cells were cultured in flexiPERM micro 12 (94.6011.436, Sarstedt) and fixed in 4% paraformaldehyde (PFA) at room temperature for 15 min. Antigen retrieval was performed using a microwave in citrate buffer (pH 6.0). Cells were washed, blocked for 1 h with 5% horse serum at room temperature and then incubated overnight at 4ºC with the primary antibodies: rabbit polyclonal anti-insulin antibody (1:100; Santa Cruz Biotechnology Inc, Texas, USA), mouse anti-vimentin antibody (1:50; Dako, Barcelona, Spain), rabbit anti-amylase (1:50; Sigma-Aldrich, St. Louis, MO, USA) and mouse anti-cytokeratin (1:80; Dako). Alexa fluor-conjugated donkey anti-rabbit and goat anti-mouse (1:400; Invitrogen) were used as secondary antibodies. Nuclei were stained with 4'6-diamidino-2-phenylindole dihydrochloride (DAPI) (300nM) (D3571, Life Technologies). Images were acquired using a Leica DFC 310FX and Leica TCS-SL filter-free spectral confocal laser scanning microscope (Leica Microsystems). Immunostaining of expanded cells was performed by the research group on Diabetes, Nutrition and Endocrine diseases, at the Institute of Biomedical Research of Bellvitge (IDIBELL).

2.4 3D CELL CULTURE

2.4.1 STANDARD 3D CULTURE TECHNIQUE IN RAD16-I PEPTIDE

Preparation of nanofiber hydrogel scaffolds was made by diluting 1% (w/v) RAD16-I (PuraMatrix^{TM}, 354250, Corning) to obtain a final concentration of peptide two-fold higher the desired one in 10% (w/v) sucrose. The working concentration of RAD16-I used in the present thesis was 0.3%. However, other concentrations were tested in order to establish the optimal working concentration for each cell type. In particular, 0.15% in the case of human islets cells and 0.15% and 0.4% for INS-1E cells. Thus, in order to prepare 1 mL of peptide hydrogel at 0.6% (stock solution), 600 µL of commercial peptide (1%) were mixed with 400 µL of 25% sucrose. Before mixing, RAD16-I commercial peptide was placed in the ultrasonic bath for 5 min. Following RAD16-I stock preparation, cells were harvested by trypsinization from the 2D culture flasks and suspended in 10% sucrose, in order to get a concentration of $4 \cdot 10^6$ cells/mL (human islet cells) and $8 \cdot 10^6$ cells/mL (INS-1E). Other cell densities were tested for human islet

cells ($8 \cdot 10^6$ cells/mL and $1.6 \cdot 10^7$ cells/mL). The following step consisted of mixing the peptide with an equal volume of cell suspension at $4 \cdot 10^6$ cells/mL (human islet cells) and $8 \cdot 10^6$ cells/mL (INS-1E) to get a final suspension of $2 \cdot 10^6$ cells/mL and $4 \cdot 10^6$ cells/mL respectively, in 0.3% RAD16-I.

Within this standard encapsulation technique, two different variants were carried out. In the first one, the suspension (20 µL or 40 µL of cell-peptide mixture for human islet cells and 40 µL for INS-1E cells) was loaded individually into 48 well culture plates. In particular, non-treated plates were used in order to avoid unspecific adhesion of the gels to the well surface. Previously, 150 µL of medium had been added into every single well. The higher ionic strength and the neutral pH of the medium induce the spontaneous self-assembling of the peptide. Then, culture plates were placed in the incubator for 20 min, time during which gelation of the RAD16-I peptide occurred. After that time 650 µL of medium were added carefully into each well and 3D cultures were eventually maintained at 37ºC in a humidified incubator with 5% CO_2. A change of medium was performed every two days, by removing 400 µL from the well and adding 400 µL of fresh medium. This method was used for both cell types. A schematic representation of this protocol is shown in Figure 2.2.

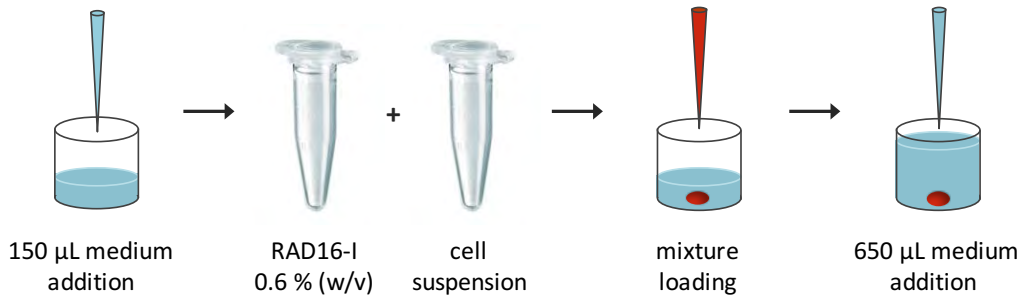

Figure 2.2. Schematic representation of the standard cell encapsulation procedure in RAD16-I self-assembling peptide. Firstly, 150 µL of medium were loaded in a 48 well culture plate. Afterwards, RAD16-I 0.6% (w/v) was mixed in a 1:1 ratio with the cell suspension. The mixture was then loaded into the center of the wells, and the higher ionic strength and the neutral pH of the medium induced the spontaneous self-assembling of RAD16-I peptide. Finally, the well was filled with cell culture medium.

On the other hand, in order to obtain thinner scaffolds, PTFE membranes were used. In this particular case, the suspension was loaded on top of hydrophilic PTFE (polytetrafluoroethylene) membranes (JHWP02500, Merck Millipore). Membranes had a diameter of 25 mm, therefore 6 well culture plates were used. Since membranes had not been wet with culture medium before loading, the cell-peptide suspension penetrated inside the membrane getting attached. This lead to the formation of a thinner layer of cell-peptide mixture. Afterwards, cell medium was added very carefully underneath the membrane, inducing gelation of RAD16-I peptide. Culture plates were kept in the incubator for 20 min and after that time a minimum amount of medium was added over the constructs, in a careful

manner, since at this moment constructs were very fragile. Cultures plates were left for another 20 min in the incubator and 2 mL of medium were added. Constructs were eventually maintained at 37ºC in a humidified incubator with 5% CO_2. A change of medium was performed every two days, by removing 1 mL from the well and adding 1 mL of fresh medium. This specific encapsulation method was only used for human islet cells with volumes of 20 and 40 µL. A schematic representation of this protocol is shown in Figure 2.3.

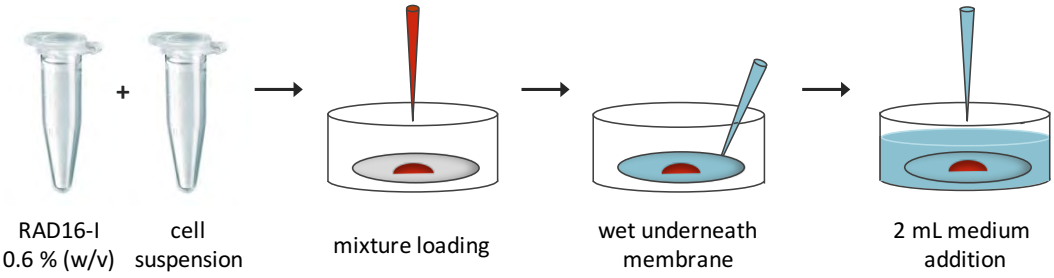

Figure 2.3. Schematic representation of the standard cell encapsulation procedure in RAD16-I self-assembling peptide, using PTFE membranes. First, RAD 0.6% (w/v) was mixed with the cell suspension. Then, the cell-peptide mixture was loaded onto PTFE membranes. Very carefully, medium was added underneath the membrane, which induced RAD16-I gelation. Finally, the well was filled with cell culture medium.

When functionalized RAD16-I was used, prototypic RAD16-I was combined with the tailor-made peptides motifs in a 95:5 ratio at the corresponding concentration. Specifically, to obtain a final concentration of 0.3%, prototypic 1% (w/v in water) RAD16-I was diluted in 25% sucrose to achieve a 0.6% concentration. The lyophilized tailor-made peptide sequences were dissolved in deionized water at 10 mg/mL (stock solution) and sonicated for 30 min. Following sonication, peptides were further diluted with 25% sucrose to a final concentration of 0.6%. Afterwards, pure 0.6% RAD16-I was mixed with each one of the 0.6% tailor-made sequences solutions at a 95:5 ratio. Finally, functionalized 0.6% RAD16-I was mixed with the cell suspension, obtaining a final concentration of functionalized RAD16-I of 0.3%.

For both versions of the standard 3D technique in RAD16-I SAP, culture medium for human islet cells and INS-1E cells was the same than the used in 2D cultures.

2.4.2 3D CULTURE TECHNIQUE IN TYPE I COLLAGEN

Collagen gels were prepared from natural type I collagen, extracted from rat tail, with a concentration of 1% (w/v) (354236, BD Biosciences). The working concentration of type I collagen was 0.3% (w/v). A stock of collagen 0.6% (w/v) was prepared by mixing 1 µL of Phenol Red with 99 µL of 10x PBS, 300 µL of tissue culture water and 600 µL of collagen type I

10mg/mL. Collagen self-assembling takes place when pH is brought to alkalinity. Thus, 0.6% collagen solution was taken to alkalinity by the addition of sodium hydroxide (NaOH) and pH was checked with a pH test paper to make sure it ranged between 8 and 9. This step was performed in ice avoiding collagen gelation before mixing the solution with the cell suspension, since at lower temperatures collagen gelation occurs in a slower way. Following collagen stock preparation, cells were harvested by trypsinization from the 2D culture flasks and suspended in PBS, in order to get a concentration of $4 \cdot 10^6$ cells/mL (human islet cells) and $8 \cdot 10^6$ cells/mL (INS-1E). The following step consisted of mixing an equal volume of $4 \cdot 10^6$ cells/mL (human islet cells) or $8 \cdot 10^6$ cells/mL (INS-1E) cell suspensions with 0.6% collagen type I, to get a final cell suspension of $2 \cdot 10^6$ cells/mL (human islet cells) and $4 \cdot 10^6$ cells/mL (INS-1E) in 0.3% (w/v) type I collagen.

As in the case of RAD16-I biomaterial, two variants of the standard collagen encapsulation method were performed (see 2.4.1 section). INS-1E and human islet cells were encapsulated following the first variant, loading 40 µL of suspension into each well (48 well non-treated plates). Plates were then placed at 37ºC for 30 min, time during which gelation occurred due to the increased temperature. Afterwards, 800 µL of medium were added on top of the constructs. 3D cultures were eventually maintained at 37ºC in a humidified incubator with 5% CO_2. A change of medium was performed every two days, by removing 400 µL and adding 400 µL of fresh medium.

On the other hand, human islet cells were also encapsulated in type I collagen using the second variant, in which PTFE membranes were used. To that end, 40 µL of suspension were loaded on top of membranes and were left 30 min at 37 ºC, to allow the gelation occur due to the increased temperature. Then, a minimum amount of medium was added over the constructs, in a careful manner, since at this moment constructs were still fragile. Culture plates were kept again in the incubator for 10 min, and finally 2 mL of medium were added into each well of the 6 well culture plate. 3D cultures were eventually maintained at 37ºC in a humidified incubator with 5% CO_2. A change of medium was performed every two days, by removing 1mL from the well and adding 1 mL of fresh medium.

For both versions of the standard 3D technique in type I collagen, culture medium for human islet cells and INS-1E cells was the same than the used in 2D cultures.

2.4.3 RAD16-I SANDWICH CULTURE SYSTEM

The sandwich culture system was carried out solely with human islet cells. Cell culture inserts (PICM01250, Merck Millipore) were placed in 24 well culture plates and coated with 40 µL of 0.3% (w/v) pure RAD16-I or RAD16-I functionalized with the RGD adhesive motif. Another concentration of RAD16-I was tested (0.15%) but peptide layer was too fragile and it broke after the addition of cells. Since RAD16-I peptide forms a hydrogel when the ionic strength increases, 200 µL of expansion medium were added underneath the insert membrane,

inducing gel formation due to a self-assembling process. This volume of peptide created a layer of 0.5 mm thickness[9]. After 30 min, 10 µL of expansion media were added to the cell culture inserts in order to equilibrate the scaffolds during another 30 min. ICCs cultured on non-adherent bacteriological Petri dishes during 48 h were detached using a cell-scrabble and were loaded into the cell culture inserts, at a cell density of 100,000 cells/insert (different cell densities were tested). ICCs were left to attach for 48 h at 37ºC and afterwards a washing step with 10% sucrose was performed to remove unattached clusters. Following the washing step, a second layer of 0.3% RAD16-I or functionalized RAD16-I/RGD was added on top of the clusters, and 200 µL of serum-free medium (CMRL 1066 5.6 mM glucose) supplemented with ITS (I3146, Sigma-Aldrich), were added beneath the insert membrane to initiate the self-assembling process of RAD16-I. Therefore, ICCs were embedded between two layers of 0.3% RAD16-I or RAD16-I/RGD peptide (sandwich culture system, Figure 2.4). The second layer of peptide was allowed to gel for 1 h in the cell incubator and a volume of 10 µL of culture medium was then added inside the insert and kept in the cell incubator for 15 min. A final volume of 120 µL of serum-free medium was carefully added on top of the second layer of RAD16-I or RAD16-I/RGD, and 400 µL were added outside the insert. The sandwich cultures were maintained for 18 days at 37ºC in a humidified incubator with 5% CO_2, and 60 µL of culture medium inside the insert and 300 µL in the well were removed and replaced with fresh medium every two days. Figure 2.4 depicts the different steps involved in this protocol. As a control condition, ICCs were cultured in non-adherent bacteriological Petri dishes for 18 days.

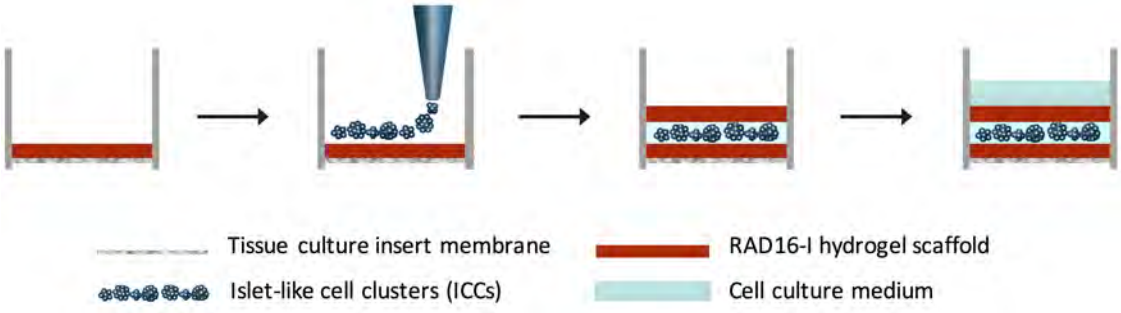

Figure 2.4. Schematic representation of the RAD16-I sandwich culture establishment. First, cell culture inserts were coated with 40 µL of pure or functionalized RAD16-I that gelled after the addition of medium. Then, ICCs were seeded on top of the thin layer of RAD16-I peptide and allowed to attach for 48 h. A second layer of pure or functionalized peptide was added, entrapping the clusters in a sandwich fashion. Finally, cell culture medium was added into the insert covering the whole construct.

2.4.4 PTFE MEMBRANE-BASED RAD16-I SANDWICH CULTURE SYSTEM

The PTFE membrane-based sandwich culture system was only carried out with human islet cells. Cell culture inserts were bigger than in standard RAD16-I sandwiches. Specifically, they had a diameter of 30 mm (4.2 cm^2) compared to the 12 mm (0.6 cm^2) of the inserts used for the standard sandwich culture system. First, PTFE membranes (JHWP02500, Merck Millipore) were cut obtaining a diameter of 20 mm (3.14 cm^2). Afterwards, membranes were modified by graft polymerization of PFM (pentafluorophenyl methacrylate) as described in 2.1.3.2 section

(day 1). Once PTFE membranes were modified by plasma grafting of PFM (PTFE/PgPFM), they were soaked overnight in an aqueous solution of NH_2-GG-RAD16-I (5 mg/mL) at room temperature and soft shaking, so that RAD16-I molecules became immobilized onto PTFE membranes surface (PTFE/PgPFM/RAD16-I), as described in Wu *et al*[2]. The same day, cell culture inserts (PICM03050, Merck Millipore) were placed in a 6 well culture plate and were coated with a very thin layer, 250 µL, of 1% RAD16-I or functionalized RAD16-I. Lower concentrations were tested, 0.3% and 0.6%, but both of them broke. Culture medium was added underneath the insert to wet the membrane and induce the gelation of RAD16-I. Plates were maintained for 1 h at 37ºC and after that time, 200 µL of expansion medium were added inside the insert to equilibrate the scaffolds and maintained for another 30 min. Then, ICCs cultured on non-adherent bacteriological Petri dishes during 48 days were detached using a cell scraper and were seeded into the cell culture inserts, at a cell density of 350,000 cells/insert (different cell densities were tested). ICCs were left to attach for 48 h at 37ºC.

The day after seeding ICCs into cell culture inserts (day 2), membranes with immobilized RAD16-I peptide on the surface, PTFE/PgPFM/RAD16-I membranes, were rinsed with 70% ethanol and autoclaved at 120ºC during 20 min. Then, PTFE/PgPFM/RAD16-I membranes were covered with 100 µL of 1% RAD16-I or functionalized RAD16-I peptide, and left 1 h without the addition of culture medium, therefore, leading to a thin coating of modified membranes. Thus, gelation occurred in a more controlled and slower way through the contact with the immobilized RAD16-I strands, as compared to the usual self-assembling process initiated by an increase of the ionic strength due to the addition of culture medium. Then, the coated membranes were dipped 10 times in deionized water in order to remove the excess on non-assembled peptide, and were left in cell culture medium until needed.

On the next day (day 3), the culture medium media contained in ICCs-seeded cell culture inserts, as well as the medium outside the insert, was withdrawn. At that moment, membranes thinly coated with RAD16-I or functionalized RAD16-I peptide were inverted and placed over the cell culture inserts and were left without medium for 5 hours. During this time, ICCs grown on cell culture inserts attached to the upper membrane, embedding ICCs between two very thin layers of peptide in a sandwich configuration. Small amounts of serum-free medium (CMRL 1066 5.6 mM glucose) supplemented with ITS (I3146, Sigma-Aldrich) were added consecutively inside the insert. The total final volume of medium inside the insert was 300 µL and 1,400 µL outside. From that moment on, cultures were maintained for 18 days at 37ºC in a humidified incubator with 5% CO_2. Medium inside the insert was replaced every day with 300 µL of fresh medium and medium outside the insert was replaced twice a week. Figure 2.5 depicts the different steps involved in this protocol.

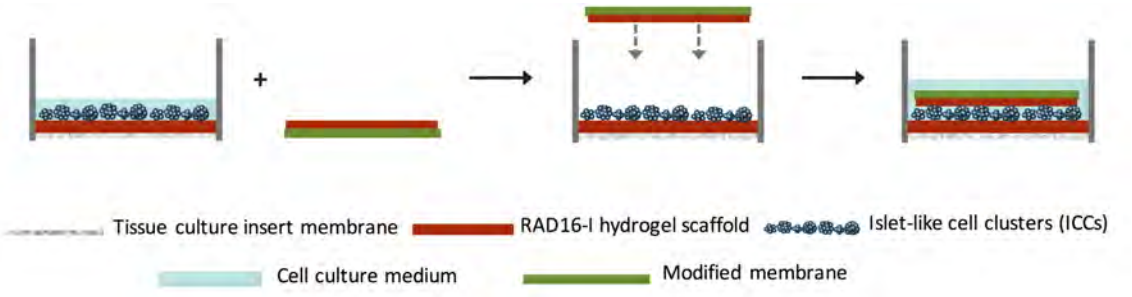

Figure 2.5. Schematic representation of the PTFE membrane-based RAD16-I sandwich culture system. First, cell culture inserts were coated with 250 µL of pure or functionalized RAD16-I that gelled after the addition of medium. Then, ICCs were seeded on top of the thin layer of RAD16-I peptide and allowed to attach for 48 h. PTFE/PgPFM membranes with a nanometric layer of pure or functionalized RAD16-I peptide were turned upside down and place on top of ICCs, entrapping the cells in a sandwich fashion. After 5 hours, cell culture medium was added.

2.5 3D CELL CULTURE CHARACTERIZATION

2.5.1 CELL MORPHOLOGY ASSESSMENT

Cell morphology and organization in 3D cultures was assessed using an inverted microscope (Nikon Eclipse TS100) at different time points. Moreover, cell morphology was also evaluated by fluorescence microscopy. To that end, staining of the cytoskeleton and nuclei were performed. Samples were washed three times with PBS and fixed with 2% (w/v) PFA during approximately 20 min. Three more washing steps with PBS were done in order to remove the excess of PFA. Following the consecutive washes, samples were incubated with 0.1% (v/v) Triton x-100, a membrane permeabilization agent, for 30 min. During that time, Phalloidin–Tetramethylrhodamine B isothiocyanate, Phalloidin-TRITC (P1951, Sigma Aldrich) and 4',6-Diamidino-2-phenylindole dihydrochloride, DAPI (D9542, Sigma Aldrich) solutions were prepared at concentrations of 1 mg/mL and 1 µg/mL, respectively, in PBS 1x, and were protected from the light. Phalloidin is conjugated to TRITC (ex 540-545 nm, em 570-573 nm) and binds to polymeric F-actin of the cytoskeleton allowing the visualization of the cytoskeleton. DAPI is a blue fluorescent probe (ex 364 nm, em 454 nm) that selectively binds to the minor groove of double stranded DNA, displaying a fluorescence approximately 20-fold greater than in the unbound state. Therefore, it enables the visualization of the cellular nuclei.

After permeabilization, three more washing steps with PBS were done. Samples were then incubated with Phalloidin-TRITC 1 mg/mL during 25 min, and without removing Phalloidin-TRITC solution, the same volume of DAPI solution 1 µg/mL was added. Samples were incubated for 5 more min and extensive washing with PBS was carried out. Samples were examined under a Zeiss Axiovert inverted microscope (Axiovert 200M, Carl Zeiss Inc.) with the

Zeiss ApoTome system, which allowed optical sectioning and subsequent 3D reconstruction (Z-stack images).

2.5.2 CELL NUMBER AND CLUSTERS AREA ASSESSMENT

ICCs number and area in standard sandwich cultures was sequentially assessed at different time points. The same inserts were analyzed at each measurement. Pictures of clusters from at least 3 inserts from 3 different islet isolations were taken using an inverted microscope (Nikon Eclipse TS100, Tokyo, Japan), and the area of at least 80 clusters/insert was measured using Image J software.

2.5.3 CELL VIABILITY ASSESSMENT

2.5.3.1 Cell viability imaging

Viability of 3D constructs was determined using the LIVE/DEAD® Viability/Cytotoxicity Kit, for mammalian cells (L3224, Invitrogen) at different time points along the cultures. Construct samples were washed 3 times with PBS. Live/dead assay reagents, calcein-AM and ethidium homodimer-1, were diluted to a final concentration of 2 µM in PBS. Both dyes become fluorescent when interacting with either live (calcein-AM) or dead (ethidium homodimer-1) cells. Calcein-AM (calcein acetomethyl ester) converts to the strongly green fluorescent calcein (ex 494nm, em 517 nm) when hydrolyzed by intracellular esterases in live cells. On the other hand, ethidium homodimer-1 enters cells with damaged membrane and produces a bright red fluorescence when bound to nucleic acids (ex 517 nm, em 617 nm). Samples were covered with the working solution for 15 min, rinsed 3 times with PBS in order to remove the excess of reagents, and examined under a Zeiss Axiovert inverted microscope (Axiovert 200M, Carl Zeiss Inc) with the Zeiss ApoTome system, which allowed optical sectioning and subsequent 3D reconstruction (Z-stack images).

In human islet cells encapsulated with the standard encapsulation system in RAD16-I cultures (using PTFE membranes), live and dead cells were counted and results were expressed as percentage of viable cells over the total number of cells. In human islet cells cultured in sandwich configuration, live and dead cells were counted and results were expressed as percentage of viable cells per ICC. Samples were examined under a Zeiss Axiovert inverted microscope (Axiovert 200M, Carl Zeiss Inc.) with the Zeiss ApoTome system, which allowed optical sectioning and the subsequent 3D reconstruction (Z-stack images).

2.5.3.2 MTT assay

3D cell cultures viability was also measured with the quantitative MTT assay[10]. This is a colorimetric assay that measures the reduction of yellow tetrazolium salt, MTT (3-(4,5-dimethylthiazolyl-2)-2,5-diphenyltetrazolium bromide) (M5655-1G, Sigma Aldrich) by dehydrogenase enzymes of the mitochondria into insoluble purple formazan crystals (Figure 2.6). The resulting intracellular purple formazan product can be solubilized with an organic solvent (DMSO), and measured spectrophotometrically at 570 nm. The amount of formazan generated is directly proportional to the number of living cells and the signal generated is dependent on the degree of activation of the cells.

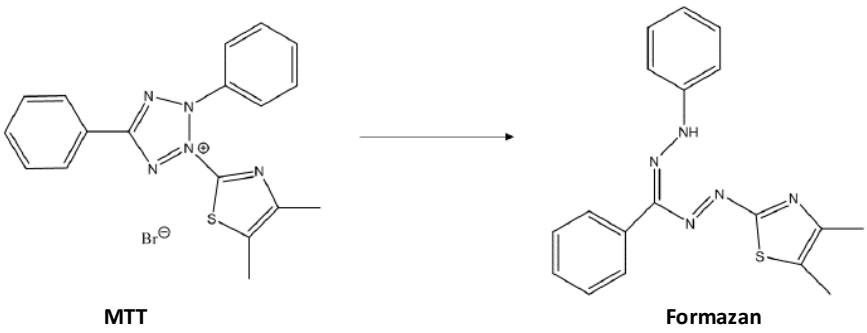

Figure 2.6. Reduction of MTT reagent to formazan. The present reaction is catalyzed by dehydrogenase enzymes of the mitochondria.

Briefly, MTT was dissolved at a concentration of 5 mg/mL in PBS (stock solution), filtered sterilized, and diluted in culture medium to a concentration of 0.5 mg/mL. In order to cover the entire sample, 500 µL were added into wells or cell culture inserts at different time points along the culture. After 3 h incubation at 37ºC, MTT solution was removed very carefully and one wash step with PBS was performed. Then, 200 µL and 400 µL of dimethyl sulfoxide (DMSO) were added for ICCs and INS-1E cells respectively, and the purple formazan crystals were solubilized by repeated pipetting. For ICCs in standard sandwich cultures, groups of three samples were pooled. Solution was then transferred to an eppendorf and vortexed for 2 min. Finally, 200 µL of the homogeneous solution were transferred to 96 well plates in triplicate, and the absorbance was read at 570 nm using a microplate reader (SpectraMax M2e). Results were expressed as optical density and the OD of blank (DMSO) was subtracted from the samples.

2.6 GLUCOSE-STIMULATED INSULIN SECRETION (GSIS)

Insulin secretion in response to glucose stimulation was determined in pure and functionalized RAD16-I cultures of INS-1E cells at the end of the culture period (day 10). Five samples from each condition were analyzed. Briefly, culture medium was removed from the wells and samples were rinsed twice with Krebs-Ringer Bicarbonate Hepes (KRBH) buffer (129 mM NaCl,

4.7 mM KCl, 1.2 mM $MgSO_4$, 2.5 mM $CaCl_2$, 5 mM $NaHCO_3$, 1.2 mM $KH2PO_4$, 0.1% BSA and 10 mM Hepes). Afterwards, samples were starved for 1 h with KRBH buffer without glucose and incubated with KRBH buffer with a low glucose concentration (2.8 mM, basal glucose concentration) for 1 h, followed by a 1h incubation in high glucose concentration (16.8 mM

glucose, stimulatory glucose concentration). High glucose concentration supernatants were collected for insulin measurement. All incubations were performed at 37ºC and continuous shaking in order to allow a better diffusion within 3D constructs. Finally, three washing steps of 10 min each with PBS were carried out, and samples were lysed by repeated pipetting in PBS.

Insulin secretion was measured using the ELISA kit for insulin (10-1250-01, Mercodia), according to the manufacturer's protocol. The principle of the insulin sandwich ELISA relies on the use of two monoclonal antibodies that are directed against separate determinants on the insulin molecule. During the incubation time, insulin reacts with the peroxidase-conjugated anti-insulin antibodies and anti-insulin antibodies bound to the well. Insulin conjugates are then detected using TMB as a substrate for peroxidase. Optical density was measured at 450 nm in a ELx808 Absorbance Reader (BioTek).

In order to normalize insulin secretion within the different samples, the DNA content of each sample was determined. To that end, samples previously lysed with PBS, were sonicated and centrifuged, and supernatants were collected. Fluorometric quantification of DNA was then performed, using the fluorescent dye bisBenzimide (Hoechst 33258) (B2883, Sigma-Aldrich). BisBenzimide binds primarily to AT sequences of the double-stranded DNA and upon excitation at 360 nm, the fluorescence emission at 460 nm of the dye increases significantly in the presence of DNA.

2.7 RNA ISOLATION, QUANTIFICATION, RETROTRANSCRIPTION AND qPCR

Total RNA was extracted from ICCs in sandwich cultures on days 10 and 18, as well as from 2D cultures using the RNAeasy Plus Mini kit (74134, Qiagen) according to the manufacturer's instructions. First, ICCs maintained in non-adherent Petri dishes and sandwich cultures were washed with PBS. Then, they were lysed with lysis buffer and repeated pipetting. For standard sandwich cultures, groups of 10 and 15 inserts from day 10 and 18 respectively, were pooled. For the modified sandwich cultures, 2 inserts were pooled.

Once purified, RNA quantity and quality was assessed with the Agilent 2100 Bioanalyzer (Agilent Technologies, Inc.). The RNA integrity (RIN) score ranged from 6.6 to 9.3. cDNA was then synthesized using High Capacity cDNA RT Kit (4368814, Applied Biosystems) followed by RNaseH treatment (18021-071, Invitrogen). qPCR reaction was carried out in triplicates using TaqMan Universal PCR Master Mix in 7900 Real-Time PCR System (Applied Biosystems).

Primers used are listed in Table 2.1 Analysis of relative gene expression was calculated using the $2^{-\Delta\Delta Ct}$ method using human TATA-box binding protein (TBP) and human large ribosomal protein (RPLP0) as endogenous controls. Cycle number of 40 was used for undetectable transcripts.

Table 2.1. List of qPCR primers

Gene Name	Gene Symbol	Taqman Probes
Cadherin-E	Cdh-1	Hs 01013953_m1
Cadherin-N	Cdh-2	Hs 00169953_m1
Glyceraldehyde-3-phosphate dehydrogenase	Gapdh	Hs 99999905_m1
Insulin	Ins	Hs 00355773_m1
MafA	MafA	Hs 01651425 s1
MafB	MafB	Hs 00534343 s1
Neuronal Differentiation 1	NeuroD1	Hs 01922995 s1
Nk6 homebox 1	Nkx6.1	Hs 00232355_m1
Pancreatic And Duodenal Homeobox 1	Pdx1	Hs 00363733 m1
Ribosomal protein large P0	Rplp0	Hs 99999902_m1
TATA-box-binding protein	Tbp	Hs 99999910_m1
Vimentin	Vim	Hs 00185584_m1

2.8 STATISTICAL ANALYSIS

Statistical analysis was performed using SPSS 15.0 and GraphPad Prism 5.0. Data were expressed as mean ± SEM and differences among means were analyzed using the one-way analysis of variance (ANOVA) and the Tukey's test for post-hoc analysis or Student's t-test, as appropriate. Data not normally distributed were expressed as median with interquartile range (Mdn [IQR]) and analyzed using Kruskal-Wallis one-way analysis of variance and the post-hoc Dunn's test. A *P* value of <0.05 was considered significant.

2.9 REFERENCES

1. Klunk, W. E., Pettegrew, J. W. & Abraham, D. J. Quantitative evaluation of congo red binding to amyloid-like proteins with a beta-pleated sheet conformation. *J. Histochem. Cytochem.* **37,** 1273–1281 (1989).

2. Wu, J. *et al.* Nanometric self-assembling peptide layers maintain adult hepatocyte phenotype in sandwich cultures. *J. Nanobiotechnology* **8,** 29 (2010).

3. Gilabert-Porres, J. *et al.* Design of a Nanostructured Active Surface against Gram-Positive and Gram-Negative Bacteria through Plasma Activation and in Situ Silver Reduction. *ACS Appl. Mater. Interfaces* **8,** 64–73 (2016).

4. Francesch, L., Garreta, E., Balcells, M., Edelman, E. R. & Borrós, S. Fabrication of bioactive surfaces by plasma polymerization techniques using a novel acrylate-derived monomer. *Plasma Process. Polym.* **2,** 605–611 (2005).

5. Ricordi, C., Lacy, P. E. & Scharp, D. W. Automated islet isolation from human pancreas. *Diabetes* **38,** 140–142 (1989).

6. Goto, M. *et al.* Refinement of the automated method for human islet isolation and presentation of a closed system for in vitro islet culture. *Transplantation* **78,** 1367–75 (2004).

7. Nacher, M. *et al.* Human serum versus human serum albumin supplementation in human islet pretransplantation culture. In vitro and in vivo assessment. *Cell Transplant.* **25,** 343–52 (2016).

8. Banerjee, M. & Otonkoski, T. A simple two-step protocol for the purification of human pancreatic beta cells. *Diabetologia* **52,** 621–5 (2009).

9. Genové, E. *et al.* Functionalized self-assembling peptide hydrogel enhance maintenance of hepatocyte activity in vitro. *J. Cell. Mol. Med.* **13,** 3387–97 (2009).

10. Gerlier, D. & Thomasset, N. Use of MTT colorimetric assay to measure cell activation. *J. Immunol. Methods* **94,** 57–63 (1986).

CHAPTER 3

DEVELOPMENT OF A BIOMIMETIC 3D MODEL TO CULTURE THE PANCREATIC RAT BETA CELL LINE INS-1E

3.1 BACKGROUND

3.1.1 OVERVIEW

Intensive insulin therapy remains the life-sustaining therapy for type 1 diabetes mellitus (T1DM) patients. Despite maintaining acceptable blood glucose levels and therefore reducing the incidence of long-term complications associated to the disease, exogenous insulin cannot completely simulate the endogenous insulin release, making it difficult to maintain physiological insulin levels. As a consequence, in some patients, intensive insulin treatments may cause severe hypoglycemic episodes[1]. Moreover, it requires multiple daily injections or the use of insulin pumps along with a continuous monitoring of blood glucose levels, and major lifestyle modifications[2]. For all these reasons, other therapeutic approaches are needed. Pancreatic islet transplantation (IT) is an alternative option that resembles more closely *in vivo* islet physiology, providing a better metabolic control and eliminating the need for exogenous insulin[3].

Although IT clinical outcomes have experienced encouraging advances along the last two decades, thanks to the improvements in islet isolation procedures and the application of the Edmonton protocol[3], several obstacles still need to be overcome[4]. The main hurdles are related to the shortage of islet supply and the efficacy of islet engraftment. Regarding islet engraftment, IT is associated with limited engraftment potential, attributed among other factors, to the destruction of the native islet microenvironment during the isolation procedure[5–7]. The enzymatic digestion of the pancreas results in the loss of the peri-insular basement membrane (BM)[8]. As a consequence, the islet-matrix relationships are disrupted, which exposes the islet cells to a variety of cellular stresses, leading to the onset of islet cell death[5]. Thereby, new strategies aimed to enhance beta cell function and survival prior to transplantation are needed.

3.1.2 IN VITRO 3D VS 2D MODELS

As already mentioned in Chapter 1, one of the aims of tissue engineering (TE) is to transform the way of studying human physiology by means of *in vitro* three-dimensional (3D) culture models[9]. Traditionally, the majority of cell-based assays have been performed in two-dimensional (2D) cultures where cells grow in monolayer. Although 2D cultures have been a valuable tool to study the diverse biological processes, their limitations have been increasingly acknowledged. In the human body, cells are embedded within an organized extracellular matrix (ECM), surrounded by other cells in a 3D fashion. The behavior of individual cells is controlled through their interactions with their immediate neighbors and the ECM, creating a local microenvironment and directing cellular features such as proliferation, migration, differentiation and apoptosis. In contrast, in 2D *in vitro* assays cells grow attached to flat and rigid plastic surfaces, with one side exposed to the cell culture medium, and the other side

facing the rigid substrate. Only a small percentage of the cell surface is actually exposed to the other cells, which is not representative of the complex cellular environment found in the human body[10]. Cells grown in monolayer assume a flat morphology and spread freely in the horizontal plane, but lose the vertical dimension, adopting as a consequence a forced apical-basal polarity based on altered cell adhesions. In fact, the spatial distribution of integrin-mediated cell adhesions is the key factor dictating the 2D or 3D geometry adopted by cells. Additionally, in 2D models the soluble factors added to the medium or secreted by the cells, diffuse in a free way through the medium allowing a rapid equilibration of the cultures[11]. This is not representative of the *in vivo* situation where gradients of soluble molecules are established. Hence, these changes in cell morphology and the lack of 3D cell-cell and cell-matrix contact interactions, 3D cell migration and 3D gradient diffusion of cell-secreted factors implies altered metabolism and gene expression patterns[12]. For all these reasons, 2D cell cultures don't adequately mimic the human physiology and therefore can provide misleading results about *in vivo* responses[13,14].

Conversely, a growing number of studies suggest that 3D cell culture systems represent more accurately the *in vivo* microenvironment of tissues and organs than 2D cultures[15]. In 3D cell-based models, cells are provided with a specific cellular and matrix microenvironment that incorporates biochemical and mechanical cues, having an impact on the experimental outcomes[16]. Regarding cell adhesion, in 3D cultures, integrin-mediated adhesions occur all around the cell surface, which has an impact on cell responses[17]. Within the body, the majority of tissues show a more compliant microenvironment than that of 2D culture surfaces. Therefore, mechanotransduction properties are also more adequately represented in 3D models, where soft gels are used to culture the cells, compared to the artificial and hard surfaces of 2D models[11]. Several works have proved the influence of matrix stiffness on the behavior of cells[18–20]. In addition, 3D models also imitate some structural traits of the native ECM, as for instance the pore size, interconnectivity, gel dimensions, cell density and charge. This spatial distribution allows the creation of soluble molecules gradients as occurs in the *in vivo* situation[11,21]. Therefore, *in vitro* 3D cultures are a powerful tool to reduce the gap between traditional cell cultures and animal models by mimicking in a more realistic way the physiological functions of the *in vivo* environment[10] (Figure 3.1).

A

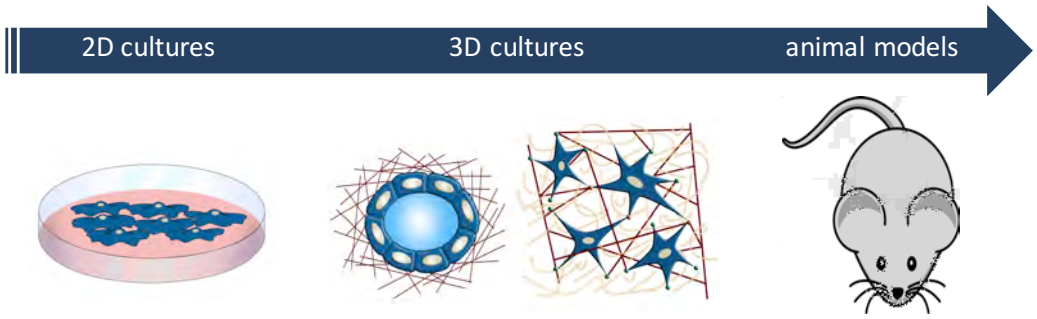

B

Biological Function	2D versus 3D	Regulatory Mechanisms
Cell Shape	Loss of epithelial cell polarity and altered epithelial and fibroblast shape in 2D	Growth factor receptors and pathways; cell-adhesion signals associated with cell survival and matrix plasticity
Gene Expression	Cells in 2D versus 3D often have different patterns of gene expression	ECM, hormones, and adhesion molecules
Growth	3D matrix-dependent regulation of cell growth	Adhesion and growth factor-related pathways plus survival or apoptotic genes
Morphogenesis	3D matrix-induced vessel sprouting and gland branching	ECM, adhesion, growth factor-related pathways and apoptotic genes
Motility	Altered single and collective cell motility patterns in 3D matrices	ECM and its regulators; adhesions and growth factor-related pathways; phospholipids
Differentiation	3D matrix-induced cell differentiation	ECM and growth factors; motor molecules

Figure 3.1. Comparison between the different models that allow the study of human physiology. (A) 2D cultures are a simplistic model unable to represent the complexity found organisms. At the opposite end of 2D cultures, animal models fail to capture some important aspects of human behavior. As an answer to these problems, a variety of 3D models have been developed, resembling more closely the in vivo cell-cell and cell-ECM matrix interactions than 2D cultures. Thus, tissue engineered 3D cultures are a powerful tool to bridge the gap between 2D cultures and animal models. (B) Different aspects of cell behavior and signaling in 2D and 3D culture models. (B) Adapted from Yamada[16].

3.1.3 NANOFIBROUS SELF-ASSEMBLING SCAFFOLDS

The maintenance of the function and differentiation of pancreatic beta cells depends strongly on the surrounding matrix. As mentioned previously, during islets isolation, the microenvironment is completely disrupted and cell-cell and cell-ECM interactions are lost. Therefore, prior to transplantation the islet microenvironment needs to be reestablished in order to recover the native conditions of the tissue. Providing pancreatic islet cells with an ECM analogue can encourage 3D structure formation, cellular migration and graft vascularization, which in turn could yield to greatest levels of engraftment[22]. Recent works showed that growing human islets on 3D scaffolds improved the outcome of the islets after being transplanted in rodents, as compared to islets non cultured on 3D conditions[23–26].

Currently, matrigel is the most widely used matrix for the culture of isolated pancreatic islets before transplantation. Matrigel is extracted from the Engelbreth-Holm-Swarm carcinoma and therefore provides different adhesion ligands and growth factors to the cells. Precisely, due to the natural component of matrigel, the role of specific ECM components on beta cell function remains undefined[27]. As explained in Chapter 1, with the use of synthetic materials this obstacle can be easily overcome.

Numerous synthetic biomaterials have been developed to provide cells with the most adequate 3D microenvironment. These systems usually begin with a liquid precursor containing suspended cells, which gels or solidifies in a hydrated manner. The obtained gels are porous to enable nutrient and waste exchange, and possess sufficient mechanical properties to be self-supporting[11]. Basically, the synthetic biomaterials that are being explored in TE applications can be classified into microfiber polymers and nanofiber hydrogels. Poly(α-hydroxy acids), including poly(glycolic acid) (PGA), poly(lactic acid) (PLA), and their copolymer poly[(lactic acid)-co-(glycolic acid)] (PLGA), are the most widely used microfiber polymeric materials in TE[28]. The main drawback of these biomaterials is their diameter and pore size, 10-50 μm and 10-200 μm respectively, which is in the same order of magnitude of an average cell size (10-100 μm in diameter)[29]. For cells to feel a true 3D microenvironment, scaffold fibers and pores must be significantly smaller than cells. In these conditions, the scaffold surrounds the cells in a similar way as the native ECM. Precisely, the fibers of the ECM and their interconnecting nanopores present nanoscale dimensions. Therefore it is reasonable that cells require the same nanostructure than the *in vivo* ECM, in order to maintain their phenotypic shape and natural behavior[30]. On the other hand, nanofiber hydrogels have a diameter of 10-20 nm and pore size of 5-200 nm, 1000 times smaller than mammalian cells. When grown in these scaffolds, cells experiment a truly 3D environment enabling cells to grow, migrate, contact other cells, change in morphology and expose membrane receptors in a proper way. In other words, cells are embedded in the hydrogel but not entrapped. Moreover, these hydrogels are permeable to gases, metabolites and macromolecules[29,31].

Among nanofiber scaffolds, self-assembling peptides (SAPs) are widely used in most of the TE applications. Molecular self-assembly is the spontaneous organization of molecules without guidance from an outside source, which under thermodynamic equilibrium conditions results into structurally well-defined arrangements by means of noncovalent interactions[32,33]. In biology, a lot of examples of self-assembly processes can be found, such as DNA self-complementary double-helix annealing. Self-assembling peptides are composed of natural aminoacid sequences, which alternate hydrophobic and hydrophilic side groups, highly soluble in water and with the tendency to form very stable β-sheet structures[31,34]. Hence, these β-sheet structures have two distinct surfaces, one polar surface with hydrophilic side chains and a non-polar surface with the hydrophobic groups[35]. The hydrophobic residues protect themselves from water creating hydrophobic interactions, meanwhile in the hydrophilic surface complementary ionic bonds with regular repeats are established. Under the appropriate conditions, the β-sheet structures spontaneously assemble to form stable macroscopic structures made of interwoven nanofibers. Besides ionic side chain interactions, conventional β-sheet backbone hydrogen bonds facilitate the self-assembling process[35]. The

complementary ionic sides are classified into 4 different moduli according to the arrangement of the alternating positively and negatively charged aminoacids. Thus, the following moduli are established, modulus I (– + – + – + –+), modulus II (– – + + – – + +), modulus III (– – – + + +) and modulus IV (– – – – + + + +) [36].

Intriguingly, a 16-aminoacid peptide, EAK16-II (AcN-AEAEAKAKAEAEAKAK-CNH_2; A: alanine, E: glutamic acid, K: lysine), was found as tandem repeats in a yeast protein, zuotin, originally characterized by binding to left-handed Z-DNA[37]. EAK16-II alternates hydrophobic and hydrophilic aminoacids, displays a β-sheet configuration and forms insoluble macroscopic membranes. This oligopeptide has been widely studied and modified to develop a new generation of peptides, such as RAD16-I (AcN-RADARADARADARADA-CNH_2; R: arginine, A: alanine, D: aspartic acid). Changes introduced include the substitution of positively charged lysines for arginines and negatively charged glutamic acids for aspartic acids. Through an increase in the ionic strength or adjustment of the pH to neutrality, RAD16-I undergoes spontaneous assembling, forming soft hydrogels stable in physiological conditions[38]. These scaffolds are made of more than 99% water and a peptide content of 1-10 mg/ml, with nanofibers diameter around 10-20 nm and pores sizes of 50-200 nm. The nanofibers are similar in scale to natural extracellular matrices (50-500 nm pore size) and since the interactions given among fibers are noncovalent, cells can freely grow, migrate, contact with other cells, and expose cell receptors properly [29]. Therefore, when cultured on RAD16-I SAP cells can experience a truly 3D environment comparable to that of the native ECM.

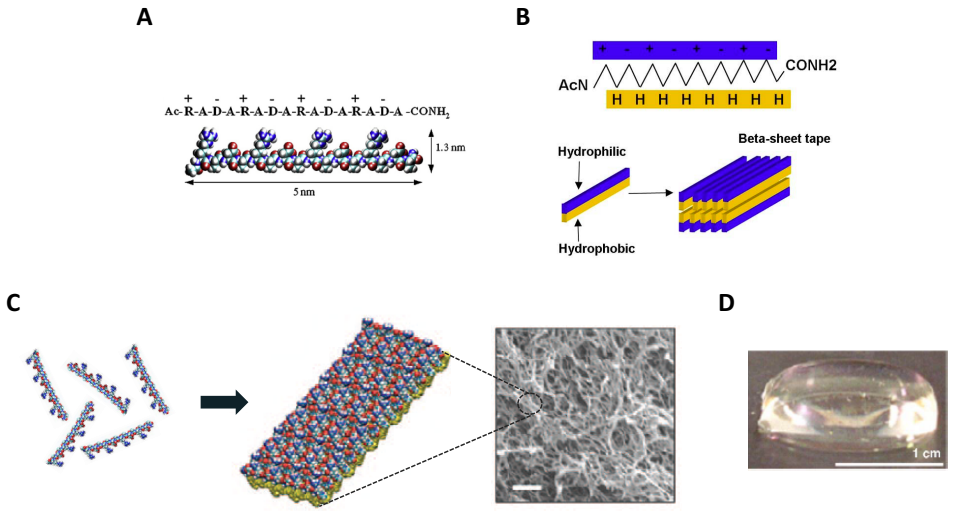

Figure 3.2. RAD16-I self-assembling peptide. (A) Amino acid sequence and molecular model of RAD16-I SAP. (B,C) Model of RAD16-I self-assembling process. RAD16-I is an amphiphilic peptide composed of alternatively repeating units of positively and negatively charged side chains, with a strong tendency to form β-sheet structures in an antiparallel configuration. Through an increase in the ionic strength or adjustment of the pH to neutrality, RAD16-I hydrogel self assembles forming nanofibers of 10-20 nm diameter and pores sizes of 50-200 nm. Scanning electron microscopy examination allows the visualization of RAD16-I nanofiber network (Right) (Scale bar 200 nm) (D) Image of RAD16-I scaffold after the gelation process (Scale bar 1 cm) (A,B,C) Adapted from Semino[38]. (D) From Nagai[39].

Other advantageous features of RAD16-I SAP as a scaffold in TE applications are the following:

- Viscoelastic properties resembling that of soft collagen scaffolds, which confers biomechanical properties similar to the natural ECM.
- The stiffness can be easily controlled by changing peptide concentration. Matching the stiffness of the matrix with that of the *in vivo* environment of the encapsulated cells provides more realistic *in vitro* conditions.
- Non-instructive environment. Peptide signaling motifs are absent in RAD16-I, this makes this hydrogel an ideal scaffold to study the different cellular responses caused by the intrinsic properties of the 3D environment *per se*.
- Tailor-made scaffold. Possibility of incorporate specific ligands for cells receptors of the ECM in order to study some particular responses, controlling that way chemical functionality.
- Chemically and physically stable at room temperature for long periods of time. These matrices are resistant to heat, to many chemical agents and to degradation by proteolytic enzymes *in vitro.*
- No harmful chemicals are used to initiate the gelation of the peptide.
- Injectable hydrogel that gels once in contact with the body, with no immune or inflammatory response.
- Biodegradable scaffold, as it is composed of aminoacids reusable by the body[32,34,35,38].

RAD16-I matrix has proved to support the attachment of multiple cell types, independently of cell adhesion mechanisms involving ECM ligands[35]. Several *in vitro* models show the potential of this biomaterial as TE scaffold. Among others, RAD16-I peptide allowed the generation of a cartilage-like tissue[31,40], the growth and proliferation of hippocampal neural cells[41], the development of functional hepatocyte-like spheroid structures from liver progenitor cells[42], the formation of confluent cell monolayers of human aortic endothelial cells[43], osteogenic differentiation of mouse embryonic stem cells and mouse embryonic fibroblasts[44], the enhancement of the hepatocyte activity *in vitro*[45,46], the study of the effect of photodynamic therapy in 3D culture environments compared to traditional 2D systems[47] and the development of bioimplants seeded with adipose progenitor cells[48]. On the other hand, some *in vivo* studies also demonstrate the efficacy of this self-assembling scaffold for tissue repair and regeneration. For instance, the application of RAD16-I in small bone defects in mice calvaria promoted bone regeneration[49]. Moreover, brain repair and axon regeneration was achieved in a functional experimental model of the optic track in the hamster, allowing the recovery of the animal's sight after severe injury[50].

Gathering all the evidence, RAD16-I SAP have demonstrated to be a promising ECM-inspired biomaterial allowing the culture, maintenance and differentiation of a wide variety of cells, from stem cells to adult cells. During the last years, SAPs other than RAD16-I have gained increasing attention as 3D matrices in pancreatic tissue engineering (PTE)[51–53]. We hypothesize that RAD16-I based models could recreate a more realistic and physiological microenvironment for pancreatic islet cells, than conventional 2D monolayer cultures.

3.1.3.1 Functionalization of self-assembling peptide scaffolds

As already mentioned, the ECM provides multifunctional adhesion ligands to the cells, such as laminin, collagen or fibronectin, which drive development and maintenance of cell function[54]. Therefore, the development of biomaterials for TE applications is focused on the design of biomimetic materials based on *in* vivo cell-ECM interactions that provide cells with the most adequate extracellular ligands. Synthetic biomaterials, which physically mimic the ECM but don't exert any biochemical signaling over the cells, allow the incorporation of bioactive molecules similar to that of the native cell matrix. These ECM-mimetic scaffolds should be capable of eliciting specific cellular responses through the recognition of the introduced biological cues[55]. Therefore, the functionalization of the synthetic biomaterials allows the study of the complex cell-ECM relationships in a more specific way.

The cell-matrix interactions can be achieved by surface or bulk modification of biomaterials, via the incorporation of native long chains of ECM proteins. However, the use of native proteins isolated from other organism implies some disadvantages, as for instance undesirable immune responses when the scaffolds are implanted into the host. Moreover, these long proteins tend to fold randomly when adsorbed into synthetic surfaces. As a result, their bioactivity may be significantly reduced[56]. In addition, proteins are subjected to proteolytic degradation and are not a good option for long-term applications[55,57]. Most of the indicated problems can be overcome by the immobilization of short peptide motifs as cell signaling molecules[58]. The short peptide motifs are signaling domains found within ECM adhesive proteins that interact with cell membrane receptors, mainly integrins, causing a specific response in cell behavior. They present higher stability, easier characterization and better cost-effectiveness than native proteins. Furthermore, since they are composed by short aminoacid sequences, space requirements are lower, being able to pack them at higher densities[57]. By far, the most widely studied adhesive peptide is the arginine-glycine-aspartate (RGD) aminoacid sequence, derived from fibronectin and laminin[59]. Extensive literature demonstrates the effectiveness of RGD motif at enhancing cell adhesion, growth, migration and differentiation of cells cultures within a variety of biomaterials[57]. Nonetheless, others peptide signaling motifs such as YIGSR and IKVAV, both derived from laminin have also been immobilized on different substrates.

RAD16-I peptide is a synthetic biomaterial that provides a non-instructive milieu, meaning that no biochemical signaling is exerted over the cells. This peptide scaffold is susceptible to be functionalized with bioactive molecules to promote or enhance desired biological activities. RAD16-I scaffold have been previously tailored with different peptide signaling motifs in specific applications, to stimulate endothelial[43], hepatic[45,46] and neural[60] functions, among others (Figure 3.3).

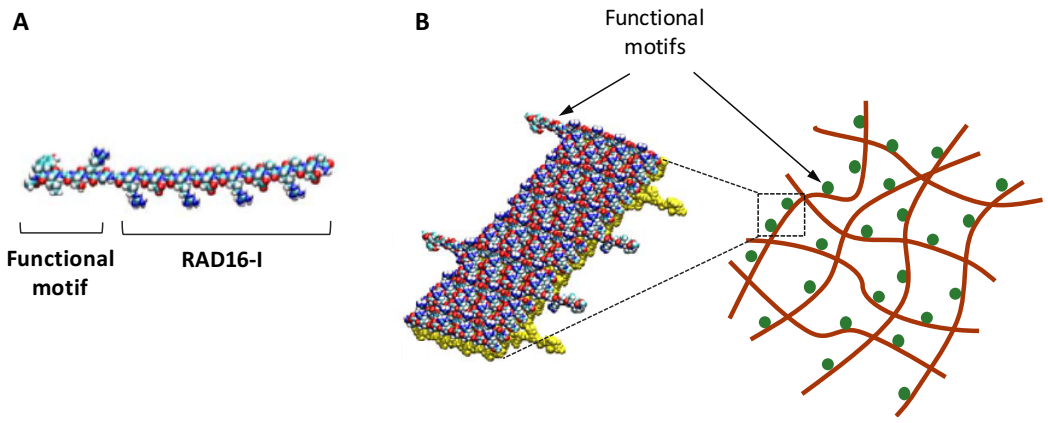

Figure 3.3. RAD16-I functionalization with bioactive functional motifs derived from the ECM proteins. (A) Molecular model of functionalized RAD16-I scaffold. The peptide signalling motifs are added to the C-termini by solid phase synthesis. (B) Molecular and schematic view of self-assembled nanofibers after mixing pure RAD16-I with the functionalized analogue. The bioactive motifs extrude from the nanofiber tape. Adapted from Genové[43].

In this chapter, the peptide scaffold RAD16-I has been used to establish an *in vitro* 3D culture platform based on the culture of the beta cells surrogate, INS-1E cell line[61]. Despite decades of attempts, human pancreatic beta cell lines that retain the characteristics of primary beta cells remain unavailable. Consequently, rodent beta cell lines have demonstrated their usefulness, and their continuous development is still essential until beta cell lines of human origin become available. Pancreatic beta cell lines with similar characteristics that insulin-releasing beta cells of pancreatic islets, are often used to assess the efficacy of new designed biomaterials aimed to improve the outcomes of pancreatic islet transplantation. Moreover, in the present chapter, in order to evaluate the influence of specific cell-matrix interactions on islet function, RAD16-I peptide has been functionalized with peptide signaling motifs found in the native islet microenvironment. The design of the RAD16-I tailor-made scaffolds was based on the islet ECM composition[62,63], recognized by the specific integrins expressed on the membrane of the islet cells [8,64–68]. Thus, various cell adhesive motifs derived from laminin and collagen IV were immobilized by solid-phase synthesis extension at the C-termini of RAD16-I peptide. In particular, five cell adhesion motifs with recognized biological activity were investigated (RGD, YIG, IKVAV, GEF and TWY). Once the functionalized peptides were obtained, they were mixed in a 95:5 ratio (pure RAD16-I:tailored RAD16-I). The peptide signaling sequences are listed in Table 3.1, as well as their cell receptors in pancreatic islets. To simplify the nomenclature of the tailor-made peptides, an abbreviation was assigned to each one of the peptides sequences.

Table 3.1. Tailor-made peptides sequences and its cell receptors

Name	Peptide Sequence	Protein	Target receptor
RAD16-I	AcN-$(RADA)_4$-$CONH_2$	None	None
RGD	AcN-GPRGDSGYRGDS-GG-$(RADA)_4$-$CONH_2$	Fibronectin/Laminin	$\alpha_V\beta_3$, $\alpha_5\beta_1$, $\alpha_3\beta_1$ integrins
YIG	AcN-YIGSRGG-$(RADA)_4$-$CONH_2$	Laminin	67 KDa Laminin Receptor
IKVAV	AcN-IKVAVGG-$(RADA)_4$-$CONH_2$	Laminin	110 KDa Laminin Receptor
GEF	AcN-GEFYFDLRLKGDKY-GG-$(RADA)_4$-$CONH_2$	Collagen IV	$\alpha_1\beta_1$, $\alpha_3\beta_1$ integrin
TWY	AcN-TWYKIAFQRNRK-GG-$(RADA)_4$-$CONH_2$	Laminin	$\alpha_6\beta_1$ integrin

3.2 HIPOTHESIS AND AIMS

Pancreatic islet isolation implies the destruction of the islet microenvironment. Our working hypothesis is that the functionalization of the self-assembling peptide RAD16-I with peptide signaling motifs will trigger the formation of controlled and specific interactions between the scaffold nanofibers and the beta cells, mimicking in a more realistic way the *in vivo* microenvironment of pancreatic islets. The creation of a more favorable environment for the cells should be able to support beta cells survival in 3D conditions and the maintenance or enhancement of islet function. Thus, the primary aim of this chapter is the development of a three-dimensional synthetic culture platform based on the reconstitution of pancreatic islet-matrix interactions. Due to the easier accessibility of beta cell lines compared to isolated human beta cells, the insulin-producing INS-1E cell line was used to establish the 3D culture model. If our hypothesis proves to be correct, it will provide a "proof of concept" for the potential of functionalized *in vitro* RAD16-I culture platforms in pancreatic tissue engineering, that could be further used with human beta cells. In particular, the specific aims of this chapter are the following:

1) To characterize physicochemically the tailor-made peptide scaffolds based on the self-assembling peptide RAD16-I.

2) To determine the optimal conditions of RAD16-I 3D matrix to encapsulate INS-1E cells (RAD16-I concentration, cell density and culture time).

3) To evaluate INS-1E behavior and viability when cultured on pure or tailor-made RAD16-I hydrogel.

4) To assess the potential of tailor-made scaffolds to maintain or enhance beta cell function, compared to pure RAD16-I.

3.3 RESULTS AND DISCUSSION

3.3.1 CHARACTERIZATION OF TAILOR-MADE PEPTIDE SCAFFOLDS

Five tailor-made peptide sequences were designed based on the most expressed integrins on pancreatic islets. For this purpose, different cell adhesion ligands, specifically, peptide signaling motifs derived from laminin and Collagen IV, were added by solid phase synthesis to the RAD16-I self-assembling (SAP) peptide. We examined the following peptides: RGD (from fibronectin and laminin), YIG (from laminin), IKVAV (from laminin), GEF (from type IV collagen) and TWY (from laminin). In all the performed experiments, pure RAD16-I was used as a control.

As a first step, the solubility in water of each one of the modified peptides was tested. The concentration used to dissolve the peptides was 1% (w/v) since it is the concentration of commercial RAD16-I (PuraMatrix). All the peptide sequences were soluble in water, except for GEF, that showed a whitish color when dissolved, and after some time a precipitate appeared. Thus, this peptide was not used for the next experiments.

To assess whether the presence of the peptide signaling motifs interfered in the self-assembling process characteristic of RAD16-I scaffold, an assay based on Congo red staining was performed (Figure 3.4). Congo red binds to the β-sheet structures present in RAD16-I nanofibers, being therefore a good indicator of the hydrogel formation capacity[69]. Conventional RAD16-I was used as a positive control. The staining was positive for RGD, YIG and IKVAV peptides, indicating that the addition of these functional motifs to RAD16-I sequence did not hinder the self-assembling process. However, TWY sequence was negative for Congo red staining, meaning that the interference caused by the added peptide sequence was too big to allow β-sheet formation impeding the gelation of this tailor-made peptide.

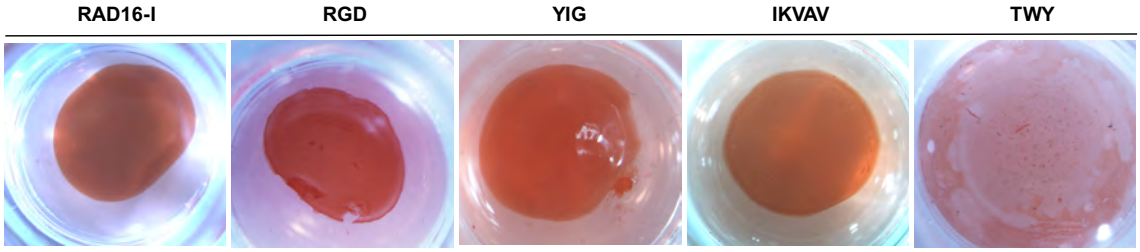

Figure 3.4. Congo red staining of conventional RAD16-I (control) and tailor-made peptides scaffolds. All the modified peptides, except for TWY, formed nanofibers gels as evidenced by the presence of β-sheet structures stained by Congo red.

In addition, circular dichroism (CD) studies were carried out to evaluate the influence of the functionalization on the β-sheet secondary structure and therefore on the self-assembling capacity of modified peptides. CD spectroscopy is a biophysical tool that refers to the differential absorption of the left and right circularly polarized radiation by chromophores

within proteins[70]. Thus, it is an excellent method to determine the secondary structure and stability of proteins and peptides. Specifically, in the far UV region (240-180 nm) that corresponds to the peptide bond absorption, the CD spectrum gives information about the content of regular secondary structural features[70]. Different structures possess characteristic CD spectra. Proteins with a β-sheet structure show a minimum molar ellipticity around 218 nm, which represents the β-sheet content and a maximum at 195 nm which corresponds to the backbone twist of the peptide in β-sheet configuration. On the other hand, α-helical structures show two minimums around 222 nm and 208 nm and a maximum at 193 nm, whereas random coil structures have very low ellipticity above 210 nm and a negative band near 195 nm[71] (Figure 3.5).

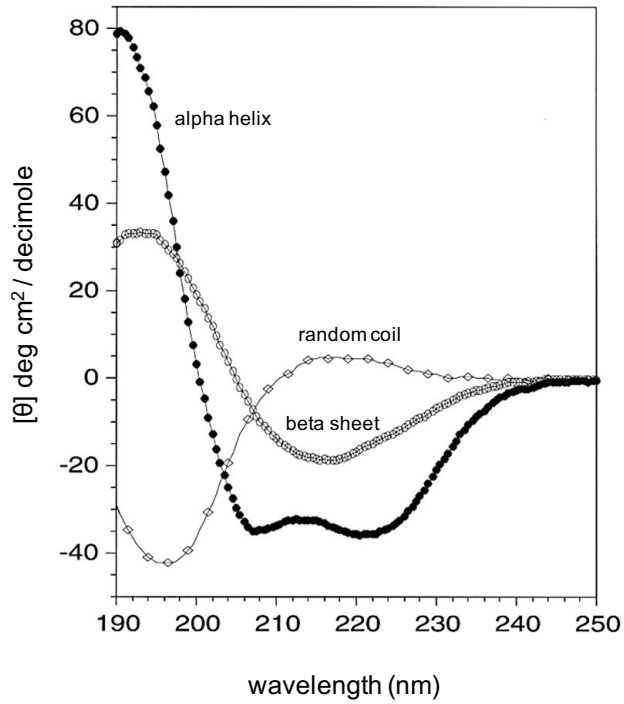

Figure 3.5. CD spectra of different proteins with representative secondary structures. Typical CD spectra of proteins with α-helical, β-sheet or random coil secondary structures. Adapted from Fändrich *et al*[72].

As seen in Figure 3.6, the CD spectrum of non-modified RAD16-I showed the typical profile of a β-sheet structure, with a minimum molar ellipticity (deg cm^2/decimole) around 216 nm and a maximum at 195 nm. On the other hand, CD spectra of functionalized peptides allowed us to monitor the changes on the secondary structure due to the addition of aminoacids that don't keep the alternating hydrophilic and hydrophobic pattern, responsible for β-sheet structures formation. The functionalized peptides, with the exception of TWY, also showed a spectrum indicative of β-sheet structure, although with a diminished β-sheet content due to the introduction of the short peptide sequences. This was depicted as a decrease in the intensity of molar ellipticity at 216 nm and 198 nm, giving place to weaker β-sheet structures. These results are in agreement with the positive results obtained for the Congo red staining. On the

other hand, the IKVAV peptide did not exhibit a similar CD spectrum compared to the RAD16-I sequence. A subtle minimum was observed although it was not exactly located at 216-217 nm but around 220 nm, slightly displaced from the typical minimum observed in a β-sheet-forming peptide. No maximum at 195 nm was either observed. Nevertheless, the positive result of the Congo red staining confirmed the presence of β-sheet structures, indicating the capacity of IKVAV sequence to form nanofibers. Moreover, IKVAV peptide has been reported to show a strong propensity to form β-sheet secondary structures in the literature and abundant TE studies using this peptide have been published [43,73]. Finally, TWY spectrum did not display a β-sheet profile, meaning that the 14 added aminoacids to the RAD16-I sequence interfered in the β-sheet conformational structure of the peptide. The lack of β-sheet structure confirms the negative results obtained for the Congo red staining. Therefore, the use of TWY peptide was excluded as a scaffold for INS-1E cells, since the β-sheet content is a prerequisite for nanofibers formation.

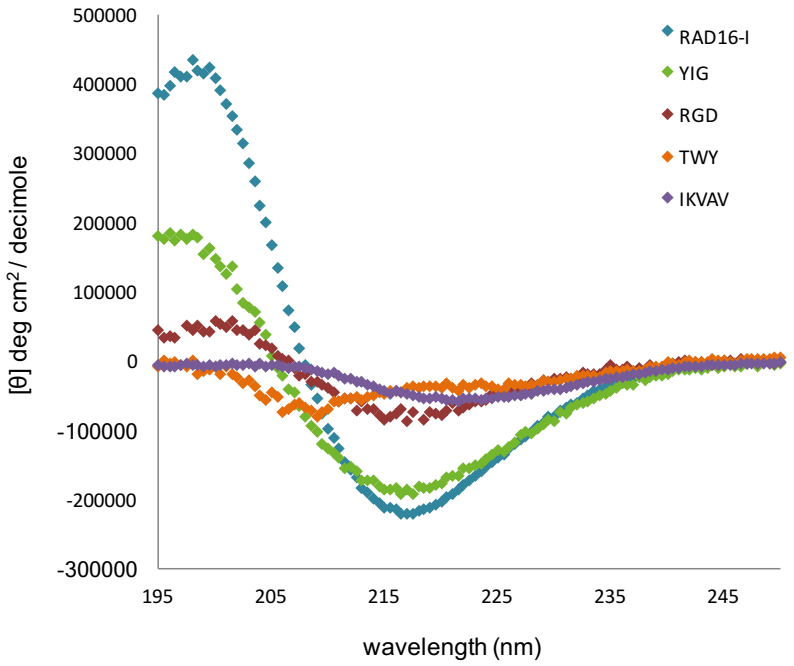

Figure 3.6. CD spectra of peptide scaffolds. RAD16-I peptide was used as a control for the β-sheet structure profile.

The following table summarizes the structural and physicochemical properties of the different tailor-made sequences based on RAD16-I peptide.

Table 3.2. Properties of tailor-made peptides

Name	Peptide Sequence	Solubility in water 1% (w/v)	Gel formation (Congo red)	Secondary Structure (CD)
RAD16-I	AcN-$(RADA)_4$-$CONH_2$	+	+	β-sheet
RGD	AcN-GPRGDSGYRGDS-GG-$(RADA)_4$-$CONH_2$	+	+	β-sheet
YIG	AcN-YIGSRGG-$(RADA)_4$-$CONH_2$	+	+	β-sheet
IKVAV	AcN-IKVAVGG-$(RADA)_4$-$CONH_2$	+	+	
GEF	AcN-GEFYFDLRLKGDKY-GG-$(RADA)_4$-$CONH_2$	-	-	
TWY	AcN-TWYKIAFQRNRK-GG-$(RADA)_4$-$CONH_2$	+	-	

3.3.2 SET-UP OF 3D CULTURE CONDITIONS TO ENCAPSULATE INS-1E CELLS IN RAD16-I SCAFFOLD

INS-1E cells were seeded in the SAP RAD16-I as detailed in Chapter 2 (section 2.4.1), in order to develop a 3D culture model based on a synthetic ECM analog. This type of culture resembles more closely the microenvironment found *in vivo* in pancreatic islets than the traditional 2D cultures. Furthermore, different variants of this model were created by the functionalization of RAD16-I peptide with active motifs derived from the pancreatic ECM proteins.

Firstly, in order to establish the optimal working concentration for the RAD16-I based platform, different peptide concentrations were tested, 0.15%, 0.30% and 0.40% (w/v). The criteria used to select a specific concentration were based on the easiness of manipulation, good growth and the capacity to form cell clusters. Since hydrogels increase in stiffness with increasing concentrations of peptide, higher concentrations provide more dens constructs and thus, easier to manipulate. The most compliant hydrogel was obtained with the lowest concentration, 0.15%, but constructs were too fragile and broke easily. Therefore, this concentration was discarded. The other two concentrations, 0.30% and 0.40%, offered a more stable structure after the self-assembling process, allowing the formation of a disc-shape hydrogel. As shown in Figure 3.7, cells were capable of forming clusters in both concentrations, but cell viability studies demonstrated that after 10 days of culture, cell death was higher in RAD16-I 0.40% hydrogels. Thus, 0.30% was the chosen RAD16-I concentration to perform the experiments. Regarding cell density, the number of cells encapsulated doubled the standard cell seeding density for human cells, that is, 160.000 cells in 40 µL of RAD16-I.

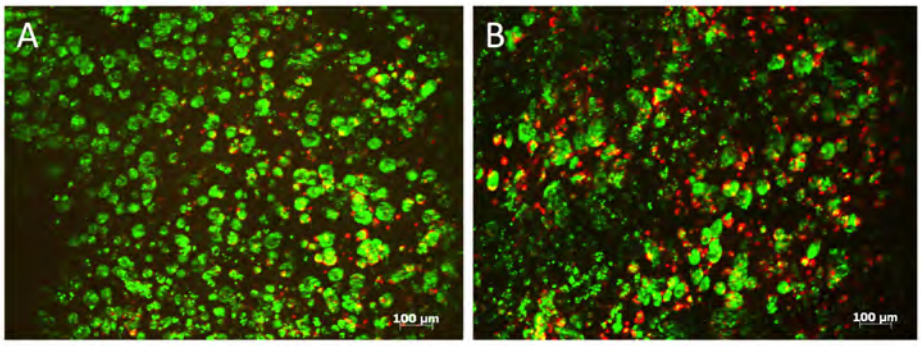

Figure 3.7. Cellular viability in RAD16-I constructs of different concentrations. (A) INS-1E viability in RAD16-I 0.3%. (B) INS-1E viability in RAD16-I 0.4%. After 10 days of culture, cells were stained with calcein dye for live cells (green) and ethidium homodimer-1 for dead cells (red). The majority of cells remained alive in both concentrations, although cell death was higher when 0.4% concentration was used. Scale bar of 100 µm.

Once peptide concentration and cell density were set, INS-1E cells were encapsulated for 14 days in order to establish the culture period. RAD16-I matrix was functionalized with the RGD, YIG, and IKVAV peptide signaling sequences, which entailed that the overall scaffold architecture was decorated with these specific biological stimuli. The functionalization ratio was 95:5, meaning that 95% of the matrix was pure RAD16-I and 5%, RAD16-I covalently linked to the bioactive sequences. We intended to tailor the RAD16-I peptide scaffold with laminin and fibronectin motifs to develop a basement membrane analogue that could enhance INS-1E cells growth and function *in vitro*.

3.3.3 INS-1E BEHAVIOR AND VIABILITY IN FUNCTIONALIZED RAD16-I SCAFFOLDS

3.3.3.1 INS-1E cell morphology in functionalized RAD16-I cultures

As depicted in Figure 3.8, INS-1E cells within RAD16-I based matrices were monitored along the culture period under a phase contrast microscope. After the first 24 hours of culture, single cells spread within the matrix and exhibited a round shape. As the culture progressed cells began to form cell aggregates (clusters) with a defined roundish morphology, easily observable during the first week of culture (day 5). By day 10, clusters size had clearly increased and cellular densities showed a marked increment compared to the first days of culture. We continued the culture until day 14, when we observed that cell clusters started to dismantle. Cell aggregates contour was no longer well defined, losing its compactness and roundish morphology. Hence, we fixed the culture period in 10 days. Looking at pure RAD16-I and functionalized matrices, no visible changes in cell morphology were appreciated due to the addition of the bioactive motifs.

RAD16-I based constructs were also visualized under a stereoscopic microscope (Figure 3.9). As already seen in Figure 3.8, the progressive increase in cell density along the culture period can be also observed at a macroscopic level, giving place to more populated and therefore opaque structures. By the end of the culture period (day 10), clusters were easily seen at macroscopic level. Regarding constructs diameters, no reduction in their dimensions were detected, indicating that no contraction of the matrix took place (data not shown). These results are in concordance with what it was expected, since beta cells are epithelial cells that grow in clusters, and unlike mesenchymal cells that display an elongated shape, they are not capable of pulling on the matrix in which they are embedded.

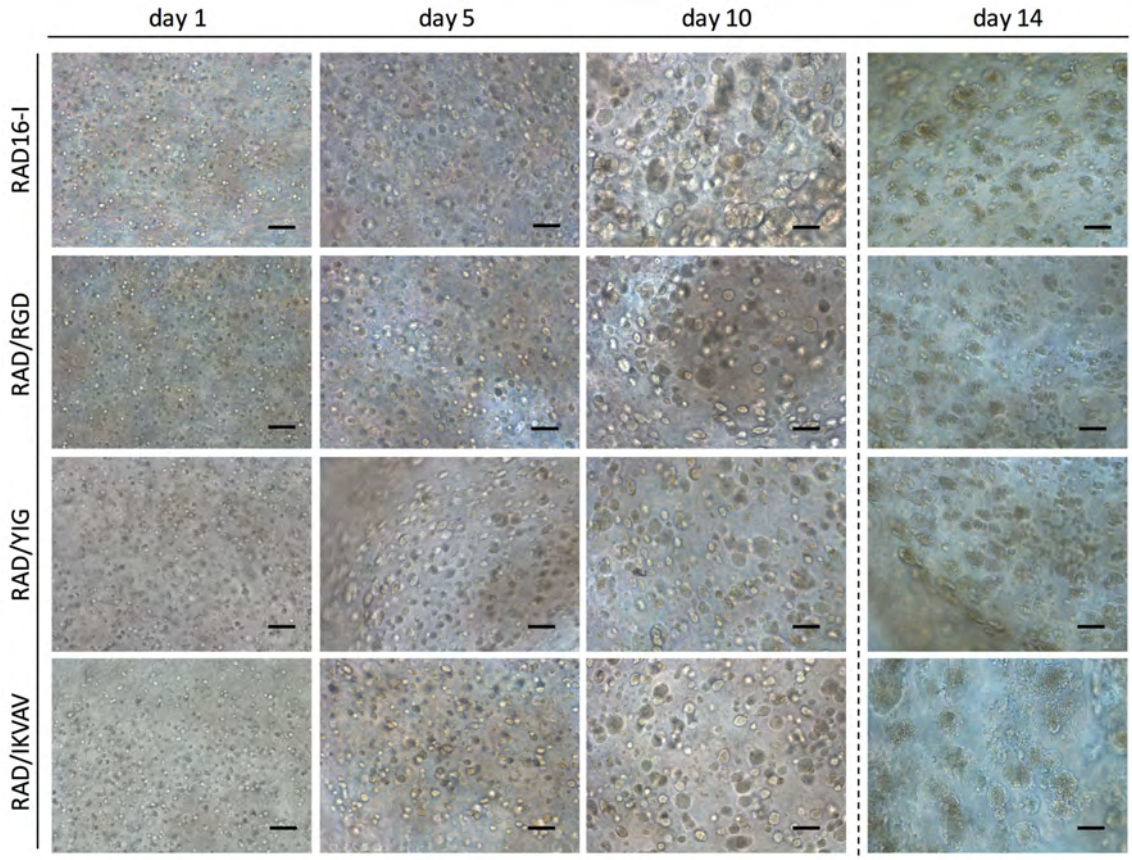

Figure 3.8. Phase contrast images of INS-1E cells cultured in pure and functionalized RAD16-I matrices. INS-1E cells were examined after 1, 5, 10 and 14 days of culture. Cells grow forming cell clusters that maintained a roundish and compact morphology until day 10 of culture. Scale bar of 100 µm.

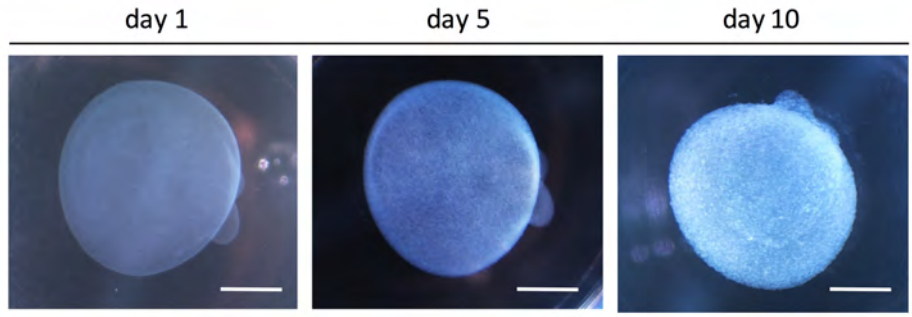

Figure 3.9. Stereoscopic images of RAD16-I constructs seeded with INS-1E cells. Cell clusters were growing progressively within RAD16-I matrix and were easily visualized by the end of the culture. Constructs dimensions remained stable along the culture period. Scale bar of 2 mm.

To further assess the evolution of cell morphology and organization within RAD16-I cultures, nuclei and actin filaments of the cytoskeleton were stained with DAPI and Phalloidin-TRITC dyes, respectively. The images taken under a fluorescence microscope allowed for a clearer visualization of cell disposition within the 3D matrix (Figure 3.10 and Figure 3.11). At the beginning of the cell culture, cells were scattered all over the matrix. As already seen in phase contrast images, after 5 days of culture it was confirmed that when grown within a 3D matrix, INS-1E cells are capable of forming spheroid cell clusters characterized by close cell-cell contacts, which is the typical growth pattern of native beta cells in pancreatic islets. From day 5 to day 10, clusters kept increasing in size, colonizing the synthetic matrix. Specifically, cell number within clusters was higher, suggesting that cell proliferation occurred during the whole culture period. Cell number is closely related with clusters size, and by the end of the culture, cell cluster diameters were estimated to be around 50-100 µm. In fact, the size of rodent islets can vary considerably, from ten or fewer cells to thousands of cells, being their diameter 20-400 µm[74]. Therefore, the size of our islet-like structures was within the range of *in vivo* pancreatic islets. Comparing pure RAD16-I and functionalized matrices, no apparent differences were observed. Nonetheless, some clusters with larger diameters were found in RAD16-I/IKVAV matrix.

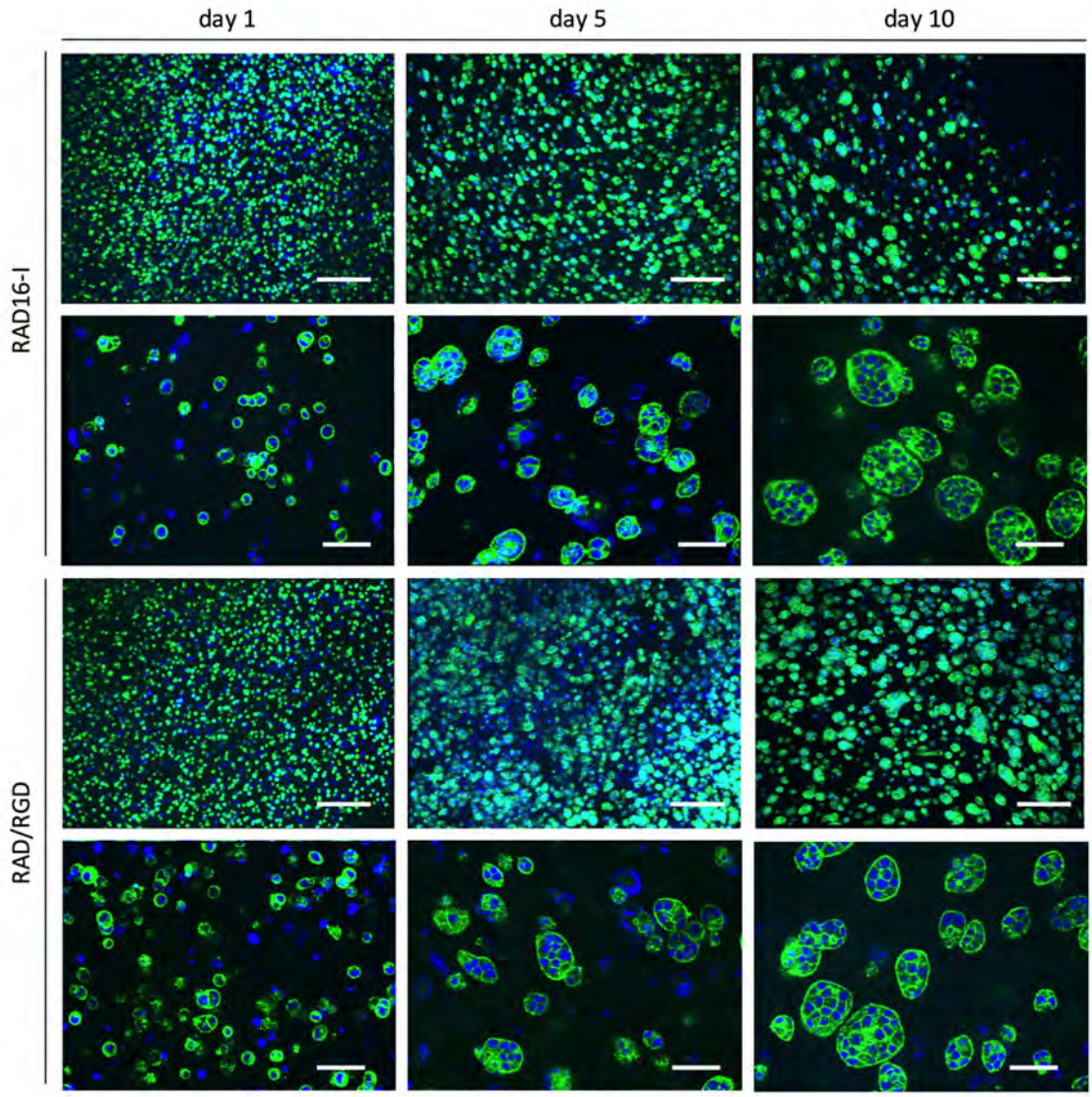

Figure 3.10. INS-1E cell morphology and organization in RAD16-I and RAD/RGD based cultures. Cells were analysed under a fluorescence microscope when cultured in pure RAD16-I and RAD16-I/RGD, functionalized matrices. Nuclei were stained in blue (DAPI) and actin filaments in green (Phalloidin). Z-stack images. Scale bar of 200 µm (Above images), and 50 µm (Below images).

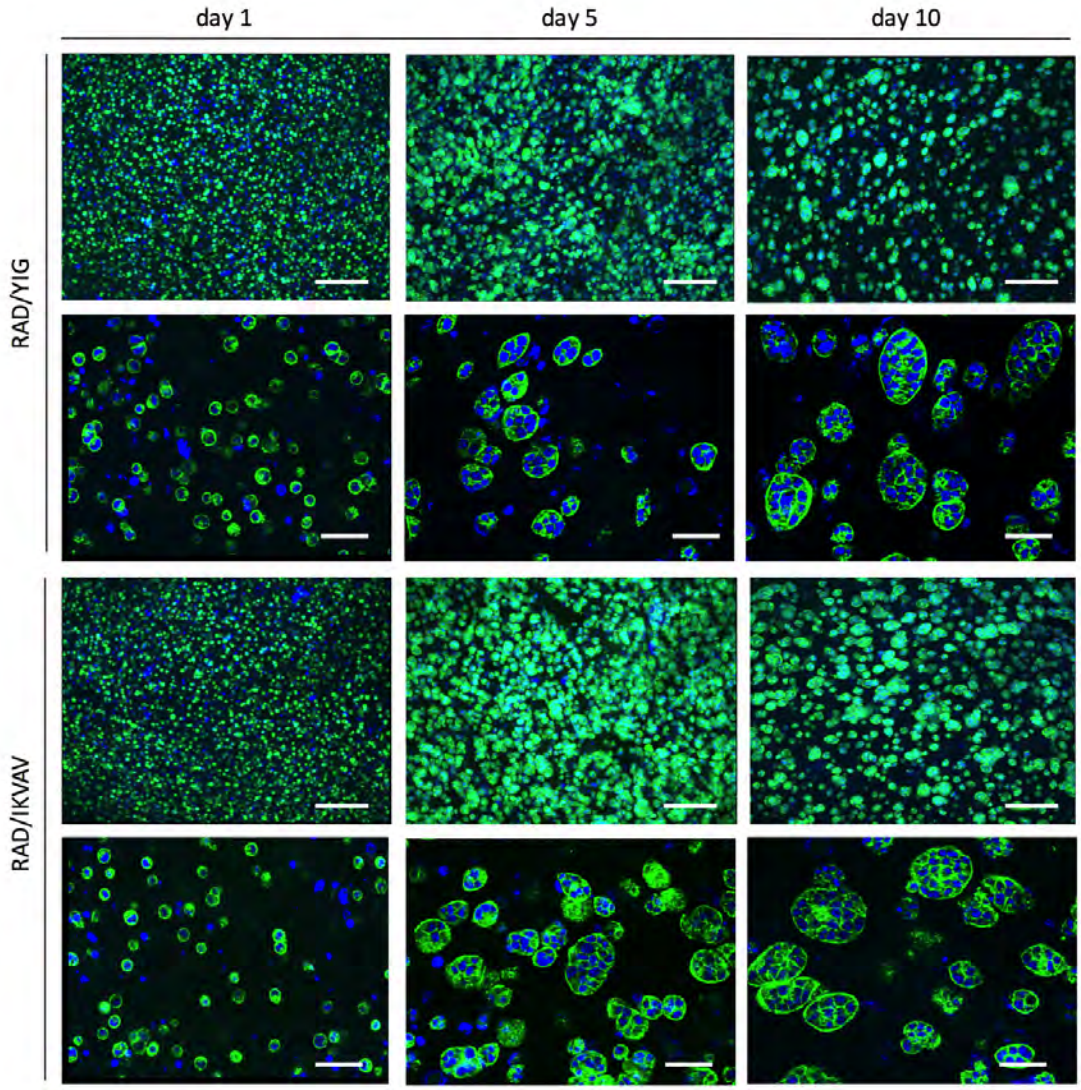

Figure 3.11. INS-1E cell morphology and organization in RAD/YIG and RAD/IKVAV based cultures. Cells were analysed under a fluorescence microscope when cultured in pure RAD/YIG and RAD16-I/IKVAV, functionalized matrices. Nuclei were stained in blue (DAPI) and actin filaments in green (Phalloidin). Z-stack images. Scale bar of 200 µm (Above images), and 50 µm (Below images).

In order to compare the morphology of INS-1E cells when cultured on different environments than the one provided by the synthetic 3D matrix RAD16-I, we assessed the growth in monolayer cultures and in 3D type I collagen matrix, a natural origin scaffold (Figure 3.12). When grown in 2D cultures INS-1E cells also form cell aggregates, but in a more dispersed manner. The aggregates were more irregular in shape and less compact than those present in RAD16-I cultures, and with some degree of cell spreading. This trait could be a consequence of cell attachment to the plastic surface, which lacks the environmental complexity of 3D matrices. Therefore, even though INS-1E cells still grow forming aggregates in 2D conditions, these structures lack the three-dimensionality needed to resemble the tissue architectures of

in vivo pancreatic islets. In type I collagen scaffolds, the same growth pattern was followed. This assay was carried out solely to compare the differences when growing beta cells in a 3D scaffold of natural origin, and therefore with intrinsic signaling properties. Despite the formation of cells clusters, these structures were less homogeneous and with a more irregular morphology. In contrast, clusters formed in RAD16-I based cultures showed a more defined and roundish architecture, mimicking more closely the islet configuration found *in vivo.*

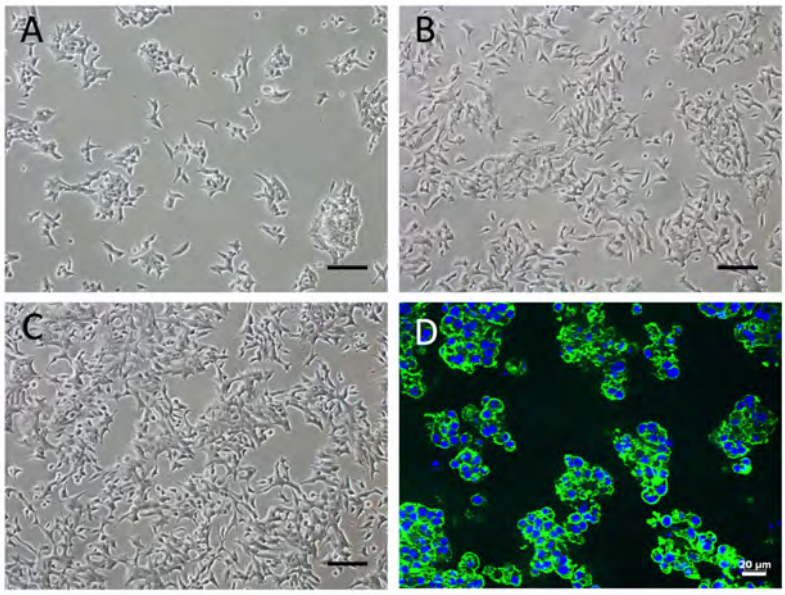

Figure 3.12. Comparison of INS-1E cell morphologies acquired when seeded on different environments. (A, B, C) Phase contrast images of INS-1E cells grown in plastic based 2D cultures at 30, 60 and 80% confluence. (D) Fluorescence images of type I collagen cultures on day 10. Nuclei were stained in blue (DAPI) and actin filaments in green (Phalloidin). Scale bar of 100 µm (A, B, C) and 20 µm (D).

Therefore, after comparing the cell morphologic traits when INS-1E cells were grown within different cell culture environments, RAD16-I showed to be a good platform for the maintenance of INS-1E cell morphology and organization in 3D conditions, with the ability to promote the formation of islet-like cell clusters.

3.3.3.2 INS-1E cell viability in functionalized RAD16-I cultures

Viability analyses were performed in order to find out whether cells remained alive along the culture period in all the established conditions. At various times during the culture (days 1, 5 and 10) cellular viability was analyzed by means of the Live and Dead qualitative assay, that distinguishes live cells from dead cells using two different dyes. Live and dead cells were labeled by green fluorescent (calcein-AM) and red fluorescent (EthD-1) reactive dyes, respectively.

As shown in Figure 3.13, several dead cells were observed on the first day of culture, in all the matrices tested. Our interpretation of the results is based on the fact that RAD16-I stock solution was too acid for cells. The SAP RAD16-I presents an acidic pH (pH 3), which is maintained until gelation occurs. At this moment RAD16-I pH value is adjusted to physiological conditions (pH 7). Thus, the high acidity to which cells are exposed during the mixing step in construct preparation might be unfavorable to cells and responsible for the early cell death. After some days of recovery from the encapsulation (day 5), the majority of the cells were alive for all the RAD16-I based cultures (images not shown). On the last day of culture (day 10), cell death ratio was higher again but not as much as in the first day of culture. One possible explanation could be the lack of oxygen and nutrients due to diffusion problems, as a result of the continued growth of INS-1E cells within the constructs.

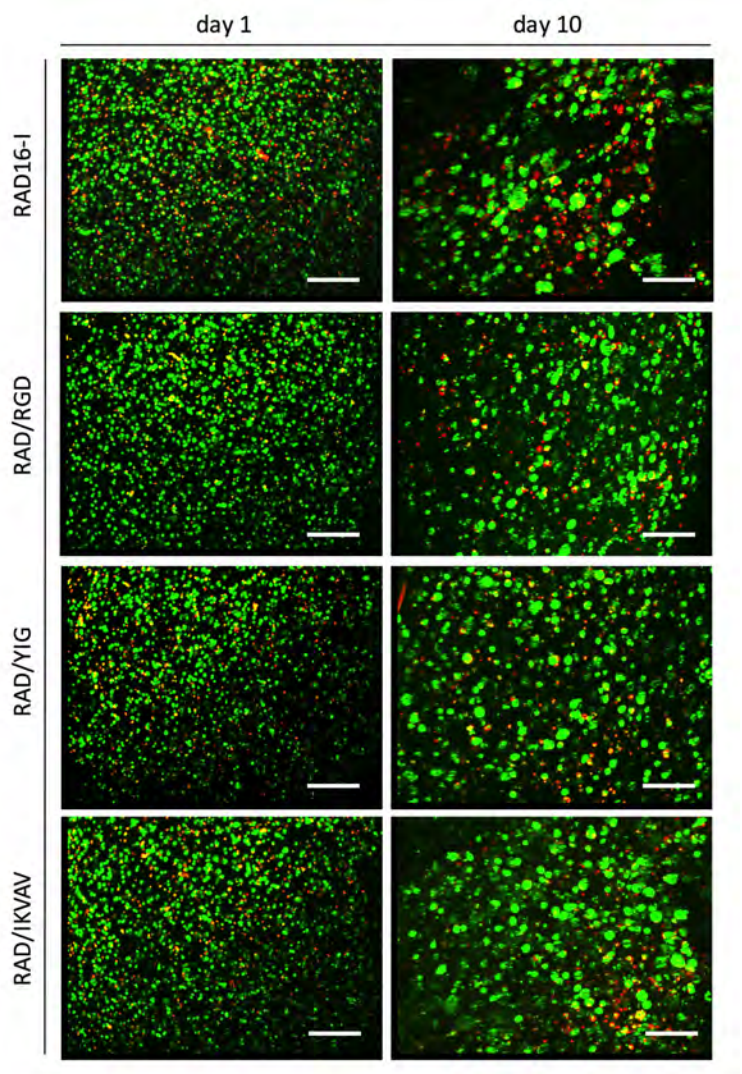

Figure 3.13. INS-1E cellular viability in 3D RAD16-I based cultures. Cells were analyzed under a fluorescence microscope when cultured in pure RAD16-I and RAD16-I/RGD, RAD16-I/YIG and RAD16-I/IKVAV functionalized matrices, by means of the Live and Dead staining. Viable cells are stained green whereas dead cells are stained red (Z-stack images). Scale bar of 200 µm.

3.3.4 ASSESSMENT OF INS-1E FUNCTION IN RAD16-I BASED CULTURES

Following the assessment of cell morphology and viability, functionality of encapsulated INS-1E cells was investigated by performing a glucose stimulated insulin secretion assay. This assay was carried out to figure out whether the introduced cell-matrix interactions entailed some improvement in terms of insulin secretion, which is the most characteristic trait of pancreatic beta cells.

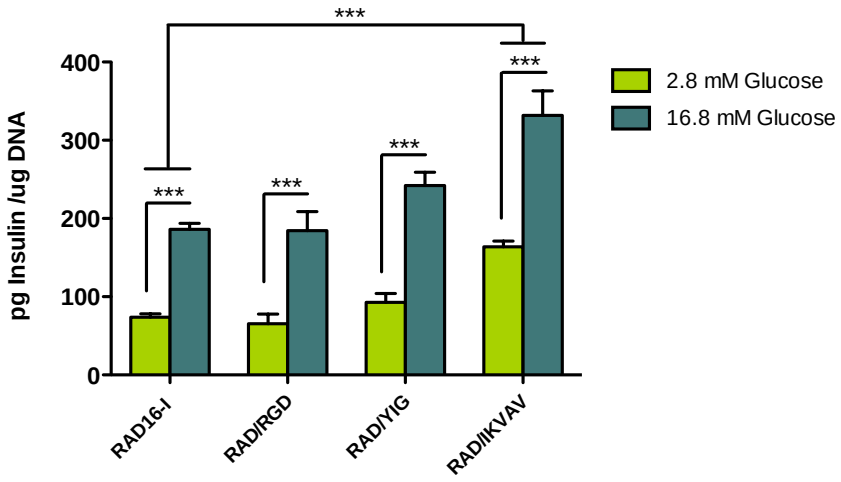

Figure 3.14. Glucose stimulated insulin release of INS-1E cells encapsulated in 3D RAD16-I scaffold after 10 days of culture. Cells cultured in functionalized RAD16-I hydrogels were exposed to a glucose challenge and insulin secretion values were compared to those of pure RAD16-I. Data are expressed as mean ± SEM (n=5) *** $p < 0.001$.

After 10 days in culture, INS-1E cells within pure RAD16-I and functionalized analogs were exposed to 2.8 and 16.8 mM glucose challenge. To avoid variations due to the differences in the number of cells in each one of the samples, the amount of insulin released from each sample in response to both glucose concentrations was normalized to the DNA content from the respective sample. The insulin release of the tailor-made scaffolds was compared to that of pure RAD16-I, used as a control (Figure 3.14). Insulin secretion in response to high glucose concentration (16.8 mM) was approximately two-fold greater than basal secretion (2.8 mM) in all the conditions tested, with no statistical differences between the different matrices. The addition of the IKVAV sequence resulted in statistically higher insulin secretion compared to cells encapsulated in the absence of cell-matrix interactions ($p<0.001$), although the stimulation index remains the same in both conditions. These results are consistent with findings from previous works in which another rodent beta cell line surrogate (MIN-6) was encapsulated in 3D PEG hydrogels[75]. It is worth noting that average insulin secretion values for cells encapsulated within another laminin derived motif, the YIG sequence, were higher than control levels, although this increase was not statistically significant. Surprisingly, the RGD

signaling motif did not cause any improvement on the insulin secretion capacity of INS-1E cells. Therefore, functionality results give evidence that the reestablishmentof cell-matrix interactions can influence in a positive way insulin secretion, by creating favorable relationships between the cells and the surrounding microenvironment. This finding increases the potential of RAD16-I based hydrogel as 3D culture platforms to restore the lost microenvironment when islet cells are isolated and cultured in monolayer conditions. Moreover, this improvement in islet function can be very useful when transplanting islet cells, since it can help reducing the amount of islet cells needed for a feasible treatment.

To further improve these results, different peptide signaling motifs should be designed and applied not only individually but also in combination since it has been demonstrated that some signaling peptide combinations possess synergistic properties[75,76].

3.4 CONCLUDING REMARKS

Pancreatic islet transplantation (IT) has proved its potential as a cell replacement therapy for type 1 diabetes patients. Five years post-transplantation, a high percentage of transplanted subjects (50%) maintain insulin independence with good glycemic control[77]. Even though these IT outcomes are very encouraging, IT feasibility needs to be improved. Among other factors, the restoration of the islet ECM-microenvironment after isolation and prior to the transplantation, is a critical step that needs to be addressed. The reestablishment of cell-matrix interactions can be achieved by the use of ECM-substrates in cell cultures. In fact, several works have already demonstrated that the use of ECM derivatives, complex or purified ECM proteins, improve the viability and function of insulin-secreting cells when grown *in vitro*[7,78,79]. Traditionally, these *in vitro* experiments have been performed in 2D coated cultures, and despite the relevant information they have provided, they don't capture the complexity found *in vivo*. On this background, a 3D culture platform based on the non-instructive RAD16-I self-assembling peptide was developed. To recreate the islet microenvironment, the synthetic matrix was functionalized with peptide signaling motifs present in the islet ECM proteins, such as laminin and fibronectin and collagen IV. Specifically, five cell adhesion motifs with recognized biological activity were covalently added to the RAD16-I sequence (RGD, YIG, IKVAV, GEF and TWY).

All the tailor-made peptides were soluble in water at 1% (w/v) concentration, except for GEF peptide being therefore excluded as a functional motif. Congo red staining helped us to figure out whether the remaining modified peptides maintained the hydrogel formation capacity of non-modified RAD16-I peptide. Three of them, RGD, YIG and IKVAV, were positive for the staining meaning that their aminoacid sequence did not interfered in the self-assembling process. In contrast, TWY sequence did not allow the gelation of the construct, and as a result it was discarded. The study of the secondary structure of the tailor-made peptides through circular dichroism studies showed the influence of the different aminoacid sequence introduced to the RAD16-I peptide, which presents the typical profile of a β-sheet structure. RGD, YIG, and IKVAV peptides also followed the profile of a β-sheet structure, although with a diminished β-sheet content. This decrease is a consequence of the bioactive motifs introduction, which don't follow the characteristic alternating hydrophilic and hydrophobic pattern of RAD16-I peptide. IKVAV peptide didn't show exactly the same profile as pure RAD16-I, but since it was capable of forming nanofibers it was not excluded.

The beta cell surrogate INS-1E cell line was seeded in pure (100% RAD16-I) and functionalized RAD16-I (95% RAD16-I:5% signaling motif), getting embedded within the synthetic matrix in a 3D configuration, and forming a disc-shape hydrogel. Among the different RAD16-I concentrations tested, 0.30% (w/v) was selected to perform the experiments, based on construct stability and viability results. At the beginning of the culture, cells were dispersed all over the matrix, exhibiting a rounded shape. By day 5 of culture, cells were capable of forming spheroid clusters with close cell-cell contacts, resembling the typical growth pattern of native beta cells in pancreatic islets. Cells aggregates were observable in all the matrices, and kept increasing in size until day 10 of culture. Despite growing in similar structures in monolayer

conditions and in collagen gels, these 3D *in vivo*-like structures characterized by a roundish defined architecture, were only fully obtained in pure or functionalized RAD16-I matrix. The addition of the cell bioactive motifs did not cause any change in clusters morphology, besides the presence of some clusters with larger diameters in IKVAV functionalized scaffolds. Cellular viability recovered after the encapsulation process, showing good values along the period culture.

Regarding beta cell functionality, the introduction of the IKVAV peptide entailed a significant enhanced insulin secretion in response to a glucose stimulation compared to the pure RAD16-I analogue. RAD16-I/YIG matrix also experienced an increase in the release of insulin, although it did not reach statistical significance. Hence, the ability of matrix interactions within a RAD16-I hydrogel environment to positively influence islet insulin secretion *in vitro,* indicates the potential of functionalized RAD16-I platforms in pancreatic tissue engineering (PTE).

3.5 REFERENCES

1. The Diabetes Control and Complications Trial group. Hypoglycemia in the Diabetes Control and Complications Trial. *Diabetes* **46,** 271 LP-286 (1997).

2. Hematti, P., Kim, J., Stein, A. P. & Kaufman, D. Potential role of mesenchymal stromal cells in pancreatic islet transplantation. *Transplant. Rev.* **27,** 21–29 (2013).

3. Shapiro, A. M. J. *et al.* Islet transplantation in seven patients with type 1 diabetes mellitus using a glucocorticoid-free immunosuppressive regimen. *N. Engl. J. Med.* **343,** 230–238 (2000).

4. Merani, S. & Shapiro, A. M. J. Current status of pancreatic islet transplantation. *Clin. Sci.* **110,** 611–625 (2006).

5. Wang, R. N. & Rosenberg, L. Maintenance of beta-cell function and survival following islet isolation requires re-establishment of the islet-matrix relationship. *J. Endocrinol.* **163,** 181–190 (1999).

6. Stendahl, J. C., Kaufman, D. B. & Stupp, S. I. Extracellular matrix in pancreatic islets: Relevance to scaffold design and transplantation. *Cell Transplant.* **18,** 1–12 (2009).

7. Nikolova, G. *et al.* The vascular basement membrane: a niche for insulin gene expression and Beta cell proliferation. *Dev. Cell* **10,** 397–405 (2006).

8. Wang, R. N., Paraskevas, S. & Rosenberg, L. Characterization of integrin expression in islets isolated from hamster, canine, porcine, and human pancreas. *J. Histochem. Cytochem.* **47,** 499–506 (1999).

9. Griffith, L. G. & Swartz, M. A. Capturing complex 3D tissue physiology in vitro. *Nat. Rev. Mol. Cell Biol.* **7,** 211–24 (2006).

10. Pampaloni, F., Reynaud, E. G. & Stelzer, E. H. K. The third dimension bridges the gap between cell culture and live tissue. *Nat. Rev. Mol. Cell Biol.* **8,** 839–45 (2007).

11. Baker, B. M. & Chen, C. S. Deconstructing the third dimension: how 3D culture microenvironments alter cellular cues. *J. Cell Sci.* **125,** 3015–24 (2012).

12. Gelain, F., Bottai, D., Vescovi, A. & Zhang, S. Designer self-assembling peptide nanofiber scaffolds for adult mouse neural stem cell 3-dimensional cultures. *PLoS One* **1,** 1–11 (2006).

13. Birgersdotter, A., Sandberg, R. & Ernberg, I. Gene expression perturbation in vitro - A growing case for three-dimensional (3D) culture systems. *Semin. Cancer Biol.* **15,** 405–412 (2005).

14. Weaver, V. M. *et al.* Reversion of the Malignant Phenotype of Human Breast Cells in Three-Dimensional Culture and In Vivo by Integrin Blocking Antibodies. **137,** 231–245 (1997).

15. Edmondson, R., Broglie, J. J., Adcock, A. F. & Yang, L. Three-dimensional cell culture systems and their applications in drug discovery and cell-based biosensors. *Assay Drug Dev. Technol.* **12,** 207–18 (2014).

16. Yamada, K. M. & Cukierman, E. Modeling tissue morphogenesis and cancer in 3D. *Cell* **130,** 601–10 (2007).

17. Beningo, K. A., Dembo, M. & Wang, Y. Responses of fibroblasts to anchorage of dorsal extracellular matrix receptors. *Proc. Natl. Acad. Sci. U. S. A.* **101,** 18024–9 (2004).

18. Engler, A. J., Sen, S., Sweeney, H. L. & Discher, D. E. Matrix Elasticity Directs Stem Cell Lineage Specification. *Cell* **126,** 677–689 (2006).

19. Paszek, M. J. *et al.* Tensional homeostasis and the malignant phenotype. *Cancer Cell* **8,** 241–54 (2005).

20. Gilbert, P. M. *et al.* Substrate elasticity regulates skeletal muscle stem cell self-renewal in culture. *Science (80-.).* **329,** 1078–1081 (2010).

21. Ramanujan, S. *et al.* Diffusion and convection in collagen gels: implications for transport in the tumor interstitium. *Biophys. J.* **83,** 1650–1660 (2002).

22. Tuch, B. E., Gao, S. Y. & Lees, J. G. Scaffolds for islets and stem cells differentiated into insulin-secreting cells. *Front Biosci (Landmark Ed)* **19,** 126–138 (2014).

23. Blomeier, H. *et al.* Polymer scaffolds as synthetic microenvironments for extrahepatic islet transplantation. *Transplantation* **82,** 452 (2006).

24. Daoud, J. T. *et al.* Long-term in vitro human pancreatic islet culture using three-dimensional microfabricated scaffolds. *Biomaterials* **32,** 1536–1542 (2011).

25. Gibly, R. F., Zhang, X., Lowe, W. L. & Shea, L. D. Porous scaffolds support extrahepatic human islet transplantation, engraftment, and function in mice. *Cell Transplant.* **22,** 811–819 (2013).

26. Salvay, D. M. *et al.* Extracellular matrix protein-coated scaffolds promote the reversal of diabetes after extrahepatic islet transplantation. *Transplantation* **85,** 1456 (2008).

27. Cheng, J. Y. C. C., Raghunath, M., Whitelock, J. & Poole-Warren, L. Matrix components and scaffolds for sustained islet function. *Tissue Eng. Part B. Rev.* **17,** 235–47 (2011).

28. Zhang, Z., Gupte, M. J. & Ma, P. X. Biomaterials and stem cells for tissue engineering. *Expert Opin. Biol. Ther.* **13,** 527–40 (2013).

29. Semino, C. E. Can We Build Artificial Stem Cell Compartments? *J. Biomed. Biotechnol.* **3,** 164–169 (2003).

30. Stevens, M. M. & George, J. H. Exploring and engineering the cell surface interface. *Science (80-.).* **310,** 1135–8 (2005).

31. Kisiday, J. *et al.* Self-assembling peptide hydrogel fosters chondrocyte extracellular matrix production and cell division:Implications for cartilage tissue repair. *PNAS* **99,** 9996 –10001 (2002).

32. Koutsopoulos, S. Self-assembling peptide nanofiber hydrogels in tissue engineering and regenerative medicine: Progress, design guidelines, and applications. *J. Biomed. Mater. Res. - Part A* **104,** 1002–1016 (2016).

33. Zhang, S. & Altman, M. Peptide self-assembly in functional polymer science and engineering. *React. Funct. Polym.* **41,** 91–102 (1999).

34. Zhang, S., Gelain, F. & Zhao, X. Designer self-assembling peptide nanofiber scaffolds for 3D tissue cell cultures. *Semin. Cancer Biol.* **15,** 413–20 (2005).

35. Zhang, S. *et al.* Self-complementary oligopeptide matrices support mammalian cell attachment. *Biomaterials* **16,** 1385–1393 (1995).

36. Zhang, S. Fabrication of novel biomaterials through molecular self-assembly. *Nat. Biotechnol.* **21,** 1171–1178 (2003).

37. Zhang, S., Lockshin, C., Herbert, A., Winter, E. & Rich, A. Zuotin , a putative Z-DNA binding protein in Saccharomyces cerevisiae. *EMBO J.* **11,** 3787–3796 (1992).

38. Semino, C. E. Self-assembling Peptides: From Bio-inspired Materials to Bone Regeneration. *J. Dent. Res.* **87,** 606–616 (2008).

39. Nagai, Y., Unsworth, L. D., Koutsopoulos, S. & Zhang, S. Slow release of molecules in self-assembling peptide nanofiber scaffold. *J. Control. Release* **115,** 18–25 (2006).

40. Fernández-Muiños, T. *et al.* Bimolecular based heparin and self-assembling hydrogel for tissue engineering applications. *Acta Biomater.* **16,** 35–48 (2015).

41. Semino, C., Kasahara, J., Hayashi, Y. & Zhang, S. Entrapment of Migrating Hippocampal Neural Cells in Three-Dimensional Peptide Nanofiber Scaffold. *Tissue Eng.* **10,** 643–655 (2004).

42. Semino, C. E., Merok, J. R., Crane, G. G., Panagiotakos, G. & Zhang, S. Functional differentiation of hepatocyte-like spheroid structures from putative liver progenitor cells in three-dimensional peptide scaffolds. *Differentiation.* **71,** 262–70 (2003).

43. Genové, E., Shen, C., Zhang, S. & Semino, C. E. The effect of functionalized self-assembling peptide scaffolds on human aortic endothelial cell function. *Biomaterials* **26,** 3341–3351 (2005).

44. Garreta, E., Genové, E., Borrós, S. & Semino, C. Osteogenic Differentiation of Mouse Embryonic Stem Cells. *Tissue Eng.* **12,** 1–13 (2006).

45. Genové, E. *et al.* Functionalized self-assembling peptide hydrogel enhance maintenance of hepatocyte activity in vitro. *J. Cell. Mol. Med.* **13,** 3387–97 (2009).

46. Wu, J. *et al.* Nanometric self-assembling peptide layers maintain adult hepatocyte phenotype in sandwich cultures. *J. Nanobiotechnology* **8,** 29 (2010).

47. Alemany-Ribes, M., García-Díaz, M., Busom, M., Nonell, S. & Semino, C. E. Toward a 3D Cellular Model for Studying In Vitro the Outcome of Photodynamic Treatments: Accounting for the Effects of Tissue Complexity. *Tissue Eng. Part A* **19,** 1665–74 (2013).

48. Soler-Botija, C. *et al.* Engineered 3D bioimplants using elastomeric scaffold, self-assembling peptide hydrogel, and adipose tissue-derived progenitor cells for cardiac regeneration. *Am. J. Transl. Res.* **6,** 291–301 (2014).

49. Misawa, H. *et al.* PuraMatrix Facilitates Bone Regeneration in Bone Defects of Calvaria in Mice. *Cell Transplant.* **15,** 903–910 (2006).

50. Ellis-behnke, R. G. *et al.* Nano neuro knitting : Peptide nanofiber scaffold for brain repair and axon regeneration with functional return of vision. *PNAS* **103,** 5054–5059 (2006).

51. Stendahl, J. C., Wang, L.-J., Chow, L. W., Kaufman, D. B. & Stupp, S. I. Growth factor delivery from self-assembling nanofibers to facilitate islet transplantation. *Transplantation* **86,** 478 (2008).

52. Khan, S., Sur, S., Newcomb, C. J., Appelt, E. A. & Stupp, S. I. Self-assembling glucagon-like peptide 1-mimetic peptide amphiphiles for enhanced activity and proliferation of insulin-secreting cells. *Acta Biomater.* **8,** 1685–1692 (2012).

53. Lim, D.-J. *et al.* Enhanced Rat Islet Function and Survival *In Vitro* Using a Biomimetic Self-Assembled Nanomatrix Gel. *Tissue Eng. Part A* **17,** 399–406 (2011).

54. Lutolf, M. P. & Hubbell, J. A. Synthetic biomaterials as instructive extracellular microenvironments for morphogenesis in tissue engineering. *Nat. Biotechnol.* **23,** 47–55 (2005).

55. Shin, H., Jo, S. & Mikos, A. G. Biomimetic materials for tissue engineering. *Biomaterials* **24,** 4353–4364 (2003).

56. Elbert, D. L. & Hubbell, J. A. Conjugate addition reactions combined with free-radical cross-linking for the design of materials for tissue engineering. *Biomacromolecules* **2,** 430–441 (2001).

57. Hersel, U., Dahmen, C. & Kessler, H. RGD modified polymers: Biomaterials for stimulated cell adhesion and beyond. *Biomaterials* **24,** 4385–4415 (2003).

58. Rahmany, M. B. & Van Dyke, M. Biomimetic approaches to modulate cellular adhesion in biomaterials: A review. *Acta Biomater.* **9,** 5431–5437 (2013).

59. Bellis, S. L. Advantages of RGD peptides for directing cell association with biomaterials. *Biomaterials* **32,** 4205–4210 (2011).

60. Zhang, Z. X., Zheng, Q. X., Wu, Y. C. & Hao, D. J. Compatibility of neural stem cells with functionalized self-assembling peptide scaffold in vitro. *Biotechnol. Bioprocess Eng.* **15,** 545–551 (2010).

61. Merglen, A. *et al.* Glucose Sensitivity and Metabolism-Secretion Coupling Studied during Two-Year Continuous Culture in INS-1E Insulinoma Cells. *Endocrinology* **145,** 667–678 (2004).

62. Otonkoski, T., Banerjee, M., Korsgren, O., Thornell, L. & Virtanen, I. Unique basement membrane structure of human pancreatic islets: implications for β-cell growth and differentiation. *Diabetes, Obes. Metab.* **10,** 119–127 (2008).

63. Virtanen, I. *et al.* Blood vessels of human islets of Langerhans are surrounded by a double basement membrane. *Diabetologia* **51,** 1181–91 (2008).

64. Kaido, T., Yebra, M., Cirulli, V. & Montgomery, A. M. Regulation of human beta-cell adhesion, motility, and insulin secretion by collagen IV and its receptor alpha1beta1. *J. Biol. Chem.* **279,** 53762–9 (2004).

65. Kaido, T. *et al.* Alphav-integrin utilization in human beta-cell adhesion, spreading, and motility. *J. Biol. Chem.* **279,** 17731–7 (2004).

66. Cirulli, V. *et al.* Expression and function of alpha(v)beta(3) and alpha(v)beta(5) integrins in the developing pancreas: roles in the adhesion and migration of putative endocrine progenitor cells. *J. Cell Biol.* **150,** 1445–60 (2000).

67. Ris, F. *et al.* Impact of integrin-matrix matching and inhibition of apoptosis on the survival of purified human beta-cells in vitro. *Diabetologia* **45,** 841–50 (2002).

68. Pinkse, G. G. M. *et al.* Integrin Signaling via RGD Peptides and Anti beta 1 Antibodies Confers Resistance to Apoptosis in Islets of Langerhans. *Diabetes* **55,** 312–317 (2006).

69. Klunk, W. E., Pettegrew, J. W. & Abraham, D. J. Quantitative evaluation of congo red binding to amyloid-like proteins with a beta-pleated sheet conformation. *J. Histochem. Cytochem.* **37,** 1273–1281 (1989).

70. Kelly, S. M. M. M. & Price, N. C. C. C. The use of circular dichroism in the investigation of protein structure and function. *Curr. Protein Pept. Sci.* **1,** 349–84 (2000).

71. Greenfield, N. Using circular dichroism spectra to estimate protein secondary structure. *Nat. Protoc.* **1,** 2876–2890 (2007).

72. Fändrich, M. & Dobson, C. M. The behaviour of polyamino acids reveals an inverse side chain effect in amyloid structure formation. *EMBO J.* **21,** 5682 LP-5690 (2002).

73. Sun, Y. *et al.* Self-assembly behaviors of molecular designer functional RADA16-I peptides: influence of motifs, pH, and assembly time. *Biomed. Mater.* **12,** 15007 (2016).

74. Huang, H. H., Ramachandran, K. & Stehno-Bittel, L. A replacement for islet equivalents with improved reliability and validity. *Acta Diabetol.* **50,** 687–696 (2013).

75. Weber, L. M., Hayda, K. N., Haskins, K. & Anseth, K. S. The effects of cell-matrix interactions on encapsulated beta-cell function within hydrogels functionalized with matrix-derived adhesive peptides. *Biomaterials* **28,** 3004–11 (2007).

76. Weber, L. M. & Anseth, K. S. Hydrogel encapsulation environments functionalized with extracellular matrix interactions increase islet insulin secretion. *Matrix Biol.* **27,** 667–73 (2008).

77. Bellin, M. D. *et al.* Potent induction immunotherapy promotes long-term insulin independence after islet transplantation in type 1 diabetes. *Am. J. Transplant.* **12,** 1576–1583 (2012).

78. Krishnamurthy, M., Li, J., Al-Masri, M. & Wang, R. Expression and function of alphabeta1 integrins in pancretic beta (INS-1) cells. *J. Cell Commun. Signal.* **2,** 67–79 (2008).

79. Hammar, E. *et al.* Extracellular Matrix Protects Pancreatic β-Cells Against Apoptosis. *Diabetes* **53,** 2034–2041 (2004).

CHAPTER 4

DEVELOPMENT OF FUNCTIONALIZED RAD16-I SANDWICH CULTURES TO PROMOTE THE REDIFFERENTIATION OF HUMAN BETA CELLS AFTER IN VITRO EXPANSION

4.1 BACKGROUND

4.1.1 OVERVIEW

Diabetes is a chronic disease that has reached epidemic proportions[1]. It is characterized by the presence of hyperglycemia that leads to the development of devastating complications and is associated with a high cardiovascular mortality and a reduced life expectancy[2,3]. The loss of insulin-producing beta cells is a common pathogenic trait of the two more common forms of diabetes. In type 1 diabetes the autoimmune disorder results in the destruction of the insulin-expressing beta cells[4]. In type 2 diabetes the reduction in beta cell mass was clearly established in the past decade[5]. Thus, beta cell replacement therapy has been proposed as a curative treatment for diabetes, and as mentioned in chapter 1, islet transplantation has provided proof of concept that cell therapy may achieve insulin-independence and restore normoglycemia in type 1 diabetes, without the need for exogenous insulin or extensive monitoring[6]. However, islet transplantation is severely restricted by the extremely limited availability of pancreatic islet tissue. Therefore, there is an urgent need to develop new strategies to generate an abundant source of insulin-producing cells[7–10]. A potential approach to the development of future therapy for diabetes is the *in vitro* expansion of adult beta cells obtained from cadaveric organ donors[11–14].

4.1.2 IN VITRO EXPANSION OF ADULT HUMAN BETA CELLS

In living organisms, cells are embedded within a complex and rich environment containing multiple extracellular matrix (ECM) components, mixed cell populations and a myriad of cell-secreted factors. It is precisely the adhesive interactions with the surrounding microenvironment what defines cell shape, organization and function. Unavoidably, the *in vitro* expansion of beta cells requires the striping of cells from these native cell-cell and cell-ECM interactions, and the introduction into the adhesive two-dimensional (2D) culture systems. Unfortunately, 2D plastic models do not faithfully recapitulate the physiological conditions found *in vivo*[15].

Although *in vivo* adult beta cells have a low replicative capacity, *in vitro* proliferation has been achieved in monolayer cultures, using a simple culture medium supplemented with serum. Specifically, adult human islet cells can be propagated for 16 passages, with an approximate doubling time of 7 days and without detectable cell apoptosis, which represents an expansion of 65,000-fold. Beyond that time, noticeable cell senescence is developed, as indicated by a decreased of the replication rate. However, this massive expansion is accompanied by a rapid dedifferentiation, implying the loss of the beta cell phenotype[11,16,17]. Within the pancreatic islet cell population, tracking of beta cells have been possible thanks to cell-lineage tracing techniques. This approach confirmed the previous results about proliferation and early dedifferentiation of beta cells *in vitro*, indicating that dedifferentiation may be a precondition

for beta cell proliferation[12]. The phenotypic changes suffered by beta cells when expanded *in vitro* resemble the epithelial to mesenchymal transition (EMT).

4.1.2.1 Epithelial to mesenchymal transition (EMT) in cultured adult beta cells

The epithelium is composed by single or multiple layer of cells that adhere and communicate with each other via specialized intercellular junctions. Epithelial cells usually interact with a basement membrane (BM) that helps to define their physiology through cell-ECM contacts, as for instance, the interactions established by BM proteins and integrins[18]. Epithelial cells are polarized, meaning that their apical and basal surfaces are different. Regularly spaced cell–cell junctions and adhesions between neighboring epithelial cells hold them together and inhibit the movement of individual cells away from the epithelial monolayer. Internal adhesiveness allows an epithelial sheet to enclose a three-dimensional space and provide it with structural definition and mechanical rigidity[19]. In culture, epithelial cells grow forming clusters maintaining strong cell-cell adhesions. On the other hand, mesenchymal cells, generally exhibit neither regimented structure nor tight intracellular adhesion. Mesenchymal cells form structures that are irregular in shape and not uniform in composition or density. Adhesions between mesenchymal cells are less strong than in epithelial tissues, allowing for increased migratory capacity. These cells also have a more extended and elongated shape, relative to epithelial cells, and possess front-to-back leading edge polarity[19]. In culture, mesenchymal cells present a fibroblast-like morphology[20].

When the epithelial to mesenchymal transition (EMT) occurs, epithelial cells undergo multiple biochemical changes that cause the acquisition of a mesenchymal phenotype, which implies enhanced cell migratory capacity, invasiveness, increased resistance to apoptosis and a highly increased production of ECM components. *In vivo* EMT, usually terminates with the degradation of the underlying BM and the migration of the mesenchymal cells away from the epithelial tissue in which was originated[21]. EMT process has been widely characterized in development, wound healing and cancer progression.

EMT is characterized by some key events, such as the deconstruction of cell-cell junctions, the loss of apical-basal polarity and acquisition of a front-rear polarity, reorganization of the cytoskeletal architecture and modification of cell shape, increased motility and ability to degrade ECM proteins, and downregulation of the most characteristic epithelial genes along with the activation of mesenchymal genes[18]. At gene expression level, a hallmark of EMT is the downregulation of the epithelial E-cadherin, that contributes to the destabilization of adherent junctions, which is accompanied by an upregulation of the mesenchymal N-cadherin. As a result of the cadherin switch, cell adhesion is seriously altered[18,21]. The plasticity of the epithelial phenotype enables the reversibility of the EMT, which implies the conversion of the mesenchymal phenotype to a partial or full epithelial phenotype. The following image shows the crucial steps of the EMT, as well as the reverse process, the MET.

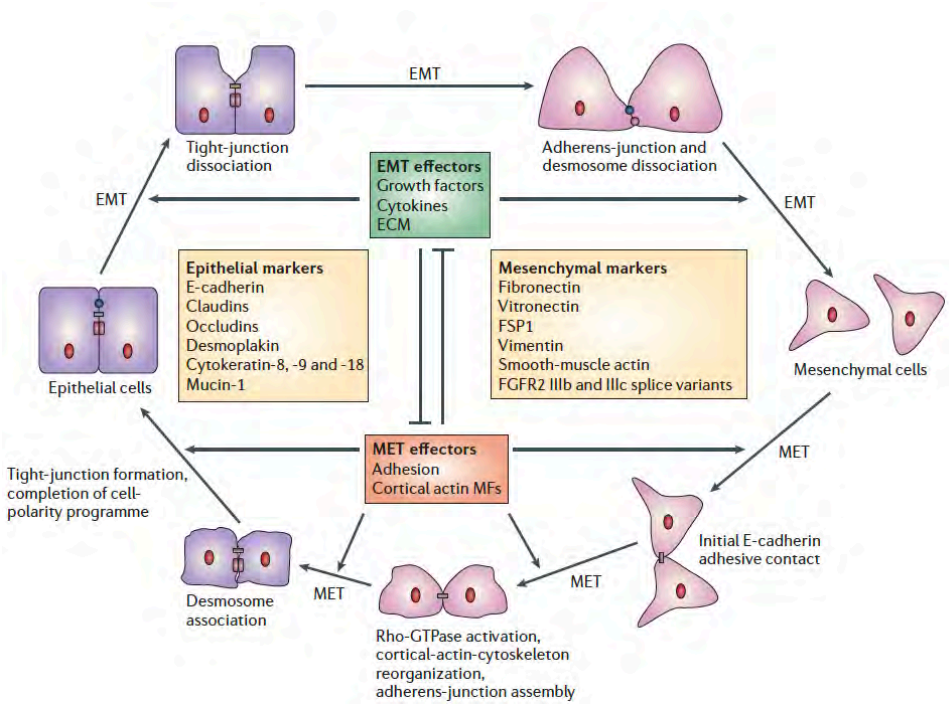

Figure 4.1. Epithelial to mesenchymal transition (EMT) and the reverse process (MET). The EMT process involves the transition of polarized epithelial cells into mobile and ECM proteins-secreting mesenchymal cells. Conversely, the regain of the epithelial phenotype is known as the mesenchymal to epithelial transition (MET). The main epithelial and mesenchymal markers commonly used to identify EMT are depicted[20].

As mentioned previously, the expansion of beta cells in monolayer cultures implies their dedifferentiation, occurring along with the EMT. When cultured beta cells were analyzed at gene expression level at different cell passages, a great decrease in the mRNA levels of insulin and E-cadherin was found. This downregulation took place along with a marked increase in the levels of mesenchymal markers, such as N-cadherin, vimentin and smooth-muscle actin (SMA). Expanded cells also expressed mesenchymal stem cell (MSC) markers, such as CD73, CD90, and CD105, although dedifferentiated cells failed to differentiate into mesodermal cell types[22] (Figure 4.2). Thus, these results based on cell lineage-tracing studies, demonstrate the existence of EMT in cultured adult primary beta cells.

As already explained in Chapter 1, the *in vitro* culture of human islet cells implies the isolation of islets from the pancreas and the subsequent dissociation into single cells. Precisely, the EMT is likely a consequence of this isolation and dissociation, and the subsequent exposure to culture conditions, which completely alters cell-cell and cell-matrix contacts due to the destruction of the islet microenvironment [22,23].

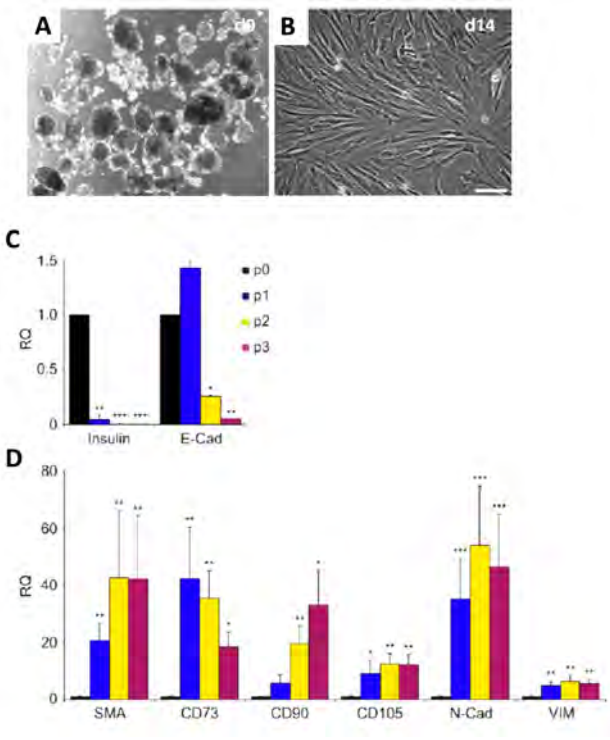

Figure 4.2. Changes in morphology and gene expression profile of isolated islets and cultured adult human islet cells at different passages. (A) Isolated pancreatic islets showing the proper cluster morphology. (B) Cultured human islet cells after 14 days of expansion displaying a fibroblast-like morphology. (C,D) Gene expression analysis of human islet cells showing a decrease in the expression of mRNA levels of insulin and E-cadherin, and an increase of the mesenchymal markers SMA, vimentin and N-cadherin demonstrate that the dedifferentiation of beta cells involves an EMT. (A,B) Adapted from Ouziel-Yahalom *et* al[11]. (C,D) From Russ *et al*[22].

4.1.3 REDIFFERENTIATION OF EXPANDED HUMAN ISLET-DERIVED CELLS

Despite the rapid dedifferentiation suffered by beta cells during *in* vitro expansion, key beta cell genes maintain a partially open chromatin structure, along with a unique DNA methylation signature, indicating the existence of an epigenetic memory. The beta-cell derived cells, even maintained this epigenetic memory after being reprogrammed into induced pluripotent stem cells[24]. Therefore, these findings demonstrate that expanded islet-derived cells maintain the potential to be redifferentiated into insulin-producing cells. Efrat and coworkers managed to redifferentiate expanded dedifferentiated beta cells into insulin-producing cells, using a combination of soluble factors in the culture medium[14]. As depicted in Figure 4.3, the redifferentiation of expanded dedifferentiated human beta cells into a beta cell-like phenotype involved a mesenchymal to epithelial transition (MET).

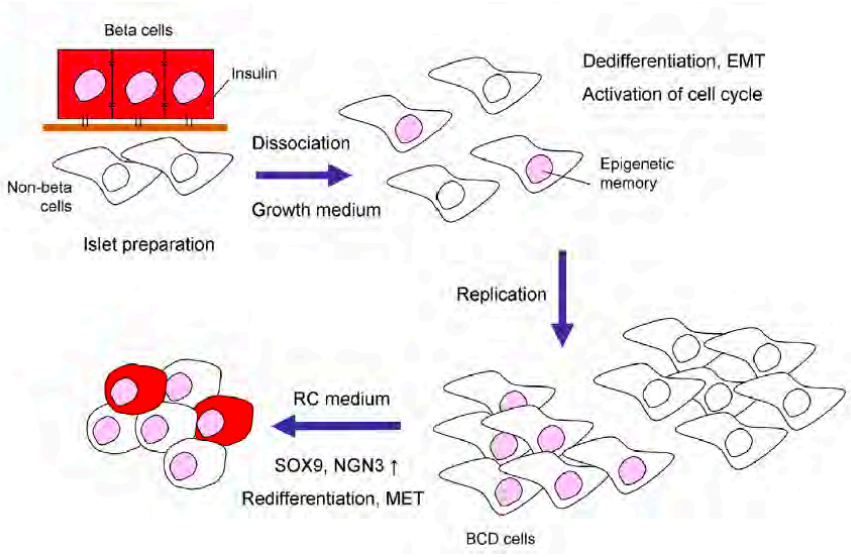

Figure 4.3. Schematic process of beta cell expansion and redifferentiation by soluble factors. Human islet cells are dissociated into single cells and expanded. Beta cell dissociation from epithelial structure, and exposure to growth factors, induce EMT and dedifferentiation, although beta cells maintained epigenetic memory. After treatment with soluble factors, 25% of the beta cell-derived (BCD) cells undergo redifferentiation, which implies MET. From Russ *et al*[14].

Gene expression analysis of cells treated with the redifferentiation cocktail revealed a gradual increase in insulin expression, as well as Pdx1 and MafA genes, markers of beta cells. The epithelial marker E-cadherin was also upregulated, in contrast to the mesenchymal marker N-cadherin, which was simultaneously downregulated. Moreover, cells expressing insulin upon redifferentiation were negative for vimentin, indicating the presence of the MET in the redifferentiation process of expanded beta cells. Hence, these findings open a new therapeutic approach for the generation of insulin-producing cells from pre-existing beta cells.

4.1.4 USE OF 3D MATRICES FOR THE REDIFFERENTIATION TOWARDS A BETA CELL PHENOTYPE

As detailed in Chapter 1, pancreatic islets extracellular matrix (ECM) is composed by the peri-islet and the vascular basement membranes (BM). The main components of the islet BM are laminin (LN) and collagen type IV, although other ECM proteins such as fibronectin (FN) and other types of collagen are also present[25–27]. As in many other tissues, ECM is one of the most important components of the islet microenvironment, playing a key role in islet survival[23,28–32], proliferation[32–34] and insulin secretion[23,35–40]. The interactions of cells to specific sites of the ECM proteins is carried out by integrins, the main cell adhesion receptors, which convert extracellular stimulus into a wide spectrum of intracellular signals[29,35,36].

The poorly controlled enzymatic digestion during pancreatic islet isolation is responsible for the destruction of the peri-islet and the vascular BM. Wang *et al* demonstrated that integrin expression is also affected by the isolation procedure, and that the disruption of cell-ECM contacts, among other factors, causes beta cell death[23]. They were able to prove that the adverse effects of islet isolation over beta cell viability and function, can be prevented or delayed by exposure of islet cells to ECM proteins. Moreover, for *in vitro* culture, isolated islets are often dissociated into single cells, a procedure that disassembles cell-cell contacts, aggravating the effects of pancreatic isolation. By reintroducing contact with other beta cells, insulin secretion was found to increase compared to dissociated single beta cells[41].

Three-dimensional (3D) culture systems provide some advantages over traditional two-dimensional (2D) cultures. In 3D cultures the native microenvironment is closely imitated due to the maintenance of more physiological structures where cell-cell and cell-matrix contacts are preserved. This is especially relevant when culturing islet cell populations, characterized by an *in vivo* environment rich in intercellular and cell-matrix contacts with the surrounding BM[42]. Complex matrices such as 804G, rich in laminin[35,37], or purified proteins from the ECM such as collagen type I[31,43], collagen type IV[40,43], LN-111[43], LN-332[29], LN-411 or LN-511[27] have been used to culture pancreatic beta cells. Compared to conventional 2D cultures, these matrices provide an improved microenvironment that increase cell viability and insulin secretion. However, cells cultured in matrices of natural origin are exposed to the influence of a large variety of unknown biochemical signals that make difficult to attribute outcomes to specific matrix components[44,45]. Furthermore, when animal-derived biomaterials are implanted into the human body an immunogenic reaction may develop[46]. On the other hand, synthetic matrices have a defined composition that can overcome these limitations[47,48].

Self-assembling peptides (SAP) nanofiber scaffolds are synthetic biomaterials that can form hydrogels with excellent properties to create three-dimensional (3D) cell cultures[49–52]. As explained in more detail in Chapter 3, the SAP hydrogel RAD16-I (AcN-RADARADARADARADA-$CONH_2$) is a peptide with a β–sheet structure that self-assembles under physiological conditions into a network of interweaving nanofibers of approximately 10-20 nm diameter that form hydrogel scaffolds with pore sizes of 50-200 nm and more than 99% water content[51], which is structurally similar to the natural ECM. Moreover, RAD16-I allows the study of the effect of a 3D environment *per se*, since it is a non-instructive material[51]. In addition, the lack of chemical signaling confers the possibility of functionalization with specific cell-binding motifs to create a basement membrane analogue. RAD16-I has been shown to promote cell adhesion, growth, proliferation and differentiation of distinct cell types[53–63]. Specifically, SAP have increased survival and insulin secretion of cultured rodent[64–69] and human islets[70].

In this chapter, the SAP RAD16-I has been used to explore different 3D *in vitro* platforms for the culture of dedifferentiated expanded islet-derived cells, aiming to promote the redifferentiation of beta cells. The first model was based on the culture platform created for the rat beta cell surrogate, INS-1E cell line (Chapter 3), where cells are encapsulated within the SAP RAD16-I. The other two models were based on the sandwich configuration[56,71], that consists on the embedding of cells between two layers of peptide. The nanofibrous structure

of RAD16-I hydrogel presents a more physiological environment for the cells, although it does not provide any chemical signaling. For this reason, and in order to mimic the islet microenvironment, RAD16-I was functionalized with short peptide signaling motifs derived from the pancreatic ECM. In particular, the adhesive motifs used to tailor the SAP are RGD, YIG and IKVAV, all of them present in laminin and fibronectin (RGD). In the case of the sandwich configuration, prior to the establishment of the 3D cultures, expanded cells were induced to re-aggregate forming islet-like cell clusters (ICCs), to promote cell-cell contacts. To determine whether redifferentiation was promoted solely by the introduction of the RGD bioactive motif, no differentiation factors were added to the culture medium. Figure 4.4 shows a schematic view of the whole process (sandwich model).

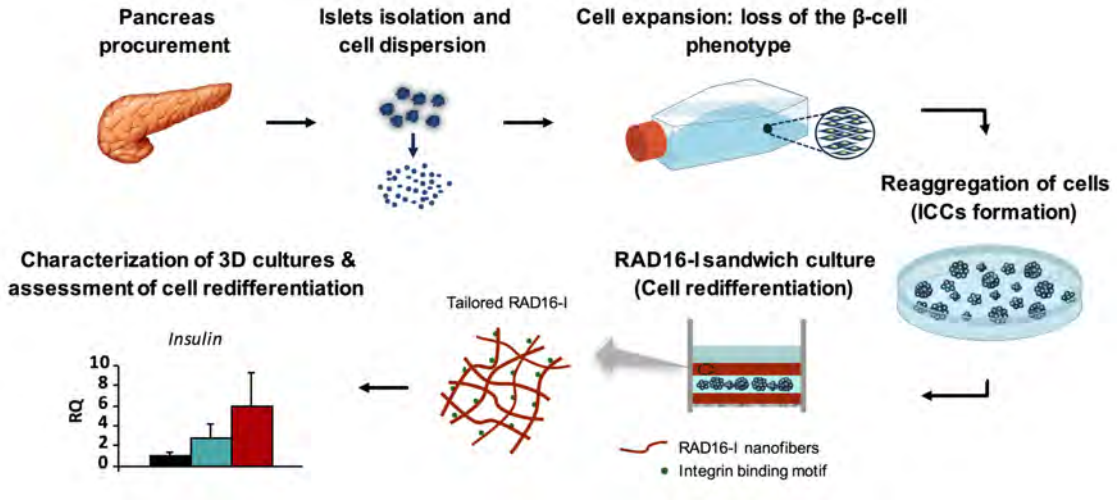

Figure 4.4. Schematic process of the 3D *in* vitro approach (sandwich model) to promote beta cell redifferentiation after human islet cells expansion in 2D cultures. After pancreas procurement, islets were isolated and dissociated into single cells. Then, cells were placed in 2D cultures in order to be expanded, which caused the dedifferentiation of human beta cells. Afterwards, dedifferentiated cells were induced to form islet-like cell clusters (ICCs) by being cultured in non-adherent plates. ICCs were then embedded in functionalized sandwich cultures, aiming to promote the redifferentiation through the reconstitution of the islet microenvironment.

4.1.5 BETA CELL AND EMT-MET MARKERS ANALYZED

In order to evaluate the redifferentiation of human islet-expanded cells after culture in 3D RAD16-I models, different endocrine and EMT cells markers were analyzed at gene expression level. A brief description of the analyzed markers is presented.

4.1.5.1 Beta cell markers

Insulin (Ins): The insulin gene provides instructions for producing the hormone insulin, which is required for normal glucose homeostasis. The insulin in the circulation of adult mammals is produced exclusively by the pancreatic beta cells and insulin deprivation results in diabetes[72]. In some animals, there are two insulin genes, although in humans a single gene is present. The insulin gene results in the translation of preproinsulin, the precursor of mature insulin. Preproinsulin is then processed to proinsulin by removal of the signal peptide and then to mature biologically active insulin, by removal of the C-peptide.

NK6 homeobox 1 (**Nkx6.1):** NKx6.1 is a bifunctional (can act as an activator or repressor) transcription factor that binds to specific A/T-rich DNA sequences in the promoter regions of a number of genes[73]. Nkx6.1 is expressed in the developing and mature pancreas and the central nervous system[74]. In the pancreas, the Nkx6.1 gene is required for the development of beta cells, being crucial for the final step of the major pathway leading to differentiation of β-cells[73]. This transcription factor binds to the insulin promoter, as it is involved in the regulation of the insulin gene. During development, Nkx6.1 is first expressed in multipotent pancreatic progenitors, where it specifies an endocrine identity by repressing the pre-acinar transcription factor Ptf1a. At later developmental stages, Nkx6.1 expression persists in common progenitor cells for the ductal and endocrine cell lineages before becoming eventually restricted to the beta cell lineage at the time of birth. The phenotype observed upon conditional activation or deletion of Nkx6.1 in endocrine precursors identifies Nkx6.1 as a potent general repressor of non-beta endocrine gene expression programs[75].

V-maf musculoaponeurotic fibrosarcoma oncogene homolog A (MafA): MafA is a beta cell specific member of the Maf family of transcription factors[76]. The Maf family proteins regulate tissue-specific gene expression and cell differentiation in a wide variety of tissues. MafA acts synergistically with other transcription factors such as Pdx1 and Beta2 to activate the insulin gene promoter. MafA is a transcription factor that binds to the promoter in the insulin gene and regulates insulin transcription in response to serum glucose levels[77]. MafA also regulates genes involved in beta cell function such as glucose transporter 2, glucagon-like peptide 1 receptor, and prohormone convertase 1/3. The abundance of MafA in beta cells is regulated at both the transcriptional and post-translational levels by glucose and oxidative stress, and may be involved in the pathogenesis of diabetes[76,78].

V-maf musculoaponeurotic fibrosarcoma oncogene homolog B (MafB): MafB is a basic region/leucine zipper transcription factors that affect transcription positively or negatively, depending on their partner proteins and the context of the target promoter. MafB along with MafA, are expressed in a unique temporal regulated manner in relation to other islet-enriched factors in developing and postnatal pancreas[79]. During embryonic development MafB is expressed earlier than MafA. Specifically, during this stage, a significant proportion of cells expressing MafB also express insulin and it regulates potential effectors of glucose sensing, hormone processing, vesicle formation and insulin secretion[80]. However, this proportion rapidly declines after birth. By contrast, the proportion of cells co-expressing insulin and MafA

increases gradually from the embryonic development to the adult stage. In the adult pancreas, there is a selective expression of MafA and MafB in beta and alpha cells, respectively. Therefore, it has been suggested that the differentiation of beta cells is preceded by a switch from MafB to MafA expression[81].

Pancreatic and duodenal homeobox 1 (Pdx1): Pdx1 is an essential transcription factor in pancreatic development, being one of the earliest genes expressed in the developing pancreas. Early in development, Pdx1 is highly expressed in a region of the posterior foregut endoderm, from which the dorsal and ventral pancreatic buds arise. As organogenesis continues, PDX1 is detected throughout the region that forms the pancreas and in part of the presumptive stomach and duodenum[82]. Its expression then becomes progressively restricted to endocrine cells, and in the adult pancreas Pdx1 is restricted to beta cells as well as a few epithelial cells in the dorsal side of the stomach and all the mucosa cells in the duodenum[83]. It regulates several genes including insulin, glucose transporter-2, and glucokinase, which are crucial to beta cell function. Moreover, recent findings indicate that in the adult pancreas acts as a master regulator of beta cell fate by simultaneously activating genes essential for beta cell identity and repressing those associated with α-cell identity[84]. Thus, Pdx1 have a dual function during development and later endocrine function. Initially is required for early pancreas formation, while later its expression is required to maintain proper hormone production by beta cells.

Neurogenic Differentiation Factor 1 (NeuroD1): NeuroD1 is a member of the NeuroD family of basic helix-loop-helix transcription factors that contributes to the regulation of several cell differentiation pathways. It is involved in the differentiation of endocrine pancreatic cells, being first expressed in the pancreatic primordium although in mature islets it is predominantly restricted to beta cells[85]. Specifically, in beta cells NeuroD1 has been shown to activate the insulin promoter.

Transcription Factor Sox9 (Sox9): Sox9 is a specific marker and maintenance factor of multipotential progenitors during pancreas organogenesis. Sox9 maintains pancreatic progenitors by stimulating their proliferation, survival and persistence in an undifferentiated state[86]. It is expressed in all epithelial cells at early developmental stages but its expression is confined to the duct cells as development proceeds. Differentiated acinar and endocrine cells do not express Sox9, but this factor is required for the induction of *Ngn3*, an indispensable gene for endocrine differentiation[87].

4.1.5.2 EMT-MET cell markers

E-cadherin (E-Cad): E-Cad gene belongs to the superfamily of cadherin genes composed by more than 100 members. E-cadherin is a transmembrane glycoprotein that mediates calcium-dependent homophilic cell-cell adhesion in most epithelial tissues. E-cadherin has long extracellular and cytoplasmic domains. The extracellular domain of E-cadherin establishes

homophilic interactions between neighboring cells, while its cytoplasmic tail associates with an array of multifunctional adaptor proteins. These intracellular adaptor proteins link cell-cell adhesion to the actin-myosin network and other intracellular signaling pathways[88]. E-cadherin plays an important role in maintaining the normal phenotype of epithelial cells.

N-cadherin (N-Cad): N-Cad gene belongs to the superfamily of cadherins genes. As in the case of E-cadherin, N-cadherin is a transmembrane glycoprotein that mediates calcium-dependent homophilic cell-cell adhesions, and presents extracellular domains that mediate homophilic interactions between adjacent cells, and cytoplasmic tails that mediate binding to catenins, responsible for the interaction with the cytoskeleton. This cadherin is expressed in some epithelial cells, including neuroepithelial cells, neurons and mesenchymal cells. Expression of N-cadherin in epithelial cells induces changes in morphology towards a fibroblastic phenotype, and is a hallmark of the EMT[89].

Vimentin (Vim): This gene encodes a member of the intermediate filament family. Intermediate filaments, along with microtubules and actin microfilaments, make up the cytoskeleton. The protein encoded by this gene is responsible for maintaining cell shape, integrity of the cytoplasm, and stabilizing cytoskeletal interactions. It functions as an organizer of a number of critical proteins involved in attachment, migration, and cell signaling. This protein is the major cytoskeletal component of mesenchymal cells. Because of this, vimentin is often used as a marker of cells undergoing an EMT.

4.2 HYPOTHESIS AND AIMS

Islet transplantation has provided proof of concept that cell therapy can restore normoglycemia in patients with diabetes. However, there is dramatic mismatch between the availability of islets and the number needed for transplantation in type 1 diabetic patients. Thus, many efforts are being placed in finding new sources of insulin-producing cells that could be used to treat diabetes. A potential approach is the *in vitro* expansion of pancreatic beta cells obtained from cadaveric organ donors. However, when human beta cells are expanded *in vitro*, they dedifferentiate and lose the expression of insulin, probably as a consequence of the islet microenvironment disruption during isolation, and the loss of cell contacts after islet dissociation into single cells.

In the previous chapter, we established a RAD16-I 3D model based on the functionalization of the synthetic matrix with cell recognition motifs, for the culture of the rat beta cell line INS-1E. That system provided good results in terms of viability, morphology and enhancement of beta cell function. Therefore, in the present chapter we apply the developed model to the culture of dedifferentiated expanded human islets cells. Moreover, we have established another 3D culture platform based on the embedding of cells between two thin layers of functionalized peptide (sandwich cultures). Our working hypothesis is that the reestablishment of cell-cell contacts, through the formation of islet-like cell clusters (ICCs) after cell expansion, and cell-matrix relationships in a biomimetic synthetic scaffold could promote the redifferentiation of human beta cells expanded *in vitro*. Thus, the specific aims of this chapter are the following:

1) To characterize the phenotype of islet-derived cells after cell sorting and *in vitro* expansion in 2D conditions.

2) To adapt the RAD16-I platform developed in the previous chapter to the culture of dedifferentiated expanded cells, in order to promote their redifferentiation.

3) To characterize the behavior and the recovery of the beta cell phenotype of dedifferentiated expanded cells, in a RAD16-I sandwich platform.

4) To characterize the behavior and the recovery of the beta cell phenotype of dedifferentiated expanded cells, in an improved RAD16-I sandwich platform.

4.3 RESULTS AND DISCUSSION

4.3.1 CHARACTERIZATION OF ISOLATED HUMAN ISLET CELLS

4.3.1.1 Phenotypic characterization of isolated and sorted cells

Human pancreatic islet cells were isolated from 12 adult cadaveric organ donors as described in Chapter 2 (section 2.2.1). After isolation, the purity of islet cell preparations used was 70 ± 4%. Since duct epithelial cells associate in a very close manner with islet cells, further methods of islet purification were needed in order to obtain purer fractions. Within the pancreas, neural cell adhesion molecule (NCAM) is known to play a key role in adhesions formed between the endocrine cells[90]. A sialylated form of the molecule, named polysialic acid–NCAM (PSA-NCAM) possess modified adhesive properties and is expressed in adult beta cells and therefore can be used as a specific beta cell marker[91,92]. Hence, following islet isolation, cells were dispersed into single cells and sorted by magnetic cell sorting (MACS) with the aim of increasing the endocrine cell purity. This method is based on a positive selection of cells expressing PSA-NCAM[93].

The application of this technique entailed a significant enrichment in insulin$^+$ cells in the PSA-NCAM positive fraction (pre-sorting: 27 ± 5%, post-sorting: 56 ± 4%), and in endocrine non-β-cells (pre-sorting: 8 ± 2%, post-sorting 22 ± 3%) (Figure 4.5). As a result, the endocrine cell purity in the post-sorting fraction was 78 ± 4%. The presence of amylase$^+$ (acinar) and cytokeratin 19$^+$ (Ck19$^+$) cells (ductal), as well as vimentin$^+$ cells (mesenchymal), was significantly reduced in the post-sorting fraction.

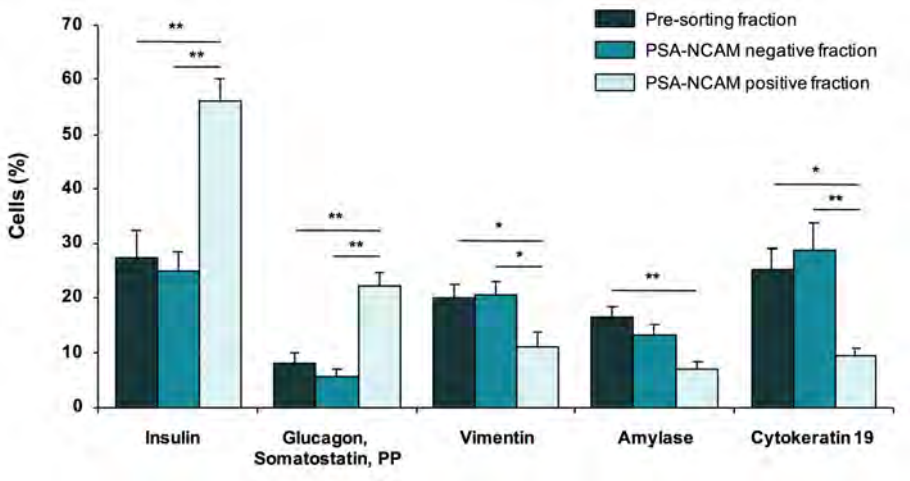

Figure 4.5. Purity of endocrine cells after islet isolation and purification by MACs. Cellular compositions of dispersed cells before (pre-sorting fraction) and after the purification step by magnetic cell sorting (PSA-NCAM positive and negative fractions). Data are means ± SEM from 8 cadaveric organ donors (n= 8) * $p < 0.05$, ** $p < 0.01$.

4.3.1.2 Phenotypic characterization of sorted cells during *in vitro* expansion

After performing the magnetic cell sorting, the enriched endocrine fraction was seeded and expanded in monolayer cultures in order to obtain a high number of cells available for beta cell replacement therapies. Beta cells have a very low proliferative capacity *in vivo*, but when dispersed into single cells and placed in 2D conditions, a significant replication has been achieved[12]. Nevertheless, once in culture, the percentage of cells expressing insulin declines drastically. Specifically, the percentage of insulin positive cells decreased from 53.4 ± 7.3% to 8.5 ± 1.9%, between day 0 and day 12, being almost undetectable at p4 (0.6 ± 0.2%). In contrast, the percentage of cells expressing the mesenchymal marker vimentin increased from 13.5 ± 2.9% on day 0 to 60.7 ± 7.9% on day 12, and to 98.0 ± 0.5 % at p4 (Figure 4.6).

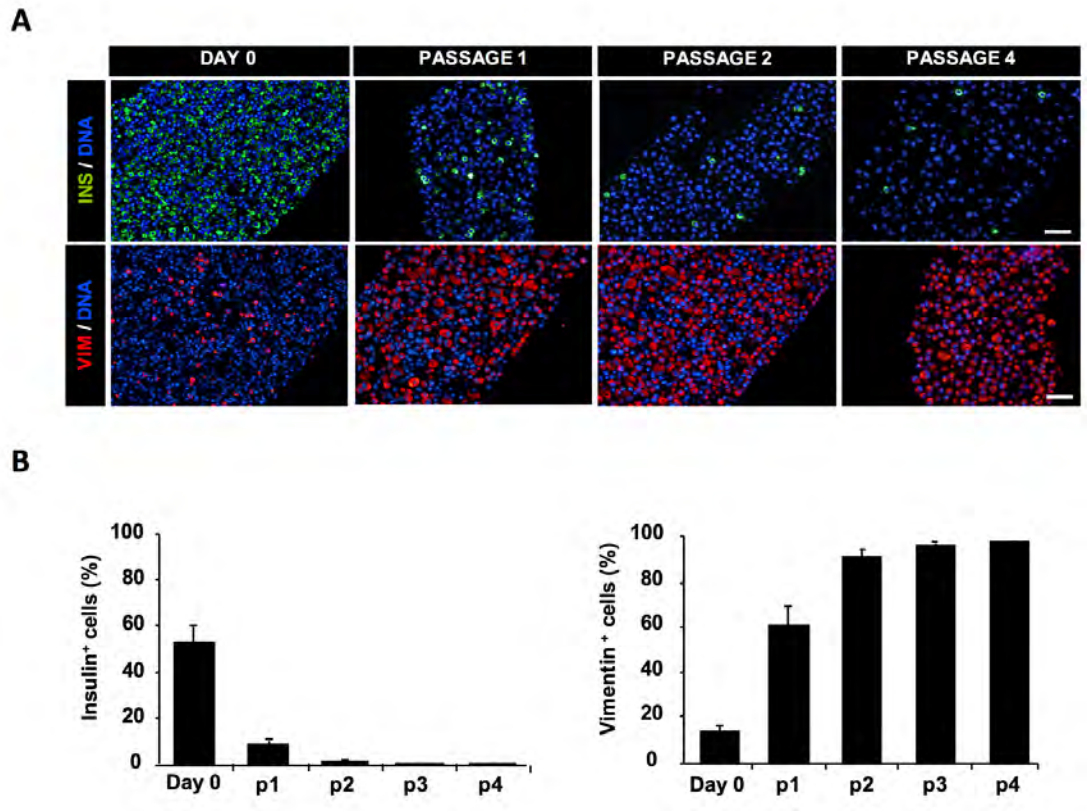

Figure 4.6. Loss of the beta cell phenotype during *in vitro* expansion. (A) Representative immunostaining images of endocrine enriched cell preparations at day 0 and at passages 1 to 4 showing epithelial to mesenchymal transition of islet cells, with loss of insulin expression and acquisition of a mesenchymal phenotype (vimentin). Cells were stained for insulin (green) and vimentin (red), and nuclei were stained with DAPI (blue). (B) Expression of insulin and vimentin along passages. A minimum of 500 positive cells for each population was counted on at least five representative fields. Scale bar of 20 µm. Data are means ± SEM from 6 cadaveric organ donors (n= 6).

Thus, the expansion of dispersed islets cells entailed the loss of the beta cell phenotype and the dedifferentiation into a population of mesenchymal-like cells that do not secrete insulin, suggesting the presence of an epithelial to mesenchymal transition (EMT) in expanded islet-derived cells. The EMT process is probably a consequence of pancreatic islet isolation and dissociation into single cells, which completely alters cell-cell and cell-matrix contacts due to the destruction of the islet microenvironment [23,94]. These results are in agreement with previous studies where massive expansion of pancreatic islet cells also caused the rapid dedifferentiation of beta cells[11,12]. In these works, cell replication was accompanied by a decrease in transcription of key genes expressed in normal beta cells, pointing out that dedifferentiation may be a requisite for beta cell replication. Efrat and coworkers proved by cell-lineage tracing studies that replicating cells derived from human adult beta cells underwent EMT[22].

The enriched endocrine fraction expanded in 2D culture conditions showed massive proliferation until passage 13. As seen in Figure 4.7.A, at passage 0, insulin-expressing cells maintained a rounded shape, typical of epithelial cells. Conversely, after undergoing cell expansion, specifically 7 passages (Figure 4.7.B), the majority of the cells presented a spindle-shape phenotype with a marked increase in vimentin expression, recapitulating some cellular traits of the EMT process. Following cell expansion, the islet-derived cells from passages 7-8 were seeded in 3D cultures.

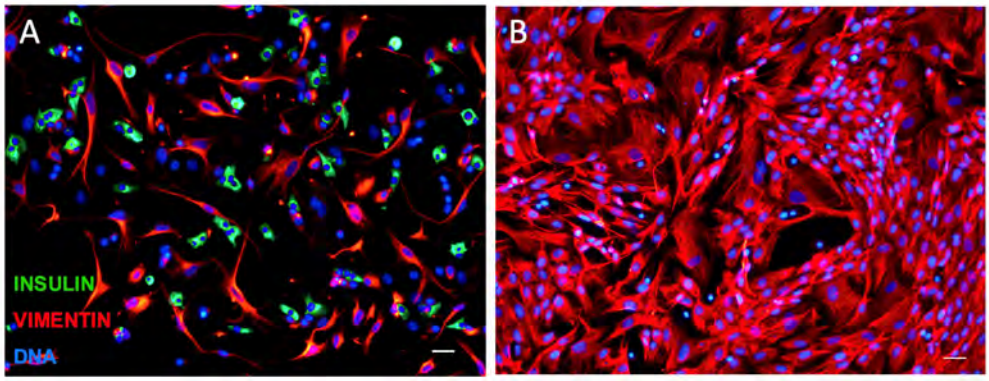

Figure 4.7. Cell morphology of islet-derived cells during cell expansion in monolayer cultures. (A) Cells from passage 0 showing different cellular morphologies. Insulin positive cells display a rounded shape characteristic of epithelial cells. (B) At passage 7, cells presented a more elongated shape with loss of insulin expression and a clear increase in vimentin expression, indicating the presence of the epithelial to mesenchymal transition (EMT). Cells were double stained for insulin (green) and vimentin (red), and nuclei were stained with DAPI (blue). Scale bars of 10 μm.

4.3.2 STANDARD 3D CULTURES OF HUMAN ISLET-DERIVED EXPANDED CELLS

4.3.2.1 Set-up of standard RAD16-I cultures of islet-derived expanded cells

After 7-8 passages in monolayer cultures, expanded human islet-derived cells were encapsulated with the RAD16-I peptide. The purpose of encapsulating expanded cells within a synthetic matrix was to provide cells with an analog of the lost ECM, as cell-ECM contacts are known to be indispensable for the maintenance of beta cells functionality[45,94].

Based on the positive results obtained when growing the insulin secreting cells INS-1E in 3D RAD16-I cultures, we aimed to set up the same RAD16-I platform to culture dedifferentiated islet-derived cells. Since RAD16-I peptide has shown to maintain viability and function of isolated pancreatic islets[70], we hypothesized that the embedding of dedifferentiated cells within this synthetic ECM would promote the establishment of cell-cell and cell-matrix contacts, providing a more favorable microenvironment for the redifferentiation into a beta cell phenotype.

Expanded cells form passages 7-8 were encapsulated with the non-instructive peptide RAD16-I 0.30%, following the standard encapsulation method described in Chapter 2 (section 2.4.1) (Figure 4.8.A). Three different cell densities were tested ($2{\cdot}10^6$, $4{\cdot}10^6$ and $8{\cdot}10^6$ cells/mL) and constructs obtained with the different cell densities were analyzed at macroscopic and microscopic level. Constructs with the highest cell density broke due to the lack of homogeneity when mixing the peptide with the cell suspension, and therefore, the $8{\cdot}10^6$ cells/mL density was considered too high and it was discarded. Moreover, two different construct volumes were assayed, 20 and 40 μL, but since no apparent differences were observed we chose the smallest volume, that results in thinner constructs. As mentioned previously, human beta cells are highly vascularized, which implies a high oxygen demand[95]. In fact, one of the challenges in tissue engineering (TE) approaches, is to obtain scaffolds capable of allowing the diffusion of oxygen and nutrients, being that influx more easily promoted when thinner scaffolds are build.

The 20 μL constructs measured 2-3 mm in diameter and 1-1.5 mm thickness. As depicted in Figure 4.8.A, on day 1 single cells were dispersed all over the RAD16-I matrix, showing a roundish morphology, as a result of the trypsinization. After the first week in culture (day 7) cells maintained the same structure, with no sign of cell elongation or cluster formation, in any of the tested cell densities. We expected that dedifferentiated cells would respond to the provided 3D environment by reestablishing cell-cell and cell-matrix contacts. However, no cell changes were appreciated during the first week of culture.

At the same time, dedifferentiated expanded cells were cultured using the same technique but with a modification. In particular, cells mixed with the RAD16-I peptide were loaded on top of a hydrophilic PTFE (polytetrafluoroethylene) membrane. The cell suspension penetrated within the membrane, and as a result, thinner constructs were obtained (detailed in Chapter 2,

section 2.4.1) (Figure 4.8.B). Constructs obtained with this method were 3-5 mm in diameter and 0.5-1 mm thickness. However, it seemed that the reduction in construct thickness did not entail any improvement in terms of cell response. As in the previous case, cells presented a rounded morphology during the first week of culture, with no apparent changes. As seen with the INS-1E beta cell line, after the encapsulation process cells suffer a traumatic insult due to the initial acidity of RAD16-I. Nonetheless, cells recovered within a few days. Specifically, INS-1E cells were capable of forming cell clusters within the first week in RAD16-I 3D cultures.

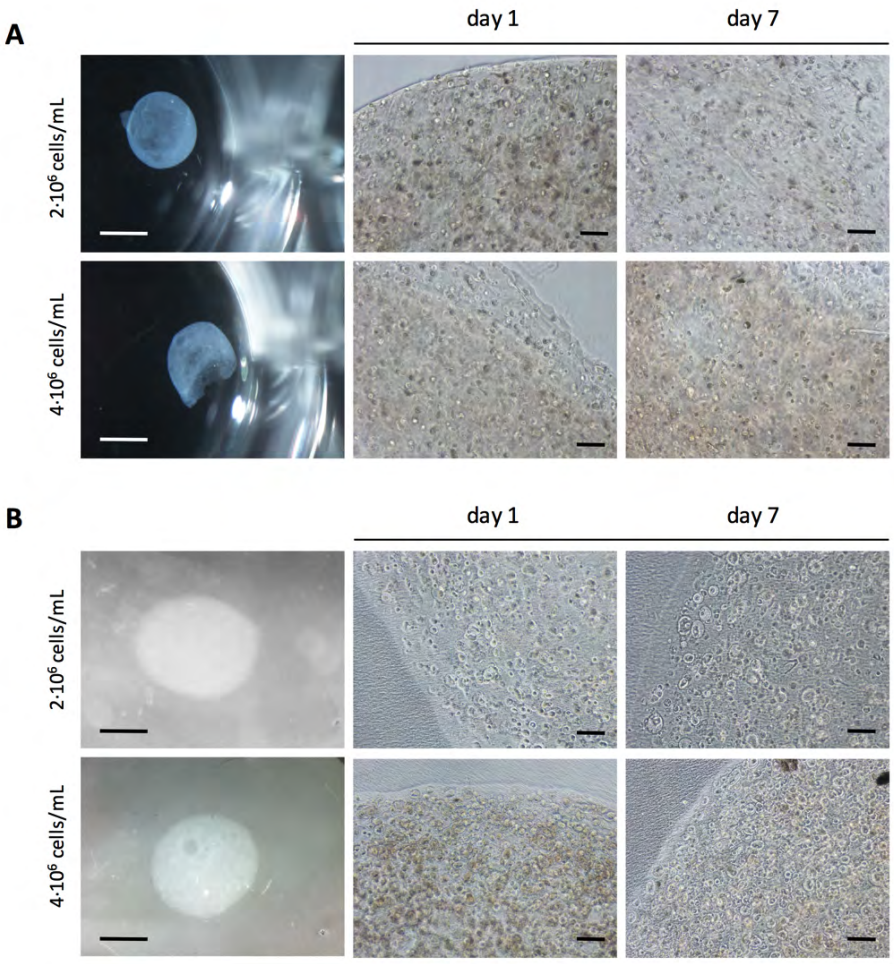

Figure 4.8. Morphology assessment of standard 3D cultures of islet-derived expanded cells at macroscopic and microscopic level. (A) Expanded cells were encapsulated with RAD16-I peptide at different cell densities ($2{\cdot}10^6$, $4{\cdot}10^6$ cells/mL) resulting in constructs of 2-3 mm in diameter and 1-1.5 mm thickness. (B) The blend of RAD6-I and cell suspension was placed on top of a PTFE membrane, obtaining thinner constructs (3-5 mm in diameter and 0.5-1 mm thickness). In both cases, cells adopted a rounded morphology with no changes during seven days of culture, giving rise to static cultures. Scale bars of 2 mm (left) and 100 μm (right).

4.3.2.2 Viability assessment of islet-derived expanded cells in RAD16-I cultures

RAD16-I peptide doesn't exert any chemical signaling over the cells. Therefore, we decided to perform a test and encapsulate expanded cells in a 3D matrix of natural origin with intrinsic signaling properties, type I collagen. Cell viability was assessed in both type of matrices, in order to find out whether the lack of cell response in RAD16-I cultures was due to cell death or to the non-instructive nature of the peptide. Thereby, on days 1 and 7 cellular viability was analyzed with the Live and Dead kit. Figure 4.9 shows that on day 1, a high cell death was present in RAD16-I cultures. This was already expected, as the acidic pH that RAD16-I presents before the self-assembling process tends to reduce cell viability. More strikingly, after one week of culture, cells were not able to recover from the encapsulation process as indicated by the decreased density of live cells. Moreover, cells did not establish contact with one another, impeding the formation of cell clusters, which is thought to be an essential step in the redifferentiation process[14,22,23]. On the other hand, most of the cells grown within the collagen matrix, and not exposed to an acidic pH during the encapsulation process, were alive on day 1. After one week in culture, cell viability was maintained and cellular morphology had changed substantially, with cell elongation as the main characteristic trait.

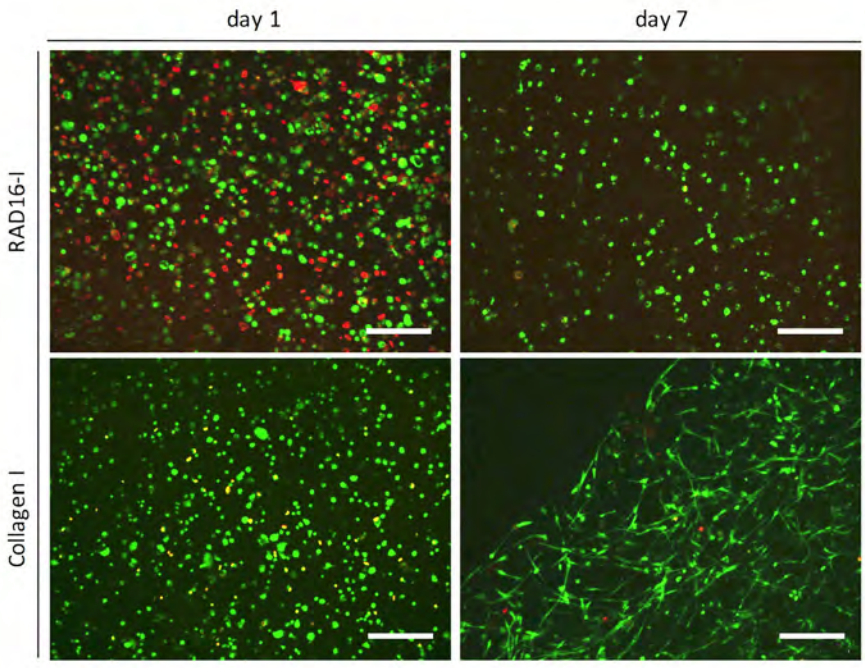

Figure 4.9. Cellular viability of 3D cultures of islet-derived expanded cells. Fluorescent images taken on days 1 and 7 of culture. Living cells were stained with calcein (green) and dead cells were stained with ethidium homodimer-1 (red). Scale bars of 200 μm.

In order to quantify the viability we performed longer cultures for cell counting. Additionally, two functionalized matrices based on the RAD16-I peptide, RAD16-I/RGD and RAD16-I/YIG, were used to create a bidirectional signaling between cells and the surrounding matrix.

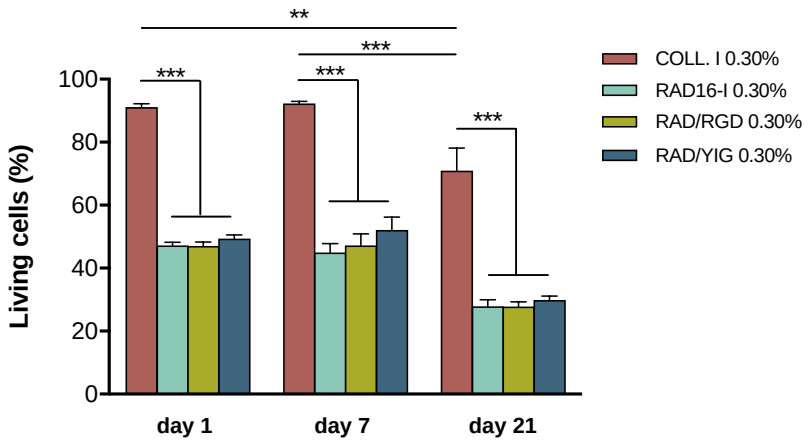

Figure 4.10. Cellular viability percentages of islet-derived expanded cells grown in 3D matrices. Quantification of cell viability in pure and functionalized RAD16-I cultures compared to type I collagen cultures (control), at different time points (days 1, 7 and 21). Quantification was performed by cell counting of Live and Dead pictures. Data are expressed as mean ± SEM, (n=3 donors). ** $p<0.01$, *** $p<0.001$.

Figure 4.10 shows the percentages of viable cells in RAD16-I and type I collagen cultures at different time points (days, 1, 7 and 21). Expanded cells cultured in type I collagen maintained viability values of around 90% during the first week of culture. When the third week of culture was reached, these values experienced a significant decrease, although, 80% of the cells still remained alive. Conversely, expanded cells cultured in RAD16-I based matrices presented significantly lower viability percentages compared to type I collagen matrix. This tendency was maintained for the whole culture period. On day 1, the percentage of living cells in RAD16-I matrices was around 50%. Lower viability percentages than those of type I collagen scaffolds were expected, due to the exposure of cells to the acidic pH of the RAD16-I. Nonetheless, cells were not able to recover from that initial event and the same viability percentages were maintained for the first seven days of culture. On day 21, viability was significantly lower than on day 7, with values around 30%. The addition of the cell signaling motifs did not entail any improvement in terms of cell viability.

Therefore, we concluded that the decreasing viability values present in RAD16-I matrices were probably due to the lack of recovery after the encapsulation process. Moreover, the chemical signaling provided by the introduction of the RGD and YIG adhesive peptides was not enough to cause any change in cell behavior.

4.3.3 CULTURE OF HUMAN ISLET-DERIVED EXPANDED CELLS IN RAD16-I SANDWICH PLATFORM

4.3.3.1 Set-up of the RAD16-I sandwich culture platform

In view of the results previously discussed, a change of strategy was needed in order to find a 3D culture platform able to sustain the viability of dedifferentiated islet-derived cells. Thus, we explored other 3D culture methods also based on the RAD16-I peptide. In particular, the sandwich culture method where cells are kept between two thin layers of peptide was chosen (explained in detail in Chapter 2, section 2.4.3). This 3D model has shown promising results for the maintenance of rat hepatocytes activity *in vitro*[56]. Prior to the establishment of the new culture platform, we induced expanded cells to form cell aggregates to mimic the *in vivo* configuration of pancreatic islets[26,45]. For that purpose, after expansion in monolayer, the dedifferentiated islet-derived cells were cultured in non-adherent Petri dishes. After 48 h of culture, cells clustered and formed independent cell colonies (islet-like cell clusters, ICCs) that were subsequently cultured into the cell culture inserts, and maintained between two layers of RAD16-I peptide.

Additionally, RAD16-I self-assembling peptide was functionalized by the covalent introduction of the ubiquitous integrin-binding motif RGD (AcN-GP**RGD**SGY**RGD**S-GG-$(RADA)_4$-$CONH_2$) aiming to support cell viability and to promote the redifferentiation towards a beta cell-like phenotype. The new peptide was blended with prototypic RAD16-I at a 95:5 ratio (pure RAD16-I:RGD motif). Figure 4.11 depicts all the steps involved in the establishment of the new approach.

By culturing the dedifferentiated cells within this configuration, we avoided cell exposure to the acidic pH of RAD16-I before self-assembling. The setting-up of the sandwich cultures involved the adjustment of the ICCs seeding density. Various cell densities were assayed, ranging between 50,000 and 400,000 cells/insert, and the 100,000 cells/insert one was the most adequate. When higher cell densities were used, ICCs tended to clump, forming bigger clusters and impeding ICCs attachment to the RAD16-I substrate. The self-assembling peptide concentration was 0.3 % (w/v). Pure RAD16-I and functionalized RAD/RGD sandwiches cultures were maintained for 18 days with the same culture medium used for the expansion, but without serum. In parallel with the sandwich cultures, ICCs were also maintained for 18 days to be used as controls. To perform all the experiments using this culture platform cells isolated from 7 cadaveric organ donors were used.

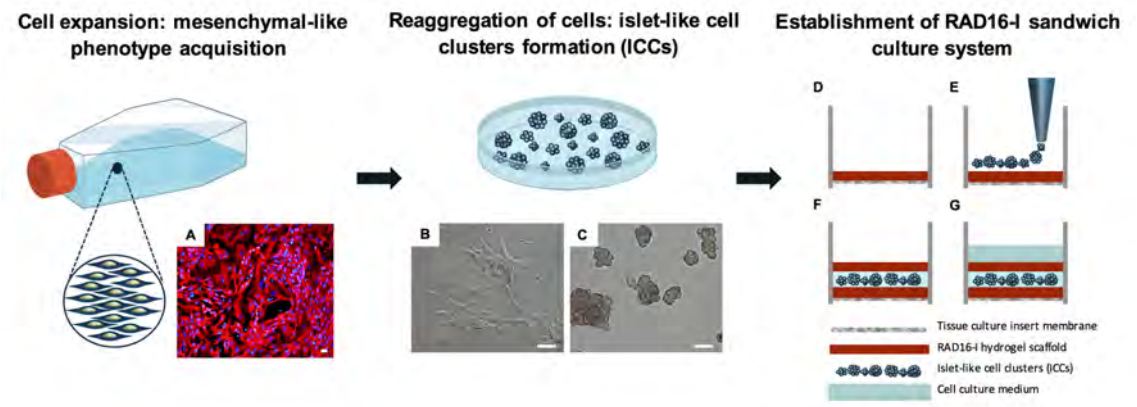

Figure 4.11. RAD16-I and RAD16-I/RGD sandwich culture model. (A) Pancreatic islet endocrine-enriched fractions were seeded in monolayer culture and expanded for 7-8 passages. Expanded cells dedifferentiated and experienced an epithelial to mesenchymal transition. (B) Expanded cells were harvested and cultured in non-adherent Petri Dishes. After 48 h in culture they formed islet-like cell clusters (ICCs). (C) The ICCs were harvested and seeded on pure RAD16-I or RAD16-I/RGD sandwich scaffolds for subsequent culture. (D) Cell culture inserts were coated with 40 µL of pure RAD16-I or functionalized RAD16-I/RGD that gelled after the addition of medium. (E) ICCs were seeded on top of the thin layer of RAD16-I or RAD16-I/RGD and allowed to attach for 48 h. (F) A second layer of peptide was added, entrapping the clusters in a sandwich fashion. (G) Cell culture medium was added into the insert, covering the whole construct. Scale bars (A) 10 µm, (B,C) 100 µm.

4.3.3.2 Expression of integrins

To evaluate the influence of cell expansion and the subsequent culture of ICCs in pure RAD16-I and RGD-functionalized sandwich cultures, gene expression of integrin subunits αV (ITGAV), β1 (ITGB1) and β3 (ITGB3) was determined. Integrin gene expression was determined initially and at the end of the expansion in monolayer culture (passage 1 and passage 7-8 respectively), in ICCs maintained in Petri dishes for 10 days (controls), and in ICCs after 10 days in culture in RAD16-I and RAD16-I/RGD sandwiches. Integrin expression was identified at all time points, supporting the rational for the use of functionalized matrices with the integrin-binding peptide RGD, in sandwich cultures. Moreover, gene expression studies revealed that no significant changes were present in the expression of integrins in any of the tested conditions (Figure 4.12). In fact, integrin gene expression was not expected to change under the RAD16-I condition since it is a non-instructive self-assembling peptide. The introduction of the RGD signaling motif did not cause any change in the expression of integrins either. Lam *et al* also showed that αV and β3 integrin expression levels were not affected by the introduction of the RGD bioactive motif in hydrogel-based cultures[96]. One possible explanation is that cells were expressing enough integrin receptors to promote the proper response during redifferentiation.

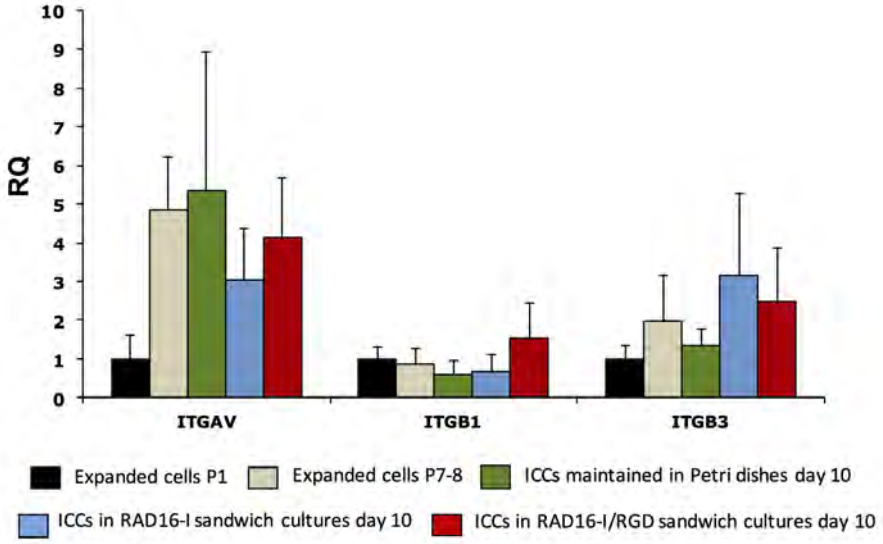

Figure 4.12. Gene expression of integrins subunits α_V (ITGAV), β1 (ITGB1) and β3 (ITGB3). Integrin expression was evaluated in expanded cells at passage 1, passage 7-8 and islet-like cell clusters (ICCs) in non-adherent Petri dishes and cultured both in RAD16-I and RAD16-I/RGD sandwich scaffolds for 10 days. Data are expressed as relative quantification (RQ) and are mean ± SEM of 4 experiments with cells from 4 different donors (n=4), except RGD condition (n=3).

4.3.3.3 Behavior of ICCs in non-adherent Petri dishes and in RAD16-I and RAD16-I/RGD sandwich cultures

The behavior of ICCs in non-adherent Petri dishes and in pure RAD16-I and functionalized RAD/RGD sandwich cultures was analyzed at microscopic and macroscopic level. As seen in the phase contrast images of Figure 4.13.A, the creation of cell-cell contacts via the formation of clusters (ICCs) was achieved. Despite the use of non-treated dishes, the majority of ICCs attached to the plate.Figure 4.13.B shows ICCs after being mechanically detached from the plastic surface. By doing so, ICCS adopted a rounded morphology. Detached clusters were subsequently seeded in cell culture inserts, previously coated with a thin layer of RAD16-I or RAD16-I/RGD 0.3%. The morphology of ICCs maintained in Petri dishes in parallel to the sandwich cultures, can also be observed in Figure 4.13.D,E. A more pronounced spindle-like morphology was clearly adopted by cells from the edges of ICCs as the culture was progressing.

The staining of cell nuclei and cytoskeleton allowed the visualization, by fluorescent microscopy, of changes in cell morphology along the culture period in the sandwich platform (Figure 4.13.E). On day 1 of sandwich culture, ICCs had a compact and rounded shape with some indication of cell spreading. On day 10, ICCs morphology had changed dramatically, with clear evidence of cell spreading and increased size. Hence, during the first days of culture ICCs spreading enable the colonization of the RAD16-I or functionalized analog matrix. By the end

of the culture, on day 18, ICCs conformation was maintained while cells in the outer part of the clusters had adopted a more elongated shape. Another significant aspect is that cell clusters spreading clearly allowed the establishment of cell contacts between cells from different ICCs, while cell-cell contacts within each cluster were maintained along the culture period. This trait seems to be critical for the redifferentiation process[14]. No apparent morphological differences were appreciated between ICCs cultured in pure RAD16-I or in RAD16-I/RGD functionalized matrices.

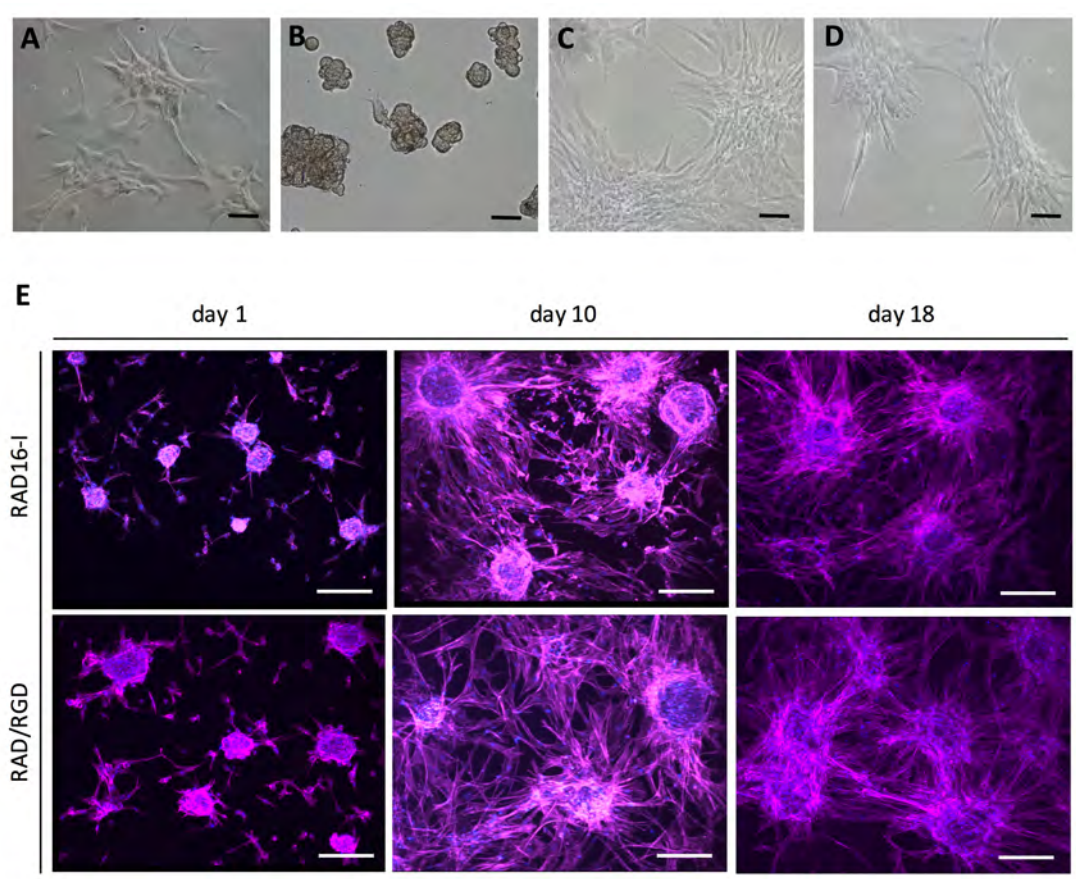

Figure 4.13. Cell morphology assessment of islet-like cell clusters (ICCs) in non-adherent Petri dishes and sandwich cultures. (A) Phase contrast image of ICCs formed after 48 h in culture in non-adherent Petri dishes. (B) ICCs after being gently detached. (C) ICCs maintained as control in non-adherent Petri dishes for 10 days. (D) ICCs maintained as control in non-adherent Petri dishes for 18 days. (E) ICCs morphology in pure RAD16-I and RGD-functionalized sandwich cultures. Nuclei were stained in blue (DAPI) and actin filaments in magenta (Phalloidin). Scale bars of 100 µm (A-D) and 200 µm (E).

In order to evaluate the effects of the RGD signaling motif on the attachment properties of the RAD16-I synthetic matrix, the number of ICCS per insert was counted by visual inspection on days 1, 10 and 18 of culture. On day 1, a significantly larger number of ICCs adhered to RAD16-I/RGD matrix than to non-modified RAD16-I (RAD16-I/RGD: 198 ± 25.0 ICCs/insert; RAD16-I: 123 ± 17.8 ICCs/insert, $p < 0.001$) (Figure 4.14.A), and the difference was similar throughout

the culture. Thus, the addition of the RGD motif to RAD16-I increased the adhesion of ICCS to the matrix. We also observed that the total number of ICCs decreased progressively in both types of matrices, but ICCs size increased significantly from day 1 to day 10 and it continued to increase from day 10 to day 18, even though the difference did not reach statistical significance (Table 4.1). The size of the individual ICCs is shown inFigure 4.14.B. The parallel reduction in the number of ICCs and the increment in size suggest that small clusters aggregated into bigger ICCs.

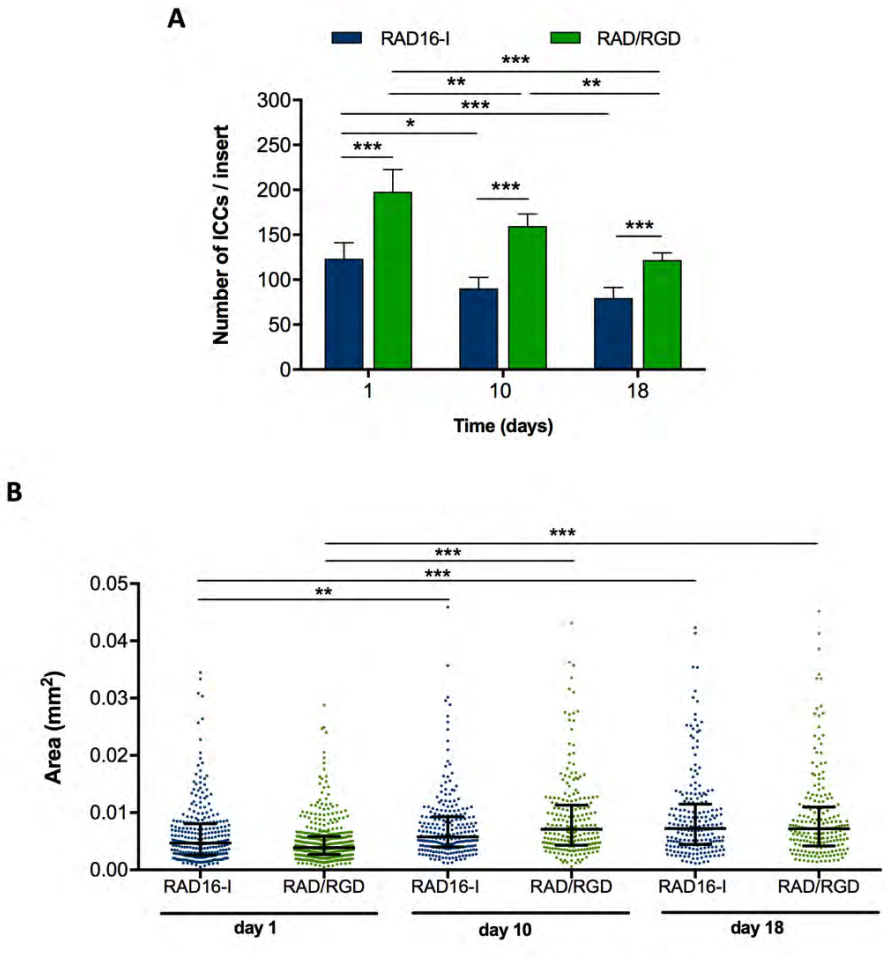

Figure 4.14. Number and size of islet-like cell clusters (ICCs) cultured in RAD16-I and RAD16-I/RGD sandwiches for 18 days. A) Number of ICCs adhered to the sandwich cultures on days 1, 10 and 18. B) Scatter plots showing ICCs area on days 1, 10 and 18 in culture. Data are expressed as mean ± SEM, (n=3 donors). ** p<0.01, *** p<0.001.

Table 4.1. ICCs area in sandwich cultures (mm^2)

Scaffold	Day 1	Day 10	Day 18
RAD16-I	$4.70x10^{-3}$ ($0.53-34.48x10^{-3}$)	$5.79x10^{-3}$($1.19-45.91x10^{-3}$)	$7.22x10^{-3}$($1.16-42.31x10^{-3}$)
RAD16-I/RGD	$3.89x10^{-3}$ ($0.47-28.76x10^{-3}$)	$7.11x10^{-3}$($0.62-43.41x10^{-3}$)	$7.20x10^{-3}$($1.38-45.19x10^{-3}$)

Values are median and range.

Thus, changes in the number and area of ICCS indicate that RAD16-I sandwich cultures are dynamic cultures characterized by the presence of a self-organizing process where ICCs clumped together to give rise to larger aggregates. The macroscopic visualization of whole sandwich constructs provides a visual assessment of the mentioned process. (Figure 4.15).

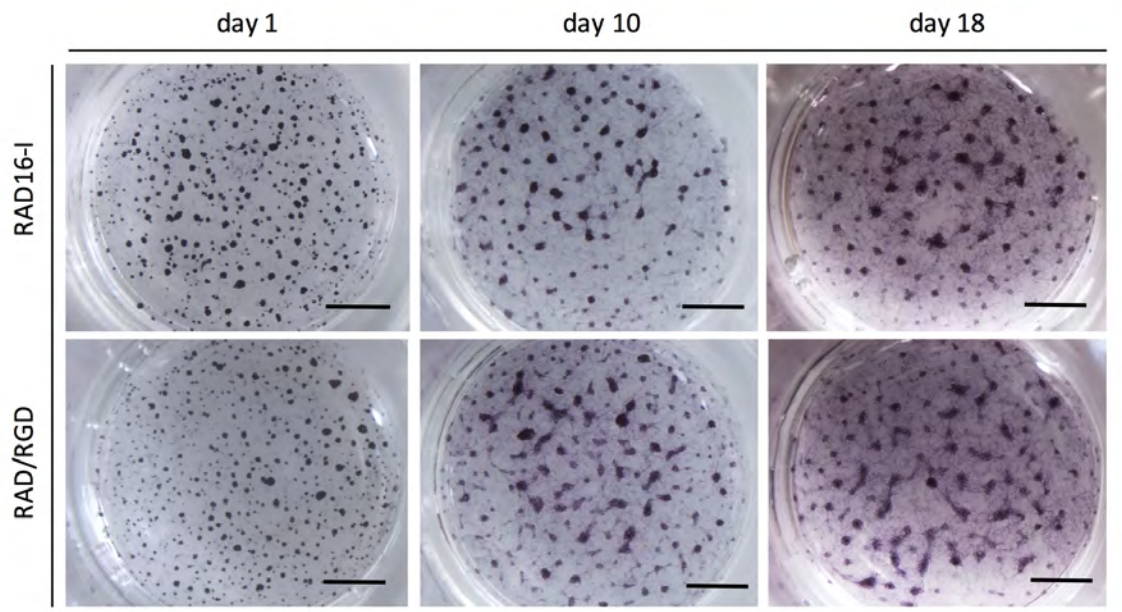

Figure 4.15. Stereoscopic images of islet-like cell clusters (ICCs) cultured in RAD16-I and RAD16-I/RGD sandwiches for 18 days. Macroscopic visualization of ICCs stained with the MTT reagent allows a clarer visualization of ICCs behavior along the culture period. Scale bars of 2 mm.

4.3.3.4 Viability and proliferation of ICCs in RAD16-I and RAD16-I/RGD sandwich cultures

To further analyze the influence of ICCs embedding in RAD16-I and RAD16-I/RGD sandwich cultures, cell viability and proliferation were analyzed by means of the Live and Dead and MTT assays at different time points. When constructs thickness is higher than 300 µm, diffusion problems may arise[97], having an impact on ICCs viability. The thickness of our construct was

500 μm, therefore viability of ICCs during the culture period could have been affected by poor oxygenation and nutrition. However, fluorescence images showed that on day 1 of sandwich culture a large majority of cells (98%) within each cluster were alive, both in RAD16-I and in RAD16-I/RGD scaffolds (Figure 4.16.A). On days 10 and 18, the percentage of viable cells was 85%, slightly decreased compared to day 1 (p: NS). Remarkably, the majority of cells located in the center of clusters remained alive for the whole culture period. Another interesting trait is that no differences in viability were observed regarding ICCs size. Surprisingly, no differences were either detected due to the introduction of the RGD signaling motif along the culture period.

On the other hand, MTT assay showed significantly higher absorbance values in RAD16-I/RGD functionalized cultures than in pure RAD16-I, probably reflecting the higher cellular adhesion to the RAD16-I/RGD scaffold, and the difference between the two matrices was maintained throughout the culture period (Figure 4.16.B). In addition, ICCs cultured in RGD-based matrix showed higher MTT values on day 10 and 18 than on day 1. In ICCs cultured in pure RAD16-I scaffold, the MTT values tended also to increase on the first 10 days of culture, but the difference did not reach statistical significance. No significant changes in MTT values were observed in ICCs cultured in RAD16-I nor in RAD16-I/RGD matrices between culture day 10 and 18. Considering that cell viability was slightly lower on day 10 than on day 1, the increased values of the MTT assay indicate that the total number of cells in the ICCs was higher on day 10 and 18 in RGD-based scaffolds, as compared to day 1 of culture, probably due to cell proliferation. However, in this type of matrix, during the second stage of culture (day 10-day 18), MTT values did not show any significant variation, suggesting therefore that cell proliferation occurred during the first days of culture (day 1-day 10) due to the introduction of the RGD integrin-binding motif. Despite the results shown by the MTT test, proliferation assessment would benefit from further studies, since MTT it is a non-direct method to measure the proliferative capacity of a cell population. For instance, the expression of the proliferation marker ki-67 could be studied.

Therefore, we can conclude that cell viability was preserved during the whole culture period, both in unmodified RAD16-I and in RGD-modified RAD16-I. Moreover, the addition of the RGD adhesive motif to the RAD16-I matrix promoted cell proliferation. Thus, these results suggest that cells specifically recognize and respond to the RGD peptide sequence present in the modified RAD16-I matrix, creating a more favorable microenvironment that improves cell attachment and proliferation conditions.

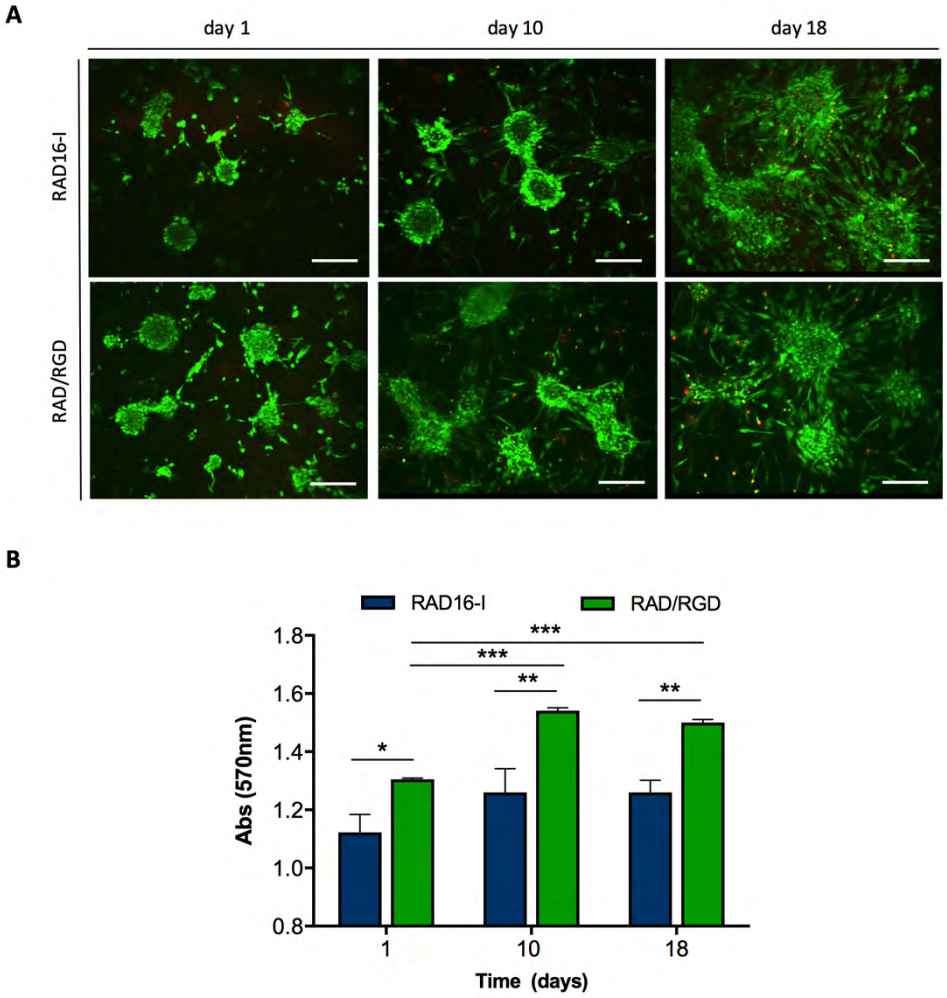

Figure 4.16. Cellular viability and proliferation of islet-like cell clusters (ICCs) cultured in RAD16-I and RAD16-I/RGD sandwiches for 18 days. (A) Living cells were stained with calcein (green) and dead cells were stained with ethidium homodimer-1 (red). Scale bars of 200 μm. (B) MTT absorbance values. Data are expressed as mean ± SEM, (n=3 donors). * $p<0.05$, ** $p<0.01$, *** $p<0.001$. Scale bars of 200 μm.

4.3.3.5 Expression of beta cell and EMT markers in ICCs cultured in RAD16-I and RAD16-I/RGD sandwich cultures

Gene expression was analyzed in ICCs cultured in non-modified RAD16-I sandwich cultures and RGD-functionalized sandwich cultures to elucidate whether the embedding of ICCs within a synthetic ECM promoted the redifferentiation towards a beta cell-like phenotype. The culture of ICCs in pure RAD16-I SAP allowed us to study the effects of the 3D environment *per se* since it is a non-instructive peptide, whereas the presence of the RGD signaling motif in RAD16-I peptide sequence, enable us to evaluate the effects of a biomimetic ECM analog on ICCs gene expression. The expression of the beta cell markers Insulin, NKx6.1, MafA, MafB, Pdx1, NeuroD1 and Sox9 was analyzed. Furthermore, the epithelial marker E-cadherin and the

mesenchymal markers Vimentin and N-Cadherin were also studied to evaluate the influence of pure RAD16-I and RGD functionalized sandwich cultures over the EMT process suffered by islet cells when expanded.

Gene expression studies in ICCs were performed on days 10 and 18, and ICCs maintained in Petri dishes for the same days and with the same culture medium than in 3D sandwich cultures were used as controls (Figure 4.17). Thereby, gene expression graphics depict the effect caused exclusively by the use of the RAD16-I based matrices. Gene expression of beta cell specific markers was markedly reduced and in the limits of detection in islet-derived expanded cells on passages 7-8 (Figure 4.17.A), and in newly formed ICCs. After 10 days in RGD-based sandwich cultures, the expression of the specific beta cell marker insulin and the beta cell transcription factors Nkx6.1 and MafA was significantly increased compared to both control condition (ICCs cultured in Petri dishes) and RAD16-I constructs. The transcription factor Pdx1 presented also an increased expression, but only when compared to non-encapsulated ICCs (Figure 4.17.B). On day 18, similar results were obtained, and insulin, Nkx6.1 and MafA gene expression levels were significantly increased compared to control ICCs cultured in non-adherent conditions (Figure 4.17.C). In addition, the transcription factors NeuroD1 and Sox9 showed a tendency to increase ($p= 0.06$, and $p= 0.07$ respectively). The expression of epithelial and mesenchymal markers E-cadherin and N-cadherin respectively, as well as vimentin, the hallmark of the mesenchymal phenotype, was similar in all groups, confirming the specificity of the increased expression of the beta cell markers in cells cultured in the RAD16-I/RGD sandwich system. The persistency of vimentin expression in 3D cultures indicates that ICCs still maintain a mesenchymal phenotype. However, the steady expression of vimentin in 3D cultures seems to be balanced by the increased expression of pancreatic beta cell markers. The similar results found on day 18 of culture provide additional support to the presence of this redifferentiation process. However, the absence of statistically significant differences between day 10 and 18 suggests that a shorter protocol (10 days) may be just as good, if not better, than prolonging the incubation 8 further days.

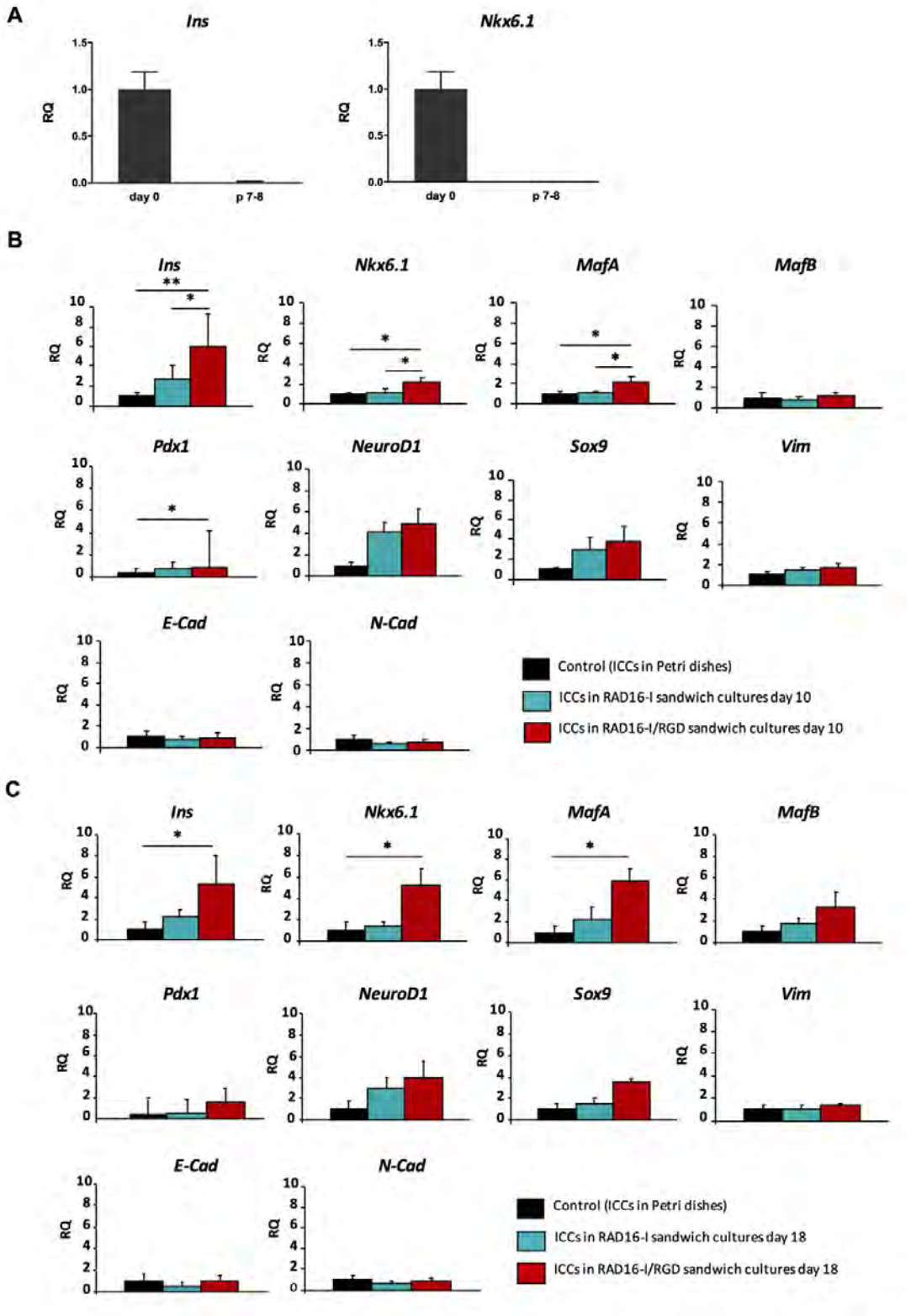

Figure 4.17. Gene expression analysis of expanded cells at p7-8 (A) (n=3) and ICCs cultured in RAD16-I and RAD16-I/RGD sandwich for (B) 10 days (n=6), and (C) 18 days (n= 4). Data are expressed as mean ± SEM of relative quantification (RQ). RQ values were calculated using expanded cells on day 0 of culture (A) and ICCs maintained in non-adherent Petri dishes (B,C) as controls. Pdx1 values did not show a normal distribution and are expressed as median and interquartile range. * $p<0.05$, ** $p<0.01$.

Thus, gene expression results show that the addition of the matrix-derived RGD sequence to the non-instructive RAD16-I induced a change in phenotype involving the over-expression of several beta cell specific genes, indicating the induction of some degree of redifferentiation towards a beta cell phenotype. Gene expression was similar in ICCs maintained in non-adherent culture conditions and ICCs cultured in RAD16-I, indicating that nanofibers were not sufficient to induce the redifferentiation, and that the addition of the integrin-binding motif RGD to the scaffold was required. Moreover, the expression of non-endocrine markers such as vimentin, E-cadherin or N-cadherin did not change confirming the specificity of the increment in beta cell markers. However, a reduction in the expression of mesenchymal markers could have been expected to occur in parallel with the redifferentiation process. It is worth noting that to better analyze the effect of the structural and biomechanical microenvironment provided by the SAP on the redifferentiation process, the culture medium used in this study was very simple, and specifically no differentiation factors were added to it. Therefore, we propose that the use of a redifferentiation media with chemical induction, along with the introduction of more peptide signaling motifs to create an BM analog closer to that of *in vivo* pancreatic islets, would enhance the redifferentiation process.

4.3.3.6 Topographical analysis of the RGD-modified RAD16-I matrix

Gene expression studies demonstrated that RGD sandwich cultures promoted some degree of redifferentiation towards a beta cell phenotype, with the upregulation of some specific beta cell markers. These results encouraged us to perform further in-depth studies on the RGD modified matrix.

The previous results could be solely attributed to the biological stimuli provided by the RGD adhesive peptide. Nonetheless, as already proved in the physicochemical characterization of the different functionalized matrices used in Chapter 3 (section 3.3.1), the introduction of the 2 RGD motifs decreased the content of the β-sheet structure present in RAD16-I, modifying the secondary structure of pure RAD16-I. Therefore, we thought that the scaffold nanostructure could have also been altered as a result of the addition of the double peptide sequence conforming the RGD motif.

With the aim to study the characteristics of the formed RAD16-I nanofibers, and whether the insertion of the RGD motifs modified the morphology of the scaffold nanostructure, non-contact atomic force microscopy (AFM) studies were performed (Figure 4.18). Pure RGD and 95:5 RAD16-I/RGD were analyzed, using prototypic RAD16-I as a control. AFM pictures allowed the visualization of nanofibers present in both peptides, pure RAD16-I and RGD. The influence of RGD peptide on the structural organization of the RAD16-I could be observed when RAD16-I and RGD peptides were blended at the same ratio used in sandwich cultures (95:5 respectively). Specifically, RAD16-I/RGD matrix provided a network of thicker nanofibers than RAD16-I alone, showing that the RAD16-I/RGD scaffold was structurally different from the conventional RAD16-I. In particular, the diameters of RAD16-I nanofibers, pure RGD and

RAD16-I/RGD blending were 19.58 ± 0.79 nm, 38.78 ± 2.04 nm and 27.85 ± 1.48 nm respectively (***p<0.001, RGD and RAD16-I/RGD compared to pure RAD16-I).

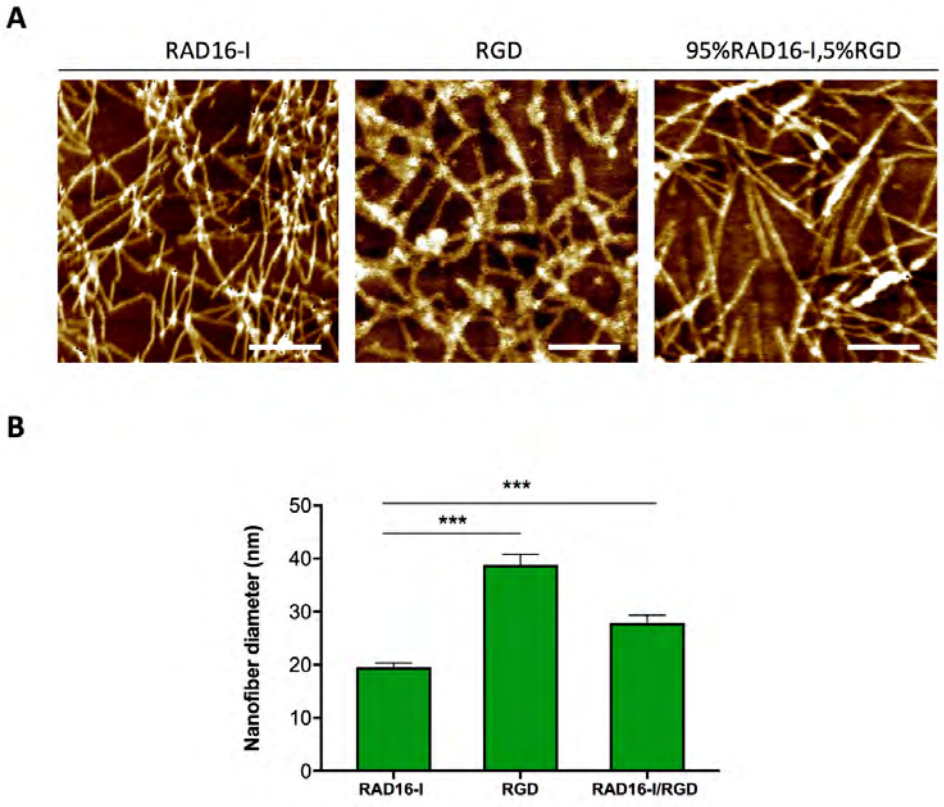

Figure 4.18. Topographical characterization of pure and functionalized RAD16-I with the signaling peptide motif RGD. (A) RAD16-I, RGD and RAD16-I/RGD SAP nanofibers were visualized by atomic force microscopy (AFM). (B) Nanofiber diameter (nm) of RGD and RAD16-I/RGD compared to non-modified RAD16-I (control). Data are expressed as mean ± SEM, ** p<0.01.

Since it is well known that cells sense the structural traits of the ECM through integrins receptors, we hypothesize that the change in ICCs behavior, including cell adhesion and gene expression profiles, could also be a consequence, together with the biochemical signaling exerted by the short peptide, of the physical changes in RAD16-I matrix when the RGD motifs were introduced.

4.3.4 CULTURE OF ISLET-DERIVED EXPANDED CELLS IN PTFE MEMBRANE-BASED SANDWICH PLATFORM

As seen in the previous section, RGD-functionalized RAD16-I sandwich cultures promoted an early redifferentiation of islet-derived expanded cells. Nevertheless, since no chemical induction was present in the culture medium, the redifferentiation process was quite modest, which encouraged us to improve our 3D culture platform.

Each individual pancreatic islet is richly vascularized by direct arteriolar blood, receiving as much as 15-20% of the pancreatic blood flow even though they only represent 1-2% of the pancreatic volume[45]. This implies that pancreatic islet cells present strict oxygen requirements. As already mentioned, 3D constructs tend to hinder oxygen transfer when their thickness is beyond 200-300 μm. Constructs assembled with the sandwich platform are approximately 500 μm. Therefore, we aimed to modify our sandwich culture configuration in order to obtain thinner constructs and enable a proper oxygen exchange and nutrient diffusion. To that end, the top RAD16-I peptide layer dimensions were optimized, by reducing them to a nanometric scale. Such modification was carried out by the previous modification of a hydrophilic PTFE (teflon) membrane with a plasma process, and the later formation of a very thin layer of RAD16-I peptide on top of it. Moreover, as in the traditional sandwich method, the self-assembling peptide was engineered with functional peptide motifs in order to activate specific cell responses that could enhance the redifferentiation towards a beta cell phenotype. The peptide signaling motifs used to tailor the PTFE membrane-based sandwich are RGD, as in the standard sandwich method, and the laminin-derived IKVAV peptide. The complete sequence for these peptides is reviewed in Chapter 3.

This new methodology, described in Chapter 2 (section 2.4.4), is an adaptation of the RAD16-I sandwich culture model used by Wu *et al* for the culture of hepatocytes[71]. The highly oxygen-demanding hepatocytes are commonly maintained in Petri dishes under oxygen-deficient culture condition, forcing the cells into anaerobic metabolic states. Thus, oxygen supply in primary hepatocyte cultures is a critical issue to be addressed[71]. With the use of this specialized bioengineering platform Wu *et al* managed to maintain the functionality of cultured hepatocytes for up to one week.

4.3.4.1 Physicochemical assessment of RAD16-I nanometric layer formation

In order to achieve a nanometric thickness for the top peptide layer of the new sandwich configuration, a hydrophilic PTFE membrane was modified with plasma grafting of pentafluorophenyl methacrylate, PFM (PgPFM). As previously mentioned, PFM coatings are used to anchor biomolecules, since this monomer offers highly reactive ester groups towards amines[98]. This modification, depicted in Chapter 2 (section 2.1.3.1), enabled the posterior attachment of RAD16-I molecules containing a primary amine.

Prior to the membrane modification by plasma grafting of PFM, we performed a test with RAD16-I covalently linked to an amino group (NH_2-GG-RAD16-I), in order to ensure the attachment of NH_2-GG-RAD16-I to the coated PFM surface. A quartz crystal microbalance with dissipation (QCM-D) monitored the adsorption of the RAD16-I SAP onto the PFM substrate. NH_2-GG-RAD16-I aqueous solution was passed through the microbalance obtaining a change in frequency, which is related to the adsorbed mass. As demonstrated in Figure 4.19, once we started flowing the NH_2-GG-RAD16-I solution, the frequency experienced a decrease of -90 Hz, indicating that mass adsorption onto the sensor surface was taking place. Once the frequency was stable, a wash with water was performed and a hardly visible frequency increase took place, indicating the RAD16-I molecules were covalently bound to the PFM coating.

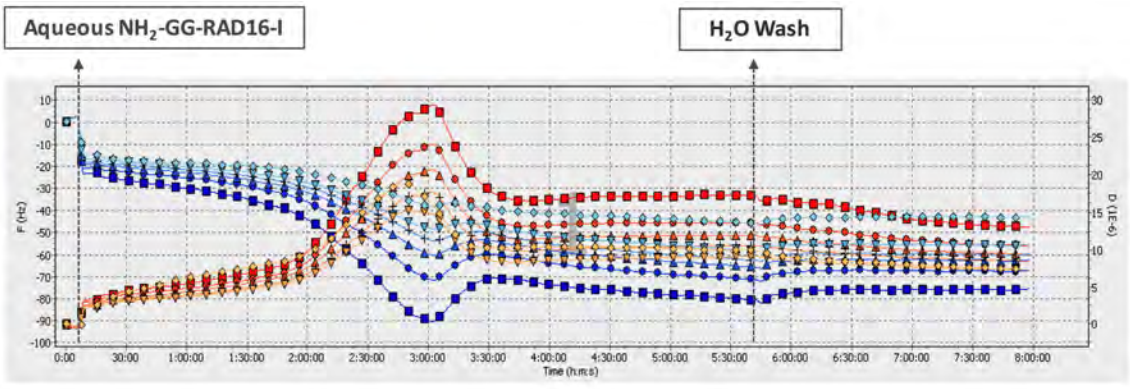

Figure 4.19. QCM-D monitoring of RAD16-I adsorption on a PFM substrate. The decreased of the frequency once NH_2-GG-RAD16-I solution was passed through the sensor surface, indicates RAD16-I adsorption onto the PFM-modified substrate.

Once we proved that PFM monomers reacted with the aqueous solution of NH_2-GG-RAD16-I, we proceeded with the PTFE membrane modification. The membrane's surface was activated by plasma and once PFM was introduced, reacted with the active groups created. At this point, membranes were modified with PFM (PTFE/PgPFM). Then, we soaked overnight PFM-modified membranes with the aqueous solution of NH_2-GG-RAD16-I (5 mg/mL), allowing the immobilization of RAD16-I peptide onto the modified membranes. The formation of RAD16-I nanofibers on top of the PFM-modified membranes was assessed by scanning electron microscopy (SEM). Comparing native PTFE membranes (Figure 4.20.A,B), with PFM-modified membranes after incubation with the aqueous solution of NH_2-GG-RAD16-I, (Figure 4.20.E), it can be easily seen how the topography of membranes changed after the incubation with the peptide solution. The close-up image (Figure 4.20.F) allows a better visualization of the individual RAD16-I nanofibers formed between the membrane pores (white arrows). As a control, non-modified membranes were also incubated with NH_2-GG-RAD16-I (Figure 4.20.C,D), and despite a slight change in topography, no nanofibers were observed. Finally, once the first nanofibers were assembled, commercial RAD16-I peptide was deposited on top of the modified membranes. Thanks to the formation of the single nanofibers, RAD16-I peptide solution was able to gel without the addition of culture medium, and after rinsing with water, a very thin layer of RAD16-I peptide remained attached to the membrane (Figure 4.20.G).

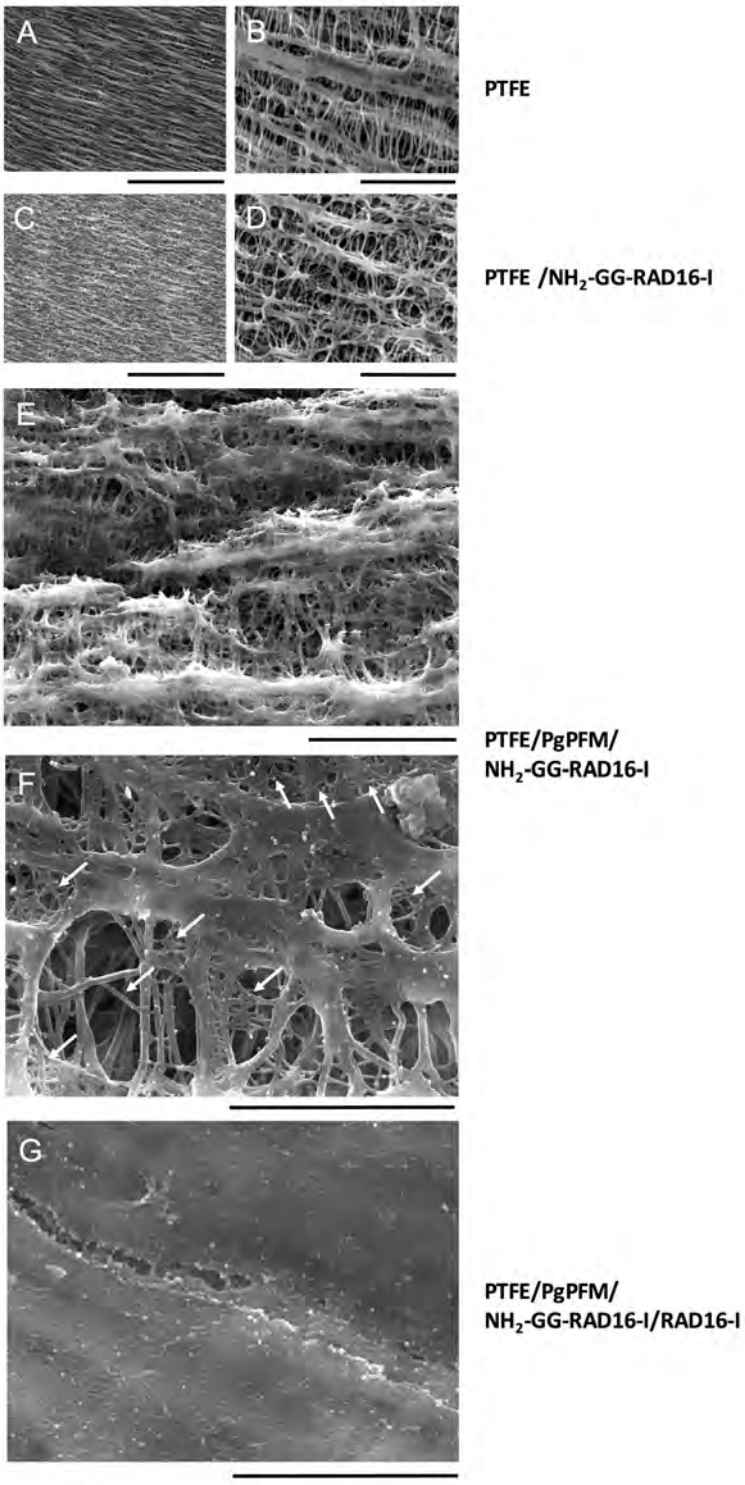

Figure 4.20. Scanning Electron Microscopy (SEM) images showing RAD16-I nanofibers formation onto PFM-modified membranes. (A,B) Native PTFE membrane. (C,D) Native PTFE membranes incubated with NH_2-GG-RAD16-I solution. (E) PFM-modified membrane after incubation with NH_2-GG-RAD16-I solution. (F) Close-up image of a PFM-modified membrane after incubation with NH_2-GG-RAD16-I solution. (G) PFM-modified membrane incubated with NH_2-GG-RAD16-I solution and with a RAD16-I layer on top. Scale bars of 70 μm (A,C), 10 μm (B,D,E) and 5 μm (F,G).

4.3.4.2 Morphology of ICCs in PTFE membrane-based RAD16-I sandwiches

In order to set-up PTFE membrane-based sandwich cultures, we started by trying to reproduce the same conditions found in standard RAD16-I sandwiches. Firstly, we tried to coat the cell culture insert, in this case of a larger diameter (30 mm), with RAD16-I 0.3%. It is worth noting that, besides the top nanometric RAD16-I layer, the bottom layer is also thinner compared to the traditional RAD16-I sandwich. Due to the fragility of the bottom layer, RAD16-I 0.3% broke after the addition of ICCs, which impeded cluster attachment. Figure 4.21 shows the broken pieces of the hydrogel (black arrows) and ICCs with no sign of cell spreading indicating that cell attachment was not accomplished. Therefore, we doubled the peptide concentration and although it provided more stability, eventually it disassembled as in the case of RAD16-I 0.3%. As a consequence, we decided to increase peptide concentration, using the maximum concentration possible (1%), as in the work presented by Wu *et al*[71]. This peptide concentration provided enough stability to allow ICCs culture for 18 days, with no fractures on the thin layer of peptide.

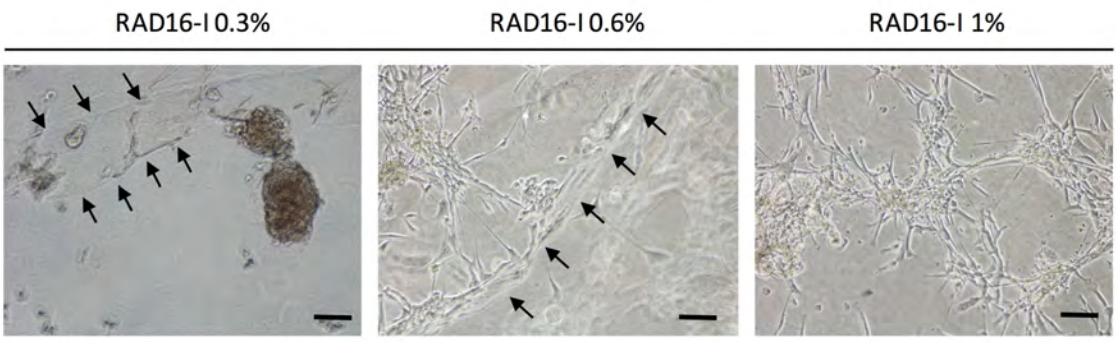

Figure 4.21. Phase contrast images of RAD16-I concentration adjustment on the bottom layer of PTFE membrane-based sandwich platform. RAD16-I 0.3%, 0.6% and 1% concentrations were tested in order to obtain a thinner bottom layer compared to the traditional sandwich culture platform. The optimal RAD16-I concentration was 1%. Scale bars of 100 μm.

Afterwards, different cell densities were tested and the one that yield to viable cultures was 350,000 cells/insert. Once cell density was adjusted, ICCs were seeded in cell culture inserts, and after attachment, the PTFE membrane with the nanometric thin layer of RAD16-I peptide was inverted and placed facing the ICCs. Thus, ICCs were embedded in a sandwich fashion characterized by the decreased thickness of the peptide layer, compared to the standard RAD16-I sandwich. Apart from pure RAD16-I, functionalized RAD16-I/RGD and RAD16-I/IKVAV were used as scaffolds, in order to induce the redifferentiation of islet-derived expanded cells. Cultures were maintained for 18 days and the evolution of ICCs along the culture period is depicted in Figure 4.22. Phase contrast images of day 1 show that ICCs spread all over the matrix although clusters were not as compact as in traditional sandwiches, due to a previous mechanic disaggregation performed before seeding. Therefore, at the beginning of the culture

period, cells were more spread which implies less cell-cell contacts. As the culture progressed, cells tended to clump and bigger clusters were formed (day 10 and 18). Hence, cluster configuration was not only maintained but enhanced during the whole culture. No appreciable differences in ICCs morphology were identified as a result of the peptide motifs introduction. ICCs counting could not be performed since the top modified membrane was highly opaque and just a few transparencies were present.

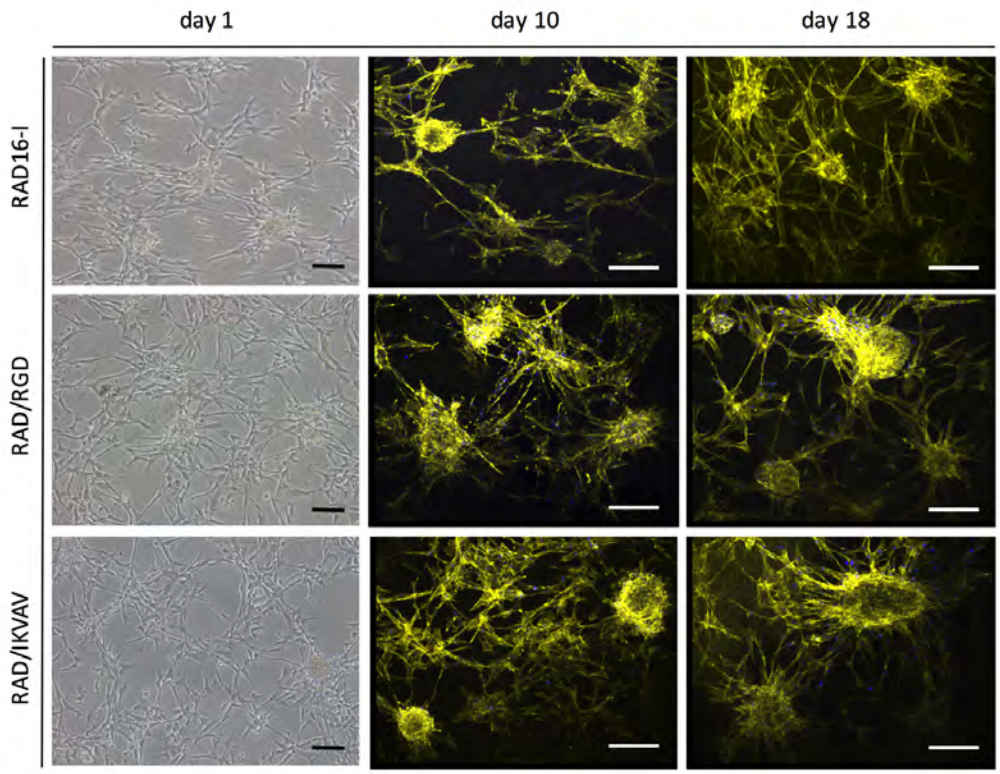

Figure 4.22. Cell morphology assessment of islet-like cell clusters (ICCs) in pure and functionalized RAD16-I sandwiches (PTFE membrane-based). Phase contrast images of day 1 show that ICCs were able to attach to the bottom layer of the sandwich. Fluorescence images show how cluster morphology was enhanced along the culture period. Nuclei were stained in blue (DAPI) and actin filaments in yellow (Phalloidin). Scale bars of 100 µm (day 1) and 200 µm (day 10 and 18).

4.3.4.3 Viability of ICCs in PTFE membrane-based RAD16-I sandwiches

Viability of ICCs cultures in PTFE membrane-based sandwich cultures was evaluated by means of the Live and Dead kit at different time points. Cellular viability assessment was especially important on day 1, in order to ensure that no cell toxicity was present due to the PFM modification of the PTFE membranes. As seen in Figure 4.23, on day 1 most of the cells were alive, as indicated by the low presence of cells stained with ethidium homodimer-1 (red cells). Thus, plasma membrane modification with PFM did not imply a decreased cellular viability.

Fluorescence images taken on days 10 and 18 of culture in both pure RAD16-I and tailor-made scaffolds (RAD16-I/RGD and RAD16-I/IKVAV), demonstrate that cell viability was preserved all along the culture period, with no signs of increase cell death.

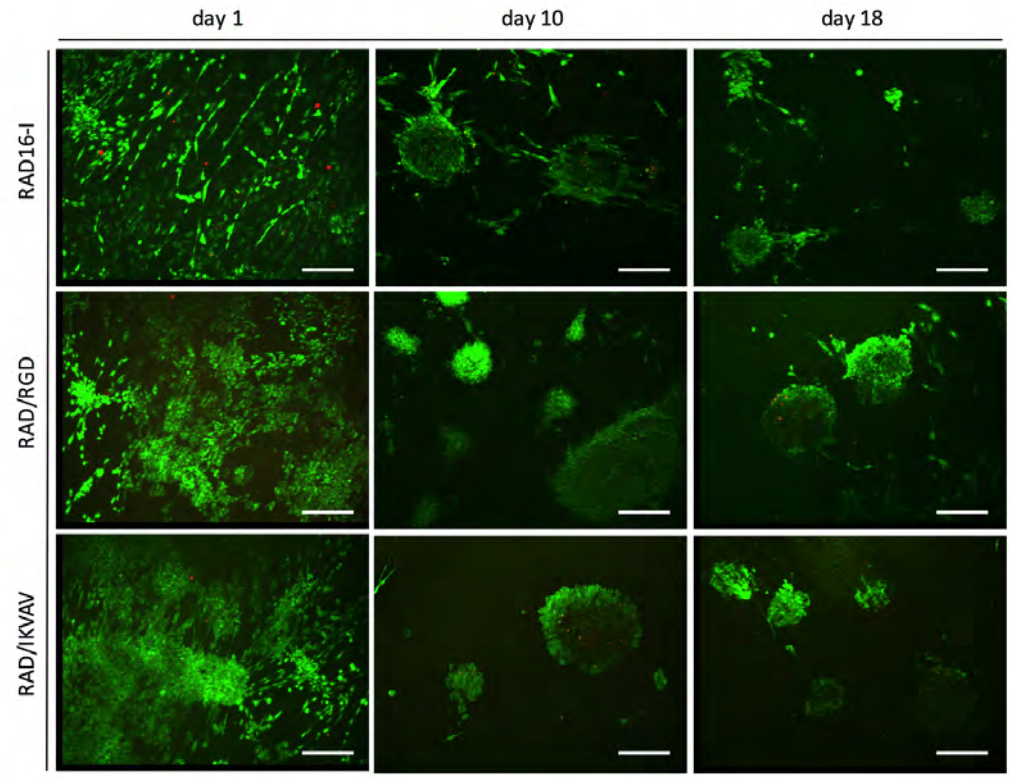

Figure 4.23. Cellular viability of islet-like cell clusters (ICCs) cultured in pure and functionalized PFM-modified RAD16-I sandwiches. Living cells were stained with calcein (green) and dead cells were stained with ethidium homodimer-1 (red). Scale bars of 200 μm.

Again, no differences were detected due to the introduction of any of the signaling motifs, since the three types of matrices provide excellent cellular viabilities.

4.3.4.4 Expression of beta cell markers in ICCs cultured in pure and functionalized PTFE membrane-based RAD16-I sandwiches

After proving that PTFE membrane-based sandwiches were able to maintain ICCs viability during the whole culture period, as well as a cluster morphology comparable to that observed in standard RAD16-I sandwiches, the next objective was to determine to what extent this new culture platform could promote the redifferentiation of islet-derived expanded cells towards a beta cell-like phenotype.

Gene expression of ICCs cultured in pure RAD16-I and functionalized PFM-modified sandwich cultures was analyzed by qRT-PCR. This assessment allowed us to compare whether the

modification introduced to RAD16-I-based sandwiches aimed to decrease the thickness of the peptide layers, entailed some improvement in terms of redifferentiation. Moreover, the addition of the laminin-derived IKVAV peptide, enabled us to determinate the influence of another biomimetic ECM analog on the redifferentiation of expanded cells.

As observed inFigure 4.24, the expression of the beta cell markers Ins, NKx6.1, MafA, MafB, Pdx1 and NeuroD1 was analyzed. Gene expression studies were performed on days 10 and 18 using ICCs maintained in Petri dishes for the same days and with the same culture medium than in sandwich cultures. Gene expression of beta cell specific markers was markedly reduced and in the limits of detection in islet-derived expanded cells on passages 7-8 and in newly formed ICCs, as previously shown. After 10 days in RAD16-I/RGD PTFE membrane-based sandwich cultures, the expression of the specific beta cell marker insulin and the beta cell transcription factors Nkx6.1, MafA and NeuroD1 was significantly increased compared to the control condition (ICCs cultured in Petri dishes) and also compared to the pure RAD16-I constructs, in the case of MafA and NeuroD1. On the other hand, the IKVAV adhesive motif also entailed the upregulation of the transcription factors MafA and NeuroD1, compared to non-encapsulated ICCs and pure RAD16-I matrix. In the case of MafA, a marker of mature beta cells, the introduction of the IKVAV motif caused significant higher levels of expression than the RGD motif. The expression of insulin and Nkx6.1 genes also tended to increase, although differences did not reach significance. Furthermore, for MafA and Nkx6.1 transcription factors, a significant increased expression was also observed when ICCs were cultured in RAD16-I with no signaling motifs, although not as pronounced as with the functionalized matrices. However, it is worth noting that the numbers of donors used for this particular experiment was 3 (day 10), and a higher number of donors is needed to obtain more robust results.

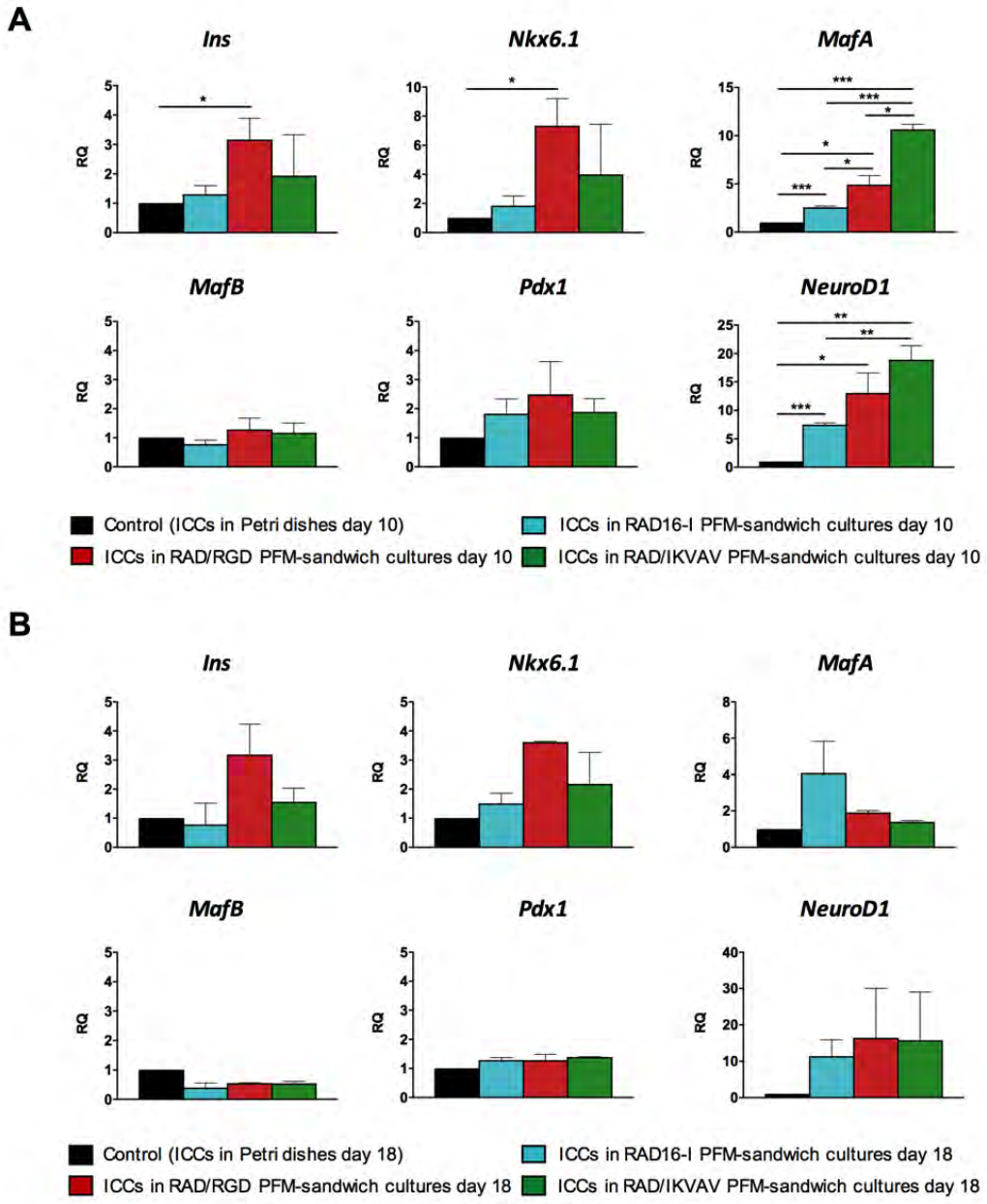

Figure 4.24. Gene expression analysis of ICCs cultured in RAD16-I, RAD16-I/RGD and RAD16-I/IKVAV PTFE membrane-based sandwiches for (A) 10 days (n=3), and (B) 18 days (n= 2). Data are expressed as mean ± SEM of relative quantification (RQ). RQ values were calculated using ICCs maintained in non-adherent Petri dishes as controls. * p<0.05, **p<0.01, ***p<0.001.

On day 18, a similar tendency seemed to be present, with the upregulation of Ins, Nkx6.1 and MafA, that in this case was more pronounced when the RGD motif was used. Nevertheless, a higher number of experiments is needed. It seems, however, that as in the case of traditional RAD16-I sandwiches, a shorter period of culture, 10 days, provides better results than the 18 days' protocol.

The comparison between the two established RAD16-I culture platforms based on the sandwich configuration, the traditional and the PFM-modified sandwich, shows that the

introduction of the RGD signaling motif promoted in both platforms some degree of redifferentiation. Regarding PTFE membrane-based sandwiches, non-functionalized RAD16-I was able to promote the upregulation of the transcription factors MafA and NeuroD1, which was not observed in the traditional sandwich model. This fact suggests that the reduced thickness of the construct, which in turn allows for a better oxygenation and nutrition, contributes to the redifferentiation process of the dedifferentiated beta cells. Nevertheless, and as mentioned previously, the same number of donors should be included in the new sandwich platform in order to obtain more robust results.

4.4 CONCLUDING REMARKS

Beta cell replacement therapy is a promising curative treatment for diabetes. Nowadays, it has been proved that islet transplantation can restore normoglycemia in type 1 diabetes[99,100]. Nevertheless, the main limitation of this approach is the scarcity of pancreatic islets available to be transplanted into diabetic patients. Thus, new strategies aimed to provide an abundant source of insulin-producing cells are needed. An attractive option is the *in vitro* expansion of adult beta cells obtained from human cadaveric organ donors[11–14]. Despite the low proliferative capacity of human beta cells *in vivo*, they can be induced to proliferate massively in 2D *in vitro* cultures. Nonetheless, the expansion is accompanied by an epithelial to mesenchymal transition (EMT), which implies the loss of the beta cell phenotype. Dedifferentiation could be due to the destruction of the islet microenvironment when pancreatic islets are isolated and to the subsequent dispersion into single cells, which also entails the loss of the cell-cell contacts.

We have studied whether the reconstitution of the islet microenvironment, through the establishment of cell-cell and cell-matrix relationships in a biomimetic synthetic scaffold, could induce the redifferentiation of pancreatic human beta cells dedifferentiated after in *vitro* expansion. With this purpose, we have developed different 3D *in vitro* culture platforms based on the non-instructive RAD16-I self-assembling peptide (SAP). The first model was based on the RAD16-I platform used to encapsulate the rat beta cell line INS-1E (Chapter 3). Despite the good results concerning viability and functionality with INS-1E cells, this model did not work with human expanded islet-derived cells, showing poor viability results and no progression of the 3D cultures. On the other hand, the other two models were based on the sandwich configuration, where cells are cultured within two thin layers of RAD16-I. In the first sandwich model, cells were embedded between two layers of equal thickness (0.5 mm total thickness), whereas in the second model, the top layer of peptide was assembled over a PTFE membrane modified with PFM. Such modification allowed the assembling of a nanometric RAD16-I layer, therefore decreasing the thickness of the whole construct. For both models, the expanded cells were allowed to reaggregate into islet-like cell clusters (ICCs) to promote the formation of cell-cell contacts, and then embedded between the two layers of the non-instructive SAP RAD16-I. Moreover, RAD16-I was functionalized by the covalent addition of the integrin-binding motif RGD (Arg-Gly-Asp) (RAD16-I/RGD), in the case of traditional sandwiches, and RGD and IKVAV (Ile-Lys-Val-Ala-Val), for the PTFE membrane-based sandwiches. The addition of the ECM-derived signaling motifs to the matrix structure was expected to promote cell-ECM interactions that could stimulate the up-regulation of beta cells markers and the redifferentiation towards a beta cell-like phenotype.

ICCs cultured in the traditional RAD16-I sandwiches were viable, maintained their cluster conformation, and increased in size by aggregation of small ICCs, suggesting a self-organizing process. ICCs cultured in functionalized RAD16-I/RGD, showed enhanced cell adhesion to the RAD16-I matrix and the re-expression of the beta cell specific genes Ins, Pdx1, Nkx6.1, and MafA. Therefore, ICCs have the capacity to respond to the microenvironment stimuli, modulating their behavior and gene expression levels. On the other hand, ICCs cultured in

PTFE membrane-based sandwiches, also showed excellent viability results and cluster conformation was maintained during the whole culture period, as in the case of traditional sandwiches. RAD16-I/RGD cultures promoted the upregulation of the beta cell markers Ins, Nkx6.1, MafA and NeuroD1. Another important aspect about PTFE membrane-based sandwiches is that, unlike traditional sandwiches, pure RAD16-I nanofibers were also able to induce the up-regulation of two important beta cell transcription factors, MafA and NeuroD1. Moreover, the introduction of the IKVAV adhesive motif in PTFE membrane-based sandwiches also caused the overexpression of MafA and NeuroD1, with higher values of overexpression than the RGD analog.

The results indicate that RGD and IKVAV functionalized SAPs in sandwich conformation are a promising 3D platform to induce the redifferentiation towards a beta cell phenotype and to generate insulin-expressing cells that could be used in cell therapy of diabetes. In order to achieve a complete redifferentiation towards a mature beta cell phenotype, different combinations of other beta cell integrin-binding motifs could be developed, in order to create a biologically functional scaffold more similar to the beta cell microenvironment.

4.5 REFERENCES

1. IDF. *International Diabetes Federation. IDF Diabetes Atlas 7th ed. Brussels, Belgium* (2015). Available at: http://www.diabetesatlas.org/.

2. Gregg, E. W. *et al.* Changes in Diabetes-Related Complications in the United States, 1990–2010. *N. Engl. J. Med.* **370,** 1514–1523 (2014).

3. Angelantonio, D., Kaptoge, Wormser, Gao, Wood, Nietert, K., Wallace, Trevisan, Cooper, Howard, S., Casiglia, Jukema, Woodward, Brunner, S. & Danesh. Association of cardiometabolic multimorbidity with mortality. *JAMA* **314,** 52–60 (2015).

4. Atkinson, M. A., Eisenbarth, G. S. & Michels, A. W. Type 1 diabetes. *Lancet* **383,** 69–82 (2014).

5. Butler, A. E. *et al.* β-cell deficit and increased β-cell apoptosis in humans with type 2 diabetes. *Diabetes* **52,** 102–110 (2003).

6. Shapiro, A. M. J. *et al.* Islet transplantation in seven patients with type 1 diabetes mellitus using a glucocorticoid-free immunosuppressive regimen. *N. Engl. J. Med.* **343,** 230–238 (2000).

7. Minami, K. & Seino, S. Current status of regeneration of pancreatic β-cells. *J. Diabetes Investig.* **4,** 131–141 (2013).

8. Bonner-Weir, S. & Weir, G. C. New sources of pancreatic beta-cells. *Nat. Biotechnol.* **23,** 857–61 (2005).

9. Domínguez-Bendala, J., Lanzoni, G., Klein, D., Álvarez-Cubela, S. & Pastori, R. L. The Human Endocrine Pancreas: New Insights on Replacement and Regeneration. *Trends Endocrinol. Metab.* **27,** 153–162 (2016).

10. Limbert, C., Päth, G., Jakob, F. & Seufert, J. Beta-cell replacement and regeneration: Strategies of cell-based therapy for type 1 diabetes mellitus. *Diabetes Res. Clin. Pract.* **79,** 389–399 (2008).

11. Ouziel-Yahalom, L. *et al.* Expansion and redifferentiation of adult human pancreatic islet cells. *Biochem. Biophys. Res. Commun.* **341,** 291–298 (2006).

12. Russ, H. A., Bar, Y., Ravassard, P. & Efrat, S. In vitro proliferation of cells derived from adult human β-cells revealed by cell-lineage tracing. *Diabetes* **57,** 1575–1583 (2008).

13. Billestrup, N. & Otonkoski, T. Dedifferentiation for replication of human beta-cells: a division between mice and men? *Diabetes* **57,** 1457–8 (2008).

14. Russ, H. A. *et al.* Insulin-producing cells generated from dedifferentiated human pancreatic beta cells expanded in vitro. *PLoS One* **6,** e25566 (2011).

15. Baker, B. M. & Chen, C. S. Deconstructing the third dimension: how 3D culture microenvironments alter cellular cues. *J. Cell Sci.* **125,** 3015–24 (2012).

16. Beattie, G. M. *et al.* Sustained proliferation of PDX-1+ cells derived from human islets. *Diabetes* **48,** 1013–9 (1999).

17. Billestrup, N. & Otonkoski, T. Dedifferentiation for Replication of Human -Cells: A Division Between Mice and Men? *Diabetes* **57,** 1457–1458 (2008).

18. Lamouille, S., Xu, J. & Derynck, R. Molecular mechanisms of epithelial-mesenchymal transition. *Natl. Rev. Mol. Cell Biol.* **15,** 178–196 (2014).

19. Lee, J. M., Dedhar, S., Kalluri, R. & Thompson, E. W. The epithelial–mesenchymal transition: new insights in signaling, development, and disease. *J. Cell Biol.* **172,** 973 LP-981 (2006).

20. Thiery, J. P. & Sleeman, J. P. Complex networks orchestrate epithelial-mesenchymal transitions. *Nat. Rev. Mol. Cell Biol.* **7,** 131–42 (2006).

21. Kalluri, R. & Weinberg, R. a. Review series The basics of epithelial-mesenchymal transition. *J. Clin. Invest.* **119,** 1420–1428 (2009).

22. Russ, H. A., Ravassard, P., Kerr-Conte, J., Pattou, F. & Efrat, S. Epithelial-mesenchymal transition in cells expanded in vitro from lineage-traced adult human pancreatic beta cells. *PLoS One* **4,** e6417 (2009).

23. Wang, R. N. & Rosenberg, L. Maintenance of beta-cell function and survival following islet isolation requires re-establishment of the islet-matrix relationship. *J. Endocrinol.* **163,** 181–190 (1999).

24. Bar-Nur, O., Russ, H. A., Efrat, S. & Benvenisty, N. Epigenetic memory and preferential lineage-specific differentiation in induced pluripotent stem cells derived from human pancreatic islet beta cells. *Cell Stem Cell* **9,** 17–23 (2011).

25. Otonkoski, T., Banerjee, M., Korsgren, O., Thornell, L. & Virtanen, I. Unique basement membrane structure of human pancreatic islets: implications for β-cell growth and differentiation. *Diabetes, Obes. Metab.* **10,** 119–127 (2008).

26. Virtanen, I. *et al.* Blood vessels of human islets of Langerhans are surrounded by a double basement membrane. *Diabetologia* **51,** 1181–91 (2008).

27. Nikolova, G. *et al.* The vascular basement membrane: a niche for insulin gene expression and Beta cell proliferation. *Dev. Cell* **10,** 397–405 (2006).

28. Pinkse, G. G. M. *et al.* Integrin Signaling via RGD Peptides and Anti beta 1 Antibodies Confers Resistance to Apoptosis in Islets of Langerhans. *Diabetes* **55,** 312–317 (2006).

29. Hammar, E. *et al.* Extracellular Matrix Protects Pancreatic Beta Cells Against Apoptosis. *Diabetes* **53,** 2034–2041 (2004).

30. Ris, F. *et al.* Impact of integrin-matrix matching and inhibition of apoptosis on the survival of purified human beta-cells in vitro. *Diabetologia* **45,** 841–50 (2002).

31. Lucas-Clerc, C., Massart, C., Campion, J. P., Launois, B. & Nicol, M. Long-term culture of human pancreatic islets in an extracellular matrix: morphological and metabolic effects. *Mol. Cell. Endocrinol.* **94,** 9–20 (1993).

32. Beattie, G. M. *et al.* A novel approach to increase human islet cell mass while preserving beta-cell function. *Diabetes* **51,** 3435–9 (2002).

33. Hayek, A. *et al.* Growth Factor/Matrix-Induced Proliferation of Human Adult β-Cells. *Diabetes* **44,** 1458–1460 (1995).

34. Parnaud, G. *et al.* Proliferation of sorted human and rat beta cells. *Diabetologia* **51,** 91–100 (2008).

35. Parnaud, G. *et al.* Blockade of beta 1 Integrin-Laminin-5 Interaction Affects Spreading and Insulin Secretion of Rat Beta Cells Attached on Extracellular Matrix. *Diabetes* **55,** 1413–1420 (2006).

36. Hammar, E. B. Activation of NF- B by Extracellular Matrix Is Involved in Spreading and Glucose-stimulated Insulin Secretion of Pancreatic Beta Cells. *J. Biol. Chem.* **280,** 30630–30637 (2005).

37. Bosco, D., Meda, P., Halban, P. A. & Rouiller, D. G. Importance of cell-matrix interactions in rat islet beta-cell secretion in vitro: role of alpha6beta1 integrin. *Diabetes* **49,** 233–243 (2000).

38. Beattie, G. M., Lappi, D. A., Baird, A. & Hayek, A. Functional impact of attachment and purification in the short term culture of human pancreatic islets. *J. Clin. Endocrinol. Metab.* **73,** 93–98 (1991).

39. Nagata, N. *et al.* Evaluation of insulin secretion of isolated rat islets cultured in extracellular matrix. *Cell Transpl.* **10,** 447–451 (2001).

40. Kaido, T. *et al.* Impact of defined matrix interactions on insulin production by cultured human beta-cells: effect on insulin content, secretion, and gene transcription. *Diabetes* **55,** 2723–9 (2006).

41. Wojtusciszyn, A., Armanet, M., Morel, P., Berney, T. & Bosco, D. Insulin secretion from human beta cells is heterogeneous and dependent on cell-to-cell contacts. *Diabetologia* **51,** 1843–1852 (2008).

42. Amer, L. D., Mahoney, M. J. & Bryant, S. J. Tissue engineering approaches to cell-based type 1 diabetes therapy. *Tissue Eng. Part B. Rev.* **20,** 455–67 (2014).

43. Krishnamurthy, M., Li, J., Al-Masri, M. & Wang, R. Expression and function of alphabeta1 integrins in pancretic beta (INS-1) cells. *J. Cell Commun. Signal.* **2,** 67–79 (2008).

44. Lee, J., Cuddihy, M. J. & Kotov, N. A. Three-Dimensional Cell Culture Matrices: State of the Art. *Tissue Eng. Part B Rev.* **14,** 61–86 (2008).

45. Stendahl, J. C., Kaufman, D. B. & Stupp, S. I. Extracellular matrix in pancreatic islets: Relevance to scaffold design and transplantation. *Cell Transplant.* **18,** 1–12 (2009).

46. Rahmany, M. B. & Van Dyke, M. Biomimetic approaches to modulate cellular adhesion in biomaterials: A review. *Acta Biomater.* **9,** 5431–5437 (2013).

47. Lutolf, M. P. & Hubbell, J. A. Synthetic biomaterials as instructive extracellular microenvironments for morphogenesis in tissue engineering. *Nat. Biotechnol.* **23,** 47–55 (2005).

48. Weber, L. M., Hayda, K. N., Haskins, K. & Anseth, K. S. The effects of cell-matrix interactions on encapsulated beta-cell function within hydrogels functionalized with matrix-derived adhesive peptides. *Biomaterials* **28,** 3004–11 (2007).

49. Matson, J. B. & Stupp, S. I. Self-assembling peptide scaffolds for regenerative medicine. *Chem. Commun.* **48,** 26–33 (2012).

50. Beniash, E., Hartgerink, J. D., Storrie, H., Stendahl, J. C. & Stupp, S. I. Self-assembling peptide amphiphile nanofiber matrices for cell entrapment. *Acta Biomater.* **1,** 387–397 (2005).

51. Semino, C. E. Self-assembling Peptides: From Bio-inspired Materials to Bone Regeneration. *J. Dent. Res.* **87,** 606–616 (2008).

52. Zhang, S., Gelain, F. & Zhao, X. Designer self-assembling peptide nanofiber scaffolds for 3D tissue cell cultures. *Semin. Cancer Biol.* **15,** 413–20 (2005).

53. Holmes, T. *et al.* Extensive neurite outgrowth and active synapse formation on self-assembling peptide scaffolds. *PNAS* **97,** 6728–6733 (2000).

54. Fernández-Muiños, T. *et al.* Bimolecular based heparin and self-assembling hydrogel for tissue engineering applications. *Acta Biomater.* **16,** 35–48 (2015).

55. Garreta, E., Genové, E., Borrós, S. & Semino, C. Osteogenic Differentiation of Mouse Embryonic Stem Cells. *Tissue Eng.* **12,** 1–13 (2006).

56. Genové, E. *et al.* Functionalized self-assembling peptide hydrogel enhance maintenance of hepatocyte activity in vitro. *J. Cell. Mol. Med.* **13,** 3387–97 (2009).

57. Genové, E., Shen, C., Zhang, S. & Semino, C. E. The effect of functionalized self-assembling peptide scaffolds on human aortic endothelial cell function. *Biomaterials* **26,** 3341–3351 (2005).

58. Kisiday, J. *et al.* Self-assembling peptide hydrogel fosters chondrocyte extracellular matrix production and cell division:Implications for cartilage tissue repair. *PNAS* **99,** 9996 –10001 (2002).

59. Marí-Buyé, N., Luque, T., Navajas, D. & Semino, C. E. Development of a Three-Dimensional Bone-Like Construct in a Soft Self-Assembling Peptide Matrix. *Tissue Eng. Part A* **19,** 870–881 (2013).

60. Quintana, L. *et al.* Early tissue patterning recreated by mouse embryonic fibroblasts in a three-dimensional environment. *Tissue Eng. Part A* **15,** 45–54 (2009).

61. Semino, C. E., Merok, J. R., Crane, G. G., Panagiotakos, G. & Zhang, S. Functional differentiation of hepatocyte-like spheroid structures from putative liver progenitor cells in three-dimensional peptide scaffolds. *Differentiation* **71,** 262–270 (2003).

62. Semino, C., Kasahara, J., Hayashi, Y. & Zhang, S. Entrapment of Migrating Hippocampal Neural Cells in Three-Dimensional Peptide Nanofiber Scaffold. *Tissue Eng.* **10,** 643–655 (2004).

63. Soler-Botija, C. *et al.* Engineered 3D bioimplants using elastomeric scaffold, self-assembling peptide hydrogel, and adipose tissue-derived progenitor cells for cardiac regeneration. *Am. J. Transl. Res.* **6,** 291–301 (2014).

64. Lim, D.-J. *et al.* Enhanced Rat Islet Function and Survival *In Vitro* Using a Biomimetic Self-Assembled Nanomatrix Gel. *Tissue Eng. Part A* **17,** 399–406 (2011).

65. Stendahl, J. C., Wang, L.-J., Chow, L. W., Kaufman, D. B. & Stupp, S. I. Growth factor delivery from self-assembling nanofibers to facilitate islet transplantation. *Transplantation* **86,** 478 (2008).

66. Khan, S., Sur, S., Newcomb, C. J., Appelt, E. A. & Stupp, S. I. Self-assembling glucagon-like peptide 1-mimetic peptide amphiphiles for enhanced activity and proliferation of insulin-secreting cells. *Acta Biomater.* **8,** 1685–1692 (2012).

67. Chow, L. W., Wang, L., Kaufman, D. B. & Stupp, S. I. Self-assembling nanostructures to deliver angiogenic factors to pancreatic islets. *Biomaterials* **31,** 6154–6161 (2010).

68. Uzunalli, G. *et al.* Improving pancreatic islet in vitro functionality and transplantation efficiency by using heparin mimetic peptide nanofiber gels. *Acta Biomater.* **22,** 8–18 (2015).

69. Zhao, M. *et al.* The three-dimensional nanofiber scaffold culture condition improves viability and function of islets. *J. Biomed. Mater. Res. Part A* **94,** 667–672 (2010).

70. Navarro-Alvarez, N. *et al.* Reestablishment of microenvironment is necessary to maintain in vitro and in vivo human islet function. *Cell Transplant.* **17,** 111–9 (2008).

71. Wu, J. *et al.* Nanometric self-assembling peptide layers maintain adult hepatocyte phenotype in sandwich cultures. *J. Nanobiotechnology* **8,** 29 (2010).

72. Ohneda, K., Ee, H. & German, M. Regulation of insulin gene transcription. *Online* **11,** 227–233 (2000).

73. Iype, T. *et al.* The transcriptional repressor Nkx6.1 also functions as a deoxyribonucleic acid context-dependent transcriptional activator during pancreatic beta-cell differentiation: evidence for feedback activation of the nkx6.1 gene by Nkx6.1. *Mol. Endocrinol.* **18,** 1363–75 (2004).

74. Sander, M. *et al.* Homeobox gene Nkx6.1 lies downstream of Nkx2.2 in the major pathway of beta-cell formation in the pancreas. *Development* **127,** 5533–5540 (2000).

75. Schaffer, A. E. *et al.* Nkx6.1 Controls a Gene Regulatory Network Required for Establishing and Maintaining Pancreatic Beta Cell Identity. *PLoS Genet.* **9,** (2013).

76. Aramata, S., Han, S.-I. & Kataoka, K. Roles and regulation of transcription factor MafA in islet beta-cells. *Endocr. J.* **54,** 659–666 (2007).

77. Zhang, C. *et al.* MafA Is a Key Regulator of Glucose-Stimulated Insulin Secretion MafA Is a Key Regulator of Glucose-Stimulated Insulin Secretion. *Mol. Cell. Biol.* **25,** 4969–76 (2005).

78. Kataoka, K. *et al.* MafA is a glucose-regulated and pancreatic ??-cell-specific transcriptional activator for the insulin gene. *J. Biol. Chem.* **277,** 49903–49910 (2002).

79. Hang, Y. & Stein, R. MafA and MafB activity in pancreatic beta cells. *Trends Endocrinol. Metab.* **22,** 364–373 (2011).

80. Artner, I. *et al.* MafA and MafB regulate genes critical to beta-cells in a unique temporal manner. *Diabetes* **59,** 2530–2539 (2010).

81. Nishimura, W. *et al.* A switch from MafB to MafA expression accompanies differentiation to pancreatic beta-cells. *Dev. Biol.* **293,** 526–539 (2006).

82. Holland, A. M., Go, L. J., Naselli, G., MacDonald, R. J. & Harrison, L. C. Conditional Expression Demonstrates the Role of the Maintenance and Regeneration of {b}-Cells in the Adult. *Diabetes* **54,** 2586–2595 (2005).

83. Gu, G., Dubauskaite, J. & Melton, D. A. Direct evidence for the pancreatic lineage: NGN3+ cells are islet progenitors and are distinct from duct progenitors. *Development* **129,** 2447–2457 (2002).

84. Gao, T. *et al.* Pdx1 maintains β cell identity and function by repressing an α cell program. *Cell Metab.* **19,** 259–271 (2014).

85. Cerf, M. E. Transcription factors regulating β-cell function. *Eur. J. Endocrinol.* **155,** 671–679 (2006).

86. Seymour, P. A. *et al.* SOX9 is required for maintenance of the pancreatic progenitor cell pool. *Proc. Natl. Acad. Sci. U. S. A.* **104,** 1865–70 (2007).

87. Kawaguchi, Y. Sox9 and programming of liver and pancreatic progenitors. *J. Clin. Invest.* **123,** 1881–1886 (2013).

88. Li, L., Bennett, S. A. L. & Wang, L. Role of E-cadherin and other cell adhesion molecules in survival and differentiation of human pluripotent stem cells. *Cell Adh. Migr.* **6,** 59–70 (2012).

89. Derycke, L. D. M. & Bracke, M. E. N-cadherin in the spotlight of cell-cell adhesion, differentiation, embryogenesis, invasion and signalling. *Int. J. Dev. Biol.* **48,** 463–476 (2004).

90. Cirulli, V. *et al.* Expression of neural cell adhesion molecule (N-CAM) in rat islets and its role in islet cell type segregation. *J. Cell Sci.* **107,** 1429–36 (1994).

91. Karaca, M., Magnan, C. & Kargar, C. Functional pancreatic beta-cell mass: involvement in type 2 diabetes and therapeutic intervention. *Diabetes Metab.* **35,** 77–84 (2009).

92. Bernard-Kargar, C., Kassis, N., Berthault, M.-F., Pralong, W. & Ktorza, A. Sialylated form of the neural cell adhesion molecule (NCAM): a new tool for the identification and sorting of beta-cell subpopulations with different functional activity. *Diabetes* **50,** S125 (2001).

93. Banerjee, M. & Otonkoski, T. A simple two-step protocol for the purification of human pancreatic beta cells. *Diabetologia* **52,** 621–5 (2009).

94. Ilieva, A. *et al.* Pancreatic islet cell survival following islet isolation: the role of cellular interactions in the pancreas. *J. Endocrinol.* **161,** 357–364 (1999).

95. Camussi, G., Zanone, M. M. & Favaro, E. From endothelial to β cells: insights into pancreatic islet microendothelium. *Curr. Diabetes Rev.* **4,** 1–9 (2008).

96. Lam, J. & Segura, T. The modulation of MSC integrin expression by RGD presentation. *Biomaterials* **34,** 3938–3947 (2013).

97. Yamada, K. M. & Cukierman, E. Modeling tissue morphogenesis and cancer in 3D. *Cell* **130,** 601–10 (2007).

98. Duque, L. *et al.* Reactions of Plasma-Polymerised Pentafluorophenyl Methacrylate with Simple Amines. *Plasma Process. Polym.* **7,** 915–925 (2010).

99. Shapiro, A. M. J. *et al.* International trial of the Edmonton protocol for islet transplantation. *N. Engl. J. Med.* **355,** 1318–1330 (2006).

100. Bellin, M. D. *et al.* Potent induction immunotherapy promotes long-term insulin independence after islet transplantation in type 1 diabetes. *Am. J. Transplant.* **12,** 1576–1583 (2012).

CONCLUSIONS

INS-1E cell line:

- A biomimetic 3D culture platform based on the use of the self-assembling peptide (SAP) RAD16-I to encapsulate the beta cell surrogate, INS-1E cell line, was developed. Even though the introduction of the RGD, YIG and IKVAV signaling motifs to RAD16-I peptide diminished the β-sheet content characteristic of RAD16-I, functionalized peptides were able to form nanofibers. GEF and TWY peptides did not maintain the capacity to form hydrogels and therefore were discarded.

- Functionalized RAD16-I matrices promoted the formation of INS-1E cell aggregates that kept growing in size up to day 10 of culture and maintained cell viability. No differences were appreciated in terms of viability or cluster size between functionalized and pure RAD16-I matrices.

- INS-1E cell cluster morphology in monolayer and 3D type I collagen cultures was less homogeneous and irregular in shape than in RAD16-I cultures. Thus, RAD16-I matrices seem to be more adequate to promote the formation of cell structures resembling that of *in vivo* pancreatic islets.

- RAD16-I/IKVAV and RAD16-I/YIG matrices enhanced glucose stimulated insulin secretion compared to non-functionalized RAD16-I matrix. These results demonstrate that the reestablishment of cell-matrix interactions in RAD16-I scaffold are able to improve islet function. Thus, functionalized RAD16-I model has proved to be a valid platform for pancreatic tissue engineering (PTE).

Human pancreatic islet-derived cells:

- Human pancreatic islets were successfully isolated and the subsequent magnetic cell sorting achieved an enrichment in insulin$^+$ cells. *In vitro* expansion of sorted cells was associated with the loss of insulin expression and a dramatic increment of vimentin$^+$ cells. These results suggest that cell expansion implies an epithelial to mesenchymal transition (EMT).

- The encapsulation of the expanded cells in RAD16-I peptide did not yield to viable cultures, as in the case of the beta cell surrogate INS-1E cell line. We hypothesize that cells were not able to recover from the stress caused by the initial acidic pH of RAD16-I.

- Pure RAD16-I and functionalized RAD16-I/RGD sandwich cultures promoted cell survival and the maintenance of cell-cell contacts throughout the culture period. Moreover, sandwich cultures proved to be dynamic cultures where cell clusters (ICCs) evolved, suggesting therefore a self-organizing process.

- The addition of the RGD signaling peptide increased cell adhesion to the RAD16-I matrix and promoted cell proliferation during the first stage of culture. Furthermore, functionalized RAD16-I/RGD sandwiches induced the re-expression of some important beta cell specific genes, including insulin.

- No significant differences in gene expression were identified when prolonging the sandwich cultures from 10 days to 18. Hence, we suggest that a shorter protocol of 10 days could be more adequate for the redifferentiation of expanded human islet-derived cells.

- Polymerization of pentafluorophenyl methacrylate (PFM) over PTFE (teflon) membranes allowed the formation of a nanometric RAD16-I peptide monolayer. Such modification enabled the establishment of a sandwich platform with reduced peptide layer thickness, compared to the traditional RAD16-I sandwich model.

- RGD and IKVAV functionalized PTFE membrane-based sandwiches, promoted cell survival and maintained cluster conformation throughout the culture period. Gene expression patterns were similar to those obtained in traditional RAD16-I sandwich cultures, although in this case non-functionalized RAD16-I was able to promote the up-regulation of two important beta cell transcription factors.

- Functionalized RAD16-I sandwich cultures are a promising 3D platform to induce the redifferentiation towards a beta cell phenotype and to generate insulin-expressing cells that could be used in cell therapy of diabetes. In order to achieve a complete redifferentiation towards a mature beta cell phenotype, different combinations of other signaling motifs and a redifferentiation cocktail could be used.

CONCLUSIONES

Línea celular INS-1E:

- Se ha desarrollado una plataforma biomimética de cultivo tridimensional (3D) basada en el uso del péptido autoensamblable (SAP) RAD16-I y la encapsulación de la línea de células beta INS-1E. A pesar de que la introducción de los motivos de señalización RGD, YIG e IKVAV en el péptido RAD16-I disminuyó el contenido de hoja beta característica del péptido, los péptidos resultantes fueron capaces de formar nanofibras. Los péptidos GEF y TWY no mantuvieron la capacidad para formar hidrogeles y por lo tanto se descartaron.

- Las matrices de RAD16-I promovieron la formación de agregados celulares, los cuales crecieron en tamaño hasta día 10 de cultivo, manteniendo la viabilidad celular. No se apreciaron diferencias en términos de viabilidad o tamaño de los agregados, entre las matrices de RAD16-I funcionalizadas y las puras.

- La morfología de los agregados celulares en los cultivos monocapa y colágeno tipo I era menos homogénea e irregular que en la matriz de RAD16-I. Por lo tanto, la matriz RAD16-I parece ser más adecuada para promover la formación de estructuras celulares semejantes a las de los islotes pancreáticos *in vivo*.

- Las matrices de RAD16-I funcionalizadas con los péptidos IKVAV y YIG causaron un aumento en la secreción de insulina estimulada por glucosa, en comparación con la matriz de RAD16-I no funcionalizada. Estos resultados demuestran que el restablecimiento de las interacciones célula-matriz es capaz de mejorar la función de los islotes pancreáticos. Así, el modelo basado en la funcionalización del péptido RAD16-I ha demostrado ser una plataforma válida para la ingeniería de tejidos pancreática (PTE).

Células humanas derivadas de los islotes pancreáticos:

- Los islotes pancreáticos humanos fueron aislados con éxito y la posterior separación mediante partículas magnéticas logró un enriquecimiento de las células positivas para insulina. La expansión *in vitro* de estas células implicó la pérdida de expresión de la insulina y un incremento de las células positivas para vimentina. Estos resultados sugieren que la expansión celular implica una transición epitelial a mesenquimal (EMT).

- La encapsulación de las células expandidas en el péptido RAD16-I no dio lugar a cultivos viables, como en el caso de la línea celular INS-1E. Nuestra hipótesis es que las células no fueron capaces de recuperarse del estrés producido por el pH acido inicial del RAD16-I.

- Los cultivos en sándwich del péptido RAD16-I puro y funcionalizado con el motivo RGD, promovieron la supervivencia celular y el mantenimiento de los contactos célula-célula a lo largo del período de cultivo. Además, los cultivos en sándwich demostraron ser cultivos dinámicos donde los agregados celulares (ICCs) evolucionaron, lo cual sugiere un proceso de auto-organización.

- La introducción del péptido de señalización RGD aumentó la adhesión celular a la matriz RAD16-I y promovió la proliferación celular durante la primera etapa de cultivo. Además, los sándwiches funcionalizados con el motivo RGD indujeron la reexpresión de algunos genes específicos de células beta, incluyendo la insulina.

- No se identificaron diferencias significativas en la expresión génica al prolongar el cultivo en sándwich de 10 a 18 días. Por lo tanto, sugerimos que un protocolo de 10 días podría ser más adecuado para la rediferenciación de las células expandidas.

- La polimerización del pentafluorofenil metacrilato (PFM) sobre membranas de teflon (PTFE) permitió la formación de una monocapa nanométrica de péptido RAD16-I. Dicha modificación permitió el establecimiento de una plataforma en configuración sándwich con un espesor de capa menor, en comparación con el modelo de sándwich RAD16-I tradicional.

- La funcionalización de los sándwiches de membrana con los motivos RGD e IKVAV promovió la supervivencia celular y el mantenimiento de los agregados celulares a lo largo del período de cultivo. Los patrones de expresión génica fueron similares a los obtenidos en los cultivos sándwich tradicionales, aunque en este caso el RAD16-I no funcionalizado fue capaz de inducir un aumento en la expresión de dos importantes factores de transcripción de célula beta.

- Los cultivos en sándwich basados en la funcionalización del péptido RAD16-I son una plataforma 3D prometedora para inducir la rediferenciación hacia un fenotipo de célula beta, generando así células que podrían ser usadas en la terapia celular de la diabetes. Con el fin de lograr una rediferenciación completa hacia un fenotipo de célula beta madura, se propone el uso de diferentes combinaciones de otros motivos de señalización y de un cóctel de rediferenciación.

CONCLUSIONS

Línia cel·lular INS-1E:

- S'ha desenvolupat una plataforma biomimètica de cultiu tridimensional (3D) basada en l'ús del pèptid autoensamblable (SAP) RAD16-I i l'encapsulació de la línia de cèl·lules beta INS-1E. Tot i que la introducció dels motius de senyalització RGD, YIG i IKVAV al pèptid RAD16-I va disminuir el contingut de fulla beta característica del pèptid, els pèptids resultants van ser capaços de formar nanofibres. Els pèptids GEF i TWY no van mantenir la capacitat per formar hidrogels i per tant es van descartar.

- Les matrius de RAD16-I van promoure la formació d'agregats cel·lulars, els quals van créixer en grandària fins a dia 10 de cultiu, mantenint la viabilitat cel·lular. No es van apreciar diferències en termes de viabilitat o grandària dels agregats, entre les matrius de RAD16-I funcionalitzades i les pures.

- La morfologia dels agregats cel·lulars en els cultius monocapa i col·lagen tipus I era menys homogènia i irregular que en la matriu de RAD16-I. Per tant, la matriu RAD16-I sembla ser més adequada per a promoure la formació d'estructures cel·lulars semblants a les dels illots pancreàtics *in vivo.*

- Les matrius de RAD16-I funcionalitzades amb els pèptids IKVAV i YIG van causar un augment en la secreció d'insulina estimulada per glucosa, en comparació amb la matriu de RAD16-I no funcionalitzada. Aquests resultats demostren que el restabliment de les interaccions cèl·lula-matriu és capaç de millorar la funció dels illots pancreàtics. Així, el model basat en la funcionalització del pèptid RAD16-I ha demostrat ser una plataforma vàlida per a l'enginyeria de teixits pancreàtica (PTE).

Cèl·lules humanes derivades dels illots pancreàtics:

- Els illots pancreàtics humans van ser aïllats amb èxit i la posterior separació mitjançant partícules magnètiques va aconseguir un enriquiment de les cèl·lules positives per insulina. L'expansió *in vitro* d'aquestes cèl·lules va implicar la pèrdua d'expressió de la insulina i un increment de les cèl·lules positives per vimentina. Aquests resultats suggereixen que l'expansió cel·lular implica una transició epitelial mesenquimal (EMT).

- L'encapsulació de les cèl·lules expandides en el pèptid RAD16-I no va donar lloc a cultius viables, com en el cas de la línia cel·lular INS-1E. La nostra hipòtesi és que les cèl·lules no es van poder recuperar de l'estrès produït pel pH àcid inicial del RAD16-I.

- Els cultius en sandvitx del pèptid RAD16-I pur i funcionalitzat amb el motiu RGD, van promoure la supervivència cel·lular i el manteniment dels contactes cèl·lula-cèl·lula al llarg del període de cultiu. A més, els cultius en sandvitx van demostrar ser cultius dinàmics on els agregats cel·lulars (ICCs) van evolucionar, la qual cosa suggereix un procés d'auto-organització.

- La introducció del pèptid de senyalització RGD va augmentar l'adhesió cel·lular a la matriu RAD16-I i va promoure la proliferació cel·lular durant la primera etapa de cultiu. A més, els sandvitxos funcionalitzats amb el motiu RGD van induir la reexpressió d'alguns gens específics de cèl·lula beta, incloent la insulina.

- No es van identificar diferències significatives en l'expressió gènica en perllongar el cultiu en sandvitx de 10 a 18 dies. Per tant, suggerim que un protocol de 10 dies podria ser més adequat per a la rediferenciació de les cèl·lules expandides.

- La polimerització del pentafluorofenil metacrilat (PFM) sobre membranes de teflon (PTFE) va permetre la formació d'una monocapa nanomètrica de pèptid RAD16-I. Aquesta modificació va permetre l'establiment d'una plataforma en configuració sandvitx amb un gruix de capa menor, en comparació amb el model de sandvitx RAD16-I tradicional.

- La funcionalització dels sandvitxos de membrana amb els motius RGD i IKVAV va promoure la supervivència cel·lular i el manteniment dels agregats cel·lulars al llarg del període de cultiu. Els patrons d'expressió gènica van ser similars als obtinguts en els cultius sandvitx tradicionals, tot i que en aquest cas el RAD16-I no funcionalitzat va ser capaç d'induir un augment en l'expressió de dos importants factors de transcripció de cèl·lula beta.

- Els cultius en sandvitx basats en la funcionalització del pèptid RAD16-I són una plataforma 3D prometedora per induir la rediferenciació cap a un fenotip de cèl·lula beta, generant així cèl·lules que podrien ser utilitzades en la teràpia cel·lular de la diabetis. Per tal d'aconseguir una rediferenciació completa cap a un fenotip de cèl·lula beta madura, es proposa l'ús de diferents combinacions d'altres motius de senyalització i d'un còctel de rediferenciació.

PUBLICATIONS

Aloy-Reverté C*, Moreno-Amador JL*, Nacher M, Montanya E, Semino CE. Use of RGD-functionalized sandwich cultures to promote the redifferentiation of human pancreatic beta cells after in vitro expansion. *Tissue Engineering Part A* (Accepted 16 June 2017). *Equal contribution.

Moreno-Amador JL, Téllez N, **Aloy-Reverté C**, Lladó L, Semino C, Nacher M, Montanya E. Epithelial to Mesenchymal Transition in human endocrine islet cells. (Submitted May 2017).

Castells-Sala, C., Alemany-Ribes, M., Fernández-Muiños, T., Recha-Sancho, L., López- Chicón, P., **Aloy-Reverté, C.,** Caballero-Camino, J., Márquez-Gil, A., Semino, C.E., *Current applications of tissue engineering in biomedicine. Biochips and Tissue Chips*, S2: 004 (2013) doi: 10.4172/2153-0777.S2-004.